ABSTRACT

Advancing an Understanding of Bioaccumulation of Contaminants of Emerging Concern in Dynamic Aquatic Ecosystems

Samuel P. Haddad, Ph.D.

Mentor: Bryan W. Brooks, Ph.D.

The aquatic environment includes complex systems on which society relies to provide ecosystem services and support biodiversity. In recent years, the demand for aquatic-ecosystem commodities has greatly increased due to rapid population growth and industrialization. This burgeoning population stresses the global water cycle in many ways including increased fossil-fuel consumption promoting climate change, altered snowpack decreasing instream flows, multiple cities utilizing the same waterways, and increased nutrient loading due to agricultural expansion.and poorly treated sewage Such alterations to aquatic systems leads to unique exposure scenarios of contaminants of emerging concern such as pharmaceuticals and cyanotoxins. Thus, an understanding of exposure, hazards, and bioaccumulation of contaminants of emerging concern in dynamic aquatic systems in necessary to support sustainable management of aquatic resources. In this dissertation, the first study examined bioaccumulation of diphenhydramine, an ionizable weak base pharmaceutical, across different life stages in an organism that demonstrated ontogenetic diet changes in an urban estuary. The findings of this study demonstrated that

ontogenetic dietary shifts do not affect the bioaccumulation of diphenhydramine, but exposure difference in water does. The second study investigated whether ionizable weak base compounds with differing properties demonstrated trophic dilution within the food web of urbanizing rivers receiving runoff from snowmelt. This study observed that multiple ionizable weak base pharmaceuticals trophicly diluted with increasing trophic position and that inhalational uptake was the main driver of bioaccumulation in rainbow trout. The third study examined the spatial and temporal fate and transport of ionizable pharmaceuticals within a dynamic aquatic system that shifted from being influenced by spring snowmelt to effluent-dominated conditions. The findings of the third study reported decreasing concentrations with increasing distance downstream regardless of season and the presence of secondary inputs from onsite waste-water systems. The fourth study developed a novel analytical method and then investigated the bioaccumulation potential of various cyanobacterial toxins in a highly eutrophic Texas reservoir. The fourth study identified several novel methodological approaches to analytically identify cyanotoxins and reported the presence of cyanotoxins in Lake Waco, Texas, USA for the first time, These observations collectively provided novel environmental assessment approaches to support an advanced understanding of bioaccumulation within dynamic aquatic ecosystems.

Bioaccumulation of Contaminants of Emerging Concern in Dynamic Ecosystems

by

Samuel P. Haddad, B.S.

A Dissertation

Approved by the Department of Environmental Science

George P. Cobb, Ph.D., Chairperson

Submitted to the Graduate Faculty of
Baylor University in Partial Fulfillment of the
Requirements for the Degree
of

Doctor of Philosophy

Approved by the Dissertation Committee

Bryan W. Brooks, Ph.D., Chairperson

J. Thad Scott, Ph.D.

Ramon Lavado, Ph.D.

C. Kevin Chambliss, Ph.D.

Scott James, Ph.D.

Accepted by the Graduate School

December 2018

J. Larry Lyon, Ph.D., Dean

Page bearing signatures is kept on file in the Graduate School.

TABLE OF CONTENTS

LIST OF FIGURES

LIST OF TABLES

ACKNOWLEDGMENTS

Greg Leeper, Thomas Craft, Cody and Shaun Reno, Brandon Hovey, William Dunn, Delta Sigma Phi Homer Pledge Class, Mike Mosely, Zach Macintyre, Dirk Tyson Masonholder, The Spirit of Peoria Crew, Tony Steck, Devin Susmark, Cara Shuman, Chris and Austin Arnold, Lily Mocharnuk, Dr. ZQ Lin, Dr. Kevin Johnson, Dr. Paul Brunkow, Dr. Bowen Du, Dr. Lauren Kristofco, Dr. Gavin Saari, Dr. Donald Legan, Dr. Alistair Brown, Dustin Dubose, Jacob Hamilton, Cagney McCauly, The McCauly Family, Terrance Hedgecoke, Victoria Faith Wilson, Bjorn Ogren, Dr. Carol Ball, Lisa Perkins, Charles Haddad, Luann Marzinzick

DEDICATION

To Dr. Kevin A. Johnson for taking a chance.

ATTRIBUTION

Co-Author Contributions

Dr. Bowen Du, Casan Scott, Gavin Saari, Christopher Breed, Martin Kelly, Linda Broach, Dr. Kevin Chambliss, Dr. Bryan Brooks, Dr. Andreas Luek, Dr. Jone Corrales, Rebekah Burket, Lauren Kristofco, Dr. Joseph Rasmussen, Micheal Luers, Clint Rogers, Raegyn Taylor, Lea Lovin, and Dr. Jeremy Conkle, all contributed intellectually and/or financially to one or more of my published works. My advisor, Dr. Bryan W. Brooks, contributed intellectually and financially to all chapters. Our discussions of experimental design and results interpretation, along with provisions of laboratory supplies and living stipend, resulted in this dissertation. Dr. Bowen Du, Casan Scott, Gavin Saari, Christopher Breed, Dr. Jone Corrales, Rebekah Burket, Raegyn Taylor, and Lea Lovin are lab mates who contributed field support, lab support, and intellectually to chapters. Dr. Kevin Chambliss advised on all analytical chemistry for all chapters. Martin Kelly and Linda Broach allowed access to the field for chapter one and contributed intellectually to the publication. Dr. Andreas Luek and Dr. Joseph Rasmussen contributed significant intellectual input into modeling efforts for chapter two. Micheal Luers and Clint Rogers contributed access, funding, and review of chapters two and three. Dr. Jeremy Conkle provided critical review of the chapter four manuscript.

CHAPTER ONE

Introduction

Background and Significance

The aquatic environment includes complex systems on which society relies to provide a wealth of ecosystem services and natural resources. In recent years, demand for aquatic-ecosystem commodities has greatly increased due to rapid population increases and industrialization (Postel 2010; Rhind 2009). Over the last 50 years the human population has gone from 2.5 to 6.8 billion (Postel 2010). This burgeoning population has stressed the global water cycle in many ways, including increased fossil-fuel consumption promoting climate change (Postel 2010) and increased nutrient loading due to agricultural demands (Chapman 2015; Brooks, et al. 2016; Heisler, et al. 2008). Due to altered weather patterns and increasing global temperatures, hot environments are getting hotter and dryer, while wet environments are getting wetter (Postel 2010). One implication is altered snowpack; over 2 billion people depend on snowmelt. However, climate change is decreasing annual snowpack and stressing surface-water inflows (Mankin, et al. 2015). Another challenge for larger populations is differential wastewater treatment capacity, food production, and fertilizer use. Increased nutrient use and poorly treated sewage is leading to eutrophication of lakes, streams, and reservoirs. Finally, it is increasingly common for multiple cities and megacities to use the same waterways, leading to a phenomenon known as the urban water cycle (Sowby 2014). Such alterations to the environment and water cycles lead to unique

environmental-exposure scenarios of contaminants of emerging concern (CECs) such as pharmaceuticals and cyanotoxins (Brooks, et al. 2016; Chapman 2015; Heisler, et al. 2008).

The occurrence of pharmaceuticals and personal care products (PPCPs) and other CECs in aquatic systems has led to new research on environmental occurrence, fate, effects, risk assessment, and treatability of these contaminants (Daughton and Ternes 1999; Kolpin, et al. 2002; Brooks, Huggett, and Boxall 2009; Daughton and Brooks 2011b; Kwon, et al. 2009). Though pharmaceuticals have received much more attention as CECs, it is critically important to recognize that traditional approaches to understand and predict exposure and effects of other environmental organic contaminant classes may not be appropriate for some CECs, which may over- or under-estimate risk (Daughton and Brooks 2011b; Kwon, et al. 2009). For example, PPCPs typically have lower log P values, are more water soluble, and are less likely to accumulate in biota (Daughton and Brooks 2011b). However, during dry months, base flows in many semi-arid rivers are increasingly dominated or even dependent on effluent discharges from wastewater-treatment plants resulting in longer biota exposure durations (Ankley, et al. 2007). These instances represents worst-case scenarios for potential aquatic exposure and ecological effects of PPCPs (Brooks, Riley, and Taylor 2006). Such considerations are important for dynamic semi-arid river systems such as those in the western USA (Du, et al. 2014a; Du, et al. 2012) because instream flows can be increasingly stressed by urban population growth and climate variability (Brooks, Riley, and Taylor 2006).

Further, with global climate change and increased nutrient use, Harmful Algal Blooms (HABs) have increased in occurrence, frequency, and duration (Brooks, et al. 2016; Merel, et al. 2013). Cyanobacteria, or blue-green algae, are prokaryotes that were

among the first photosynthesizing organisms on Earth (Merel, et al. 2013). Cyanobacteria are globally distributed in water bodies including rivers, lakes, streams, ponds, reservoirs, and estuaries (Codd, et al. 2005; Kaloudis, et al. 2013). Under the proper conditions**,** cyanobacteria exponentially produce biomass and form dense blooms. Some cyanobacteria also produce harmful secondary metabolites known as cyanotoxins, which pose significant health risks to humans and animals through multiple exposure pathways (Merel, et al. 2013). HABs occur when the increased biomass of cyanobacteria releases cyanotoxins during growth**,** or lysis, causing the surrounding environment to become toxic (Lajeunesse, et al. 2012).

Because anthropogenic stressors are increasing in complexity, large-scale dynamic system questions are posed in this dissertation. The bioaccumulation, fate, and transport of CECs, specifically pharmaceuticals and cyanotoxins, through dynamic aquatic systems will be examined. The overarching goal is to advance to science to better characterize potential bioaccumulation and associated risks of these CECs to aquatic systems. This dissertation (1) explores exposure and accumulation of CECs across trophic positions in dynamic systems, including whether or not ionizable weak-base compounds demonstrate trophic magnification in an effluent-dominated semi-arid system, (2) determines whether bioaccumulation of CECs across trophic positions in effluent-dominated streams are affected by spatial (e.g., longitudinal) and temporal factors (e.g., snowmelt), and (3) develops an understanding of cyanotoxin occurrence and biomagnification across multiple trophic levels within highly eutrophic reservoir-transition zones.

Ontogenetic Dietary Shifts in Estuarine Fish and Bioaccumulation of Pharmaceuticals

Reports of human pharmaceuticals accumulating in aquatic biota from inland surface waters have increased in recent years, particularly from rapidly urbanizing regions (Brooks, et al. 2005; Du, et al. 2014a; Du, et al. 2012; Kolpin, et al. 2002; Ramirez, et al. 2009). Though there is increasing information relative to freshwater, there remains a poor understanding of the occurrence, bioaccumulation, and risks of human pharmaceuticals in coastal and marine systems (Daughton and Brooks 2011a; Alvarez, et al. 2014; Gaw, Thomas, and Hutchinson 2014; Jiang, Lee, and Fang 2014; Lazarus, et al. 2015; Meador, et al. 2016). Coastal waters receive freshwater inflows, which are influenced by watershed practices including discharge from municipal and industrial wastewater treatment plants (WWTPs) and runoff from storm water in agricultural and urban areas. Instream flows of many freshwater streams in semiarid regions of the world are dominated by or even dependent on effluent discharge (Brooks, Riley, and Taylor 2006). These urban systems likely represent worst-case scenarios for potential ecological effects of pharmaceuticals in developed countries because effective exposure duration increases with limited dilution of continuous chemicals introduction (Ankley, et al. 2007). Such exposure scenarios for consumer chemicals are also critically important to understand in rapidly urbanizing coastal systems (Brooks, Riley, and Taylor 2006). In fact, a recent global horizon scanning workshop identified developing an understanding of the bioaccumulation and risk associated with PPCPs in wildlife among the top questions necessary to understand corresponding environmental risks (Boxall, et al. 2012a). Coastal contamination from urban areas was also identified as a priority research need for marine science (Rudd 2014).

The stripped mullet, *Mugil cephalus,* is a versatile species with a wide range of occurrences in tropical, subtropical, and temporal coastal waters in all major oceans between the latitudes of 42° N and 42° S (Thompson 1966). In most coastal populations, *M. cephalus* lays its eggs in the marine environment near shore. Floating eggs are suspended by the marine currents until they hatch (Strydom and d'Hotman 2005). After a month at sea and in the surf zone, the early juveniles enter coastal estuaries for the remainder of the juvenile and part of the sub-adult life stages (Hsu, et al. 2009; Lawson 2010) before returning to the ocean as adults to spawn and lay eggs. This species is tolerant to ranges of diverse environmental conditions including salinity (Cardona 2006) and temperature (Marais 1978). *Mugil cephalus* can be used as a 'sentinel' species to monitor changes and effects in the environment due to its global distribution and tolerance of a range of conditions (Whitfield, Panfili, and Durand 2012). Recent studies have looked at the induction of oxidative stress with exposures to contaminants in the United States (Maruya, Francendese, and Manning 2005) and Portugal (Ferreira, Moradas-Ferreira, and Reis-Henriques 2005), the effects of climate change in Queensland, Australia (Meynecke, et al. 2006; Meynecke and Lee 2011), and biomonitoring in the Tumen Estuary, Sea of Japan (Oksyuzyan and Sokolovsky 2003) using *Mugil cephalus*. *Mugil cephalus* were thus selected for study to examine pharmaceutical bioaccumulation in estuarine systems. Pharmaceutical exposures in these esturaries are affected by diel salinity and pH (Scott, et al. 2016) so environmental tolerances are important considerations when using this species to examine bioaccumulation of pharmaceuticals.

Ontogenetic shifts in diet occur in larval and smaller individuals (1 to 100 mm SL) (Eggold and Motta 1992). , and possibly larger individuals (>100 mm SL) of *M. cephalus*,

where smaller individuals selectively browse while larger individuals opportunistically feed on detritus and benthos. During their larval phase, *M. cephalus* are primarily planktonic feeders (Zismann, Berdugo, and Kimor 1975; Nash, Kuo, and McConnel 1974; Gisbert, Cardona, and Castello 1996). Between 10 and 20 mm SL, the juvenile fish undergo a shift in diet, first feeding on small invertebrates in the water column, then transitioning to benthic organisms (Blaber and Whitfield 1977; Whitfield, Panfili, and Durand 2012). Eventually, as they increases in size (20 to 100 mm SL) they will feed more frequently on detritus and inorganic matter (sand) (Eggold and Motta 1992; Desilva and Wijeyaratne 1977). The trend in shifting from feeding on organisms in the water column to feeding on benthic organism and detritus was noted by De Silva and Wijeyaratne (Desilva and Wijeyaratne 1977). This study shows that there was little sand or detritus in any sample below 25 mm SL and that sand and detritus occurrence increases with an increase in fish size. This trend was then confirmed by Eggbold and Matta (1992) (Eggold and Motta 1992), who separated the fish into cohorts based on size and showed a trend of increasing inorganic content and detritus in the stomach. Further, a recent study noted that the $\delta^{15}N$ and thus the trophic level of *M. cephalus* shifted up as the size of the fish increased (Akin and Winemiller 2006).

Spatio-temporal Ecosystem Exposure and Accumulation

Increased pharmaceutical occurrence in lotic systems has led to an increase in observed pharmaceutical bioaccumulation in multiple aquatic matrices (e.g., sediment, water, periphyton, mussels, macroinvertebrates, fish) in freshwater and coastal ecosystems influenced by urban effluent discharges (Ramirez, et al. 2009; Metcalfe, et al. 2010; Du, et al. 2016; Du, et al. 2014a; Maruya, et al. 2014; Tanoue, et al. 2015; Xie, et al. 2015;

Ruhi, et al. 2016; Gaw, Thomas, and Hutchinson 2014; Subedi, et al. 2012). Partitioning dynamics of ionizable pharmaceuticals are rarely reliant on hydrophobic interaction relative to persistent organic pollutants (Ramirez, et al. 2009), but more often rely on hydrogen bonding, cation interactions, and surface complexation (Brooks, Huggett, and Boxall 2009). Uptake is influenced in fish (Nichols, et al. 2015) and invertebrates (Meredith-Williams, et al. 2012) by pH affecting the ionization state and bioavailability of ionizable pharmaceuticals in the stream (Nichols, et al. 2015; Valenti, et al. 2012; Valenti, et al. 2009; Valenti, et al. 2011). Further, the bioaccumulation of pharmaceuticals may be elevated due to a poor ability to biotransform some pharmaceuticals, which may lead to a higher accumulation for certain compounds (Connors, et al. 2013). Due to considerations listed above, traditional model organisms and endpoints used to define aquatic effects may not be as useful for therapeutics (Brooks, et al. 2003) such that the U.S. Environmental Protection Agency has recently proposed modifying traditional water-quality criteria to develop approaches to account for unique potencies of pharmaceuticals (Ankley, et al. 2009). Further, the realistic occurrence, ecological effects, and exposure scenarios of ionizable pharmaceuticals in aquatic and terrestrial systems were recently identified as a major research need (Boxall, et al. 2012a; Arnold, et al. 2014) and are germane to managing environmental quality and the conservation of ecosystem resources (Brooks 2014). Thus, a non-traditional and more advanced approach to assessing exposure, accumulation, hazards, and risks of pharmaceuticals is required (Tanoue, et al. 2014).

One approach gaining popularity in the regulatory arena is the use of trophic magnification factors (TMF), a weight-of-evidence assessment of bioaccumulation under the European Union's Registration, Evaluation, Authorization and Restriction of

Chemicals (REACH) program (Kim, et al. 2016). TMFs are empirically derived relationships used to assess bioaccumulation across different trophic levels in a food web and to examine chemical behavior (partitioning and uptake) in the environment at large (McLeod, et al. 2015; Burkhard, et al. 2013). Currently, there are several studies that provide a summary of the state-of-the-science (Kim, et al. 2016; Borga, et al. 2012; Conder, et al. 2012; McLeod, et al. 2015; Burkhard, et al. 2013). However, there are major uncertainties when formulating a TMF including: characterization of ionizable compounds within the TMF framework, concentration gradients within the system, and species home range (Kim, et al. 2016; Burkhard, et al. 2013). To date, there are few studies that examine pharmaceuticals in a TMF framework (Du, et al. 2016; Du, et al. 2014a; Xie, et al. 2015). Subsequently, little is known about ionizable pharmaceuticals in the context of trophic magnification that recent global synthesis efforts (including 1591 compounds) did not have any pharmaceutical data present because of limited study (Walters, et al. 2016; Lagesson, et al. 2016). Another source of variability within the TMF framework is the existence of spatial gradients within dynamic systems (e.g., estuaries, reservoir transition zones, snowmelt to urban streams) that are expected to exist for PPCPs specifically due to point-source discharges (Kim, et al. 2016).

In a comprehensive review of pharmaceuticals accumulation in aquatic organisms, Daughton and Brooks (2011a) recently identified that studies examining the influence of combined spatial and temporal factors on bioaccumulation and potential risks of pharmaceuticals and other CECs to aquatic life is decidedly lacking. Few studies, directly investigated spatial and temporal factors affecting bioaccumulation and trophic magnification factors (Moreno, et al. 2015; Li, et al. 2015). Variation in uptake from

different species within functional food chains can occur due to exposure scenarios influenced by species specific traits (foraging range, feeding behavior, migration, and morphology) (Brodin, et al. 2014; Brown, et al. 2014; Meredith-Williams, et al. 2012; Kim, et al. 2016; Burkhard, et al. 2013). For example, Du, Haddad et al. 2016 (Du, et al. 2016) recently reported that accumulation of diphenhydramine was significantly different in fish occupying different freshwater and saltwater habitats in a coastal system. Such observations could have been influenced by spatio-temporal factors influencing pH and salinity (Scott, et al. 2016), morphology of freshwater fish vs saltwater fish, or habitat and niche use (Du, et al. 2016). Combining spatio-temporal factors (season and distance) with bioaccumulation studies, including TMFs, and ecological assessments may provide a more robust understanding of CEC bioaccumulation, particularly in dynamic systems.

Spatial and Temporal Predicted and Observed Fish Plasma Levels of CECs

In order to understand exposure to aquatic organisms in a lotic system, occurrence, transport and fate of CECs within streams must be understood. Often, tracking CECs through a stream system can be difficult because sources of CECs may be uncertain. However, certain anthropogenic tracers, such as sucralose and caffeine, can provide a way to trace other CECs from defined sources (Du, et al. 2014b; Soh, et al. 2011). Sucralose is a highly conserved target analyte that doesn't degrade under UV light or within environmentally relevant pHs and temperatures. Further, due to a low log $P = -1$, sucralose does not tend to transition to other environmental compartments or bioaccumulate. Sucralose is also poorly removed from wastewater by both WWTPs and onsite septic systems (Du, et al. 2014b). As such, sucralose has been proposed for use as an environmental tracer (Soh, et al. 2011). Caffeine isbiodegradable during the wastewater

treatment process and in the environment under environmentally relevant conditions (Soh, et al. 2011; Du, et al. 2014b). In fact, it was found that the wastewater treatment process removed almost all caffeine during some treatment processes (Du, et al. 2014b). However, much caffeine is consumed, resulting in releases through effluents. Further, onsite septic systems were only found to remove ~50% of caffeine from treated water (Du, et al. 2014b) and approximately 20% of Americans use onsite waste treatment systems. Thus, sucralose provides a useful indicator of effluent discharge from WWTPs, and elevated levels of caffeine may provide an indicator of influence from onsite systems.

Translating surface-water concentrations of CECs to potential risk to aquatic life has also received increasing attention. Understanding internal doses of drugs, for example, in plasma and target tissues of aquatic organisms (e.g., fish) is actually more important for pharmaceuticals than traditional body-burden approaches that have been applied to whole organisms for conventional contaminants (Brooks, et al. 2009; Kwon, et al. 2009; Huggett, et al. 2003; Daughton and Brooks 2011a) because critical tissue or plasma levels can be linked to therapeutic and side-effect activity and resulting ecologically adverse outcomes (Brooks, et al. 2009). For example, Fick et al (Fick, et al. 2010a) recently quantified several pharmaceuticals in plasma of trout caged in several Swedish rivers influenced by wastewater effluents – one of these drugs exceeded human therapeutic concentrations and a number of therapeutics were present at concentrations higher than a fish plasma model proposed by Huggett et al (Huggett, et al. 2003). Further, Tanoue et al. (2015) presented an approach to anticipate specific fish-tissue concentrations based on plasma concentrations and can be used to more effectively understand where pharmaceuticals will ultimately accumulate within an organism. Because many pharmacological targets are

evolutionarily conserved in aquatic organisms (Gunnarsson, et al. 2008), mammalian pharmacology and toxicology data may be leveraged to study and even predict adverse effects to aquatic life (Kwon, et al. 2009; Ankley, et al. 2009; Ankley, et al. 2007; Berninger and Brooks 2010; Huggett, et al. 2003). Very limited corollaries to the Fick et al (2010a) study are available in North America; no efforts have examined temporal and spatial instream flow influences on internal dose levels of CECs. This consideration is particularly important for arid systems because instream flows can be increasingly stressed by population growth and climate variability (Brooks, Riley, and Taylor 2006). During dry months, base flows in many southwestern US rivers are increasingly dominated or even dependent upon effluent discharges from WWTPs, which represents worst-case scenarios for potential aquatic effects of CECs in developed countries (Brooks, Riley, and Taylor 2006).

Detection and Bioaccumulation of Cyanotoxins in Water and Fish

Harmful algal blooms, particularly by cyanobacteria, appear to be increasing in magnitude, frequency and duration in inland waters. There is no standard definition for what constitutes a cyanobacterial bloom; however, it is generally considered to be a high production of biomass over a short period of time (Merel, et al. 2013). Increased bloom formation can be attributed to several factors, such as climate change, temperature, and nutrient loading (Brooks, et al. 2016; Chapman 2015; Merel, et al. 2013):. Cyanobacteria prefer water temperatures of >25°C based on optimal growth rates. Global climate change has increased the selection of cyanobacteria over eukaryotic algae (Merel, et al. 2013; Arheimer, et al. 2005; Dale, Edwards, and Reid 2006; El-Shehawy, et al. 2012; Johnk, et al. 2008; O'Neil, et al. 2012). Cyanobacteria require a minimum amount of light for

photosynthesis. Whereas light profiles are species specific, the pigmentation of cyanobacteria protects from intense light and allows for a greater absorption over a broad spectrum. Thus, the duration of light exposure is far more important than intensity or quality as a growth factor (Merel, et al. 2013), yet the concentration and stoichiometry of nutrients limits bloom dynamics (Downing, Watson, and McCauley 2001). Further, certain cyanobacteria can fix nitrogen, which allows a competitive advantage when nitrogen levels are limiting (Scott, et al. 2009).

There are about 40 genera of cyanobacteria capable of producing cyanotoxins including *Anabaena*, *Cylindrospermopsis*, *Microcystis*, *Nostoc*, *Lyngbya*, and *Oscillatoria (Plantothrix)* (van Apeldoorn, et al. 2007; Greer, et al. 2016). All cyanotoxins are produced as internal metabolites (van Apeldoorn, et al. 2007; Wiegand and Pflugmacher 2005) except for cylindrospermopsin, which is up to 90% extracellular (Sotton, et al. 2015; van Apeldoorn, et al. 2007). Cyanotoxins are classified by two criteria: mechanism of action and structure (Ferrao-Filho Ada and Kozlowsky-Suzuki 2011). The most studied toxins, microcystins and nodularins, are hepatotoxic cyclic peptides that illicit toxicity by the inhibition of protein phosphatase 1 and 2A resulting in liver failure and hepatic hemorrhaging (van Apeldoorn, et al. 2007; Wiegand and Pflugmacher 2005). The ß-amino acid ADDA ((2S, 3S, 8S, 9S)-3-amino-9-methoxy-2,6,8-trimethyl-10-phenyl deca-4,6-dienoic acid) is responsible for toxicity associated with microcystins and nodularins because it conjugates to diene (Ferrao-Filho Ada and Kozlowsky-Suzuki 2011; Zervou, et al. 2017; van Apeldoorn, et al. 2007; Merel, et al. 2013). Cylindrospermopsin is a cytotoxic, dermotoxic, and hepatotoxic cyclic guanidinic alkaloid (de la Cruz, et al. 2013; Ferrao-Filho Ada and Kozlowsky-Suzuki 2011). The main mechanism of action for

cylindorspermopsin is the inhibition of protein synthesis, which results in liver and kidney failure (van Apeldoorn, et al. 2007). Anatoxin-a is a neurotoxic, bicyclic secondary amine (2-acetyl-9-azabicyclo[4,2,1]non-2-ene) (Zervou, et al. 2017). Anatoxin-a was the first described neurotoxic cyanotoxin and has a mechanism of action that irreversibly binds the nicotinic acetylcholine receptor resulting in muscular paralysis and ultimately death by suffocation, which is where its nickname "Very Fast Death Factor" appears to have originated (Ferrao-Filho Ada and Kozlowsky-Suzuki 2011; Merel, et al. 2013; van Apeldoorn, et al. 2007). Saxitoxin is also known as paralytic shellfish poison or toxin (PSP or PST) because it was first identified in edible shellfish (Ferrao-Filho Ada and Kozlowsky-Suzuki 2011). Saxitoxin has a mechanism of action that binds the sodium ion channels in nerves resulting in ataxia, convulsions, and paralysis (Merel, et al. 2013; van Apeldoorn, et al. 2007). Death from saxitoxin occurs from suffocation.

Exposures to cyanotoxins in food, drinking water, medical water, and recreational water have been globally responsible for illness and death in humans and animals (Roegner, et al. 2014; Merel, et al. 2013). Death from ingestion of cyanotoxins was first reported in an Australian lake in 1878. The lake was reported to contain a slimy scum and animals that drank from the lake died shortly afterward (Francis 1878). Another fatal incident occurred in Caruaru, Brazil when 131 patients at a local hospital receiving hemodialysis were exposed to microcystins and cylindrospermopsin by dirty water used in the process. One hundred of those patients died of acute liver failure (Pouria, et al. 1998). Another exposure to cylindrospermopsin in 1979 in Australia resulted in hospitalization of 140 children. A pesticide was administered to a lake to kill the scum that had formed. The massive cell lysis released cylindrospermopsin (Byth 1980). Over the last 100 years,

saxitoxin has been associated with numerous poisonings resulting in numbness, paralysis, and death. However, exposures to saxitoxin from drinking water have not been observed (Merel, et al. 2013), while anatoxin-a has resulted in multiple animal poisoning, but none to humans to date (Merel, et al. 2013). In 2014, a HAB in Lake Erie left over 400,000 people without drinking water in Toledo, Ohio when microcystins were detected in the water supply (Allinger and Reavie 2013; Michalak, et al. 2013). Sampling of Lake Erie showed levels of microcystin-LR between 10 and 20 µg/L, while tests at the Toledo water treatment facility measured levels at 2.5 µg/L, which is above the World Health Organizations recommended limit of 1.0 µg/L (Greer, et al. 2016; WHO 2011). Many countries have regulatory values for microcystin-LR that are in agreement with the World Health Organization at 1 µg/L (Merel, et al. 2013). However, few regulations exist for nodularin, cylindrospermopsin, anatoxin-a, or saxitoxin despite the numerous human exposures and economic losses (Merel, et al. 2013). Recently, the US Environmental Protection Agency (EPA) added cyanotoxins, specifically microcystin-LR, anatoxin-a, and cylindrospermopsin to the Contaminant Candidate List 3 and 4 (CCL3&4) (U.S.EPA 2016a). The EPA also issued health advisories for cylindrospermopsin and microcystin (U.S.EPA 2015a).

While cyanobacteria HABs have increased in frequency, duration, and magnitude in recent years, cyanobacteria blooms are not synonymous with the occurrence of cyanotoxins because not all strains produce toxic metabolites (Sarazin, et al. 2002; Brooks, et al. 2016). Only those strains containing the appropriate genes to produce toxins will results in HABs (Kurmayer and Christiansen 2009; Pearson, et al. 2016). However, even a bloom of a toxin-producing strain does not guarantee production of toxins because most

strains have the ability to activate genes depending on conditions (Merel, et al. 2013). Thus, understanding toxin production by cyanobacteria and bioaccumulation in aquatic systems is germane to ensuring high-quality food and water for consumption and recreation. Advanced analytical chemistry monitoring efforts are needed to support allocation of fiscal resources to help mitigate exposures to humans and animals.

CHAPTER TWO

Ontogenetic Dietary Shifts and Bioaccumulation of Diphenhydramine in *Mugil cephalus* from an Urban Estuary

This chapter published as: Haddad SP, Du B, Scott WC, Saari GN, Breed C, Kelly M, Broach L, Chambliss CK, Brooks BW. 2017. Ontogenetic Dietary Shifts and Bioaccumulation of Diphenhydramine in *Mugil cephalus* from an Urban Estuary. *Marine Environmental Research*. 127:155-162.

Abstract

Though bioaccumulation of pharmaceuticals has received attention in inland waters, studies of pharmaceutical bioaccumulation in estuarine systems are limited. Further, an understanding of pharmaceutical bioaccumulation across size classes of organisms displaying ontogenetic feeding shifts is lacking. We selected the striped mullet, *Mugil cephalus,* a euryhaline and eurythermal species that experiences dietary shifts with age, to identify whether a model weak base, diphenhydramine, accumulated in a tidally influenced urban bayou. We further determined whether diphenhydramine accumulation differed among size classes of striped mullet over a two-year study period. Stable isotope analysis identified ontogenetic feeding shifts of *M. cephalus* occurred from juveniles to adults. However, bioaccumulation of diphenhydramine did not significantly increase across age classes of *M. cephalus* but did correspond to surface water levels of the pharmaceutical, which suggests inhalational exposure of diphenhydramine was more important than dietary exposure in this urban estuary.

Introduction

Reports of human pharmaceuticals accumulating in aquatic biota from inland surface waters have increased in recent years, particularly from rapidly urbanizing regions (Brooks, et al. 2005; Du, et al. 2014a; Du, et al. 2012; Kolpin, et al. 2002; Ramirez, et al. 2009). Though there is increasing information for freshwater, there remains a poor understanding of the occurrence, bioaccumulation and risks of human pharmaceuticals in coastal systems (Daughton and Brooks 2011a; Alvarez, et al. 2014; Gaw, Thomas, and Hutchinson 2014; Jiang, Lee, and Fang 2014; Lazarus, et al. 2015; Meador, et al. 2016). Coastal waters receive freshwater inflows, which are influenced by watershed practices, including discharge from municipal and industrial wastewater treatment plants (WWTPs), and runoff from stormwater in agricultural and urban areas. Instream flows of many freshwater streams in semi-arid regions of the world are dominated by or even dependent on effluent discharge (Brooks, Riley, and Taylor 2006). These urban systems likely represent worst-case scenarios for potential ecological effects of pharmaceuticals because effective exposure duration increases with limited dilution of continuous chemicals introduction (Ankley, et al. 2007). Such exposure scenarios for consumer chemicals are also critically important to understand in rapidly urbanizing coastal systems (Brooks, Riley, and Taylor 2006). In fact, a recent global horizon scanning workshop identified developing an understanding of the bioaccumulation and risk associated with pharmaceuticals and personal care products (PPCPs) in wildlife among the top questions necessary to understand risks of PPCPs in the environment (Boxall, et al. 2012a). Coastal contamination from urban areas was also identified as a priority research need for marine science (Rudd 2014).

Our recent research observed accumulation of a calcium channel blocker, diltiazem, in plasma of multiple fish species exceeding human therapeutic plasma doses (Scott, et al. 2016). We also identified bioaccumulation of several other pharmaceuticals in fish from four estuaries of the Gulf of Mexico in Texas, USA, with differential land use and urbanization features (Du, et al. 2016). Whether these observations extend across life history stages of fish or other aquatic life is poorly understood. Further, influences of dietary exposure on bioaccumulation of ionizable contaminants in species displaying ontogenetic feeding shifts across their life histories are not known. In the current study we selected the striped mullet, *Mugil cephalus*, to explore whether accumulation of an ionizable pharmaceutical differs among life history stages. Ontogenetic shifts in diet specifically occur in smaller *M. cephalus* (1-100 mm; (Eggold and Motta 1992; Akin and Winemiller 2006)), but have received limited study in larger individuals.

The striped mullet is an estuarine species with a wide distribution in tropical, subtropical, and temporal coastal waters in all major oceans between the latitudes of 42° N and 42° S (Thompson 1966). In most coastal populations *M. cephalus* lay eggs near shore in the marine environment where these eggs remain suspended until hatch (Strydom and d'Hotman 2005). After a month at sea in the surf zone, early juveniles transition to coastal estuaries where juvenile and part of the sub-adult life stages are lived (Hsu, et al. 2009; Lawson 2010) before returning to the ocean as adults to spawn. A euryhaline (Cardona 2006) and eurythermal teleost (Marais 1978), *M. cephalus* may represent a 'sentinel' species to monitor environmental changes (Whitfield, Panfili, and Durand 2012). Herein, an understanding of exposure and accumulation of most contaminants of emerging concern

(CECs), including pharmaceuticals, is unknown as organisms grow, but necessary to reduce uncertainty during environmental hazard and risk assessment.

In the present study, we examined whether a model ionizable weak base, diphenhydramine (DPH), was accumulated by *M. cephalus* from a tidally influenced urban bayou, which receives municipal effluent from Houston, Texas, USA. We then determined whether DPH accumulation differed with size of *M. cephalus* over a two year study period. Stable isotope analysis was employed to identify if ontogenetic feeding shifts of *M. cephalus* occurred with age.

Materials and Methods

Study Site

Buffalo Bayou (Figure 2.1) begins in Fort Bend County, Texas, flows to the Houston Ship Channel, and then on to Galveston Bay, a critically important commercial fishery and port in the Gulf of Mexico. Buffalo Bayou was selected for study because this intensively urbanized watershed is the receiving system for appreciable effluent discharge and stormwater runoff from the City of Houston, Texas, the fourth largest city in the USA. During an initial study, we observed a number of pharmaceuticals and other CECs in the surface waters of Houston (Watkins, et al. 2014). We sampled downstream of the 69th Street WWTP, which is the largest WWTP (~200 Million Gallons Daily) in the US EPA Region 6 states of Texas, New Mexico, Louisiana, Arkansas and Oklahoma.

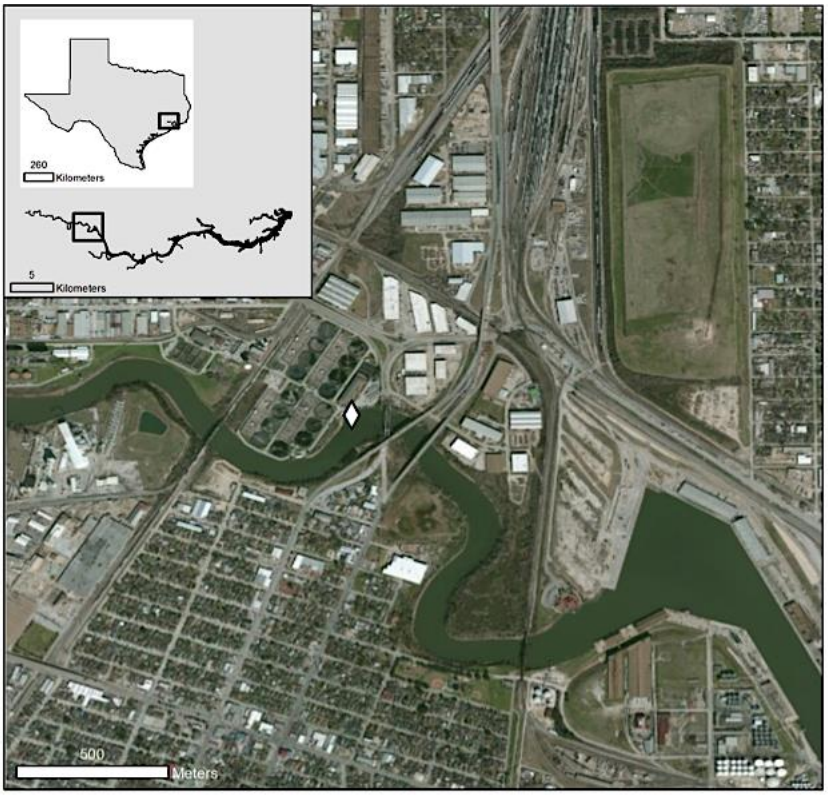

Figure 2.1. Buffalo Bayou in Houston, Harris County, Texas, USA. The diamond symbol denotes an effluent discharge from a major waste water treatment plant.

Field Sampling

Surface water and biological samples were collected on two different sampling events in October 2012 and September 2013. September and October are considered by the Texas Commission on Environmental Quality as important periods for monitoring surface water quality because these months represent a time of the year when rainfall, and thus instream dilution, is typically lowest, and subsequent exposure to aquatic contaminants is expected to be highest (TCEQ 2012). Sample collection followed Texas Commission on Environmental Quality methods by boat electrofishing, minnow trapping, and cast netting (TCEQ 2012). Specific boat electrofishing locations within a 200 m radius of the discharge were determined by salinity influences on electrofishing. Fish length and weight were

measured on site immediately after anesthetization using MS-222. All samples were transported to the lab on ice and stored at -20 °C until further analyses. During each sampling event, duplicate surface water samples were collected ~50 m downstream of the discharge in 4-L pre-rinsed amber glass bottles, transported on ice to the lab, and stored for less than 48 h at 4 °C in the dark prior to filtration and extraction.

Pharmaceutical Analysis in Water and Fish Tissue

Analytical methods for surface water and tissue followed previously reported procedures by our research team (Du, et al. 2014a; Du, et al. 2012), which were adapted from earlier reported methods (Vanderford and Snyder 2006; Lajeunesse, Gagnon, and Sauvé 2008). Information for other pharmaceutical occurrence in water and bioaccumulation for other fish species from Buffalo Bayou can be found elsewhere (Du, et al. 2016). Isotope dilution was used to compensate for matrix interference with an isotopically-labeled internal standard for the target analyte (Du, et al. 2014a; Du, et al. 2016).

All tissue samples were analyzed using liquid chromatography-tandem mass spectrometry (LC-MS/MS) following a previously reported method, in which instrumentation parameters, separation strategy, detection of the target analyte, calibration method, and method detection limits (MDLs) were detailed (Du, et al. 2012). MDLs for the analyte represented the lowest concentration that was reported with 99% confidence that the concentration was different from zero in a given matrix. One method blank sample and a pair of matrix spikes were also analyzed in each analytical sample batch. Matrix spike samples were spiked with 100 μg/kg of the target analyte. All matrix spike recoveries were within 80-120% of this spiking value.

Stable Isotope Analysis

Stable isotopes ($\delta^{15}N$, $\delta^{13}C$) were determined in the Stable Isotope Core Laboratory at Baylor University using a dual-inlet gas-source Stable Isotope Mass Spectrometer (Thermo-Electron, Waltham, Massachusetts, USA) and an Elemental Analyzer (Costech, Valencia, CA, USA). Whole biological tissue samples were dried for 24 h at 95 °C in a drying oven to constant weight and crushed to a fine powder using a mortar and pestle. Dried, crushed samples were weighed to approximately 1 mg and wrapped in Sn capsules prior to the instrumental analysis. Data was calibrated using internationally recognized standards USGS-40 and USGS-41 with analytical precision of ± 0.02 %. Isotopic ratios are calculated using the following equation:

$$\delta X\ (‰) = (R_{sample}/R_{standard} - 1) \times 1000$$

where the heavier isotope X is ^{15}N or ^{13}C, R_{sample} is the ratio of heavy to light isotope in the analyzed sample, and $R_{standard}$ is the ratio of heavy to light isotope in the standards (Jardine, Kidd, and Fisk 2006).

Statistical Analysis

Individual *M. cephalus* were partitioned to size classes from <149 mm (<1 year juveniles), 150 – 249 mm (~12-24 month old juveniles), 250 – 349 mm (~2 year old juveniles to adults), or > 350 mm (adults). Because the maximum size of *M. cephalus* at one year is reported to be 148 mm in Texas (McDonough and Wenner 2003), the smallest size class ended at 149 mm and was considered to be fish < 24 months old. Sexual maturity occurs between 250 to 300 mm for males and between 250 to 350 mm for females (Amuer, Bayed, and Benazzou 2003), so another size class of 250 – 349 mm was intended to encompass late juveniles and early adult *M. cephalus*. The largest size class of > 350 mm

was selected to represent more mature adult mullet. ANOVA, Tukeys HSD, and one-way T-tests were performed using JMP Pro (alpha of 0.05; Version 9, SAS institute Inc., Cary, NC, USA) and regression conducted with SigmaPlot 13 (Systat Software, San Jose, CA, USA).

Results and Discussion

Studies of pharmaceutical occurrence, bioaccumulation and risks in estuaries of the United States and other parts of world are rare (Meador, et al. 2016). In the current study, surface water concentrations of DPH were 15 ng/L and 42 ng/L in 2012 and 2013, respectively. The presence of other pharmaceuticals and CECs detected in fish species from Buffalo Bayou appeared to vary among fish species depending on habitat preferences (Du, et al. 2016). In addition to our recent observations in urban estuaries of the Gulf of Mexico (Du, et al. 2016; Scott, et al. 2016), three other studies, from San Francisco Bay, California (Klosterhaus, et al. 2013), the Chesapeake Bay, Maryland (Lazarus et al., 2015) and the Puget Sound, Washington (Meador, et al. 2016), have reported DPH occurrence in urban estuaries of the USA. Levels of DPH in surface water from the current study were typically 5 to 35 times higher than those previously reported from other estuaries (Scott, et al. 2016). Similarly, DPH accumulation in *M. cephalus* was generally elevated compared to other locations and estuarine species in the USA. Individual *M. cephalus* accumulated DPH ranging from 0.06 to 0.28 μg/kg in 2012 to slightly higher levels (0.29 to 2.01 μg/kg) during 2013 (Table 2.1).

Table 2.1. *Mugil cephalus* mean (±SD) weight (g), δ13C, δ15N, diphenhydramine (DPH) tissue levels and bioaccumulation factors (BAF) by size classes from an urban estuary, Buffalo Bayou, Texas, USA, in 2012 and 2013.

Size Class (mm)	n	Weight (g)	$\delta^{13}C$	$\delta^{15}N$	DPH (μg kg^{-1})	BAF (L kg^{-1})
2012						
350 >	4	779.6 ± 203.8	−25.59 ± 2.39	18.07 ± 2.58	0.06 ± 0.00	3.7 ± 0.0
250 - 349	7	265.8 ± 81.5	−25.75 ± 1.90	15.89 ± 2.24	0.25 ± 0.06	17 ± 4.0
150 - 249	9	89.9 ± 31.0	−26.09 ± 1.71	15.08 ± 3.10	0.19 ± 0.09	13 ± 6.0
< 149	5	27.4 ± 5.4	−23.50 ± 2.98	12.98 ± 1.78	0.17 ± 0.07	11 ± 4.5
2013						
150 - 249	6	111.4 ± 28.9	−26.17 ± 1.65	15.72 ± 1.11	0.73 ± 0.57	17 ± 13
< 149	9	24.6 ± 7.1	−21.51 ± 2.06	15.01 ± 2.06	1.2 ± 0.51	28 ± 12

Compared to other estuarine fish species from our recent research (Du, et al. 2016), *M. cephalus* accumulated the highest amount of DPH in whole body homogenates (μg/kg). Our observations of DPH in *M. cephalus* from 2012 were similar to DPH levels in salmon and sculpin from Washington, even though surface water DPH concentrations in Buffalo Bayou were 10-15 times higher than in Puget Sound (Meador, et al. 2016). However, during 2013 accumulation of DPH in *M. cephalus* was 1-8 times higher than salmon and sculpin from Puget Sound, and significantly greater ($p > 0.05$) than observations from fall 2012. If human ingestion of pharmaceuticals in fish from Buffalo Bayou is considered (Brooks, et al. 2005), exposure to DPH from consumption of *M. cephalus* is well below a typical daily dose of DPH. For example, considering a single fish serving is commonly estimated to be 0.289 kg (USEPA 1989), ~135,000 kgs of *M. cephalus* would need to be consumed in one meal to equal a DPH dose of 25 mg.

Though previous research partitioned juvenile *M. cephalus* among smaller size classes (20-100 mm) associated with shifts among different prey items with fish growth (Eggold and Motta 1992), in the present study we examined fish size classes up to 400 mm in length. DPH bioaccumulation in the largest fish (>350 mm) was significantly lower

($p<0.05$) than smaller size classes from the 2012, but not the 2013, sampling event (Figure 2.2). When field BAFs were calculated (Arnot and Gobas 2006) for both sampling dates, a consistent decrease in BAFs corresponded to increasing size of *M. cephalus*. For example, the highest BAF (28) was observed in 2013 for smaller fish (<149 mm) while the lowest BAF (3.7) was observed in 2012 for the largest size class (> 350 mm) (Table 2.1).

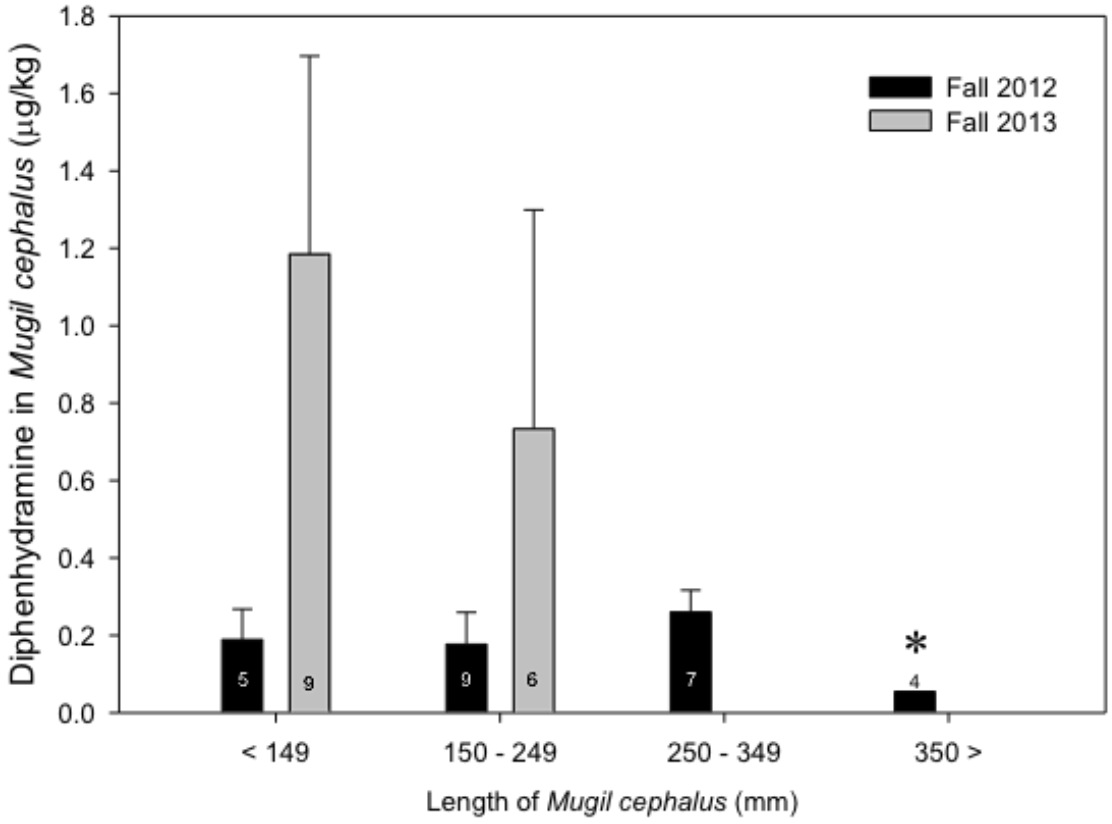

Figure 2.2. Mean (±SD) concentration of diphenhydramine across size classes of Mugil cephalus in Buffalo Bayou, Houston, Texas, USA, for two different sampling years. Numbers in bars represent n for each group. *: $p < 0.05$.

Observed DPH accumulation differences in fish may have been influenced by several factors, such as species movement, variable surface water diphenhydramine exposure, pH, salinity, and dietary exposure. Because bioaccumulation does not occur instantaneously (Arnot and Gobas 2006), the home range of this species must be considered. Movement *of M. cephalus* above and below the WWTP discharge likely

occurred during the current study due to foraging behavior. *M. cephalus* school and move within an estuary to feed on detritus and available food along the benthos (Whitfield, Panfili, and Durand 2012). Additionally, adult striped mullet leave estuaries and return to the open ocean to spawn (Ibanez and Benitez 2004). *M. cephalus* are considered adults when they are sexually mature enough to reproduce, which is typically greater than 250 mm (Amuer, Bayed, and Benazzou 2003).

In the present study, we examined a heavily influenced urban watershed and sampled surface waters downstream from a large (~200 MGD) discharge. Surface water concentrations of DPH and other contaminants may be expected to generally decrease with distance downstream from a WWTP discharge. As water moves away from the WWTP discharge through Buffalo Bayou toward Galveston Bay, it is increasingly diluted by more saline Bay water. For example, dilution was observed in DPH water concentrations a short distance between the effluent discharge (200 ng/L) and surface water (42 ng/L) sampled 50 m downstream in 2013 (Du, et al. 2016). However, exposure to DPH also occurs above this discharge due to tidal influence and other upstream effluent sources (Scott, et al. 2016). Surface water sampling efforts during the present study were not intended to characterize the range of exposure scenarios *M. cephalus* experience temporally and spatially across their life cycle. Decreased DPH levels observed in older fish may have resulted from more time spent away from effluent discharge.

DPH levels in striped mullet may also have been influenced by dietary exposure. During the larval phase *M. cephalus* are primarily planktonic feeders (Zismann, Berdugo, and Kimor 1975; Nash, Kuo, and McConnel 1974; Gisbert, Cardona, and Castello 1996), then begin to shift as juveniles (e.g., ~10-20 mm) to feed on small invertebrates and benthic

organisms (Whitfield, Panfili, and Durand 2012; Blaber and Whitfield 1977). As striped mullet increase in size they will feed more frequently on detritus and inorganic matter (sand) (Eggold and Motta 1992; Desilva and Wijeyaratne 1977). Though we did not examine potential DPH exposure from detritus, partitioning of DPH and other ionizable contaminants deserve additional study. For example, Al-Khazrijy and Boxall (2016) recently noted challenges associated with predicting sediment partitioning behavior of ionizable pharmaceuticals, which do not conform to equilibrium partitioning expectations for nonionizable organic contaminants.

A previous study observed $\delta^{15}N$ signatures of *M. cephalus* from Matagorda Bay, Texas, to increase with increasing fish size, which most likely resulted from ontogenetic dietary shifts with age (Akin and Winemiller 2006). Though ontogenetic dietary shifts have been studied in juvenile *M. cephalus* (1-100 mm; (Eggold and Motta 1992), ontogenetic dietary shifts from juveniles (100 to 300 mm) and adults (>300 mm) of this species are not well understood. In the present study, we employed stable isotopes ($\delta^{15}N$, $\delta^{13}C$) across various *M. cephalus* size classes, from juvenile to adult, to identify whether potential ontogenetic feeding shifts occurred in larger individuals (Table 2.1). In 2012 $\delta^{15}N$ significantly increased ($p < 0.05$) in larger striped mullet, which suggests a change in feeding and thus trophic position (Figure 2.3A). A similar relationship was not observed in 2013 (Figure 2.3B); however, *M. cephalus* in the largest adult classes, which were electrofished in 2012, were not encountered during collection efforts in the following sampling period (Table 2.1). Though such differences in $\delta^{15}N$ provide a reasonable surrogate for dietary uptake and assimilation, future studies examining ontogenetic feeding

shifts in mullet should confirm observations in the present study using stomach content analysis.

Ontogenetic dietary shifts, similar to those exhibited by the striped mullet, have received previous study for influencing bioaccumulation of nonionizable organic contaminants (e.g., PCBs) and mercury (Kraemer, Evans, and Dillon 2012; Szczebak and Taylor 2011). In the present study we observed significantly lower levels of DPH only in the highest size class during 2012 (Figure 2.2). Conversely, tissue concentrations of conventional nonionizable organic contaminants that do not experience appreciable biotransformation generally increase with age and trophic position. In addition, lengths and weights of fish in biomonitoring studies are typically reported as a range and then less regarded compared to tissue concentrations during studies of contaminant accumulation (Waltham, Teasdale, and Connolly 2013). Such a practice is often relevant when lipid normalization is employed for organic contaminants. However, as we previously identified with DPH and other ionizable weak bases, partitioning to fish does not solely occur by hydrophobic mechanisms, which is common for nonionizable organic contaminants (e.g., PCBs, dioxins, furans); thus, lipid normalization of weak bases in aquatic organisms is less relevant for bioaccumulation studies (Ramirez, et al. 2009).

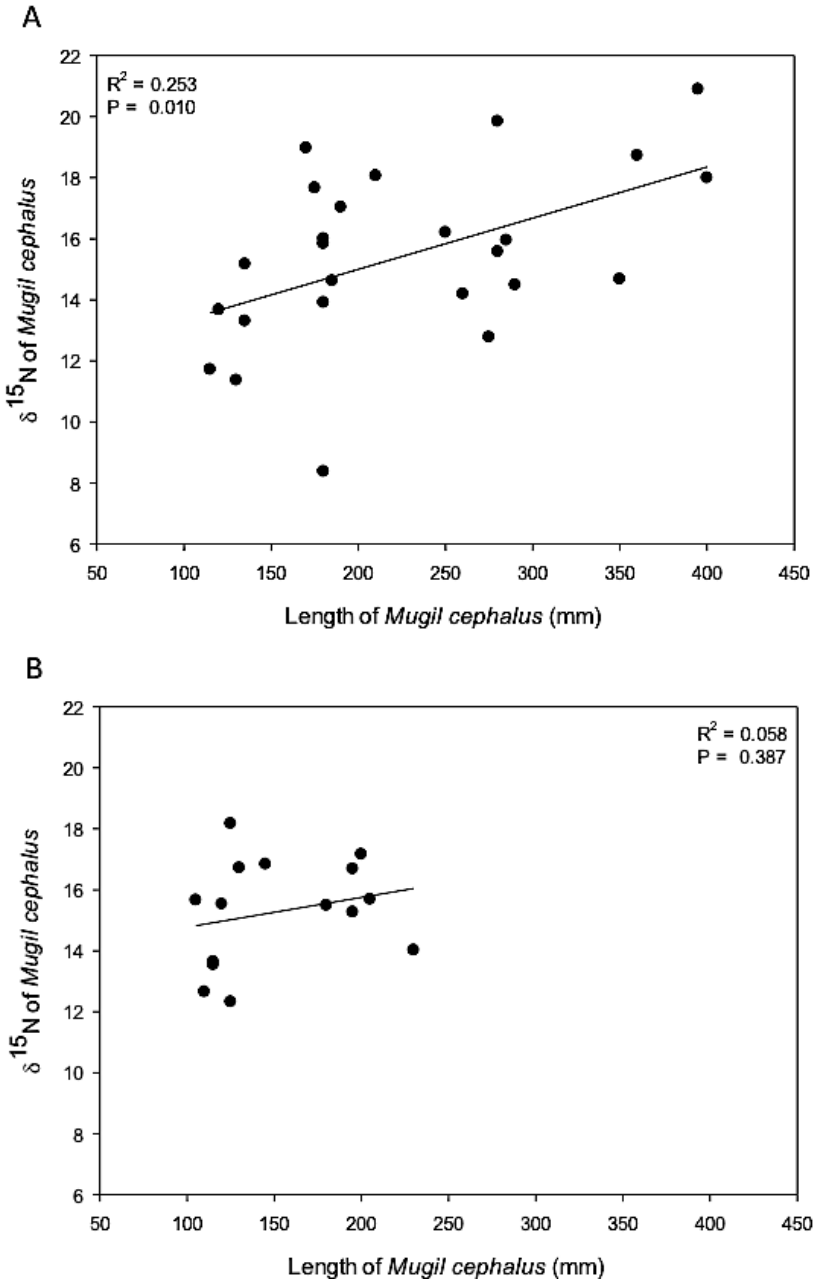

Figure 2.3. Relationship between δ15N and length (mm) in Mugil cephalus vs the length (mm) during two study years (A = 2012, B = 2013).

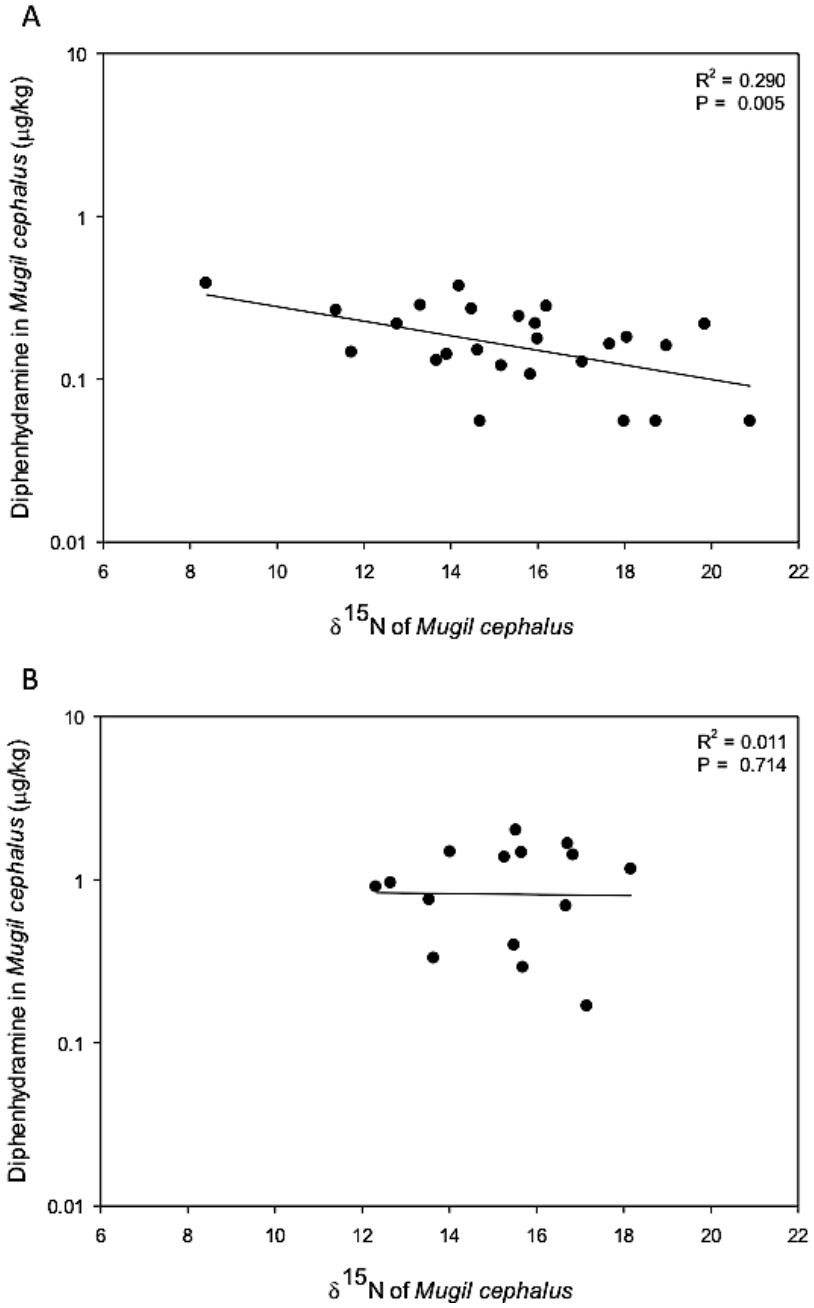

Figure 2.4. Relationship between δ15N and diphenhydramine (µg/kg) in Mugil cephalus during two study years (A = 2012, B = 2013).

The apparent volume of distribution, an important pharmacokinetic parameter, value for DPH of ~3-8 L/kg in humans is almost identical to fish (Nichols, et al. 2015). Though observations from the present study indicate that ontogenetic feeding shifts to higher trophic positions did not significantly increase DPH bioaccumulation by *M. cephalus* (Figure 2.4), future studies are needed to examine other ionizable organic contaminants in estuarine and marine organisms.

Bioconcentration of DPH by freshwater fish increases as pH approaches the pKa value, and uptake occurs rapidly with steady state conditions achieved within 24-96 hrs (Nichols, et al. 2015). In the present study, significantly higher tissue levels of DPH were observed in M. cephalus collected during 2013 compared to the previous year. Similarly, elevated surface water concentrations were observed in 2013 (42 ng/L) compared to 2012 (15 ng/L) (Table 2.1). It thus appears possible that increasing DPH levels in tissue correspondingly increased with increasing waterborne exposure. A similar relationship may exist between DPH in surface water and fish tissue from a recent study in Puget Sound, though DPH from grab samples of surface water were lower in the Puget Sound (0.96 – 1.5 ng/L) than the current study. Observations in the present study are in agreement with another recent study that identified DPH and several other ionizable weak bases do not exhibit trophic magnification in a municipal effluent-dependent freshwater system (Du, et al. 2014a). Thus, inhalational uptake, compared to diet, appears to be a more important route of exposure (Du, et al. 2014a). Comparative pharmacokinetic studies in estuarine and marine fish are lacking but necessary to understand bioaccumulation dynamics of these CECs and other ionizable contaminants.

Acknowledgements

The present study was supported in part by an institutional grant (NA10OAR4170099) to the Texas Sea Grant College Program from the National Sea Grant Office, National Oceanic and Atmospheric Administration, US Department of Commerce (to BWB and CKC). BWB received additional support as the Fulbright Canada Visiting Research Chair in Water and the Environment at the University of Lethbridge. We thank Dr. Ren Zhang, Dr. Kristin Connors, Lauren Kristofco, Bekah Burket, David Dreier, Catherine Sotelo, Maddie Baxter, Craig Calvert, and Valerie Toteu-Djomte for laboratory support.

CHAPTER THREE

Spatio-temporal Bioaccumulation and Trophic Transfer of Ionizable Pharmaceuticals in a Semi-arid Urban River Influenced by Snowmelt

This chapter published as: Haddad SP, Luek A, Corrales J, Scott WC, Saari GN, Burket SR, Kristofco LA, Rasmussen JB, Chambliss CK, Luers M, Rogers C, Brooks BW. 2018. Spatio-temporal assessment of bioaccumulation and trophic transfer of ionizable pharmaceuticals in a semi-arid stream influenced by snowmelt. *Journal of Hazardous Materials* 359: 231-240.

Abstract

Bioaccumulation of pharmaceuticals in aquatic organisms is increasingly reported in the peer-reviewed literature. However, seasonal instream dynamics including occurrence and bioaccumulation across trophic positions are rarely studied, particularly in semiarid streams with flows influenced by seasonal snowmelt and municipal effluent discharges. Thus, we selected East Canyon Creek in Park City, Utah, USA to examine spatio-temporal bioaccumulation of select ionizable pharmaceuticals across trophic positions using trophic magnification factors calculated at incremental distances (0.15, 1.4, 13 miles) downstream from a municipal effluent discharge during spring (May), Summer (August), and fall (October). Nine target analytes were detected in all species during all sampling events. Trophic dilution was consistently observed for amitriptyline, caffeine, diphenhydramine, diltiazem, fluoxetine, and sertraline, regardless of seasonal instream flows or distance from effluent discharge, where calculated TMFs ranged from 0.01-0.71. Negative slopes were observed for all 35 regressions, with significantly ($p<0.05$) negative slopes observed in 32 of the 35 regressions. Further, this study presents the first empirical study to investigate normalizing pharmaceutical concentrations to lipids, phospholipid or

protein fractions using pair matched samples from fish. Our results confirm that normalization of ionizable pharmaceuticals to neutral lipids, polar lipids, or the protein fraction is inappropriate and thus not recommended.

Introduction

Over the last 50 years the human population has grown from 2.5 to 6.8 billion worldwide, and is predicted to increase to 9.8 billion by 2050, with 66% of people residing in urban centers (Postel 2010; "United Nations, World Urbanization Prospects: The 2017 Revision, United Nations Population Division" 2017). Global industrialization has focused populations in urban areas including megacities (Rhind 2009; Bryan W. Brooks, et al. 2012) and increased fossil fuel consumption has led to altered weather patterns and elevated global temperatures (Postel 2010). Water resource management has thus become more complex in response to increased demand for already stressed aquatic resources, and diverse anthropogenic stressors (Postel 2010; Rhind 2009). For example, elevated global temperatures and altered weather patterns are decreasing snowpack, which is currently relied on by over 2 billion people annually for water resources and instream flows (Mankin, et al. 2015). Further, it is increasingly common for multiple urban centers to utilize common watersheds for water withdrawals and return flows of reclaimed water, leading to an urbanizing water cycle (Sowby 2014) that results in concentrated effluent discharge to receiving systems (Carey and Migliaccio 2009; Rice and Westerhoff 2017). Such discharges include diverse contaminants of emerging concern (CECs), including active pharmaceutical ingredients (APIs).

With ~3000 APIs currently administered in Europe, the United States, and Asia, studies have increasingly examined bioaccumulation, hazards and risks to aquatic

organisms (Rice and Westerhoff 2017; Xie, et al. 2015). Because APIs and their metabolites are designed to be biologically active molecules (Ebele, Abou-Elwafa Abdallah, and Harrad 2017) and have conserved targets across vertebrates, a range of sub-lethal responses and adverse outcomes in aquatic organisms can be linked to therapeutic activity at sufficient internal concentrations (Gunnarsson, et al. 2008; Brodin, et al. 2014; Brooks 2014). Pharmaceuticals were historically considered to be less likely than legacy persistent organic contaminants to bioaccumulate in aquatic systems due to greater water solubility routine detection at ng/L to μg/L levels in developed countries (Bryan W. Brooks, et al. 2012; Daughton and Brooks 2011b). However, during dry months, particularly in arid and semi-arid regions, base flows of urban rivers and streams can be effluent dominated or even dependent, resulting in increased effective exposure durations of APIs to aquatic life (Ankley, et al. 2007). Effluent influenced urban ecosystems can represent worst-case scenarios for potential accumulation and effects of APIs and other consumer chemicals in surface waters (Rice and Westerhoff 2017; Brooks, Riley, and Taylor 2006). Thus, identifying conditions where APIs pose higher risks to aquatic wildlife and understanding the bioaccumulation potential, exposure pathways, and trophic transfer of APIs in ecosystems was recently identified as major research needs to define ecological risks (Boxall, et al. 2012a; Brooks 2014; Rudd, et al. 2014) and ensure sustainable environmental management and ecosystem services (Brooks 2014; Burkhard, et al. 2013; Walters, et al. 2016).

Trophic magnification represents a particularly important aspect of bioaccumulation studies because dietary exposure can result in increasing concentrations of a contaminant with increasing trophic position, and ultimately present risks of adverse

outcomes to aquatic and terrestrial wildlife and humans (Borga, et al. 2012). The extent of trophic magnification in an ecosystem can be quantified using trophic magnification factors (TMFs), defined as an empirical relationship of contaminant concentration with trophic positions (Borga, et al. 2012; McLeod, et al. 2015; Burkhard, et al. 2013; Walters, et al. 2016). High quality field based TMF studies are proposed as highly relevant to assess and identify bioaccumulative substances because such studies possess all relevant routes of exposure and ecological processes that may influence bioaccumulation (Kim, et al. 2016; Walters, et al. 2016; Borga, et al. 2012). To date TMF studies have mainly been calculated for nonionizable chemicals (Walters, et al. 2016; Mackay, et al. 2016) and TMF studies investigating APIs have mainly occurred in laboratory experiments (Bostrom, et al. 2017; Ding, et al. 2015b; Ding, et al. 2015a; Heynen, et al. 2016; Lagesson, et al. 2016; Orias, Simon, and Perrodin 2015; Ruhi, et al. 2016), while field studies investigating trophic transfer of ionizable APIs in aquatic ecosystems are scarce (Xie, et al. 2017; Du, et al. 2014a; Xie, et al. 2015). The first TMF study performed on APIs was in the North Bosque River, a semi-arid effluent dominated stream located in Texas, USA, which observed trophic dilution (TMF <1.0) as opposed to trophic magnification (TMF >1.0) for two pharmaceuticals, diphenhydramine and carbamazepine (Du, et al. 2014a). Later studies in Lake Taihu, China identified trophic dilution for eight additional pharmaceuticals (Xie, et al. 2015; Xie, et al. 2017). However, clearly many questions still remain in regards to trophic transfer of APIs and warrant additional investigation. For instance, when deriving a field TMF a typical assumption is that exposure and ecosystem conditions are ubiquitous for all organism, downplaying the importance of sampling location. This assumption ignores non-uniform patterns in exposure concentrations, which have been shown to

significantly affect the calculation of TMFs, at different sampling sites even when such gradients are expected to exist, especially for APIs, due to point source discharges such as waste water treatment plants (Borga, et al. 2012; Kim, et al. 2016). Additionally, TMFs have mainly been calculated for hydrophobic chemicals requiring fugacity normalization (lipid)(Mackay, et al. 2016), which was recently identified as inappropriate for quantify APIs in fish (Bostrom, et al. 2017; Ramirez, et al. 2009). Though normalization to the protein or phospholipid fraction may be appropriate because a majority of APIs bind plasma proteins and phospholipids within organisms (Armitage, et al. 2017).

Here, we examined the spatial and temporal exposure, bioaccumulation, and trophic transfer of APIs in multiple trophic positions from a semi-arid river, East Canyon Creek, Utah, USA. In this dynamic system, instream flow fluctuates due to seasonal snow melt and continuous effluent discharge. Target pharmaceuticals were quantified in water and biota samples from East Canyon Creek collected during spring, summer, and fall sampling events at an upstream reference site and incremental distances downstream from an effluent discharge. To examine the influence of pharmaceutical partitioning on bioaccumulation in brown trout (*Salmo trutta)* the octanol-water distribution coefficient *(D_{ow})*, membrane-water distribution coefficient (D_{mw}), albumin-water distribution coefficient (D_{BSAw}), and muscle protein-water distribution coefficient (D_{mpw}) were calculated and regressed against calculated BAFs. Total lipids, neutral (storage) lipids, polar (phospholipids) lipids, and protein content were determined in paired fish samples to examine whether fugacity normalization of ionizable APIs to protein or phospholipids was appropriate. Finally, stable isotopes $\delta^{15}N$ and $\delta^{13}C$ were measured to map functional food chains and identify trophic positions of sampled stream biota, and TMFs were calculated

at each site downstream from a municipal effluent discharge during three seasons to examine whether spatial and temporal differences influenced trophic transfer of APIs.

Methods and Materials

Study Site

The East Canyon Creek watershed is located east of Salt Lake City, Utah, USA, spread over the western stretch of Summit and Morgan Counties (Figure 3.1). The East Canyon Water Reclamation Facility (ECWRF) discharges to East Canyon Creek near Park City, Utah. ECWRF has a design capacity of 4.0 million gallons/day (MGD) with a mean daily load of ~3 MGD. East Canyon Creek is located in the semi-arid mountainous region of Utah and receives ~60% of annual precipitation during the winter. As a result, stream discharges in East Canyon Creek are elevated due to snowmelt during spring and early summer months.

Field Sampling

Samples from East Canyon Creek were collected during spring (4-7 May), summer (17-21 August), and fall (27-31 October) of 2014. Sampling dates encompassed high flow conditions from snow melt (spring) and lower flow semi-arid condition later in the year (summer and fall). Collection occurred at an upstream reference site, previously investigated by our research team (Du, et al. 2012), and at incremental distances downstream (0.15, 1.4, 13 miles) from the ECWRF discharge (Figure 3.1). Traditional water quality parameters and nutrients were measured for each sampling event. pH, specific conductance, DO, and temperature were measured with calibrated multi-parameter

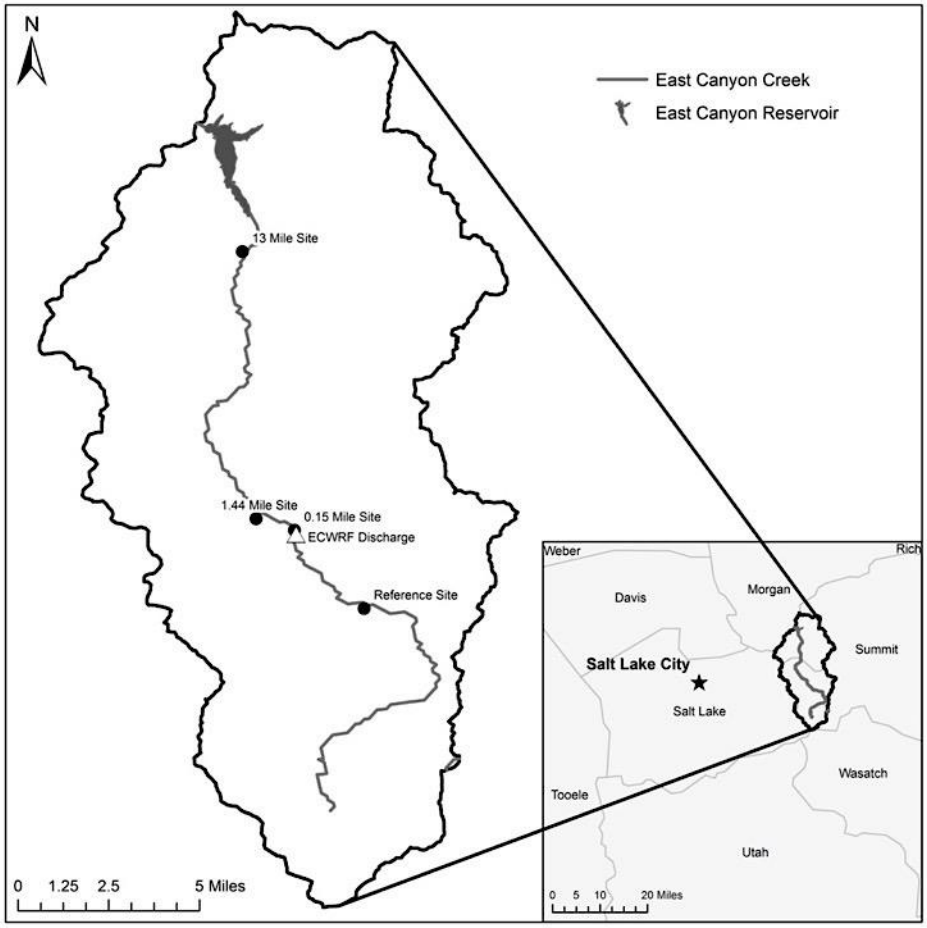

Figure 3.1. A map of the East Canyon Creek watershed in Park City, Utah, USA, showing sampling locations relative to the East Canyon Water Reclamation Facility discharge.

datasondes (YSI 600 XLM, 6920, YSI Instruments, Yellow Springs, OH, USA) at each downstream study site for ~24 hours. Data were collected at 15-minute intervals. Datasondes were calibrated at room temperature within 24 hours prior to data collection, and then rechecked after deployment (TCEQ 2007; TCEQ 2008). Post-calibration checks following data collection were completed using error limits for pH, dissolved oxygen, specific conductance, and temperature of 0.5 standard units, ±5% error at saturation, ±5% in µS/cm, and ±1 °C, respectively (TCEQ 2007; TCEQ 2008). Water samples for total nitrogen, total phosphorus, dissolved nitrogen, and orthophosphate were collected from

each site and the effluent discharge. Total N concentrations were determined using sulfanilamide method on persulfate digested samples (EPA 353.2). Total P concentrations were determined using the molybdate-blue method on persulfate digested samples (EPA 365.1). Nitrogen and phosphorous concentrations were measured colorimetrically using a Lachat Quickchem 8500 Flow Injection Autoanalyzer (Loveland, CO, USA). Discharge measurements were available from the U.S. Geological Survey for two gaging stations located in East Canyon Creek. Stations #10133800 and #10133980 located approximately 0.15 and 13 miles downstream from the ECWRF discharge; thus, water and biological sampling sites were located adjacent to these gaging stations. A unique geological barrier exists between the upstream site and the ECWRF discharge that allows organisms to move downstream but not back upstream ensuring that organisms sampled from the upstream site had not been influenced by the ECWRF discharge.

Duplicate water samples for targeted APIs were collected using acetone cleaned 4 L amber glass bottles at each sampling site and from the ECWRF discharge during each sampling event. Utah Department of Natural Resources (UDNR) protocols were followed for backpack electroshock collection of two common fish species, the brown trout (*Salmo trutta*) and mottled sculpin (*Cottus bairdii*). Fish length and weight were measured on site immediately after anesthetization using MS-222. Periphyton was collected by scrapping a 2 x 2 inch cross section of rocks found at each sampling site. We specifically collected and sorted macroinvertebrates including mayflies (*Ephemerella sp.*), crane fly *(Tipula sp.)*, snails (*Lymnaeidea* & *Physidae)*, and caddis fly (Trichopterans: *Helicopsyche sp*. & *Hydropsyche sp*.) using standard kick net techniques.

Chemicals and Analytical Standards

All chemicals and their corresponding isotopically-labeled analogs were obtained with various vendors. Acetaminophen (ACE), acetaminophen-*d*4, amitriptyline (AMI), amitriptyline-*d*3, aripiprazole (ARI), aripiprazole-*d*8, benzoylecgonine (BEN), benzoylecgonine -*d*3, buprenorphine (BUP), buprenorphine-*d*4, caffeine (CAF), carbamazepine (CAR), carbamazepine-*d*10, diclofenac (DIC), diltiazem (DIL), diphenhydramine (DIP), diphenhydramine-*d*3, duloxetine (DUL), duloxetine-*d*3, fluoxetine (FLU), fluoxetine-*d*6, methylphenidate (MPH), methylphenidate-*d*9, norfluoxetine (NOR), norfluoxetine-*d*6, , promethazine (PROM), promethazine-*d*3, and sertraline (SER) were purchased as certified analytical standards from Cerilliant (Round Rock, TX, USA). Amlodipine (AML), amlodipine-*d*4, caffeine-*d*9, desmethylsertraline (DES), desmethylsertraline-*d*4, diclofenac-*d*4, diltiazem-*d*3, and sertraline-*d*3 were purchased from Toronto Research Chemicals (Toronto, Ontario, Canada). Sucralose (SUC) was purchased from Sigma-Aldrich (St. Louis, MO, USA) and sucralose-*d*6 was purchased from Santa Cruz Biotechnology (Santa Cruz, CA, USA). All chemicals were reagent grade and used as received. HPLC grade methanol (MeOH), methyl tert-butyl ether (MTBE), and chloroform were obtained from Fisher Scientific (Fair Lawn, NJ, USA), formic acid was purchased from VWR Scientific (Radnor, PA, USA), and a Thermo Barnstead™ Nanopure™ (Dubuque, IA, USA) Diamond UV water purification system was used throughout sample analysis to provide 18 MΩ water.

Sample Preparation

Water samples were filtered and concentrated to solid phase extraction (SPE) cartridges following previously reported methods (Du, et al. 2014b; Lajeunesse, Gagnon,

and Sauve 2008; Vanderford and Snyder 2006; Bean, et al. 2018). Described briefly samples were filtered through three different sized filters to remove particulate: a glass fiber prefilter (1.0-μm pore size, 47 mm, Pall Corporation, Port Washington, NY, USA), a nitrocellulose filter (0.45-μm pore size, 47 mm, GE Healthcare, Little Chalfont, BUX, UK), and a Nylaflo™ filter (0.2-μm pore size, 47 mm, Pall Corporation, Port Washington, NY, USA). 2 L were separated into 2 – 1 L volumetric flasks for extraction with an Oasis HLB (6 cc, 200 mg, Waters Corporation, Milford, MA, USA) cartridge and a Strata SCX (6 cc, 500 mg, Phenomenex, Torrance, CA, USA) cartridge. 50 μL of prepared 2000 (ng mL^{-1}) internal standard was spiked into each sample. Strata SCX samples were then spiked with an additional 100 μL of 85 % phosphoric acid and 5 mL of MeOH. Oasis HLB cartridges were pretreated with 5 mL MTBE, 5 mL MeOH, and 5 mL nanopure water respectively. Strata SCX cartridges were pretreated with 5 mL MEOH and 5 mL nanopure water respectively. Samples were extracted via a 24 port Visiprep™ vacuum manifold (Supelco Inc., Bellefonte, PA, USA) with a flow rate of approximately 10 ml/min. Oasis HLB cartridges were eluted with 5 mL MeOH and 5 mL 10:90 (v v^{-1}) MeOH:MTBE. Strata SCX cartridges were first washed with 5 mL of aqueous 0.1% HCl solution, then eluted with 5 mL MeOH and 6 mL 5:95 (v v^{-1}) NH_4OH:MeOH. Eluates were blown to dryness under a gentle stream of nitrogen in a Turbovap (Zynmark, Hopkinton, MA, USA) set to 45°C, then reconstituted to 1 mL with 5:95 (v v^{-1}) MeOH:aqueous 0.1% formic acid.

Tissue samples were extracted following previously reported methods (Du, et al. 2014a; Du, et al. 2015; Du, et al. 2016; Ramirez, et al. 2007) with some modification. Briefly, whole body homogenates were prepared for fish samples. Periphyton and macro invertebrates were pooled into larger ~1g sample composites and homogenized. Then 1g

w/w of all samples were separated and placed in a 20 mL borosilicate glass vial (Wheaton; VWR Scientific, Rockwood, TN, USA). Next, 50 μL of 2000 μg/L ISS was spiked in each sample. Then 4 mL of MeOH and 4mL of aqueous 0.1 M acetic acid (pH 4.0) were added to the sample vials. Vials were inverted by hand for 30 seconds to mix the contents prior to placement on a rotating table at 15 rpm for 25 minutes. After mixing, samples were centrifuged at 7500 rpm for 45 minutes. Following centrifugation, supernatant was collected and blown to dryness under a gentle stream of nitrogen in a Turbovap (Zynmark, Hopkinton, MA, USA) set to 45°C, then reconstituted to 1 mL with 5:95 (v v^{-1}) MeOH:aqueous 0.1% formic acid.

All reconstituted samples were syringe filtered using a BD 1 mL TB syringe (BD, Franklin Lakes, NJ, USA) and Acrodisc® hydrophobic Teflon Supor membrane syringe filters (13-mm diameter; 0.2-μm pore size, Pall Corporation, Port Washington, NY, USA) and placed in 2 mL analytical vials (Agilent Technologies, Santa Clara, CA, USA) for analysis.

Instrumental Analysis

Samples were analyzed using isotope-dilution liquid chromatography-tandem mass spectrometry (LC-MS/MS) with an Agilent Infinity 1260 autosampler/quaternary pumping system, Agilent jet stream thermal gradient electrospray ionization source (ESI), and model 6420 triple quadrupole mass analyzer (Agilent Technologies, Santa Clara, CA, USA). A binary gradient method consisting of aqueous 0.1 % formic acid as solvent A, and MeOH as solvent B, was used. Separation was performed using a 10 cm × 2.1 mm Poroshell 120 SB-AQ column (120Å, 2.7 μm, Agilent Technologies, Santa Clara, CA, USA) preceded by a 5 mm × 2.1 mm Poroshell 120 SB-C18 attachable guard column

(120Å, 2.7 μm, Agilent Technologies, Santa Clara, CA, USA). The flow rate was held constant at 0.5 mL/min with a column temperature maintained at 60 °C. The injection volume was 10 μL. Cycle time was adjusted to 500 ms for acquisition of data. Multiple reaction monitoring (MRM) transitions for target analytes and associated instrument parameters can be found elsewhere (Bean, et al. 2018).

Quantitation was performed using an isotope dilution calibration method. Calibration standards, containing mixture of internal standards and variable concentrations of target compounds, were prepared in 95:5 0.1% (v v^{-1}) aqueous formic acid–methanol. The linear range for each analyte (0.1 – 500 ng mL^{-1}) was confirmed from plots of sensitivity (i.e., response factor; RF) versus analyte concentration. Our criterion for linearity required that the relative standard deviation of RFs for standards spanning the noted range was ≤ 15%. Internal standard calibration curves were constructed for each analyte using eight standards that were within the corresponding linear range. Calibration data were fit to a linear regression, and correlation coefficients (r^2) for all analytes were ≥ 0.995. Quality assurance and quality control measures included running a continued calibration verification (CCV) sample every five samples to check calibration validity during the run. A criterion of ± 20% of CCV concentration was held to be acceptable for all analytes. One blank (i.e., reference water with internal standards only), one field blank, and duplicate matrix spikes were included in each analytical sample batch. Method detection limits (MDLs) represented the lowest concentration of an analyte reported with 99% confidence that the concentration is different from zero in a given matrix. The EPA guideline (40 CFR Part 136, Appendix B) for generating method detection limits was followed to generate MDLs in water, periphyton, invertebrates, and fish (Table 3.1). In the

present study <MDL is defined as analytes that were detected in the matrices, but below corresponding MDLs.

Table 3.1. Limit of Detection (LOD), Limit of Quantitation (LOQ), Solid Phase Extraction (SPE) cartridge, and Method Detection Limits (MDLs) for target analytes in whole body fish homogenates, periphyton, and invertebrates.

Analyte	LOD	LOQ	SPE	MDLs			
				Water (ng/L)	Fish (µg/kg)	Periphyton (µg/kg)	Invertebrates (µg/kg)
Acetaminophen	0.02	0.07	HLB	3.47	2.84	1.82	2.33
Amitriptyline	0.01	0.04	SCX	5.30	0.99	1.49	1.66
Amlodipine	0.04	0.13	SCX	12.03	2.11	1.76	1.78
Aripiprazole	0.04	0.14	SCX	2.21	2.28	NA	1.41
Benzoylmethylecgonine	0.02	0.07	SCX	0.05	0.10	0.07	0.08
Buprenorphine	0.01	0.03	SCX	6.35	2.27	1.88	4.10
Caffeine	0.05	0.18	HLB	4.43	1.69	1.89	1.33
Carbamazepine	0.10	0.33	HLB	0.27	0.16	0.19	0.18
Desmethylsertraline	NA	NA	SCX	7.16	2.19	1.77	1.72
Diclofenac	0.04	0.12	HLB	4.74	2.31	2.30	2.13
Diltiazem	0.01	0.03	HLB	0.31	0.06	0.10	0.11
Diphenhydramine	0.01	0.03	SCX	0.11	0.13	0.24	0.05
Duloxetine	0.03	0.10	SCX	6.79	2.36	2.52	2.60
Fluoxetine	0.01	0.02	SCX	2.39	0.85	0.76	0.85
Methylphenidate	0.02	0.07	SCX	0.14	0.06	0.08	0.08
Norfluoxetine	0.02	0.07	SCX	1.77	0.99	1.23	1.02
Promethazine	0.00	0.01	HLB	9.65	2.60	1.68	1.44
Sertraline	0.02	0.06	SCX	1.52	0.99	2.22	1.28
Sucralose	0.66	2.19	HLB	2.62	2.91	NA	NA

Bioconcentration Factors (BCFs) and Bioaccumulation Factors (BAFs)

BCFs for periphyton BAFs for all other organisms are defined as the ratio of target analyte detected in biota and associated water concentration. Periphyton do not ingest food, therefore BCFs are calculated to reflect only exposure from ambient water concentrations as opposed to higher organism where BAFs are used to account for respiratory and dietary exposure routes (Arnot and Gobas 2006).

$$BCF_{periphyton} = C_{periphyton}/C_{water}$$

$$BAF_{biota} = C_{biota}/C_{water}$$

where C_{biota} and $C_{periphyton}$ are the measured concentration of a contaminant in the organism, and C_{water} is the measured concentration of the contaminant in the water column. If target analytes were not detected or detected <MDL in water, but were detected in biota, half MDL values of the water concentration were used to calculate BCFs and BAFs. If target analytes detected in biota were <MDL, half MDL values were used to calculate BCFs and BAFs.

Stable Isotope Analysis

Stable isotopes, $\delta^{15}N$ and $\delta^{13}C$, were determined with a dual-inlet gas-source Stable Isotope Mass Spectrometer (Thermo-Electron, Waltham, MA, USA) and an Elemental Analyzer (Costech, Valencia, CA, USA) at the Stable Isotopes Core Laboratory at Baylor University. Data were calibrated with USGS isotopic reference materials, USGS40 and USGS41. Analytical precision was ±0.2%. Isotopic ratios in delta notation were calculated using the following equation:

$$\delta X\ (‰) = (R_{sample}/R_{standard} - 1) \times 1000$$

where X represents the heavier isotope, R_{sample} represents the ratio of heavy to light isotope in the analyzed sample, and $R_{standard}$ represents the ratio of heavy to light isotope in the standards (Jardine, Kidd, and Fisk 2006).

2.4 Trophic Transfer of Pharmaceuticals

Trophic position (TP) was determined as (Borga, et al. 2012):

$$TP_{sample} = ((\delta^{15}N_{sample} - \delta^{15}N_{baseline}) / \Delta^{15}N) + 2$$

where TP_{sample} and $\delta^{15}N_{sample}$ represent the TP and stable isotope abundance, respectively, of an organism. $\delta^{15}N_{baselione}$ represents the baseline $\delta^{15}N$ of the trophic structure. $\Delta^{15}N$ represents the nitrogen-enrichment factor; an enrichment factor of 3.4‰ was chosen for the current study. Trophic transfer was examined by calculating TMFs (Eq. 3) using the slope (b) of Eq. 2 derived from the log transformed contaminant level and TP of biota (Borga, et al. 2012):

$$\log[\text{contaminant}] = b(TP) + a$$

$$TMF = 10^{b}$$

Total Lipid, Neutral Lipid, and Polar Lipid Determination

Total lipid content was measured by gravimetric methods performed on whole-body homogenates of *Salmo trutta* (~1 g) using a modified version of the Bligh and Dyer method (Bligh and Dyer 1959; Drouillard, Hagen, and Haffner 2004). Briefly, 1 g (wet weight) of homogenate was lyophilized for 72 hours to determine water content. The remaining tissue (~200 mg dry weight) was combined with 10 mL of 1:1 chloroform:methanol in a 20 mL borosilicate vial. Subsequently, the samples were placed on a rotatory extractor in an incubator (35°C) for 24 hours at 85 rpm to gently mix samples with end over end rotation. 5 mL of nanopure water was then added to each vial and shaken by hand vigorous to mix the organic and aqueous phase. Samples were then allowed to settle and separate back into aqueous and organic phase. The organic phase (chloroform on the bottom) was removed carefully with a pasture pipette and placed into a preweighed 20 mL test tube. 10 mL of chloroform was then added to each sample and hand shaken to mix the phases. After phase separation, the organic layer was removed and combined with the first extract. extracts were blown to dryness under a gentle stream of nitrogen in a

Turbovap (Zynmark, Hopkinton, MA, USA) set to 65°C. Residues were dried to a constant weight in an over at 40°C for 24 hours. Percent lipid content was calculated by dividing the weight of the residue in the test tube by the wet weight of the sample prior to extraction.

Crude residues were further fractionated into polar (phospholipids) and neutral (storage) lipid fractions using a previously published protocol (Juaneda and Rocquelin 1985). Briefly, crude lipid extracts were suspended in 500 µL of chloroform then loaded to a dry Sep-pak Silica (6 cc, 500 mg, Waters Corporation, Milford, MA, USA) SPE cartridge. After adsorption of the sample to the SPE, 20 mL of chloroform was allowed to gravity drip through the SPE to extract the neutral lipid fraction into a preweighed 20 mL test tube. The polar lipid fraction was then extracted by allowing 20 mL of methanol to gravity drip into a second preweighed 20 mL test tube. Extracts were dried to a constant weight in a vented oven at 70°C for 24 hours. Percent polar and neutral lipid content was calculated by dividing the weight of the residue in the test tube by the wet weight of the sample prior to total lipid extraction.

Total Protein Determination

Total protein was determined on whole-body homogenates of *Salmo trutta*. Homogenate samples were thawed and kept on ice to weigh out a 150 mg ± 15 tissue aliquot. Each sample was homogenized in 1 mL MES buffer and 10 µl Halt™ Protease Inhibitor Cocktail (Thermo Scientific, Rockford, IL). Samples were centrifuged at 12,000 x *g* for 10 min at 4°C. The supernatant was used to determine the total protein concentration using the Bradford protein assay (Bradford 1976). Finally, protein concentrations from the assay were normalized to tissue weight and used to calculate percent protein content of each sample.

Estimation of D_{ow}, D_{mw}, D_{mpw}, and D_{BSAw}

Estimated values of the acid dissociation constant (pK_a) and the octanol-water partitioning coefficient (K_{ow}) were obtained from SCIfinder. D_{ow} values were estimated following the methods from Armitage et al. (Armitage, et al. 2013):

$$\text{Log } K_{ow(ion)} = \text{Log } K_{ow(neutral)} - \Delta_{ow}$$

$$\text{Log } D_{ow} \text{ (pH 7.99-8.28)} = \text{Log}(f_{nuetral} \cdot K_{ow(neutral)} + f_{ion} \cdot K_{ow(ion)})$$

$$f_{nuetral} = 1/1+10^{(pKa-pH)}$$

$$f_{ion} = 1- f_{nuetral}$$

where Δ_{ow} was assumed to be 3.5 log units lower than the neutral species (Trapp and Horobin 2005), f_{ion} and $f_{nuetral}$ are the fractions of ionized form and neutral form of the chemical respectively as predicted by the Henderson-Hasselbalch equation based on measured pH at each site during each season (Table 3.2). D_{mw} was determined following the method by Droge et al. (Droge, et al. 2017):

$$\text{Log } K_{mw(neutral)} = 1.01 \cdot \text{Log } K_{ow} + 0.12 \text{ (Endo et al. (Endo, Escher, and Goss 2011))}$$

$$\text{Log } K_{mw(ion)} = \text{Log } K_{mw(neutral)} - \Delta_{mw}$$

$$\text{Log } D_{mw} \text{ (pH 7.99-8.28)} = \text{Log}(f_{nuetral} \cdot K_{mw(neutral)} + f_{ion} \cdot K_{mw(ion)})$$

where Δ_{mw} = -1.4 for 1˚ polar amines, -0.57 for 2˚ polar amines, and 0.35 for 3˚ polar amines. D_{BSAw} (pH 7.4) and D_{mpw} (pH 7.0) were estimated following the methods from Henneberger et al. (Henneberger, Goss, and Endo 2016b; Henneberger, Goss, and Endo 2016a) with polyparameter linear free energy relationships (PP-LFER) models.

Table 3.2. Physiochemical properties and estimated distribution coefficients of select pharmaceuticals.

Analyte	Fraction ionized at pH 7.99-8.28 (%)	Pk_a	Log $K_{ow(nuetral)}$	Log D_{ow} (pH 7.99-8.28)	Log D_{mw} (pH 7.99-8.28)	Log D_{mpw} (pH 7.0)	Log D_{BSAw} (pH 7.4)
Diphenhydramine	75.1-85.5	8.76	3.27	2.43-2.67	3.14-3.19	1.27	0.98
Diltiazem	82.0-89.9	8.94	4.70	3.70-3.95	4.57-4.60	1.00	-0.03
Norfluoxetine	85.5-92.0	9.05	3.70	2.60-2.86	5.19-5.22	1.44	1.64
Amitriptyline	92.9-96.2	9.40	4.95	3.52-3.80	4.79-4.81	2.17	1.66
Fluoxetine	98.5-99.2	10.10	4.57	2.46-2.74	5.30	2.18	2.37
Sertraline	93.9-96.8	9.47	5.08	3.59-3.86	5.80-5.81	2.58	2.43

Table 3.3. Substance descriptors used to estimate D_{BSAw} and D_{mpw}.

Analyte	E	S	A	B	V	E_i	S_i	A_i	B_i	V_i	J_i^+	J_i^-	Na_i
Diphenhydramine	1.31	1.11	0.00	1.22	2.19	1.16	3.94	1.46	0.00	2.21	2.24	0.00	1
Diltiazem	2.66	2.14	0.00	2.22	3.14	2.51	6.85	2.51	0.00	3.16	3.91	0.00	1
Norfluoxetine	1.23	1.27	0.17	1.11	2.10	1.08	3.75	2.38	0.00	2.12	1.53	0.00	3
Amitriptyline	1.92	1.42	0.00	1.08	2.40	1.77	3.75	1.70	0.00	2.42	2.45	0.00	1
Fluoxetine	1.00	1.30	0.10	0.93	2.24	0.85	3.33	2.18	0.00	2.26	1.26	0.00	2
Sertraline	1.83	1.50	0.10	0.82	2.27	1.68	3.16	2.18	0.00	2.29	1.81	0.00	2

Neutral species descriptors (E, S, A, B, V) was taken from the UFZ-LSER database (Ulrich, et al. 2017). Where, E is excess molar refraction, S is polarizability parameter, A is the H bond donor properties, B is the H-bond acceptor properties, and V is the molar volume. Ionic species (E_i, S_i, A_i, B_i, V_i, J_i^+, J_i^-) were subsequently calculated using the empirical equations from Abraham et al. (Abraham and Acree 2010) (Table 3.3). Ionic species were then inserted into the following models to predict distribution coefficients (Henneberger, Goss, and Endo 2016b; Henneberger, Goss, and Endo 2016a):

$$\text{Log } D_{BSAw} = 0.85 + 0.63E_i - 0.63S_i - 0.05A_i - 2.08B_i + 2.06V_i - 1.16J_i^+ + 3.13J_i^-$$

$$\text{Log } D_{mpw} = -0.237 + 0.675E_i - 0.764S_i - 0.196A_i - 2.285B_i + 2.511V_i - 0.682J_i^+ + 2.89J_i^-$$

Data Analysis

Statistical analyses were performed using SigmaPlot 13 by Systat Software (San Jose, CA, USA), the statistical package PAST3 (Hammer, Harper, and Ryan 2001), and the programming language R (R Core Team 2013), with an alpha of 0.05. Spatial and temporal bioaccumulation of individual pharmaceuticals in *Salmo trutta, Cottus bairdii,* Trichoptera, and periphyton were examined using a two-way ANOVA (location, season were experimental factors) of detected target analyte concentrations, with a post-hoc pair-wise analysis (Holm-Sidek method). Spatial and temporal accumulation of target analytes in *Salmo trutta, Cottus bairdii,* Trichoptera, and periphyton were visualized with non-metric multidimensional scaling (NMDS) ordinations constructed in unconstrained space using the Bray-Curtis dissimilarity measure in the R package vegan (Oksanen, et al. 2017) and plotted using the package ggplot2 (Wickham 2016). Observed patterns in multivariate space were tested for significance by performing a one-way randomized/permutation analysis of variance (PERMANOVA; location or season were experimental factors; permutation N = 9999) (Anderson 2001) with post-hoc pair-wise analysis (Holm-Bonferroni method) using Bray-Curtis dissimilarity. Species-specific accumulation was investigated using box plots of calculated BAFs and BCFs with a one-way PERMANOVA (permutation N = 9999) using Bray-Curtis dissimilarity and a post-hoc pair-wise analysis (Holm-Bonferroni method) to test for significant differences between species. Influence of pharmaceutical physicochemical properties on bioaccumulation in *Salmo trutta* was examined by regressing the partitioning coefficients D_{ow}, D_{mw}, D_{mpw}, and D_{BSAw} against calculated BAFs. Regression analyses relating protein, total lipids, neutral lipids, and polar lipids to concentrations of target analytes were performed.

Results

Stream Characterization and Traditional Water Quality Parameters

During 2014, Park City, UT received 32% less average rainfall and 74% less average snowfall than normal, resulting in lower than average instream flows in East Canyon Creek. Water quality parameters (Table 3.4) and measured concentrations of nutrients (Table 3.5) were determined for all sampling events. Water temperature was highest ($p<0.05$) in summer (14.67-24.06 ºC), followed by spring (7.83-12.58 ºC), and the lowest in fall (3.21-12.24 ºC). Dissolved oxygen and pH were lower ($p<0.05$) in the summer compared to spring and fall. Phosphate levels were highest ($p<0.05$) during spring, and decreased with each subsequent sampling in summer, then fall. Ammonia concentrations were highest ($p<0.05$) in fall, followed by spring and summer.

Table 3.4. Temperature, specific conductivity, dissolved oxygen (DO), and pH at sites downstream (0.15 miles, 1.4 miles, 13 miles) of the ECWRF discharge during three sampling seasons in 2014.

		Temperature (°C)			Sp. Cond. (mS/cm °C)			DO (mg/L)			pH		
Season	Site (mi)	Mean	Min	Max	Mean	Min	Max	Mean	Min	Max	Median	Min	Max
Spring	0.15	9.93	7.83	12.13	0.7	0.67	0.77	9.18	7.9	11.3	8.16	7.9	8.53
	1.4	-	-	-	-	-	-	-	-	-	-	-	-
	13	10.1	7.89	12.58	0.71	0.69	0.75	11.54	10.5	13.5	8.23	8.17	8.47
Summer	0.15	21.83	20.03	24.06	0.45	0.45	0.46	9.38	8.56	10.08	8.07	7.87	8.37
	1.4	17.35	14.67	23.53	0.86	0.8	0.93	10.57	7.59	15	8.14	7.85	8.87
	13	18.29	15.52	23.66	1.45	1.09	1.61	8.8	6.12	12.99	8.03	7.71	8.64
Fall	0.15	7.73	3.21	12.17	1.1	1.06	1.18	11.56	8.49	15.18	8.06	7.93	8.44
	1.4	7.66	3.27	12.09	1.2	1.14	1.25	9.75	7.59	12.93	7.99	7.79	8.72
	13	7.41	3.61	12.24	0.93	0.91	0.96	9.95	9.01	11.72	8.28	8.17	8.83

Table 3.5. Measured nutrient data from upstream, downstream (0.15 miles, 1.4 miles, 13 miles) and at the ECWRF effluent discharge during three sampling seasons in 2014.

Season	Site	Phosphate (µg/L)	Ammonia (µg/L)	Nitrite/Nitrate (µg/L)	Total Phosphorous (µg/L)	Total Nitrogen (µg/L)
Spring	Upstream	22.7	20.1	102	40	375
	Effluent	10	17.6	2810	27.3	3260
	0.15 mile	16.4	5.1	285	40.6	646
	1.4 mile	14.9	4.2	319	31.8	586
	13 mile	22.4	44.3	36.1	27.7	289
Summer	Upstream	17.3	< MDL	29.8	21.2	232
	Effluent	14.7	11.9	4930	51.1	5025
	0.15 mile	16.9	< MDL	2080	33.8	2365
	1.4 mile	12.3	< MDL	2030	25.2	2290
	13 mile	12	< MDL	500.5	35.4	839
Fall	Upstream	2.9	< MDL	60.8	22.2	196
	Effluent	7.61	3400	5170	85.9	8475
	0.15 mile	5.8	1010	1430	24.2	3390
	1.4 mile	4.1	404.5	840.5	16.4	1895
	13 mile	3.2	< MDL	101	17.1	339

Aqueous concentrations of total nitrogen, total phosphorous, and nitrate/nitrite did not differ significantly ($p<0.05$) over the course of this study.

Occurrence of Pharmaceuticals in Water and Biota

Seventeen of nineteen target analytes were detected in water at one or more sites during at least one of the three sampling events (Table 3.6). Target analytes were typically detected at the highest levels in effluent and then decreased in concentration with increased distance downstream. Nine target analytes were detected in all species during all sampling events (Table 3.7-3.9). Due to ubiquitous detection at all sites downstream of the effluent discharge during all seasons AMI, DIL, DIP, FLU, and SER were specifically selected to evaluate potential spatial and temporal accumulation differences in collected biota. Trichoptera were collected at all sites during all seasons, which allowed for robust

comparisons between sites and sampling events. Specifically, spatial accumulation of individual target analytes, regardless of season, were significantly ($p<0.05$) higher at sites closer to the effluent discharge and then decreased with increasing distance from the discharge for all five target analytes in periphyton (Figure 3.2), Trichoptera (Figure 3.3), *C. bairdii* (Figure 3.4), and *S. trutta* (Figure 3.5). Temporal accumulation of DIP and DIL in periphyton were significantly ($p<0.05$) higher in the spring, while SER was higher in the fall (Figure 3.2). No significant ($p>0.05$) temporal differences in accumulation by Trichoptera were observed for any target analytes (Figure 3.3). *C. bairdii* accumulation of DIP was significantly ($p<0.05$) elevated during the spring and summer, while SER, FLU, and AMI accumulations were higher only during the summer (Figure 3.4). Accumulation of DIL and SER in *S. trutta* were significantly ($p<0.05$) higher in summer and fall, while accumulation of FLU was higher during summer (Figure 3.5).

Table 3.6. Human pharmaceuticals in mean (n = 2) water samples collected from upstream, downstream (0.15 miles, 1.44 miles, 13 miles) and at the ECWRF effluent discharge during three sampling seasons in 2014. ND, No Detect; <MDL, below method detection limit.

Season	Site	ACE (ng/L)	AMI (ng/L)	AML (ng/L)	BEN (ng/L)	BUP (ng/L)	CAF (ng/L)	CAR (ng/L)	DES (ng/L)	DIC (ng/L)	DIL (ng/L)	DIP (ng/L)	DUL (ng/L)	FLU (ng/L)	MPH (ng/L)	NOR (ng/L)	SER (ng/L)	SUC (ng/L)
Spring	Upstream	ND	ND	ND	2.3	ND	7.3	0.5	ND	ND	<MDL	0.11	ND	3.4	ND	ND	ND	3.6
	Effluent	<MDL	170	<MDL	77	<MDL	17	50	ND	94	87	320	<MDL	46	9.0	5.4	2.0	1600
	0.15 mile	<MDL	ND	ND	5.2	ND	7.1	3.8	ND	ND	1.5	11	ND	ND	0.58	ND	ND	200
	1.4 mile	<MDL	ND	ND	4.8	ND	6.7	3.5	ND	ND	6.3	6.7	ND	ND	0.41	ND	ND	170
	13 mile	<MDL	ND	ND	3.1	ND	5.0	3.5	ND	ND	2.7	2.8	ND	ND	0.19	ND	ND	140
Summer	Upstream	ND	ND	ND	1.5	ND	22	<MDL	6.6	ND	<MDL	0.49	ND	ND	ND	ND	ND	8.5
	Effluent	15	140	<MDL	26	<MDL	21	110	55	69	32	82	<MDL	58	6.8	ND	37	1900
	0.15 mile	7.6	29	ND	7.2	<MDL	30	34	ND	23	9.4	26	ND	15	2.0	ND	ND	750
	1.4 mile	17	24	ND	11	<MDL	33	34	ND	14	9.0	20	ND	ND	1.4	ND	ND	770
	13 mile	3.1	ND	ND	9.0	ND	20	26	ND	ND	1.5	1.6	ND	ND	<MDL	ND	ND	560
Fall	Upstream	<MDL	ND	ND	0.36	ND	120	ND	<MDL	ND	ND	<MDL	ND	39	ND	ND	ND	7.1
	Effluent	23	150	ND	61	<MDL	105	100	36	160	38	140	<MDL	33	6.8	9.0	28	1700
	0.15 mile	8.8	28	ND	16.5	<MDL	45	31	18	22	9.3	33	<MDL	38	1.6	28	15	820
	1.4 mile	6.3	5.8	ND	8.6	<MDL	44	17	18	5.5	2.8	12	<MDL	39	0.58	47	11	550
	13 mile	4.0	8.6	ND	6.8	<MDL	150	11	ND	ND	0.51	0.86	<MDL	22	<MDL	ND	7.5	440

Table 3.7. Human pharmaceuticals in biota (mean ± s.d.; μg kg^{-1}) during May (Spring) of 2014. AMI, amitriptyline; CAF, caffeine; DIL, diltiazem; DPH, diphenhydramine; FLU, fluoxetine; MPH methylphenidate; NOR, norfluoxetine; SER, sertraline; ND, not detected; <MDL, below method detection limit.

		Analyte																	
		AMI (μg/kg)		CAF (μg/kg)		CAR (μg/kg)		DIL (μg/kg)		DIP (μg/kg)		FLU (μg/kg)		MPH (μg/kg)		NOR (μg/kg)		SER (μg/kg)	
Site	Organism	Mean ± SD	Freq.	Mean ± SD	Freq.	Mean ± SD	Freq.	Mean ± SD	Freq.	Mean ± SD	Freq.	Mean ± SD	Freq.	Mean ± SD	Freq.	Mean ± SD	Freq.	Mean ± SD	Freq.
Upstream	*Salmo trutta*	ND	0/11	<MDL	2/11	ND	0/11	ND	0/11	ND	0/11	ND	0/11	3.0 ± 2.1	11/11	ND	0/11	ND	0/11
	Cottus bairdii	ND	0/10	<MDL	9/10	ND	0/10	0.14	2/10	ND	0/10	ND	0/10	ND	0/10	ND	0/10	ND	0/10
	Diptera	ND	0/10	<MDL	3/10	ND	0/10	0.88 ± 0.50	8/10	ND	0/10	0.57 ± 0.29	4/10	ND	0/10	ND	0/10	ND	0/10
	Trichoptera	ND	0/9	17 ± 8.6	9/9	ND	0/9	0.27 ± 0.15	6/9	ND	0/9	11	1/9	ND	0/9	ND	0/9	ND	0/9
	Baetidae	ND	0/6	ND	0/6	ND	0/6	0.72 ± 1.2	5/6	ND	0/6	ND	0/6	ND	0/6	ND	0/6	ND	0/6
	Periphyton	5.4	1/10	5.7 ± 2.2	10/10	ND	0/10	1.2 ± 1.6	10/10	ND	0/10	8.5	1/10	ND	0/10	ND	0/10	<MDL	2/10
0.15 mile	*Salmo trutta*	4.1 ± 3.4	8/10	<MDL	5/10	ND	0/10	0.15 ± 0.08	10/10	1.1 ± 1.0	10/10	1.5 ± 1.4	10/10	2.7 ± 1.7	10/10	1.6 ± 1.3	10/10	1.1 ± 1.1	10/10
	Cottus bairdii	5.0 ± 2.1	9/9	0.76 ± 0.17	4/9	ND	0/9	0.42 ± 0.06	9/9	3.7 ± 0.78	9/9	1.7 ± 0.42	9/9	ND	0/9	5.6 ± 1.1	9/9	2.6 ± 0.81	9/9
	Diptera	ND	0/4	ND	0/4	ND	0/4	0.21	1/4	0.68 ± 0.34	4/4	0.69	2/4	ND	0/4	ND	0/4	ND	0/4
	Trichoptera	ND	0/5	8.7 ± 3.2	5/5	ND	0/5	0.56 ± 0.31	5/5	5.1 ± 0.84	5/5	2.8 ± 0.53	5/5	ND	0/5	ND	0/5	4.4 ± 1.9	5/5
	Baetidae	ND	0/4	3.2 ± 0.77	4/4	ND	0/4	0.34 ± 0.13	4/4	1.7 ± 0.17	4/4	ND	0/4	ND	0/4	ND	0/4	ND	0/4
	Periphyton	34 ± 13	10/10	4.5 ± 2.2	10/10	ND	0/10	15 ± 12	10/10	29 ± 15	10/10	8.6 ± 4.5	10/10	0.11 ± 0.08	10/10	ND	0/10	14 ± 5.8	10/10
1.4 mile	*Salmo trutta*	1.9 ± 0.62	5/10	<MDL	7/10	ND	0/10	0.11 ± 0.02	10/10	0.76 ± .38	10/10	1.2 ± 1.2	10/10	2.7 ± 2.2	9/10	2.4 ± 1.1	9/10	0.69 ± 0.42	10/10
	Cottus bairdii	4.8 ± 1.7	9/10	<MDL	3/10	ND	0/10	0.71 ± 0.79	10/10	3.4 ± 0.48	10/10	1.6 ± 0.65	10/10	ND	0/10	4.5 ± 1.1	10/10	2.0 ± 0.52	10/10
	Diptera	ND	0/4	<MDL	4/4	ND	0/4	0.15	1/4	0.9 ± 0.42	4/4	1.0	2/4	ND	0/4	ND	0/4	ND	0/4
	Trichoptera	ND	0/1	3.1	1/1	ND	0/1	ND	0/1	3.4	1/1	2.0	1/1	ND	0/1	ND	0/1	ND	0/1
	Baetidae	ND	0/7	2.3 ± 1.1	5/7	ND	0/7	0.24	1/7	1.1 ± 0.16	7/7	ND	0/7	ND	0/7	ND	0/7	ND	0/7
	Periphyton	15 ± 4.0	10/10	4.8 ± 1.4	10/10	ND	0/10	4.4 ± 3.0	10/10	33 ± 9.1	10/10	6.7 ± 1.8	10/10	ND	0/10	2.5	2/10	8.5 ± 2.9	10/10
13 mile	*Salmo trutta*	ND	0/10	<MDL	5/10	ND	0/10	0.08 ± 0.03	10/10	0.19 ± 0.09	10/10	<MDL	9/10	3.0 ± 1.9	10/10	1.1 ± 0.43	7/10	ND	0/10
	Cottus bairdii	1.6 ± 1.2	4/10	1.3 ± 0.9	5/10	ND	0/10	0.24 ± 0.08	10/10	0.81 ± 0.12	10/10	<MDL	8/10	ND	0/10	2.4 ± 1.1	10/10	0.65 ± 0.29	8/10
	Diptera	ND	0/6	1.0 ± 0.8	5/6	ND	0/6	0.38 ± 0.21	3/6	0.93 ± 1.3	6/6	ND	0/6	ND	0/6	ND	0/6	ND	0/6
	Trichoptera	ND	0/2	2.0	2/2	ND	0/2	0.38	2/2	0.73	2/2	ND	0/2	ND	0/2	ND	0/2	ND	0/2
	Baetidae	ND	0/4	ND	0/4	ND	0/4	0.27	1/4	0.46 ± 0.06	4/4	ND	0/4	ND	0/4	ND	0/4	7.0	1/4
	Periphyton	4.8 ± 1.9	8/10	2.4 ± 1.5	10/10	ND	0/10	0.40 ± 0.18	10/10	10 ± 5.3	10/10	2.8 ± 2.5	10/10	ND	0/10	7.3	1/10	2.5 ± 0.27	4/10

Table 3.8. Human pharmaceuticals in biota (mean ± s.d.; μg kg^{-1}) during August (Summer) of 2014. AMI, amitriptyline; CAF, caffeine; CAR, carbamazepine; DIL, diltiazem; DPH, diphenhydramine; FLU, fluoxetine; MPH methylphenidate; NOR, norfluoxetine; SER, sertraline; ND, not detected; <MDL, below method detection limit.

		Analyte																	
		AMI (μg/kg)		CAF (μg/kg)		CAR (μg/kg)		DIL (μg/kg)		DIP (μg/kg)		FLU (μg/kg)		MPH (μg/kg)		NOR (μg/kg)		SER (μg/kg)	
Site	Organism	Mean ± SD	Freq.	Mean ± SD	Freq.	Mean ± SD	Freq.	Mean ± SD	Freq.	Mean ± SD	Freq.	Mean ± SD	Freq.	Mean ± SD	Freq.	Mean ± SD	Freq.	Mean ± SD	Freq.
Upstream	*Salmo trutta*	<MDL	1/10	2.0 ± 2.8	10/10	0.57 ± 0.32	5/10	0.12	2/10	ND	0/10	ND	0/10	3.0 ± 3.6	10/10	<MDL	3/10	ND	0/10
	Cottus bairdii	ND	0/10	<MDL	10/10	ND	0/10	0.69	1/10	ND	0/10	ND	0/10	ND	0/10	ND	0/10	ND	0/10
	Trichoptera	ND	0/2	4.2	2/2	ND	0/2	ND	0/2	ND	0/2	ND	0/2	ND	0/2	ND	0/2	ND	0/2
	Lymnaeidea & Physidae	ND	0/6	2.8 ± 0.5	6/6	ND	0/6	ND	0/6	0.20 ± 0.06	2/6	ND	0/6	ND	0/6	ND	0/6	ND	0/6
	Periphyton	ND	0/5	5.3 ± 4.0	5/5	ND	0/5	ND	0/5	ND	0/5	ND	0/5	ND	0/5	ND	0/5	ND	0/5
0.15 mile	*Salmo trutta*	4.7 ± 4.4	10/10	1.1 ± 0.73	8/10	ND	0/10	0.17 ± 0.15	10/10	0.80 ± 0.52	10/10	4.8 ± 3.1	10/10	1.6 ± 1.4	10/10	2.3 ± 0.81	10/10	3.8 ± 2.6	10/10
	Cottus bairdii	9.2 ± 2.1	10/10	1.3 ± 1.0	10/10	0.22 ± 0.05	10/10	0.39 ± 0.11	10/10	2.1 ± 0.54	10/10	4.1 ± 1.2	10/10	0.04 ± 0.01	10/10	5.8 ± 1.3	10/10	5.3 ± 1.3	10/10
	Trichoptera	ND	0/2	2.4	1/2	0.72	2/2	0.33	2/2	2.1	2/2	4.0	2/2	ND	0/2	3.9	2/2	8.4	2/2
	Periphyton	40 ± 14	5/5	1.5 ± 1.3	5/5	0.16 ± 0.09	5/5	0.69 ± 0.18	5/5	16 ± 11	5/5	10 ± 3.9	5/5	0.10 ± 0.04	5/5	ND	0/5	27 ± 7.8	5/5
1.4 mile	*Salmo trutta*	3.7 ± 2.2	10/10	<MDL	9/10	ND	0/10	0.14 ± 0.06	10/10	0.69 ± 0.32	10/10	2.8 ± 1.0	10/10	3.1 ± 2.3	10/10	2.4 ± 0.70	10/10	1.7 ± 1.0	10/10
	Cottus bairdii	10 ± 4.1	10/10	<MDL	10/10	0.21 ± 0.05	10/10	0.46 ± 0.11	10/10	2.7 ± 1.3	10/10	3.8 ± 1.0	10/10	0.05 ± 0.03	9/10	5.7 ± 1.4	10/10	4.3 ± 1.3	10/10
	Trichoptera	23 ± 2.5	5/5	0.98 ± 0.43	5/5	0.54 ± 0.08	5/5	0.55 ± 0.14	5/5	4.5 ± 0.71	5/5	3.9 ± 0.94	5/5	<MDL	1/5	2.1 ± 2.1	5/5	23 ± 27	5/5
	Lymnaeidea & Physidae	25 ± 5.6	4/4	<MDL	4/4	0.15 ± 0.06	4/4	0.26 ± 0.06	4/4	4.1 ± 1.1	4/4	5.1 ± 0.87	4/4	0.05 ± 0.02	4/4	<MDL	1/4	24 ± 8.1	4/4
	Periphyton	22 ± 8.2	5/5	<MDL	5/5	<MDL	5/5	0.42 ± 0.12	5/5	8.5 ± 6.8	5/5	5.5 ± 1.9	5/5	0.07 ± 0.03	5/5	ND	0/5	13 ± 5.3	5/5
13 mile	*Salmo trutta*	ND	0/10	<MDL	9/10	ND	0/10	0.11 ± 0.13	10/10	<MDL	10/10	<MDL	8/10	1.9 ± 2.5	4/10	0.81 ± 0.55	10/10	1.7 ± 3.1	7/10
	Cottus bairdii	0.38	1/9	<MDL	8/9	0.55 ± 0.35	9/9	0.14 ± 0.03	9/9	0.27 ± 0.04	8/9	<MDL	9/9	ND	0/9	1.7 ± 0.46	9/9	<MDL	9/9
	Trichoptera	ND	0/3	2.8 ± 0.76	3/3	0.44	2/3	0.19 ± 0.01	3/3	1.6 ± 0.10	3/3	1.2	2/3	ND	0/3	1.6	1/3	1.8	2/3
	Periphyton	ND	0/5	1.2 ± 0.65	5/5	ND	0/5	0.12 ± 0.05	5/5	4.6 ± 2.8	5/5	ND	0/5	ND	0/5	ND	0/5	ND	0/5

Table 3.9. Human pharmaceuticals in biota (mean ± s.d.; μg kg^{-1}) during October (Fall) of 2014. AMI, amitriptyline; CAF, caffeine; CAR, carbamazepine; DIL, diltiazem; DPH, diphenhydramine; FLU, fluoxetine; MPH methylphenidate; NOR, norfluoxetine; SER, sertraline; ND, not detected; <MDL, below method detection limit.

		Analyte																	
		AMI (μg/kg)		CAF (μg/kg)		CAR (μg/kg)		DIL (μg/kg)		DIP (μg/kg)		FLU (μg/kg)		MPH (μg/kg)		NOR (μg/kg)		SER (μg/kg)	
Site	Organism	Mean ± SD	Freq.	Mean ± SD	Freq.	Mean ± SD	Freq.	Mean ± SD	Freq.	Mean ± SD	Freq.	Mean ± SD	Freq.	Mean ± SD	Freq.	Mean ± SD	Freq.	Mean ± SD	Freq.
Upstream	Salmo trutta	ND	0/10	<MDL	5/10	ND	0/10	ND	0/10	0.10 ± 0.05	3/10	1.0	1/10	2.2 ± 1.7	10/10	1.1	1/10	ND	0/10
	Cottus bairdii	ND	0/10	<MDL	4/10	ND	0/10	ND	0/10	0.08 ± 0.04	10/10	ND	0/10	ND	0/10	ND	0/10	ND	0/10
	Lymnaeidea & Physidae	ND	0/4	ND	0/4	ND	0/4	ND	0/4	ND	0/4	ND	0/4	ND	0/4	ND	0/4	1.7	1/4
	Trichoptera	ND	0/6	ND	0/6	ND	0/6	ND	0/6	ND	0/6	ND	0/6	ND	0/6	ND	0/6	ND	0/6
	Diptera	ND	0/5	<MDL	5/5	ND	0/5	<MDL	2/5	ND	0/5	ND	0/5	ND	0/5	ND	0/5	ND	0/5
	Periphyton	ND	0/5	<MDL	4/5	ND	0/5	ND	0/5	ND	0/5	ND	0/5	ND	0/5	ND	0/5	ND	0/5
0.15 mile	*Salmo trutta*	5.8 ± 6.3	8/10	<MDL	2/10	ND	0/10	0.21 ± 0.19	6/10	0.85 ± 0.76	10/10	2.2 ± 0.94	10/10	2.3 ± 1.7	10/10	2.1 ± 1.0	10/10	3.3 ± 1.5	10/10
	Cottus bairdii	4.7 ± 1.1	10/10	<MDL	3/10	<MDL	10/10	0.24 ± 0.07	10/10	1.7 ± 0.05	10/10	1.3 ± 0.50	10/10	ND	0/10	3.6 ± 0.68	10/10	2.6 ± 1.1	10/10
	Trichoptera	4.3 ± 0.54	5/7	ND	0/7	0.30 ± 0.06	7/7	0.17 ± 0.13	7/7	2.8 ± 0.78	7/7	2.4 ± 1.4	7/7	ND	0/7	1.8 ± 0.21	3/7	4.9 ± 2.8	6/7
	Periphyton	41 ± 6.9	5/5	<MDL	5/5	ND	0/5	0.55 ± 0.09	5/5	7.8 ± 0.61	5/5	8.9 ± 1.5	5/5	0.13 ± 0.03	5/5	1.2 ± 0.66	5/5	54 ± 9.0	5/5
1.4 mile	*Salmo trutta*	3.2 ± 0.32	5/10	<MDL	1/10	ND	0/10	0.06	1/10	0.46 ± 0.11	10/10	1.7 ± 1.3	10/10	2.2 ± 1.5	10/10	1.6 ± 0.99	10/10	2.1 ± 1.3	10/10
	Cottus bairdii	6.1 ± 3.8	10/10	<MDL	10/10	ND	0/10	0.62 ± 0.74	10/10	2.2 ± 0.82	10/10	1.5 ± 0.75	10/10	ND	0/10	3.4 ± 1.1	10/10	2.3 ± 1.0	10/10
	Trichoptera	ND	0/5	ND	0/5	ND	0/5	0.21 ± 0.10	4/5	3.5 ± 1.4	5/5	3.6 ± 1.8	5/5	ND	0/5	ND	0/5	9.1	2/5
	Periphyton	20 ± 8.5	5/5	<MDL	5/5	ND	5/5	0.33 ± 0.14	5/5	8.5 ± 3.2	5/5	5.5 ± 3.1	5/5	0.06 ± 0.03	5/5	ND	0/5	18 ± 10	5/5
13 mile	*Salmo trutta*	ND	0/10	<MDL	9/10	ND	0/10	0.09	2/10	0.11 ± 0.11	10/10	0.70 ± 0.68	6/10	1.7 ± 1.3	10/10	0.80 ± 0.57	10/10	1.2	1/10
	Cottus bairdii	7.2	1/10	2.9 ± 2.5	10/10	ND	0/10	0.13 ± 0.02	8/10	0.29 ± 0.07	10/10	<MDL	2/10	ND	0/10	0.91 ± 0.52	10/10	0.64 ± 0.32	5/10
	Trichoptera	ND	0/7	ND	0/7	ND	0/7	0.12 ± 0.04	6/7	0.97 ± 0.52	7/7	ND	0/7	ND	0/7	ND	0/7	ND	0/7
	Periphyton	ND	0/5	ND	0/5	ND	0/5	0.18 ± 0.02	5/5	4.8 ± 0.52	5/5	ND	0/5	ND	0/5	ND	0/5	4.2 ± 2.2	5/5

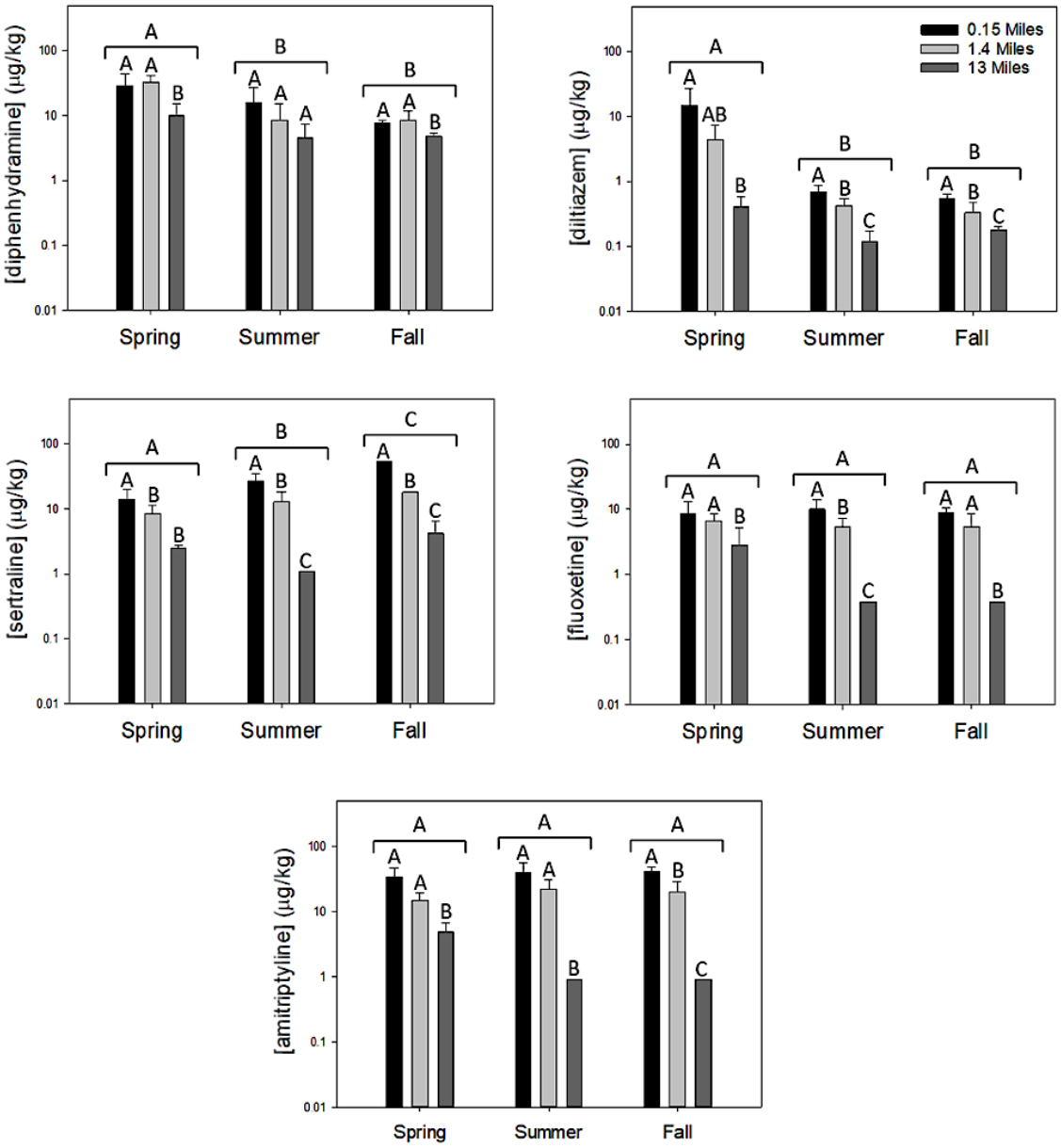

Figure 3.2. Mean (± SD) concentration of diphenhydramine, diltiazem, sertraline, fluoxetine, and amitriptyline in periphyton at three distances (0.15, 1.4, 13 miles) downstream of the East Canyon Water Reclaimation Facility discharge, during three different seasons (spring, summer, fall) of 2014. Spatial and temporal bioaccumulation differences were tested for significance using a two-way ANOVA with a post-hoc pair-wise analysis (Holm-Sidek method). If target analytes were not detected or detected as <MDL, in each organism, half MDL values were utilized for statistical analysis. Letters above bars represent significant ($p<0.05$) differences in accumulation between sites. Letters above brackets represent significant ($p<0.05$) differences in accumulation between season.

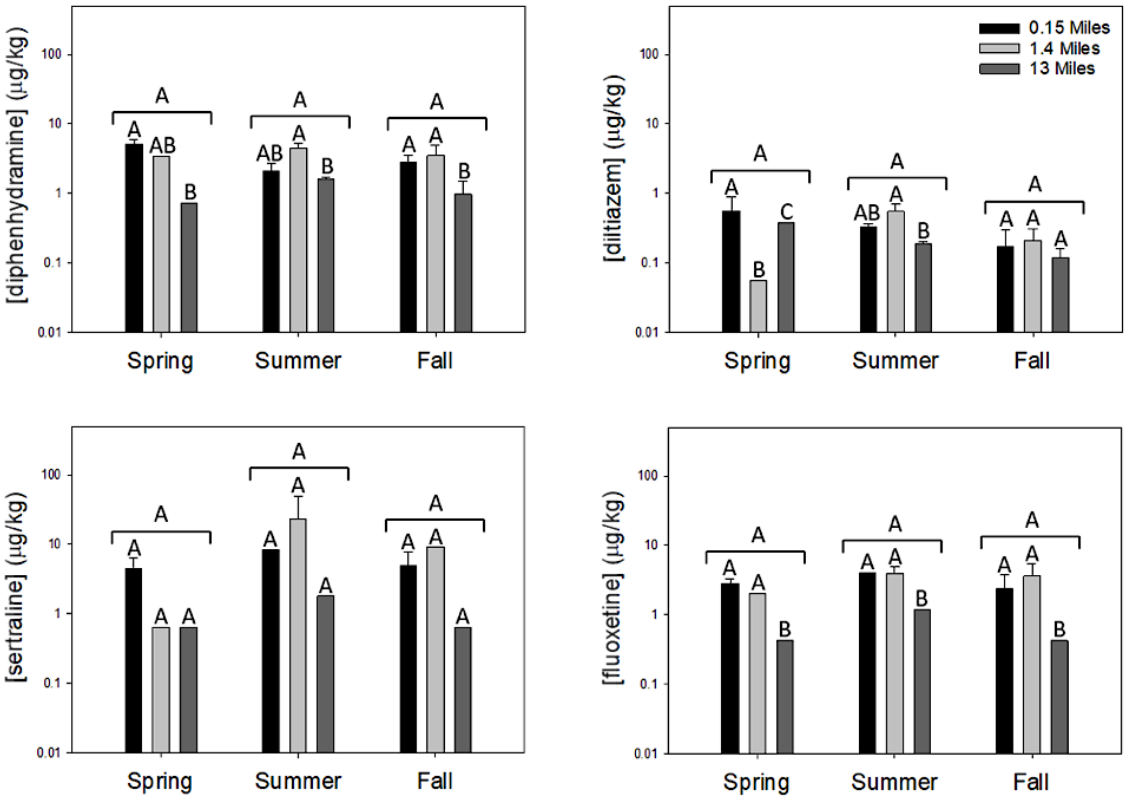

Figure 3.3. Mean (± SD) concentration of diphenhydramine, diltiazem, sertraline, and fluoxetine in Trichoptera at three distances (0.15, 1.4, 13 miles) downstream of the East Canyon Water Reclaimation Facility discharge, during three different seasons (spring, summer, fall) of 2014. Spatial and temporal bioaccumulation differences were tested for significance using a two-way ANOVA with a post-hoc pair-wise analysis (Holm-Sidek method). If target analytes were not detected or detected as <MDL, in each organism, half MDL values were utilized for statistical analysis. Letters above bars represent significant ($p<0.05$) differences in accumulation between sites. Letters above brackets represent significant ($p<0.05$) differences in accumulation between season.

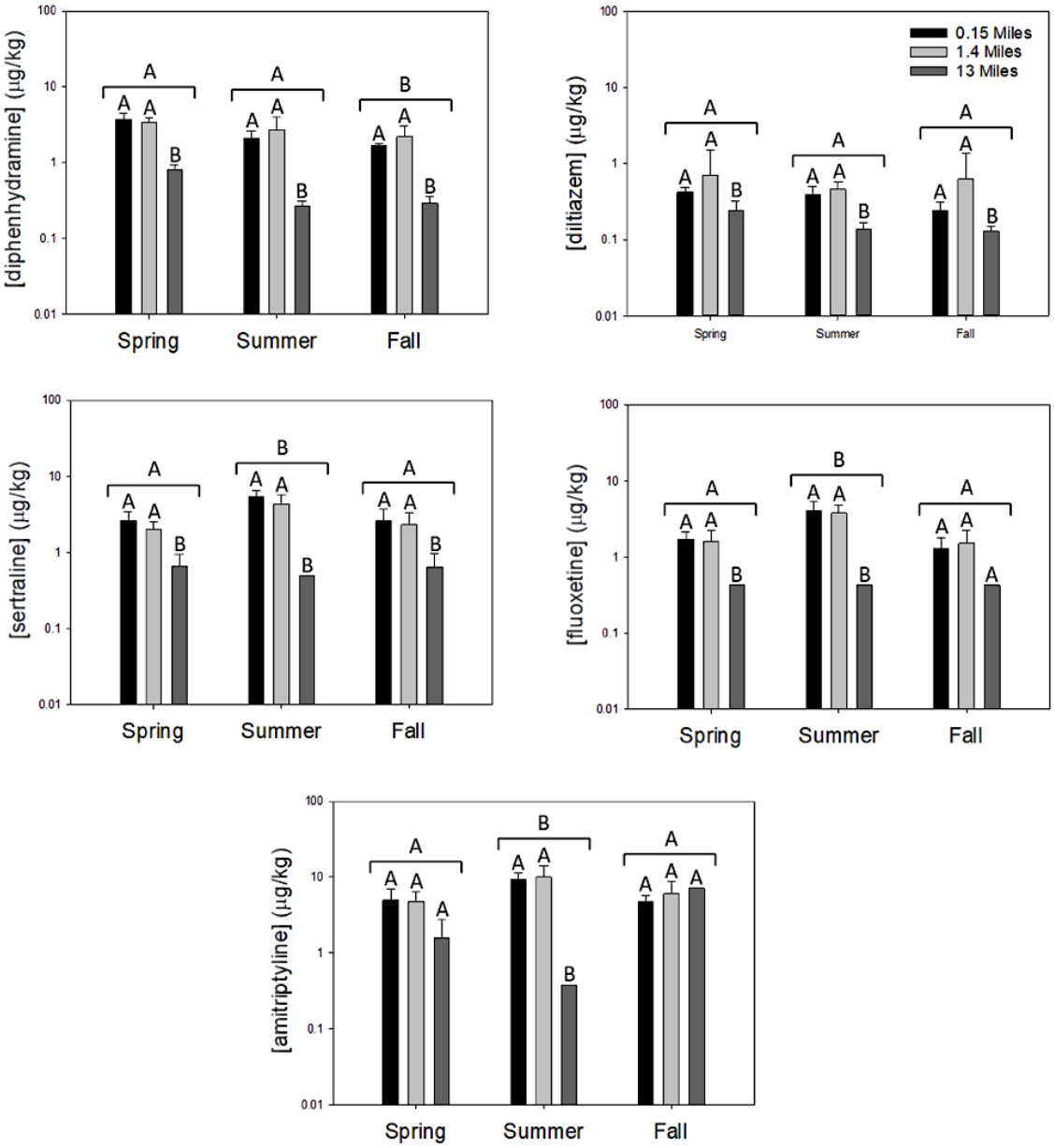

Figure 3.4. Mean (± SD) concentration of diphenhydramine, diltiazem, sertraline, fluoxetine, and amitriptyline in Cottus bairdii at three distances (0.15, 1.4, 13 miles) downstream of the East Canyon Water Reclaimation Facility discharge, during three different seasons (spring, summer, fall) of 2014. Spatial and temporal bioaccumulation differences were tested for significance using a two-way ANOVA with a post-hoc pair-wise analysis (Holm-Sidek method). If target analytes were not detected or detected as <MDL, in each organism, half MDL values were utilized for statistical analysis. Letters above bars represent significant ($p<0.05$) differences in accumulation between sites. Letters above brackets represent significant ($p<0.05$) differences in accumulation between season.

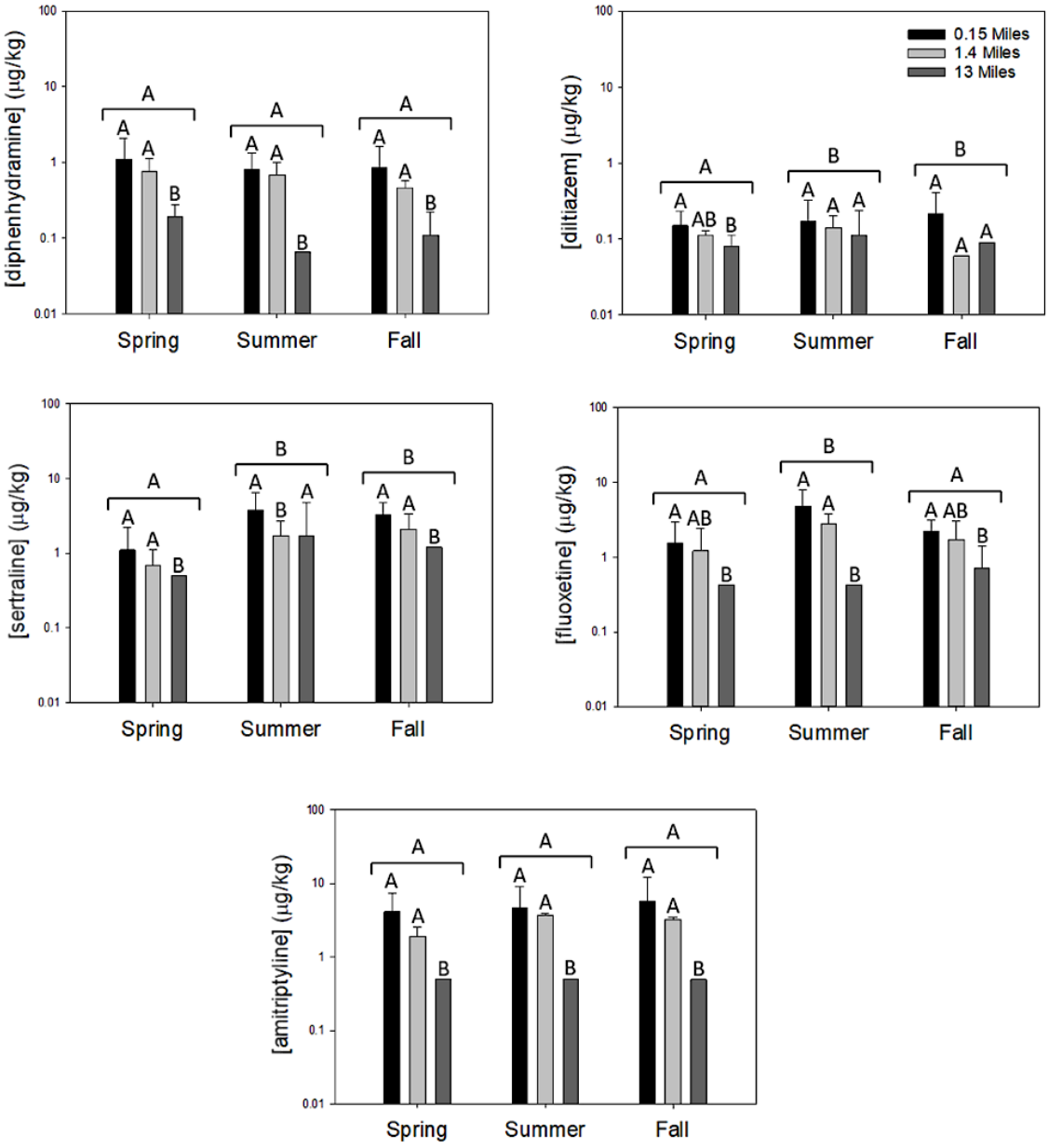

Figure 3.5. Mean (± SD) concentration of diphenhydramine, diltiazem, sertraline, fluoxetine, and amitriptyline in Salmo trutta at three distances (0.15, 1.4, 13 miles) downstream of the East Canyon Water Reclaimation Facility discharge, during three different seasons (spring, summer, fall) of 2014. Spatial and temporal bioaccumulation differences were tested for significance using a two-way ANOVA with a post-hoc pair-wise analysis (Holm-Sidek method). If target analytes were not detected or detected as <MDL, in each organism, half MDL values were utilized for statistical analysis. Letters above bars represent significant ($p<0.05$) differences in accumulation between sites. Letters above brackets represent significant ($p<0.05$) differences in accumulation between season.

NMDS ordinations for periphyton, Trichoptera, *Cottus bairdii*, and *Salmo trutta* display spatial and temporal dissimilarity in accumulation patterns for each organism in multivariate space by site and season (Figure 3.6). The horizontal axis (NMDS 2) ordered by sampling site, while the vertical axis (NMDS 1) ordered by sampling season. The difference in scale between NMDS1 and NMDS 2 show a greater dissimilarity between locations than between seasons. Location (shape) and season (color) were applied to organism in multivariate space as categorical variables to investigate dissimilarity in spatial and temporal accumulation of target analytes in individuals. Spatial accumulation in periphyton was significantly different ($F = 33.95$, $p = 0.0001$) between all sites. Temporally, accumulation is periphyton during the spring was significantly different ($F = 4.047$, $p = 0.0027$) from summer and fall. Spatial accumulation in Trichoptera at the 13-mile site was significantly different from the 0.15 and 1.4 mile sites ($F = 18.21$, $p = 0.001$). Temporal accumulation in Trichoptera was not significantly different ($F = 1.73$, $p = 0.1202$) between seasons. Spatial accumulation in *Cottus bairdii* at the 13-mile site was significantly different ($F = 55.43$, $p = 0.0001$) from the 0.15 and 1.4 mile sites. Temporal accumulation in *Cottus bairdii* during spring was significantly different ($F = 3.9$, $p = 0.0058$) from summer; however, fall was not significantly different from spring or summer. Spatial accumulation in *Salmo trutta* was significantly different ($F = 29.77$, $p = 0.0001$) between all sites. Temporal accumulation in *Salmo trutta* during the spring was significantly different ($F = 3.835$, $p = 0.0033$) from summer and fall.

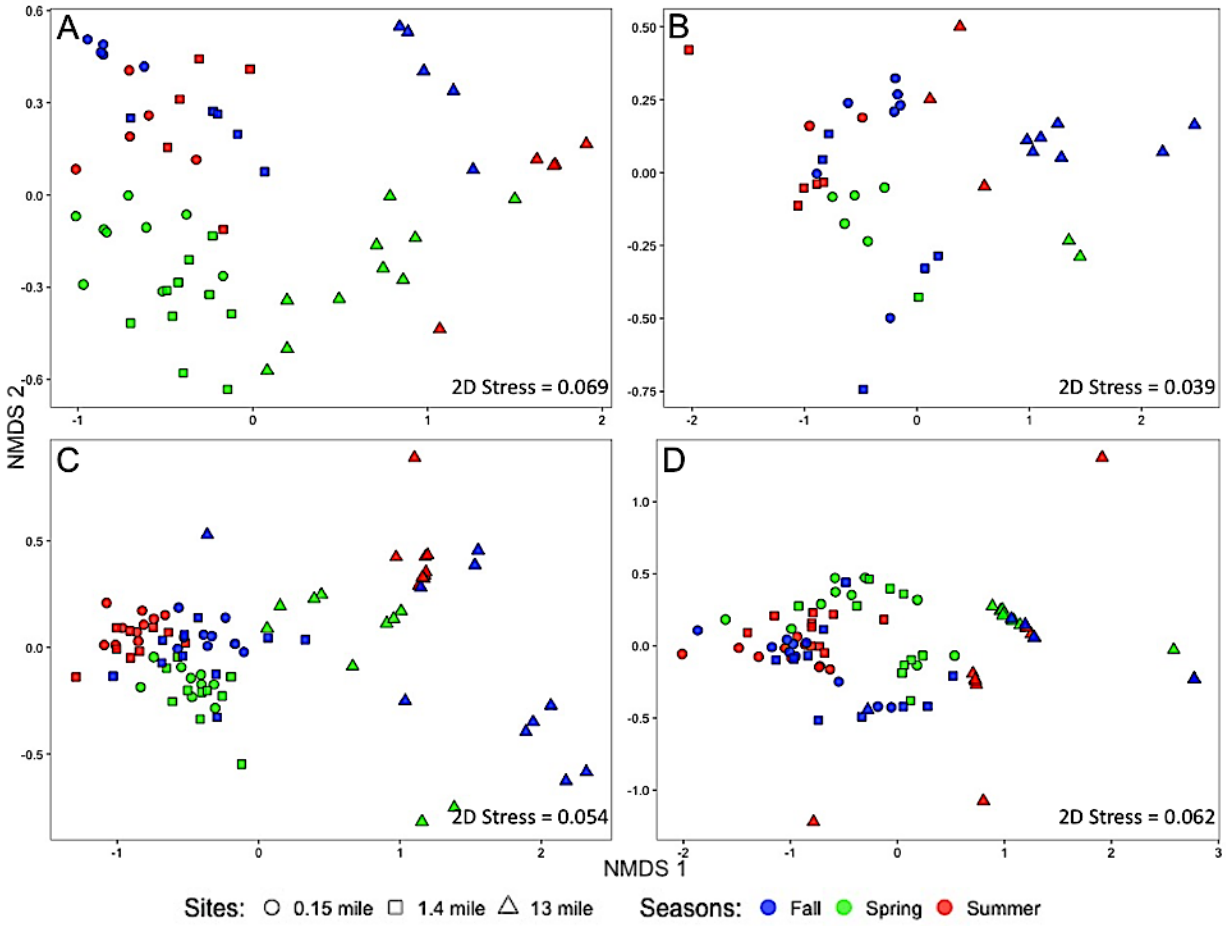

Figure 3.6. NMDS of target analyte concentrations (amitriptyline, diltiazem, diphenhydramine, fluoxetine, and sertraline) in periphyton (A), Trichoptera (B), Cottus bairdii (C), and Salmo trutta (D) at all distance during all seasons downstream of the East Canyon Water Reclamation Facility discharge to East Canyon Creek, Park City, Utah, USA. Target analytes measured <MDL were substituted with half MDL values to represent a detect and no detect values were substituted with a zero for that sample.

The minimum-maximum and median BCFs and BAFs from all sites during all seasons downstream of the discharge are presented in Tables 3.10-3.12. Box plots of BAFs and BCFs demonstrated that organisms at lower TPs (i.e. periphyton and Trichoptera) had significantly ($p<0.05$) higher accumulations of AMI ($F = 36.58$, $p = 0.0001$), DIL ($F = 39.73$, $p = 0.0001$), DIP ($F = 161.3$, $p = 0.0001$), FLU ($F = 11.51$, $p = 0.0001$), NOR ($F = 4.87$, $p = 0.0023$), and SER ($F = 18.81$, $p = 0.0001$), than organisms at higher TPs (i.e., fish) for all examined compounds (Figure 3.7).

Pharmaceutical Partitioning and Normalization to Proteins or Phospholipids

Calculated values for the partitioning coefficients D_{ow}, D_{mw}, D_{mpw}, *and* D_{BSAw} are given in Table 3.2. Positive relationships between BAFs and partitioning coefficients were observed for D_{mw} ($R^2 = 0.295$, $p = <0.001$), D_{BSAw} ($R^2 = 0.360$, $p = <0.001$) and D_{mpw} ($R^2 = 0.263$, $p = <0.001$) in *S. trutta* (Figure 3.8). However, no relationship was observed for D_{ow} ($R^2 = 0.000$, $p = 0.961$). Mean (±SD) trout samples in the present study consisted of 1.90% ± 0.66 protein, 5.01% ± 2.28 total lipids, 2.71% ± 1.28 neutral (storage) lipids, and 1.47% ± 0.56 polar lipids. Overall R^2 for regressions between biological fractions and measured pharmaceutical concentrations (Figures 3.9-3.14) were below 0.1 except for two regressions relating percent protein to AMI ($R^2 = 0.248$, $p = <0.001$) and DIL ($R^2 = 0.168$, $p = <0.001$). Interestingly, these relationships indicated a decrease in concentration with an increase in total protein.

Table 3.10. Median (range) of calculated BAFs (L/kg) for biota during May (spring) of 2014. AMI, amitriptyline; CAF, caffeine; CAR, carbamazepine; DIL, diltiazem; DPH, diphenhydramine; FLU, fluoxetine; MPH methylphenidate; NOR, norfluoxetine; SER, sertraline.

		Analyte								
Site	Organism	AMI (L/kg)	CAF (L/kg)	CAR (L/kg)	DIL (L/kg)	DIP (L/kg)	FLU (L/kg)	MPH (L/kg)	NOR (L/kg)	SER (L/kg)
0.15 mile	*Salmo trutta*	1605 (419-5581)	119		80 (40-233)	85 (31-355)	1004 (356-4268)	3966 (724-9138)	1413 (559-5424)	651 (651-4737)
	Cottus bairdii	2047 (1349-4465)	119 (70-119)		267 (233-380)	327 (255-491)	1423 (1088-2092)		5763 (4746-8136)	3026 (2500-5658)
	Diptera				140 (140-140)	70 (22-86)	580 (356-803)			
	Trichoptera		1056 (873-1972)		280 (207-733)	491 (364-545)	2510 (1674-2762)			5789 (3421-9342)
	Baetidae		451 (338-563)		223.5 (160-287)	145 (136-173)	356 (356-356)			3026 (3026-3026)
	Periphyton	17209 (5581-24186)	634 (133-1070)		8667 (1867-26000)	2182 (1455-5364)	6192 (3515-15900)	155 (69-500)		14474 (10263-34211)
1.4 mile	*Salmo trutta*	1023 (558-1256)	126		19 (11-24)	105 (64-269)	551 (356-3515)	8537 (927-13659)	2147 (1130-5085)	651 (651-1842)
	Cottus bairdii	2279 (1302-3442)	126		72 (54-444)	522 (388-597)	1214 (803-2594)		4859 (3616-7571)	2500 (1842-3947)
	Diptera		99		24	125 (81-209)	837 (837-837)			
	Trichoptera		463			507 (507-507)	1674 (1674-1674)			
	Baetidae		299 (209-597)		38	149 (124-194)				
	Periphyton	7442 (4279-9767)	642 (507-1194)		548 (175-1746)	4702 (3284-7910)	5607 (3431-7866)		2769 (2260-3277)	11382 (5132-17105)
13 mile	*Salmo trutta*		169		30 (11-48)	73 (23-121)	356	155267 (1895-30000)	1469 (559-1695)	
	Cottus bairdii	1163 (791-1488)	169 (169-580)		93 (41-130)	281 (236-357)	356		2373 (559-4520)	651 (651-1579)
	Diptera		133 (133-494)		104 (93-226)	164 (100-1250)				
	Trichoptera		400 (280-520)		141 (133-148)	261 (243-279)				
	Baetidae				100	168 (136-182)				9211 (9211-9211)
	Periphyton	1977 (347-4000)	424.5 (189-880)		137 (48-307)	2858 (1357-6429)	1800 (318-7615)		8249 (8249-8249)	1461 (1461-8553)

Table 3.11. Median (range) of calculated BAFs (L/kg) for biota during August (summer) of 2014. AMI, amitriptyline; CAF, caffeine; CAR, carbamazepine; DIL, diltiazem; DPH, diphenhydramine; FLU, fluoxetine; MPH methylphenidate; NOR, norfluoxetine; SER, sertraline.

		Analyte								
Site	Organism	AMI (L/kg)	CAF (L/kg)	CAR (L/kg)	DIL (L/kg)	DIP (L/kg)	FLU (L/kg)	MPH (L/kg)	NOR (L/kg)	SER (L/kg)
0.15 mile	*Salmo trutta*	119 (48-552)	28 (28-97)		11 (9-61)	23 (18-85)	227 (187-867)	625 (45-2150)	2091 (1808-4746)	3750 (1974-13158)
	Cottus bairdii	300 (217-448)	28 (28-113)	6.5 (2-8)	46 (23-56)	83 (50-112)	260 (140-440)	15 (15-35)	6328 (3503-8701)	6974 (4737-10921)
	Trichoptera		80	21 (21-21)	35 (33-37)	81 (65-96)	264 (247-280)		4351 (4068-4633)	11053 (6316-15789)
	Periphyton	1379 (690-2069)	32 (32-127)	3 (3-8)	74 (51-101)	500 (223-1308)	547 (447-1067)	50 (20-70)		34211 (22368-50000)
1.4 mile	*Salmo trutta*	132 (50-346)	26		14 (8-29)	30 (14-70)	2134 (1088-4268)	2179 (21-4643)	2712 (1469-3955)	2106 (651-5000)
	Cottus bairdii	392 (225-792)	26	6 (5-9)	47 (38-76)	110 (90-290)	2929 (2008-4603)	21 (21-71)	6102 (4407-9379)	5526 (3421-8421)
	Lymnaeidea & Physidae	917 (833-1208)	20 (20-45)	15 (14-19)	53 (48-86)	220 (180-280)	3431 (2008-4100)	29	2034 (576-6441)	15789 (11711-93421)
	Trichoptera	1083 (750-1250)	20	4.5 (3-6)	27 (22-37)	225 (125-240)	4352 (3264-4937)	29 (29-57)	576 (576-576)	30263 (21053-42105)
	Periphyton	833 (542-1375)	29	3 (3-3)	48 (29-62)	325 (115-900)	5523 (2510-6025)	57 (29-86)		19737 (6842-25000)
13 mile	*Salmo trutta*		42		40 (20-293)	41	356	13715 (2286-81429)	559 (559-2373)	651 (651-11579)
	Cottus bairdii	177	42	3 (3-7)	87 (60-127)	175 (125-200)	356		1808 (1243-3051)	651
	Trichoptera		150 (100-175)	17 (14-20)	127 (120-127)	1000 (938-1063)	1005 (837-1172)		1808	2303 (2237-2368)
	Periphyton		47 (47-120)		80 (33-113)	2125 (1625-5875)				

Table 3.12. Median (range) of calculated BAFs (L/kg) for biota during October (fall) of 2014. AMI, amitriptyline; CAF, caffeine; CAR, carbamazepine; DIL, diltiazem; DPH, diphenhydramine; FLU, fluoxetine; MPH methylphenidate; NOR, norfluoxetine; SER, sertraline.

		Analyte								
Site	Organism	AMI (L/kg)	CAF (L/kg)	CAR (L/kg)	DIL (L/kg)	DIP (L/kg)	FLU (L/kg)	MPH (L/kg)	NOR (L/kg)	SER (L/kg)
0.15 mile	*Salmo trutta*	143 (46-750)	19		15 (6-62)	21 (7-88)	53 (26-103)	1313 (244-3438)	70 (36-168)	240 (93-420)
	Cottus bairdii	161 (107-236)	19	3 (3-3)	25 (16-39)	48 (33-73)	32 (11-55)		132 (82-161)	153 (113-360)
	Trichoptera	161 (121-168)		10 (7-13)	13 (6-41)	79 (64-121)	47 (26-124)		61 (57-71)	224 (193-640)
	Periphyton	1536 (1036-1643)	21		60 (46-72)	239 (209-258)	232 (179-289)	81 (56-100)	46 (22-79)	3600 (2733-4400)
1.4 mile	*Salmo trutta*	552 (466-621)	19		21	38 (29-57)	39 (11-108)	3190 (569-7414)	31 (11-66)	169 (53-382)
	Cottus bairdii	1009 (276-2586)	19		122 (57-893)	171 (73-275)	38 (11-64)		68 (47-117)	182 (109-400)
	Trichoptera				67 (46-125)	250 (167-483)	77 (56-172)			823 (755-891)
	Periphyton	3103 (2069-5862)	21		100 (68-200)	575 (533-1167)	118 (82-282)	69 (69-190)		1455 (773-3182)
13 mile	*Salmo trutta*		6		167 (157-176)	76 (76-477)	19 (19-95)	21429 (1000-62857)	559 (559-2486)	160
	Cottus bairdii	837	15 (6-56)		265 (176-294)	360 (209-465)	19		559 (559-1921)	66 (66-160)
	Trichoptera				265 (108-314)	1279 (291-1744)				
	Periphyton				373 (294-392)	5581 (5000-6512)				600 (148-880)

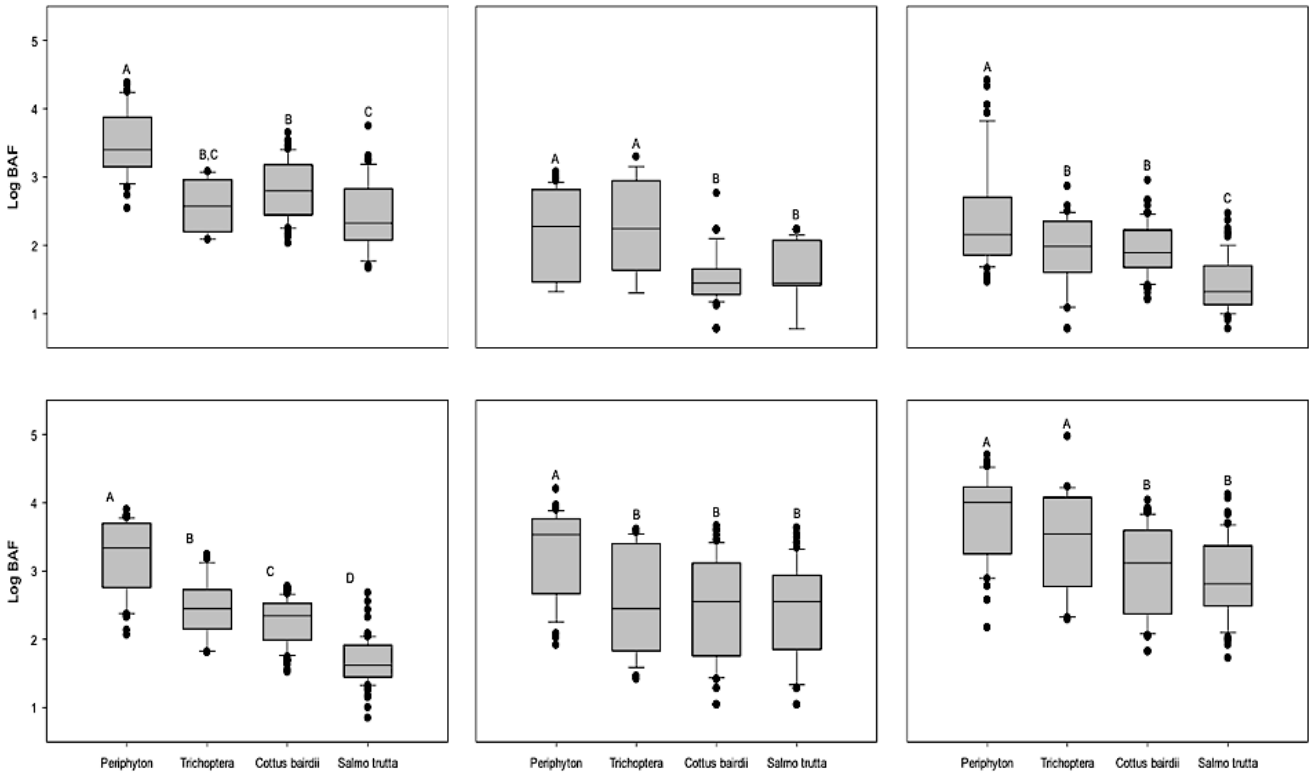

Figure 3.7. Boxplots of periphyton, Trichoptera, Cottus bairdii, and Salmo trutta BAFs for amitriptyline (A), diltiazem (B), diphenhydramine (C), fluoxetine (D), norfluoxetine (E), and sertraline (F) at all distance during all seasons downstream of the East Canyon Water Reclamation Facility discharge to East Canyon Creek, Park City, Utah, USA. Letters above boxplots represent significant ($p<0.05$) differences in accumulation between species.

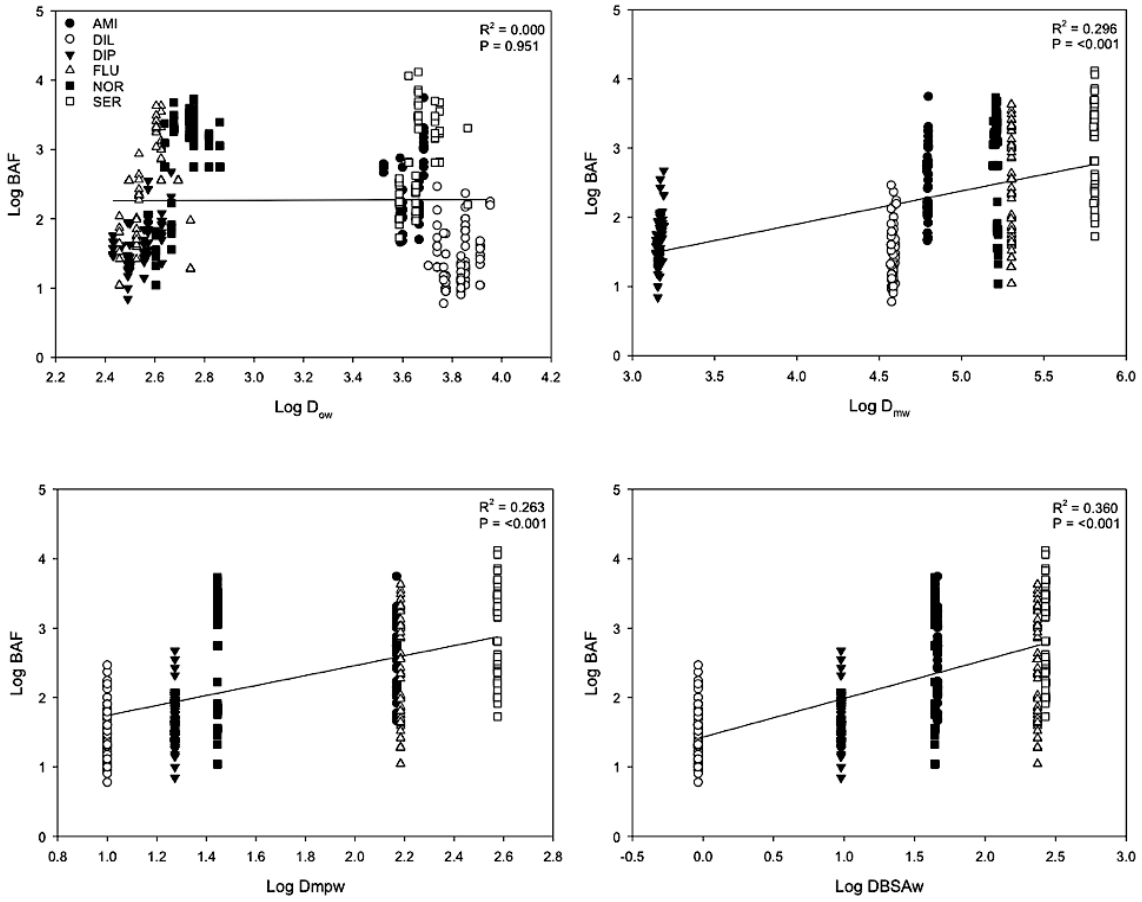

Figure 3.8. Relationship between the calculated bioaccumulation factoss (BAFs) of amitriptyline, diltiazem, diphenhydramine, fluoxetine, norfluoxetine, and sertraline in Salmo trutta versus calculated distribution coefficients (Log Dow, Log Dmw, Log Dmpw, and Log DBSAw).

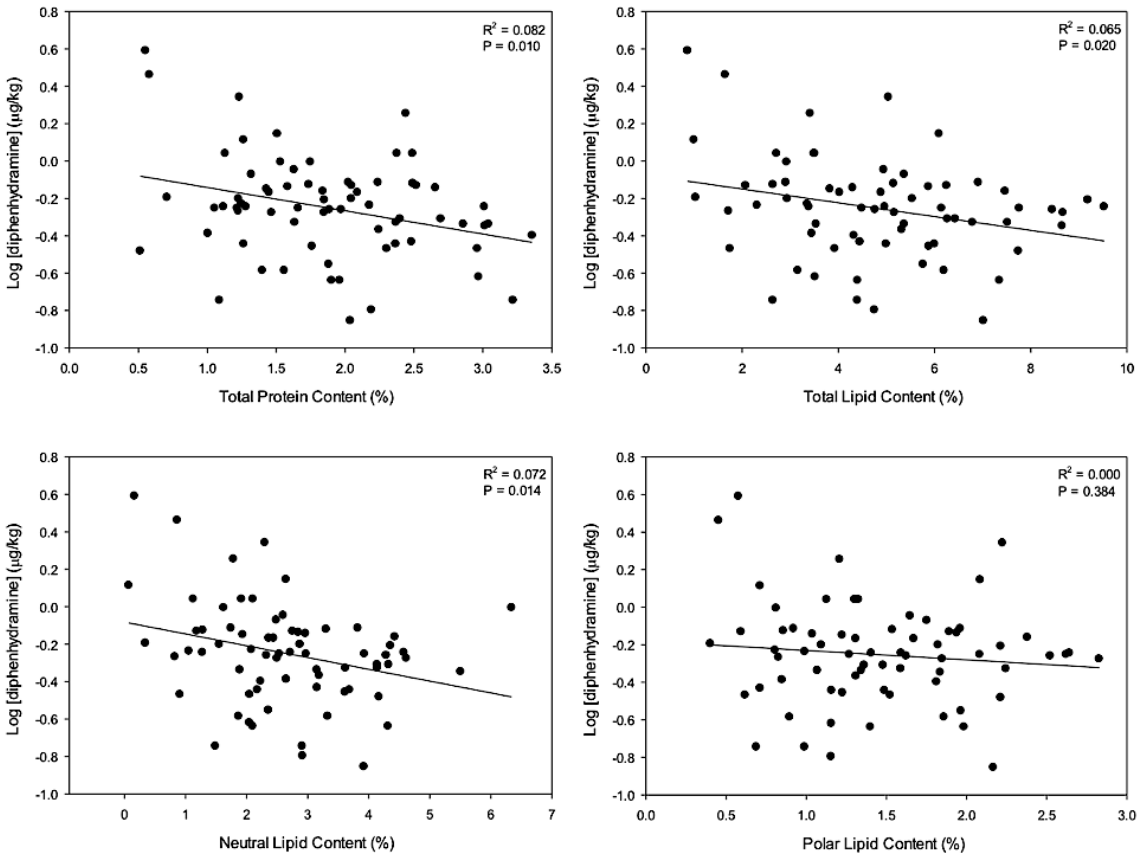

Figure 3.9. Relationship between the concentration of diphenhydramine (µg/kg) to total protein (%), total lipid (%), neutral lipids (%), and storage lipids (%) in Salmo trutta from all sites during all seasons downstream of the East Canyon Water Reclaimation Facility discharge.

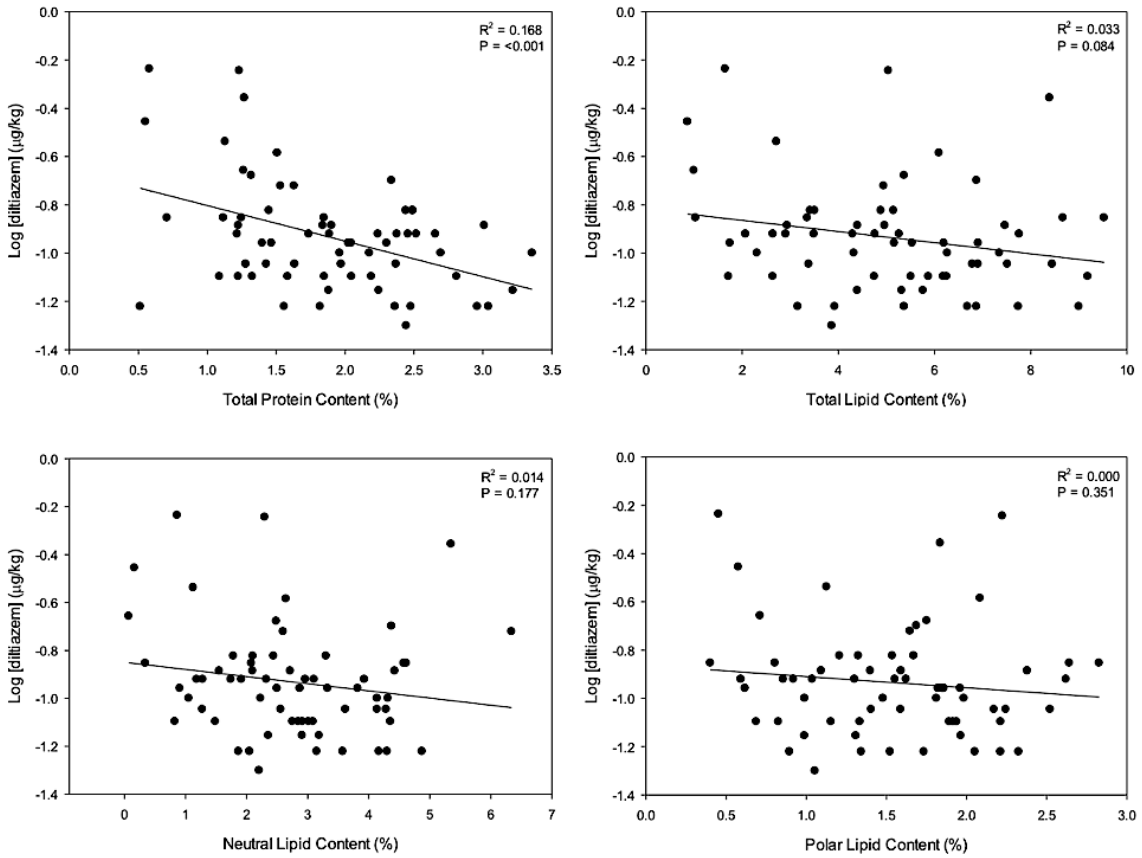

Figure 3.10. Relationship between the concentration of diltiazem (µg/kg) to total protein (%), total lipid (%), neutral lipids (%), and storage lipids (%) in Salmo trutta from all sites during all seasons downstream of the East Canyon Water Reclaimation Facility discharge. Target analytes with >50% detection above the MDL were used in regression analysis.

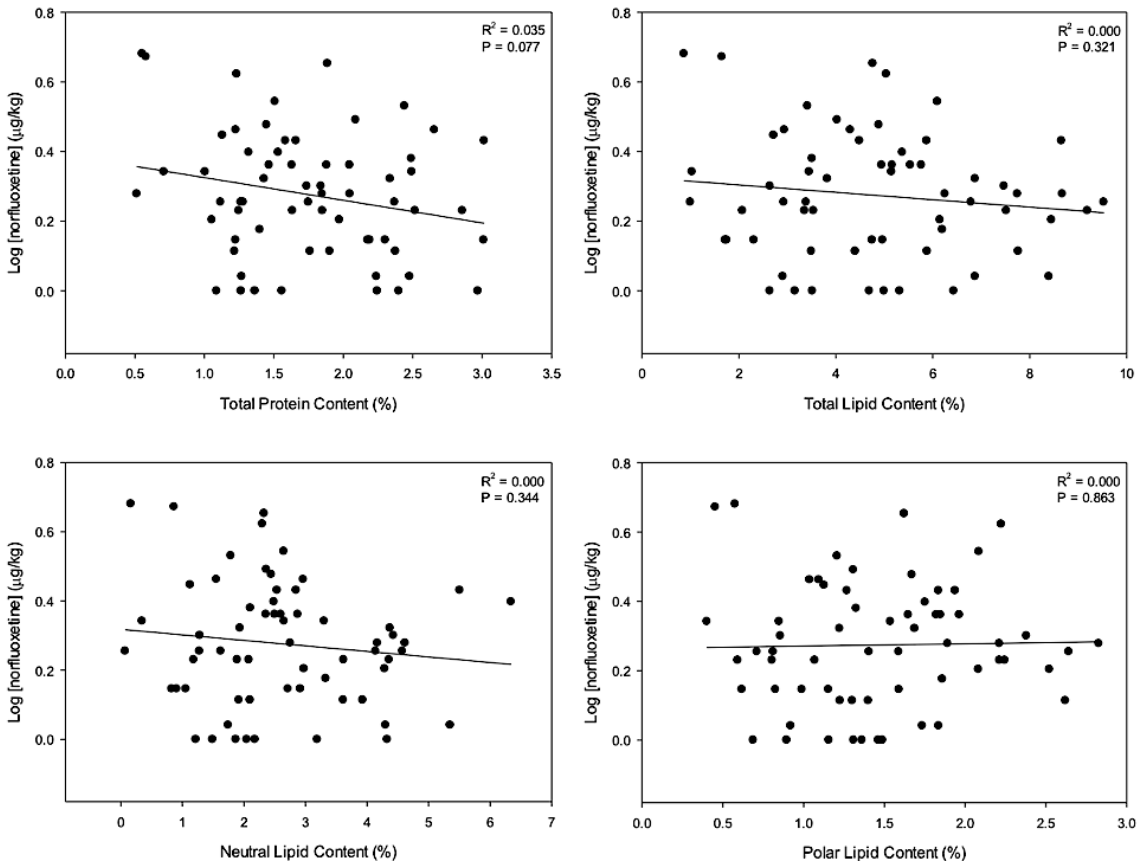

Figure 3.11. Relationship between the concentration of norfluoxetine (µg/kg) to total protein (%), total lipid (%), neutral lipids (%), and storage lipids (%) in Salmo trutta from all sites during all seasons downstream of the East Canyon Water Reclaimation Facility discharge. Target analytes with >50% detection above the MDL were used in regression analysis.

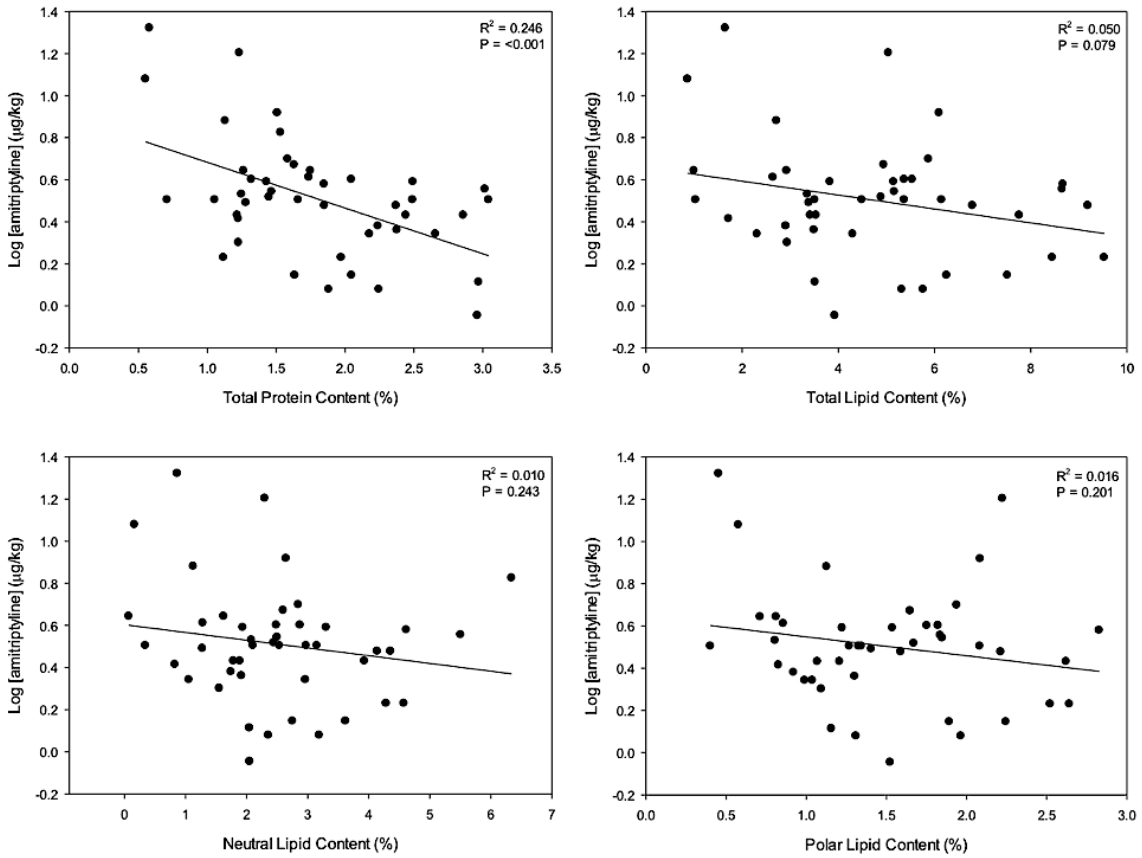

Figure 3.12. Relationship between the concentration of amitriptyline (µg/kg) to total protein (%), total lipid (%), neutral lipids (%), and storage lipids (%) in Salmo trutta from all sites during all seasons downstream of the East Canyon Water Reclaimation Facility discharge. Target analytes with >50% detection above the MDL were used in regression analysis.

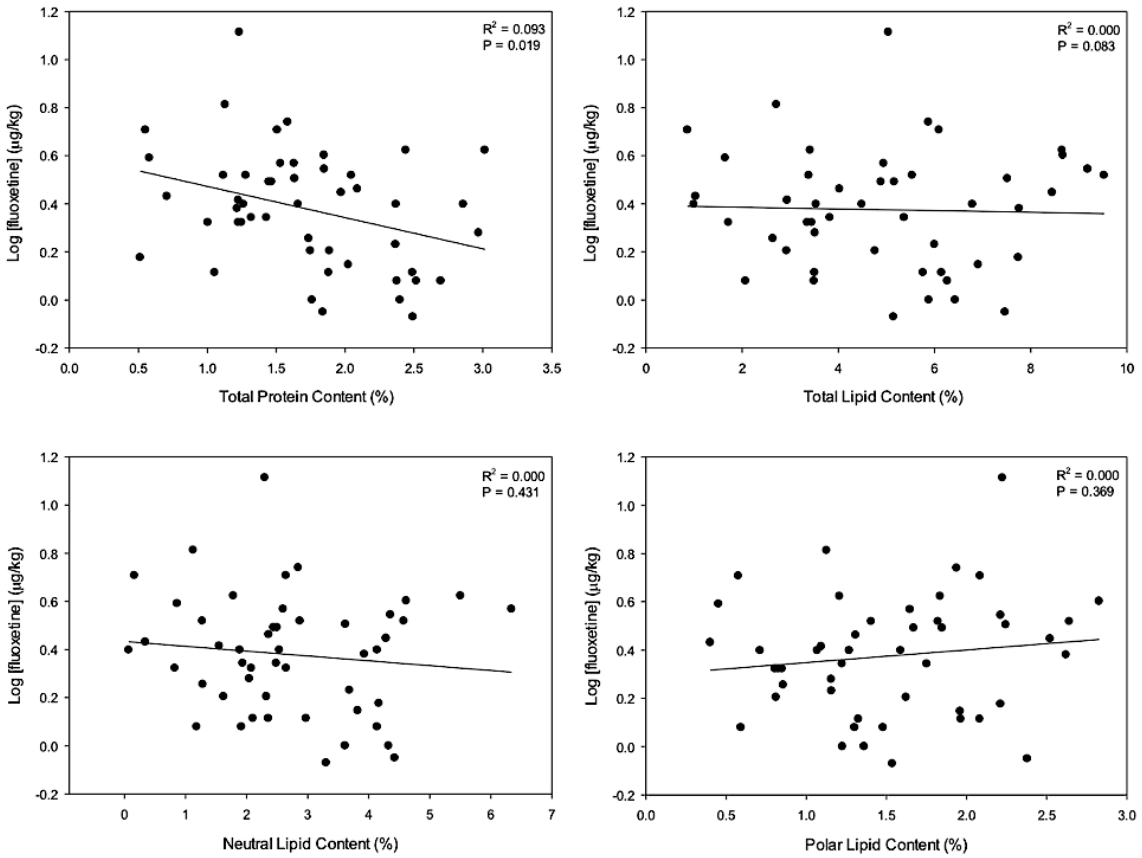

Figure 3.13. Relationship between the concentration of fluoxetine (µg/kg) to total protein (%), total lipid (%), neutral lipids (%), and storage lipids (%) in Salmo trutta from all sites during all seasons downstream of the East Canyon Water Reclaimation Facility discharge. Target analytes with >50% detection above the MDL were used in regression analysis.

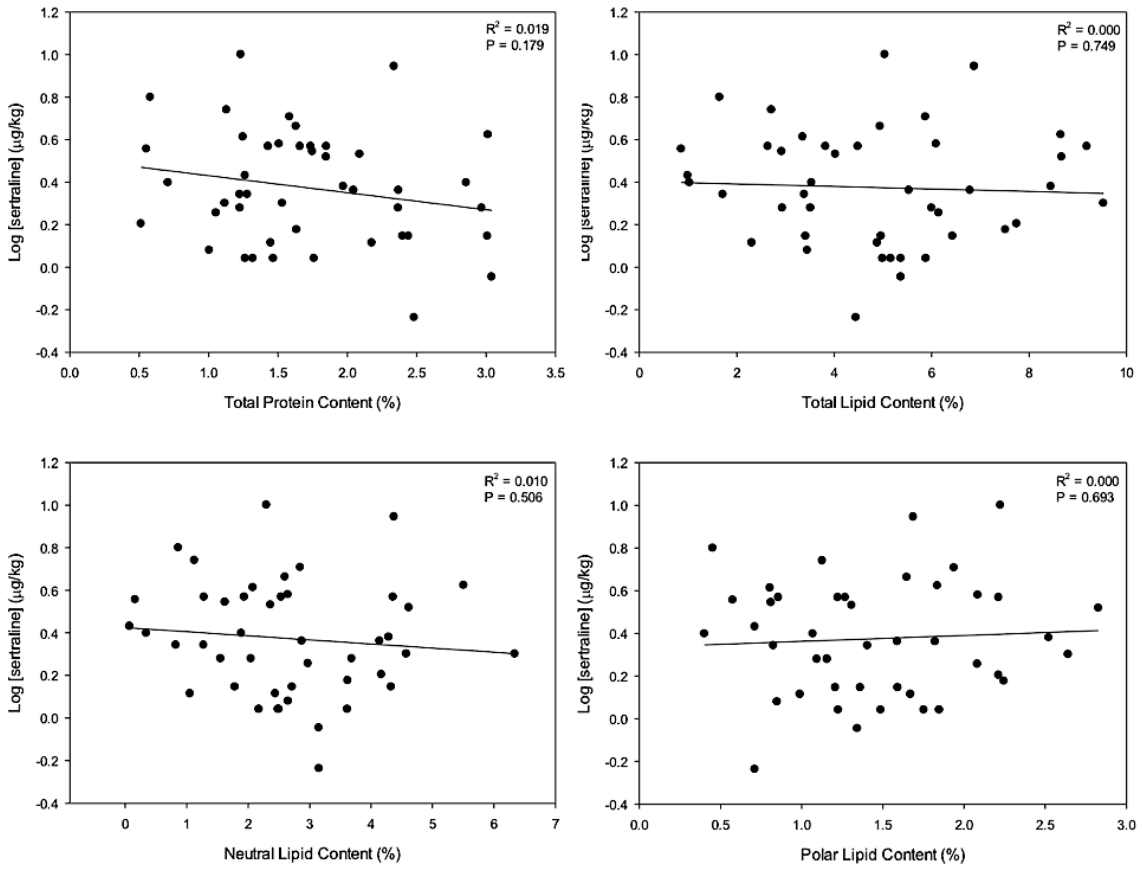

Figure 3.14. Relationship between the concentration of sertraline (µg/kg) to total protein (%), total lipid (%), neutral lipids (%), and storage lipids (%) in Salmo trutta from all sites during all seasons downstream of the East Canyon Water Reclaimation Facility discharge. Target analytes with >50% detection above the MDL were used in regression analysis.

Characterization of the Food Web

Functional food chains were identified by examining $\delta^{13}C$ in the mixing space of $\delta^{15}N$ to $\delta^{13}C$ bi-plots (Figure 3.15). Stable isotopes ($\delta^{15}N$, $\delta^{13}C$), TPs for organisms collected, and baseline values used to calculate TPs are given in Tables 3.13-3.15. TPs for all organisms ranged from 1.82-4.06 ($\delta^{15}N$ 9.80-20.00 ‰) during spring, 1.66-3.39 ($\delta^{15}N$ 10.18-20.32 ‰) during summer, and 0.23-3.09 ($\delta^{15}N$ 5.41-20.28 ‰) during fall. Periphyton was assumed to occupy the lowest TP (primary producers) and make up the bottom of the food chain. The range of TPs for periphtyton were 1.96-3.03 ($\delta^{15}N$ 10.02-15.04 ‰) during spring, 1.66-2.86 ($\delta^{15}N$ 10.18-17.82 ‰) during summer, and 0.23-1.72 ($\delta^{15}N$ 5.41-17.21 ‰) during fall. Invertebrates were considered to occupy the next TP (primary consumers) ranging from 1.82-2.89 ($\delta^{15}N$ 9.80-16.01 ‰) during spring, 1.79-2.63 ($\delta^{15}N$ 10.35-18.20 ‰) during summer, and 1.46-2.41 ($\delta^{15}N$ 9.59-19.04 ‰) during fall. *Cottus bairdii* were considered to occupy the next TP (secondary consumers) with TPs ranging from 3.12-3.96 ($\delta^{15}N$ 13.78-19.66 ‰) during spring, 2.09-3.04 ($\delta^{15}N$ 13.66-19.41 ‰) during summer, and 2.29-2.98 ($\delta^{15}N$ 13.73-20.25 ‰) during fall. Finally, *Salmo trutta* were considered to occupy the highest TP (tertiary consumer) with TPs ranging from 3.25-4.06 ($\delta^{15}N$ 14.60-20.00 ‰) during spring, 2.59-3.39 ($\delta^{15}N$ 14.01-20.32 ‰) during summer, and 1.15-3.09 ($\delta^{15}N$ 13.68-20.28 ‰) during fall.

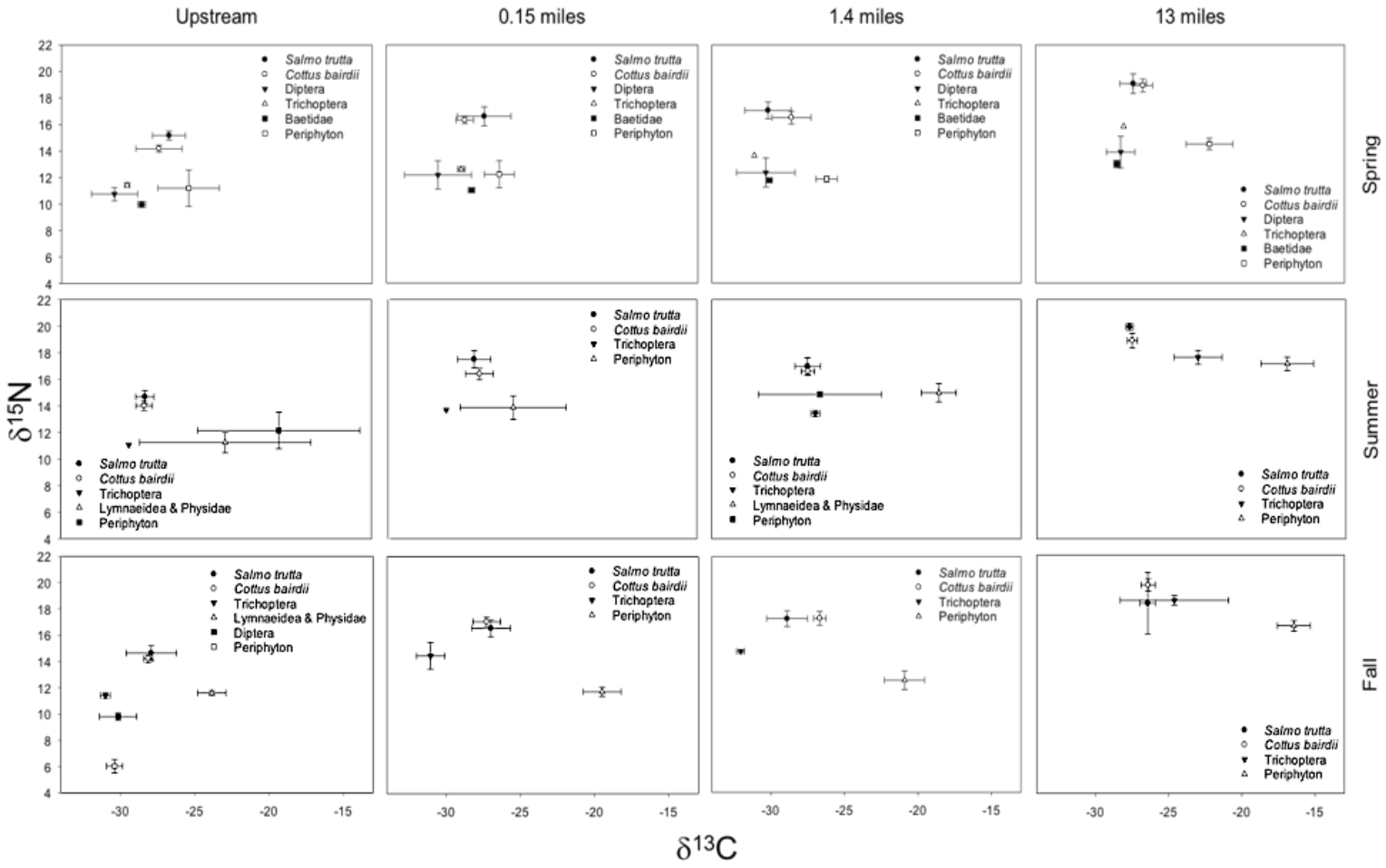

Figure 3.15. δ13C to δ15N scatter plot of all species collected during three seasons (spring, summer, fall) at three distances (0.15, 1.4, 13 miles) downstream of the East Canyon Water Reclamation Facility discharge and the upstream reference site in Park City, Utah, USA.

Table 3.13. Summary of stable isotopes ($\delta^{13}C$ & $\delta^{15}N$) and trophic position for all organisms at three distances downstream of the ECWRF discharge during spring 2014. Bold values represent the baseline at each site used to calculate trophic position.

			$\delta^{13}C$ (‰)	$\delta^{15}N$ (‰)	Trophic Position
Site	Organism	n	Mean ± SD	Mean ± SD	Mean ± SD
Upstream	Salmo trutta	5	-26.75 ± 1.12	15.17 ± 0.34	3.53 ± 0.10
	Cottus bairdii	5	-27.42 ± 1.56	14.18 ± 0.25	3.23 ± 0.07
	Diptera	5	-30.44 ± 1.56	10.75 ± 0.50	2.23 ± 0.15
	Trichoptera	5	-29.58 ± 0.15	11.43 ± 0.12	2.42 ± 0.03
	Baetidae	5	-28.60 ± 0.26	**9.98** ± 0.21	2.00 ± 0.06
	Periphyton	5	-25.42 ± 2.08	11.20 ± 1.38	2.36 ± 0.40
0.15 mile	Salmo trutta	5	-27.41 ± 1.81	16.60 ± 0.72	3.64 ± 0.21
	Cottus bairdii	5	-28.72 ± 0.59	16.32 ± 0.27	3.56 ± 0.08
	Diptera	4	-30.53 ± 2.26	12.17 ± 1.07	2.34 ± 0.03
	Trichoptera	5	-28.95 ± 0.26	12.61 ± 0.17	2.47 ± 0.05
	Baetidae	4	-28.27 ± 0.22	**11.02** ± 0.13	2.00 ± 0.04
	Periphyton	5	-26.40 ± 1.01	12.22 ± 1.03	2.35 ± 0.30
1.4 mile	Salmo trutta	5	-30.19 ± 1.57	17.05 ± 0.63	3.55 ± 0.19
	Cottus bairdii	5	-28.60 ± 1.33	16.51 ± 0.48	3.39 ± 0.14
	Diptera	4	-30.34 ± 1.99	12.35 ± 1.10	2.17 ± 0.32
	Trichoptera	1	-31.12	13.64	2.55
	Baetidae	5	-30.09 ± 0.19	**11.77** ± 0.06	2.00 ± 0.02
	Periphyton	5	-26.21 ± 0.72	11.86 ± 0.23	2.03 ± 0.07
13 mile	Salmo trutta	5	-27.37 ± 0.90	19.07 ± 0.74	3.79 ± 0.22
	Cottus bairdii	5	-26.71 ± 0.67	18.93 ± 0.48	3.74 ± 0.14
	Diptera	5	-28.22 ± 0.97	13.90 ± 1.20	2.26 ± 0.35
	Trichoptera	2	-28.02	15.84	2.83
	Baetidae	4	-28.49 ± 0.20	**13.00** ± 0.28	2.00 ± 0.08
	Periphyton	5	-22.19 ± 1.59	14.51 ± 0.44	2.44 ± 0.13

Table 3.14. Summary of stable isotopes ($\delta^{13}C$ & $\delta^{15}N$) and trophic position for all organisms at three distances downstream of the ECWRF discharge during summer 2014. Bold values represent the baseline at each site used to calculate trophic position.

			$\delta^{13}C$ (‰)	$\delta^{15}N$ (‰)	Trophic Position
Site	Organism	n	Mean ± SD	Mean ± SD	Mean ± SD
Upstream	Salmo trutta	5	-28.32 ± 0.62	14.69 ± 0.47	3.06 ± 0.14
	Cottus bairdii	5	-28.37 ± 0.55	14.02 ± 0.37	2.87 ± 0.11
	Trichoptera	2	-29.40	**11.08**	2.00
	Lymnaeidea & Physidae	5	-22.89 ± 5.78	11.25 ± 0.77	2.05 ± 0.23
	Periphyton	5	-19.26 ± 5.48	12.16 ± 1.38	2.32 ± 0.41
0.15 mile	Salmo trutta	5	-28.24 ± 1.14	17.51 ± 0.65	3.12 ± 0.19
	Cottus bairdii	5	-27.88 ± 0.95	16.41 ± 0.43	2.80 ± 0.13
	Trichoptera	2	-30.15	**13.70**	2.00
	Periphyton	5	-25.57 ± 3.61	13.89 ± 0.87	2.06 ± 0.26
1.4 mile	Salmo trutta	5	-27.50 ± 0.86	16.99 ± 0.62	3.04 ± 0.18
	Cottus bairdii	5	-27.49 ± 0.45	16.61 ± 0.30	2.93 ± 0.09
	Trichoptera	5	-26.97 ± 0.30	**13.44** ± 0.22	2.00 ± 0.07
	Lymnaeidea & Physidae	4	-18.58 ± 1.18	14.99 ± 0.68	2.46 ± 0.20
	Periphyton	5	-26.66 ± 4.18	14.87 ± 0.18	2.42 ± 0.05
13 mile	Salmo trutta	5	-27.70 ± 0.25	19.95 ± 0.25	2.67 ± 0.07
	Cottus bairdii	5	-27.52 ± 0.34	18.92 ± 0.55	2.37 ± 0.16
	Trichoptera	3	-23.05 ± 1.63	**17.66** ± 0.51	2.00 ± 0.15
	Periphyton	5	-16.98 ± 1.79	17.18 ± 0.50	1.86 ± 0.15

Table 3.15. Summary of stable isotopes ($\delta^{13}C$ & $\delta^{15}N$) and trophic position for all organisms at three distances downstream of the ECWRF discharge during fall 2014. Bold values represent the baseline at each site used to calculate trophic position.

			$\delta^{13}C$ (‰)	$\delta^{15}N$ (‰)	Trophic Position
Site	Organism	n	Mean ± SD	Mean ± SD	Mean ± SD
Upstream	Salmo trutta	5	-27.93 ± 1.69	14.64 ± 0.57	2.94 ± 0.17
	Cottus bairdii	5	-28.13 ± 0.30	14.21 ± 0.30	2.82 ± 0.09
	Trichoptera	5	-31.01 ± 0.34	**11.42** ± 0.20	2.00 ± 0.06
	Lymnaeidea & Physidae	4	-23.85 ± 0.94	11.60 ± 0.17	2.05 ± 0.05
	Diptera	5	-30.15 ± 1.25	9.81 ± 0.28	1.50 ± 0.08
	Periphyton	5	-30.39 ± 0.54	6.04 ± 0.50	0.42 ± 0.15
0.15 mile	Salmo trutta	5	-26.99 ± 1.29	16.56 ± 0.64	2.62 ±0.19
	Cottus bairdii	5	-27.28 ± 0.92	17.06 ± 0.35	2.76 ± 0.10
	Trichoptera	7	-31.06 ± 0.94	**14.46** ± 1.01	2.00 ± 0.30
	Periphyton	5	-19.49 ± 1.28	11.74 ± 0.34	1.20 ± 0.10
1.4 mile	Salmo trutta	5	-28.89 ± 1.39	17.26 ± 0.59	2.73 ± 0.17
	Cottus bairdii	5	-26.68 ± 0.42	17.28 ± 0.53	2.74 ± 0.16
	Trichoptera	5	-32.04 ± 0.27	**14.76** ± 0.14	2.00 ± 0.04
	Periphyton	5	-20.91 ± 1.36	12.56 ± 0.71	1.35 ± 0.21
13 mile	Salmo trutta	5	-26.43 ± 0.54	18.37 ± 2.33	1.94 ± 0.69
	Cottus bairdii	5	-26.40 ± 0.48	19.74 ± 0.46	2.34 ± 0.14
	Trichoptera	7	-24.61 ± 3.70	**18.58** ± 0.35	2.00 ± 0.10
	Periphyton	5	-16.44 ± 1.12	16.66 ± 0.39	1.55 ± 0.11

Trophic Transfer of Select Pharmaceuticals

In total, 35 regressions for six target analytes, DIP (Figure 3.16), AMI, CAF, DIL, FLU, and SER (Figures 3.17-3.21), were performed to calculate TMFs, which ranged from 0.01-0.71 (Table 3.16). Negative slopes were observed for all 35 regressions, with significantly ($p<0.05$) negative slopes observed in 32 of the 35 regressions. Statistical power for 8 of these 35 regression relationships fell below a recommended value of 0.80 (Conder, et al. 2012). However, the calculated 95% confidence intervals around the TMFs demonstrated that the calculated TMF values for all significant ($p<0.05$) regressions fell below 1.

Discussion

We recently observed trophic dilution of the ionizable weak base pharmaceutical DIP (Du, et al. 2014a) in an effluent dependent stream in central Texas, USA. In the present study, we extended these efforts to other classes of pharmaceuticals to examine whether trophic transfer of APIs would differ with ecological and spatiotemporal complexity. Consistent with our previous observations (Du, et al. 2014a), trophic dilution was observed for DIP in the present study (Figure 3.16). Further, trophic dilution was observed for five other pharmaceuticals, AMI, CAF, DIL, FLU, and SER (Figures 3.17-3.21). Such observed trophic dilution of ionizable pharmaceuticals are in agreement with recent observations from a freshwater lake system (Xie, et al. 2015; Xie, et al. 2017) and several constructed field and laboratory systems (Bostrom, et al. 2017; Ding, et al. 2015b; Ding, et al. 2015a; Lagesson, et al. 2016; Ruhi, et al. 2016). It is important to note that a common assumption when calculating a TMF is that exposure and ecosystem conditions are ubiquitous for all organism within a system.

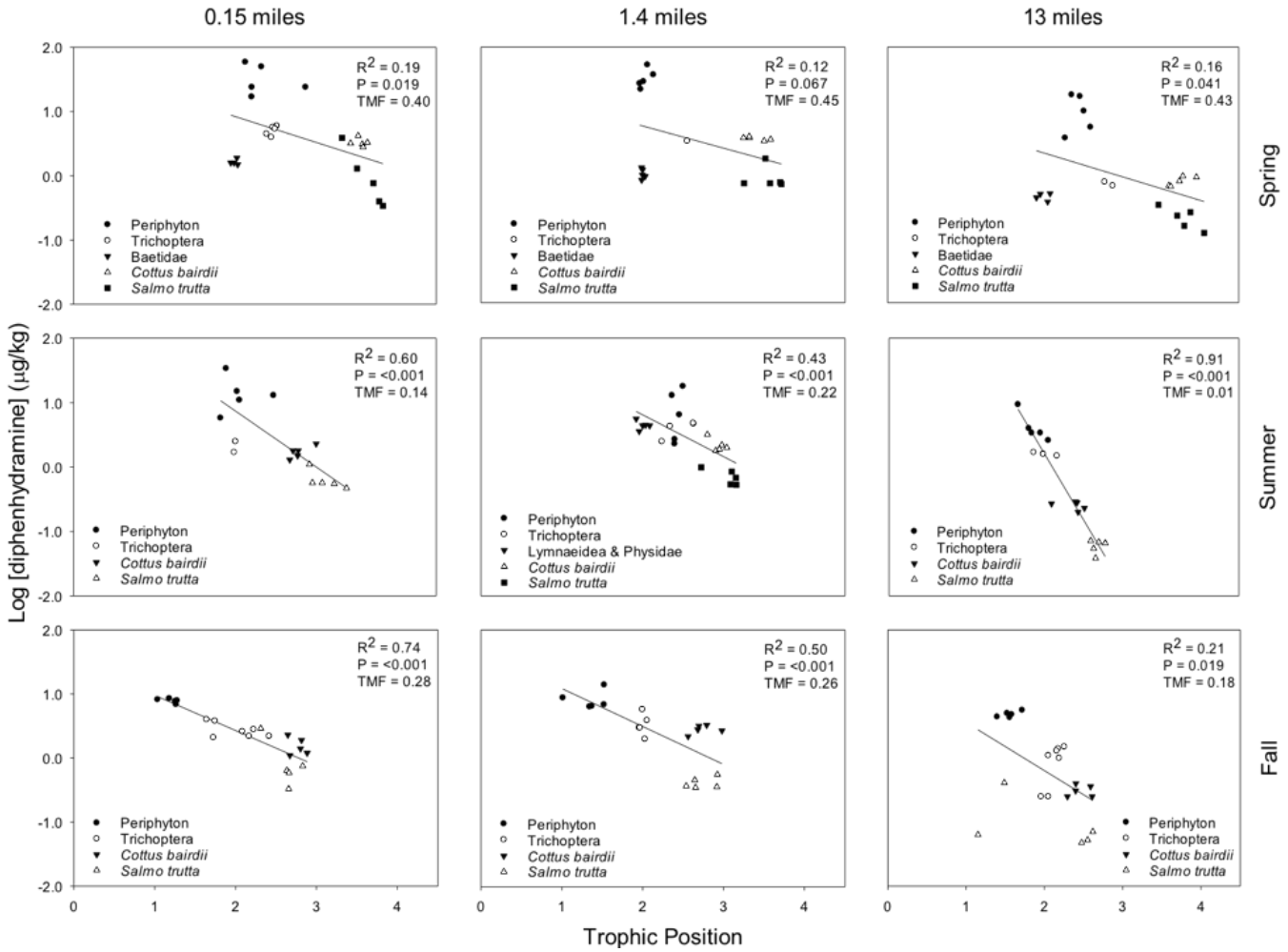

Figure 3.16. Diphenhydramine trophic magnification factors (TMFs) for three sites (0.15, 1.4, 13 miles) downstream of the East Canyon Water Reclamation Facility discharge to East Canyon Creek, Park City, Utah, USA during three different seasons (spring, summer, fall).

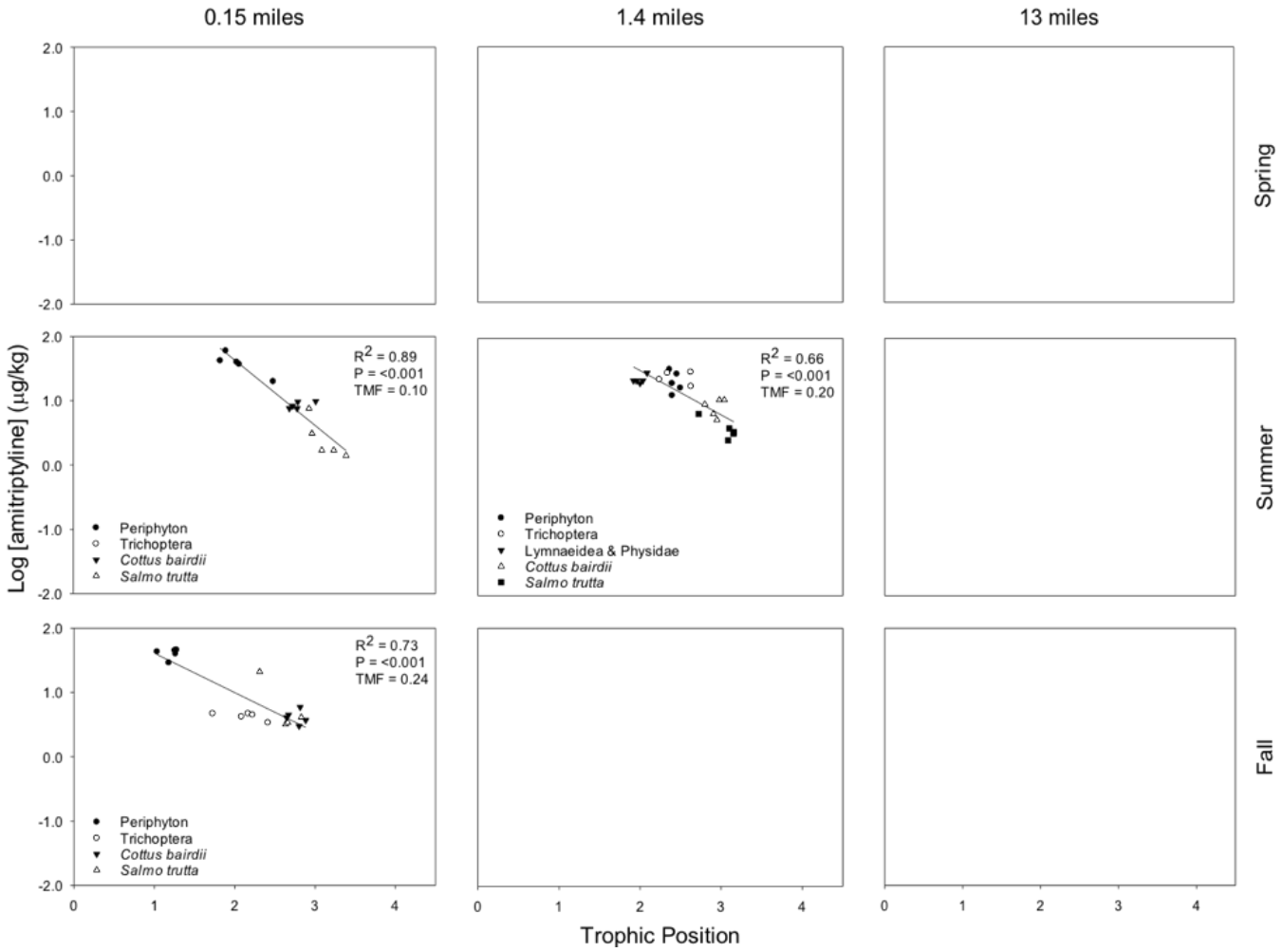

Figure 3.17. Amitriptyline trophic magnification factors (TMFs) for three sites (0.15, 1.4, 13 miles) downstream of the East Canyon Water Reclamation Facility discharge at East Canyon Creek, Park City, Utah, USA during three different seasons (spring, summer, fall) of 2014.

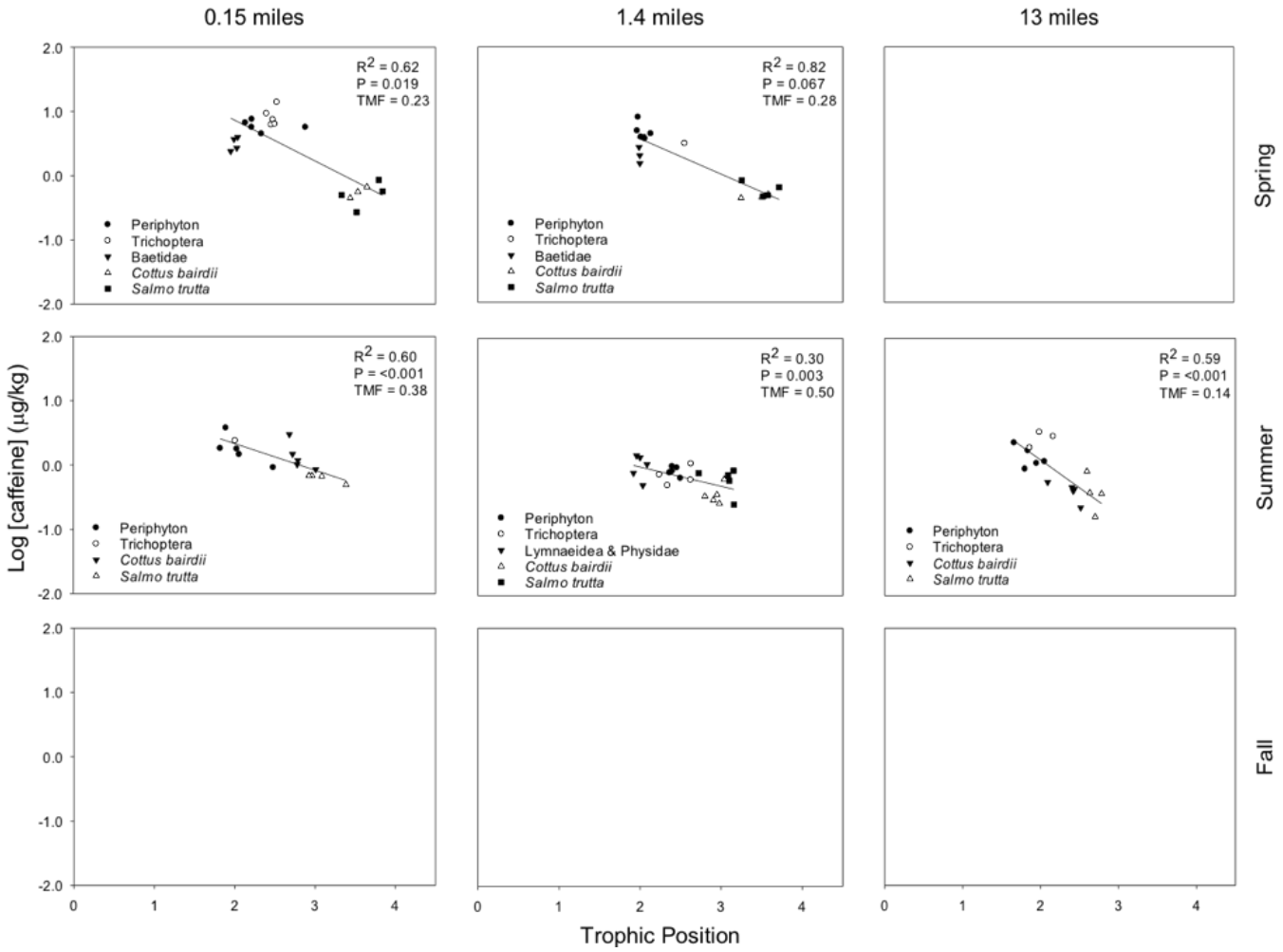

Figure 3.18. Caffeine trophic magnification factors (TMFs) for three sites (0.15, 1.4, 13 miles) downstream of the East Canyon Water Reclamation Facility discharge at East Canyon Creek, Park City, Utah, USA during three different seasons (spring, summer, fall) of 2014.

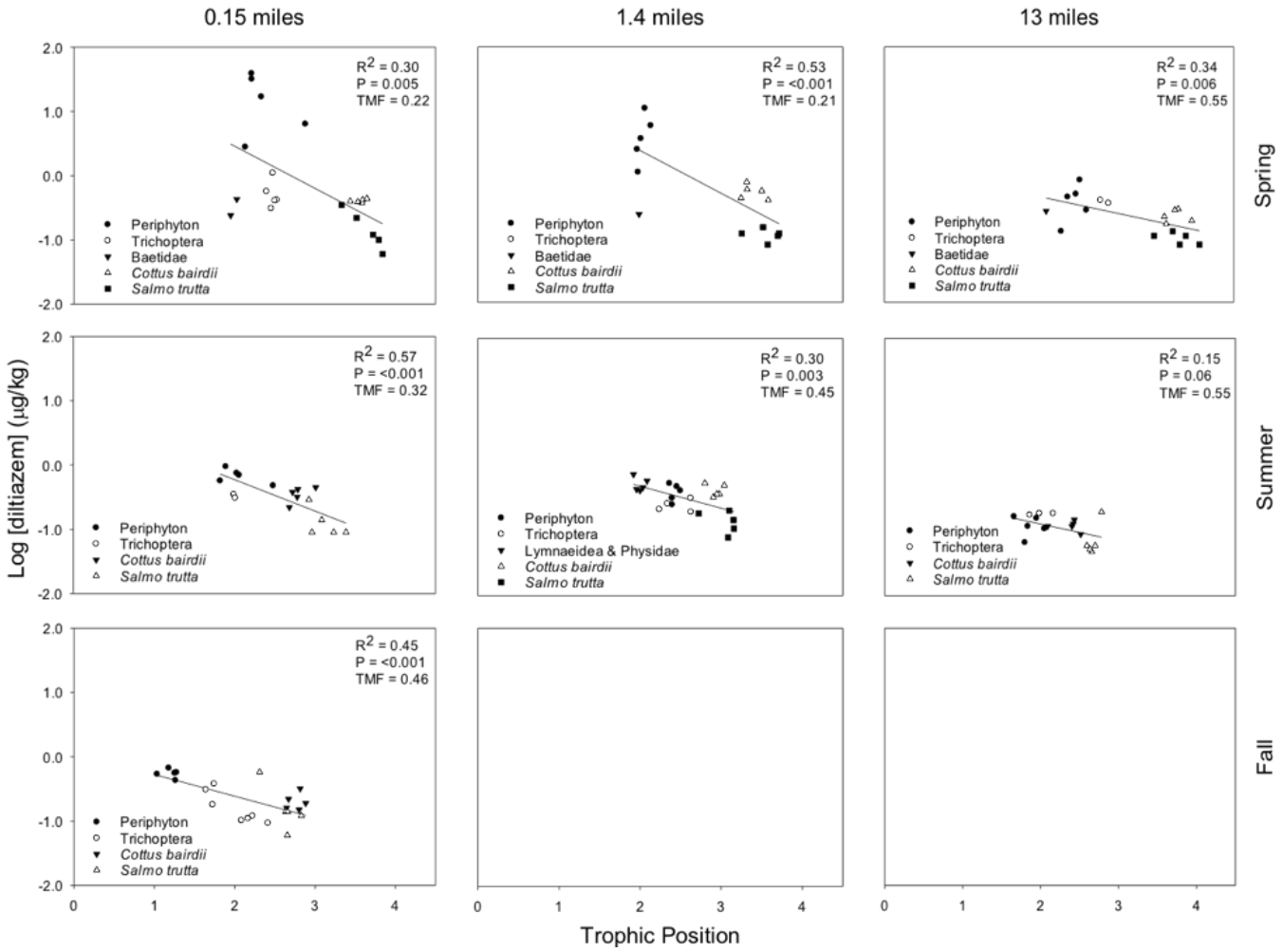

Figure 3.19. Diltiazem trophic magnification factors (TMFs) for three sites (0.15, 1.4, 13 miles) downstream of the East Canyon Water Reclamation Facility discharge at East Canyon Creek, Park City, Utah, USA during three different seasons (spring, summer, fall) of 2014.

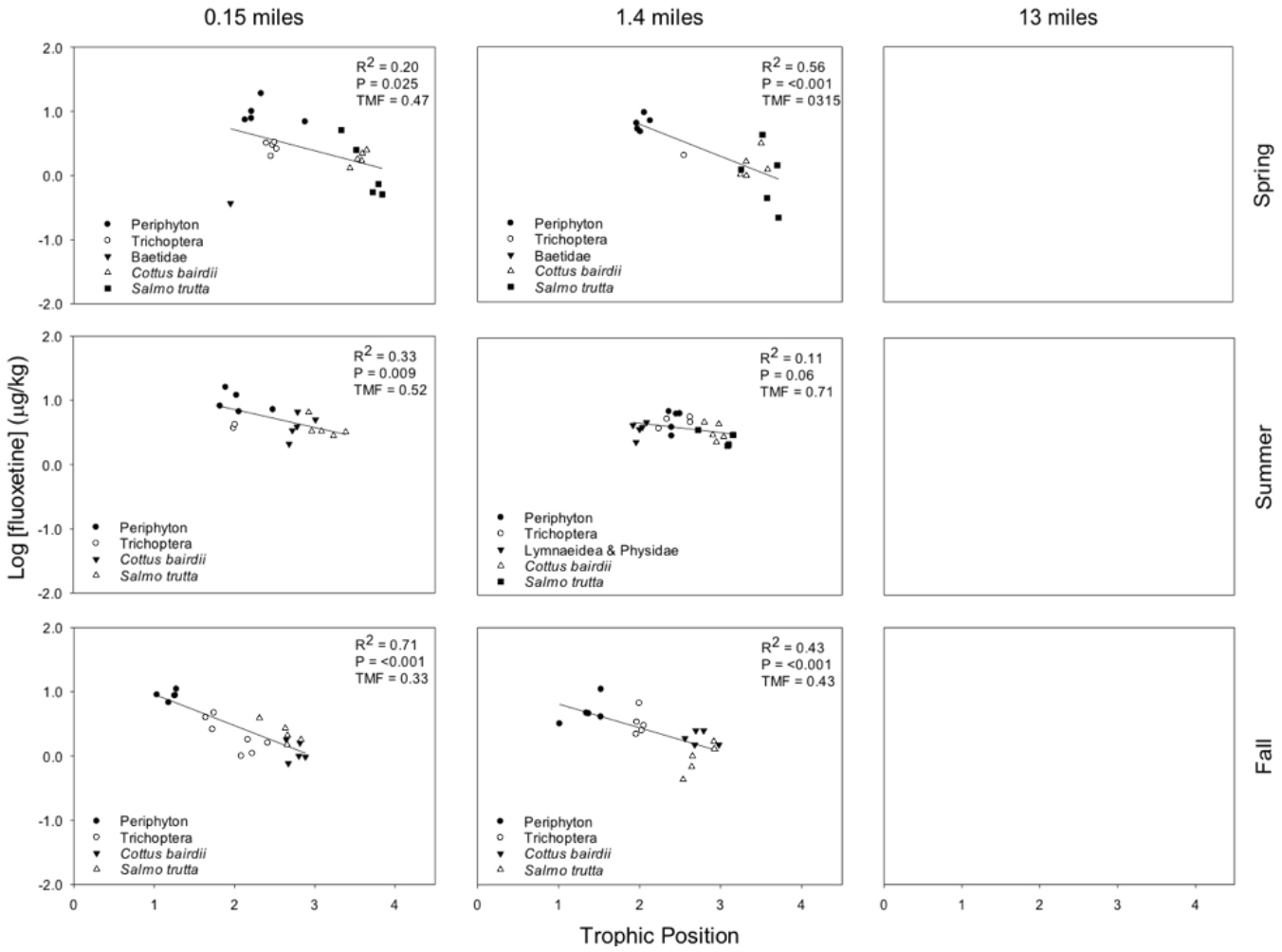

Figure 3.20. Fluoxetine trophic magnification factors (TMFs) for three sites (0.15, 1.4, 13 miles) downstream of the East Canyon Water Reclamation Facility discharge at East Canyon Creek, Park City, Utah, USA during three different seasons (spring, summer, fall) of 2014.

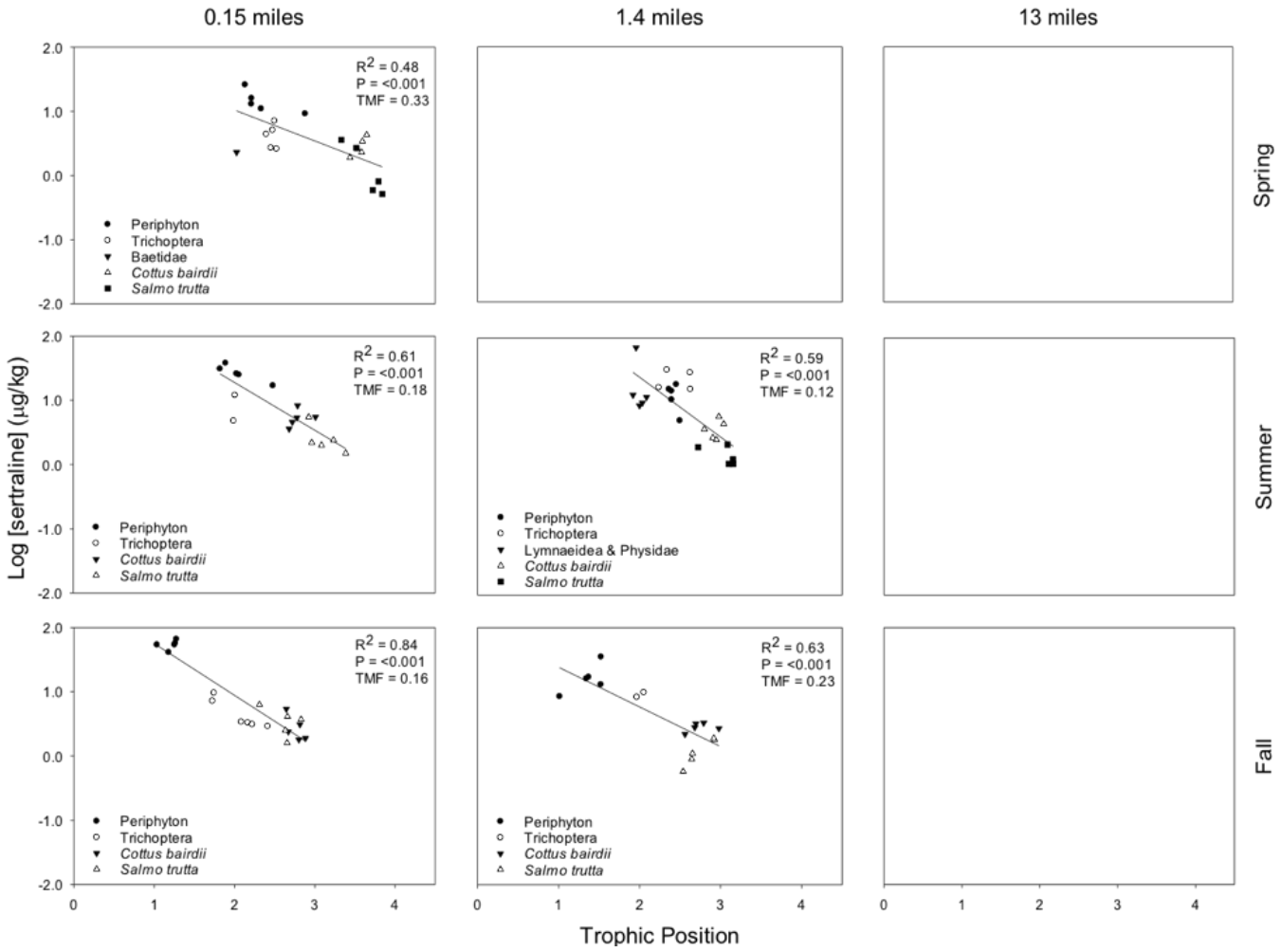

Figure 3.21. Sertraline trophic magnification factors (TMFs) for three sites (0.15, 1.4, 13 miles) downstream of the East Canyon Water Reclamation Facility discharge at East Canyon Creek, Park City, Utah, USA during three different seasons (spring, summer, fall) of 2014.

Table 3.16. Calculated trophic magnification factors (TMFs) and 95% confidence intervals for amitriptyline, caffeine, diltiazem, diphenhydramine, fluoxetine, and sertraline at sampling locations downstream of the East Canyon Water Reclamation Facility discharge during spring, summer, and fall of 2014 in Park City, Utah, USA. TMFs were calculated for compounds at sites with >75% detection and a minimum of three trophic levels. All analyte detection data, including < MDL detections, were used to calculate TMFs. <MDL values were substituted with the measured value as long as the value was above the limit of detection (LOD) and limit of quantification (LOQ) found in Table S12. Additional regression parameters including slope, intercept, 95% confidence intervals of slope and intercept, statistical power, and significance level are reported for each calculated TMF. TMF regressions were considered significant when $p<0.05$.

Analyte	Season	Site (mi)	n	R^2	Slope ± SE	Slope 95% CI	Intercept ± SE	Intercept 95% CI	Power	p-value	TMF	TMF 95% CI
Amitriptyline	Summer	0.15	15	0.89	-1.02 ± 0.10	-1.23, -0.81	3.67 ± 0.26	3.10, 4.23	1.00	<0.001	0.10	0.06 - 0.16
		1.4	24	0.66	-0.69 ± 0.10	-0.90, -0.48	2.88 ± 0.27	2.32, 3.43	1.00	<0.001	0.20	0.13 - 0.33
	Fall	0.15	19	0.73	-0.61 ± 0.09	-0.79, -0.43	2.22 ± 0.20	1.81, 2.63	1.00	<0.001	0.24	0.16 - 0.37
Caffeine	Spring	0.15	21	0.62	-0.64 ± 0.11	-0.86, -0.41	2.14 ± 0.31	1.50, 2.78	0.96	<0.001	0.23	0.14 - 0.39
		1.4	17	0.82	-0.55 ± 0.06	-0.69, -0.42	1.67 ± 0.18	1.29, 2.05	1.00	<0.001	0.28	0.20 - 0.38
	Summer	0.15	15	0.60	-0.42 ± 0.09	-0.61, -0.22	1.17 ± 0.23	0.66, 1.67	0.84	<0.001	0.38	0.25 - 0.60
		1.4	24	0.30	-0.30 ± 0.09	-0.49, -0.11	0.60 ± 0.24	0.11, 1.09	0.85	0.003	0.50	0.33 - 0.77
		13	17	0.59	-0.87 ± 0.18	-1.25, -0.49	1.84 ± 0.40	0.99, 2.70	0.98	<0.001	0.14	0.06 - 0.32
Diltiazem	Spring	0.15	22	0.30	-0.66 ± 0.21	-1.10, -0.22	1.78 ± 0.63	0.47, 3.08	0.81	0.005	0.22	0.08 - 0.60
		1.4	16	0.53	-0.67 ± 0.16	-1.01, -0.33	1.72 ± 0.47	0.70, 2.73	0.94	<0.001	0.21	0.10 - 0.47
		13	18	0.34	-0.26 ± 0.08	-0.44, -0.09	0.18 ± 0.27	-0.40, 0.75	0.80	0.006	0.55	0.37 - 0.82
	Summer	0.15	17	0.57	-0.49 ± 0.10	-0.71, -0.27	0.75 ± 0.27	0.18, 1.33	0.97	<0.001	0.32	0.20 - 0.54
		1.4	24	0.30	-0.34 ± 0.10	-0.56, -0.13	0.39 ± 0.27	-0.17, 0.95	0.86	0.003	0.45	0.28 - 0.74
		13	18	0.15	-0.26 ± 0.13	-0.54, 0.01	-0.36 ± 0.30	-0.99, 0.26	0.47	0.06	0.55	0.29 - 1.03
	Fall	0.15	22	0.45	-0.34 ± 0.08	-0.50, -0.17	0.06 ± 0.18	-0.31, 0.43	0.96	<0.001	0.46	0.31 - 0.67
Diphenhydramine	Spring	0.15	24	0.19	-0.40 ± 0.16	-0.73, -0.07	1.72 ± 0.46	0.77, 2.68	0.66	0.019	0.40	0.19 - 0.84
		1.4	21	0.12	-0.35 ± 0.18	-0.72, 0.03	1.46 ± 0.51	0.40, 2.52	0.45	0.067	0.45	0.19 - 1.06
		13	21	0.16	-0.37 ± 0.17	-0.72, -0.02	1.08 ± 0.53	-0.02, 2.18	0.54	0.041	0.43	0.19 - 0.96
	Summer	0.15	17	0.60	-0.87 ± 0.17	-1.24, -0.50	2.61 ± 0.46	1.64, 3.58	0.98	<0.001	0.14	0.06 - 0.32
		1.4	24	0.43	-0.65 ± 0.15	-0.96, -0.34	2.11 ± 0.39	1.29, 2.92	0.96	<0.001	0.22	0.11 - 0.46
		13	18	0.91	-2.04 ± 0.16	-2.38, -1.70	4.29 ± 0.36	3.52, 5.05	1.00	<0.001	0.01	0.00 - 0.02
	Fall	0.15	22	0.74	-0.55 ± 0.07	-0.70, -0.40	1.53 ± 0.16	1.20, 1.86	1.00	<0.001	0.28	0.20 - 0.40
		1.4	20	0.50	-0.59 ± 0.13	-0.87, -0.31	1.68 ± 0.30	1.04, 2.31	0.97	<0.001	0.26	0.14 - 0.49
		13	22	0.21	-0.74 ± 0.29	-1.36, -0.14	1.31 ± 0.62	0.03, 2.59	0.66	0.019	0.18	0.04 - 0.72
Fluoxetine	Spring	0.15	21	0.20	-0.33 ± 0.14	-0.61, -0.05	1.37 ± 0.41	0.52, 2.22	0.62	0.025	0.47	0.25 - 0.90
		1.4	16	0.56	-0.50 ± 0.11	-0.74, -0.26	1.79 ± 0.34	1.06, 2.52	0.96	<0.001	0.31	0.18 - 0.55
	Summer	0.15	17	0.33	-0.28 ± 0.09	-0.48, -0.08	1.42 ± 0.25	0.90, 1.95	0.75	0.009	0.52	0.33 - 0.83
		1.4	24	0.11	-0.15 ± 0.07	-0.30, 0.01	0.97 ± 0.19	0.57, 1.37	0.47	0.06	0.71	0.50 - 1.02
	Fall	0.15	22	0.71	-0.49 ± 0.15	-0.62, -0.35	1.45 ± 0.15	1.14, 1.75	1.00	<0.001	0.33	0.24 - 0.45
		1.4	20	0.43	-0.37 ± 0.09	-0.57, -0.17	1.18 ± 0.21	0.73, 1.63	0.93	<0.001	0.43	0.27 - 0.67
Sertraline	Spring	0.15	21	0.48	-0.48 ± 0.11	-0.71, -0.25	1.99 ± 0.33	1.29, 2.68	0.97	<0.001	0.33	0.19 - 0.56
	Summer	0.15	17	0.61	-0.74 ± 0.12	-0.99, -0.50	2.77 ± 0.31	2.11, 3.42	0.98	<0.001	0.18	0.10 - 0.32
		1.4	24	0.59	-0.93 ± 0.16	-1.26, -0.60	3.25 ± 0.42	2.38, 4.12	1.00	<0.001	0.12	0.05 - 0.25
	Fall	0.15	21	0.84	-0.81 ± 0.08	-0.97, -0.64	2.56 ± 0.17	2.19, 2.92	1.00	<0.001	0.16	0.11 - 0.23
		1.4	17	0.63	-0.63 ± 0.12	-0.88, -0.38	2.02 ± 0.28	1.43, 2.61	0.99	<0.001	0.23	0.13 - 0.42

This assumption ignores non-uniform patterns in exposure concentrations, even when exposure gradients are expected to exist to point source discharges, which introduces systematic bias in calculations of TMFs (Borga, et al. 2012; Kim, et al. 2016). To account for systematic bias, it has been recommended that sampling be performed at locations where exposure gradients are non-existent or limited (Kim, et al. 2016). A TMF previously calculated for DIP in the North Bosque River of central Texas generally followed this assumption (Du, et al. 2014a). However, in the present study, clear exposure gradients existed between study locations in East Canyon Creek and seasonal surface water exposures differed up to an order of magnitude for some compounds (Table 3.6). Regardless, we consistently observed trophic dilution for AMI, CAF, DIL, DIP, FLU, and SER at all sites across seasons with TMFs ranging from 0.01-0.45 (Table 3.16). The results of the current study are in agreement with another TMF study of pharmaceuticals (Xie, et al. 2017), which showed that calculated TMFs were apparently independent of exposure concentrations both spatially and temporally.

Understanding and accounting for potential sources of variation in calculated TMFs are essential to compare TMFs among ecosystems (Burkhard, et al. 2013; Kim, et al. 2016). Two major sources of variation within TMF regressions commonly arise from measured contaminant concentrations and TP calculation based on stable isotopes. Advances in analytical methods, including the robust isotope dilution approach employed in the current study, can reduce concerns associated with contaminants measurements; however, fewer studies have evaluated variability associated with measured $\delta^{15}N$ values and the estimation of trophic position (Borga, et al. 2012; Starrfelt, et al. 2013). In the present study, $\delta^{15}N$ signatures in biota increased between 3.02-4.75 ‰ during spring, 4.90-6.58 ‰ during

summer, and 3.73-10.62 ‰ during fall along the downstream river gradient (Tables 3.13-3.15). Enrichment of $\delta^{15}N$ along the sampling gradient in the present study can be contributed to anthropogenic N input (Brinkmann, Rasmussen, and Kidd 2012) from effluent discharge, animal waste, and onsite wastewater systems along East Canyon Creek. Additional anthropogenic N to aquatic systems and subsequent incorporation to food webs is well established (Costanzo, et al. 2005), and can alter the $\delta^{15}N$ signature of primary producers when used as a baseline to calculate TPs (Anderson and Cabana 2005). Further, periphytic $\delta^{15}N$ in spring and summer was higher than the $\delta^{15}N$ of primary consumers, causing calculated TPs to be higher in periphyton (Figure 3.15). Such observations of higher $\delta^{15}N$ values in primary producers are not unique to the present study, and have been previously reported where a pulse of enriched N caused the $\delta^{15}N$ of primary producers to be elevated above consumer species because of differential stable nitrogen assimilation rate (O'Reilly, et al. 2002; Loomer, et al. 2015). Stable nitrogen turnover in primary producers is on the order of a few days (O'Reilly, et al. 2002), while invertebrates range from 1 to 2 weeks, and fish range from 1 to 3 months (Loomer, et al. 2015). Thus, consumer species collected at the same time as prey species may not respond in a similar fashion to large variations in $\delta^{15}N$ at the base of the food chain (Loomer, et al. 2015; O'Reilly, et al. 2002). Due to the variability of $\delta^{15}N$ in primary producers, both naturally and in urban systems influenced by effluent discharges, $\delta^{15}N$ of longer lived primary consumers was used as a baseline to calculate TPs in the current study because primary consumer $\delta^{15}N$ values are more stable (Post 2002; Vander Zanden and Rasmussen 1999).

TMFs have primarily been studied for nonionizable hydrophobic chemicals, which requires lipid normalization (Mackay, et al. 2016). Such an approach is inappropriate to

interpret ionizable API levels in fish (Ramirez, et al. 2009). However, normalization of pharmaceutical concentrations to polar lipids (phospholipids) or protein fractions of biota has been suggested because these compartments can contribute significantly to overall partitioning processes (Armitage, et al. 2017). For example, positive relationships between pharmaceutical BCFs and predicted distribution coefficients were reported for phospholipids (D_{mw}) and proteins (D_{BSAw} & D_{mpw}) observed in a recent laboratory study (Chen, Gong, and Kelly 2017). In the present study, similar significant positive relationships were observed for these distribution coefficients (Figure 3.8, Table 3.2) using field collected *Salmo trutta.* Such positive relationships observed for D_{mw}, D_{mpw}, and D_{BSAw} suggest that membrane or protein partitioning may be an important consideration when trying to predict or understand bioaccumulation and partitioning of ionizable pharmaceuticals in field settings. Thus, incorporating more specific partitioning parameters like D_{mw}, D_{mpw}, and D_{BSAw} appear useful during bioaccumulation assessments. However, while these distribution coefficients may increase an understanding of partitioning mechanisms for ionizable contaminants, results from the current study indicate that normalization of pharmaceuticals to the neutral lipid, polar lipid, or protein fractions were not useful (Figures 3.9-3.14). To our knowledge, this is the first study to relate analytically measured concentrations of pharmaceuticals from biological samples to paired fractions of neutral lipids, polar lipids, and proteins. Future studies examining the influences of internal partitioning (e.g., plasma protein binding) on bioaccumulation of ionizable environmental contaminants, including pharmaceuticals, are needed.

Studies examining differential uptake and accumulation of ionizable APIs among organisms of differing TPs are limited. In the present study, we examined spatial and

temporal exposure and bioaccumulation patterns of pharmaceuticals in aquatic organisms at different TPs (Figures 3.6 & 3.2-3.6). Spatial accumulation in all organisms, regardless of season, was higher at sites closer to the effluent discharge and then decreased with increasing distance from the discharge. Likewise, target analyte concentrations in water typically decreased at sampling sites with increasing distance downstream of the ECWRF discharge, effectively lowering exposure concentrations with increasing distance, again regardless of season (Table 3.6). Spatially, pharmaceutical concentrations in surface water most likely decreased due to instream attenuation and dilution from groundwater and smaller tributaries along East Canyon Creek. The extent of pharmaceutical attenuation or transformation with distance from discharge is inherently influenced by chemical, biological and physical factors (Acuna, et al. 2015). Thus, we initially hypothesized that seasons with higher instream dilution due to snowmelt (spring) would have decreased instream analyte levels in water and biological tissues relative to drier seasons (summer, fall). In fact, the mean stream flow immediately downstream from the effluent discharge was at least three-fold higher during the spring (55 ft^3/s) than during summer (12 ft^3/s) or fall (14 ft^3/s). This altered effluent dilution in which the highest instream effluent percentage was observed in the summer (33.3%), followed by fall (21.9%) and spring (7.4%). However, target analyte concentrations in effluent varied seasonally, where the highest observed concentrations of AMI, DIL, and DIP were during spring, while elevated FLU and SER levels were observed in the summer (Table 3.6). Observed temporal accumulation patterns may have resulted from differential population consumption and discharge of these target analytes to East Canyon Creek through time. Such temporal dynamics deserve additional study.

We generally observed the highest levels of AMI, DIL, DIP, FLU, and SER in periphyton and Trichoptera (Figure 3.7, Tables 3.7-3.9). Higher accumulation in autotrophic organisms are not unique and has been observed for a number of pharmaceutical compounds in lab and field settings (Ding, et al. 2015a; Ding, et al. 2015b; Lagesson, et al. 2016; Ruhi, et al. 2016; Bostrom, et al. 2017; Du, et al. 2014a; McLeod, et al. 2015; Miller, et al. 2017; Xie, et al. 2015; Xie, et al. 2017). Such observations are attributed to sorptioning of pharmaceuticals to extracellular polymeric substances (EPS), used to maintain structure within periphytic biofilms (Rodney 2002; Lagesson, et al. 2016; Ruhi, et al. 2016; Ding, et al. 2015b; Ding, et al. 2015a; Bostrom, et al. 2017; Huerta, et al. 2016). EPS is comprised of polysaccharides, proteins, nucleic acids, and lipids containing many functional groups that effectively increase sorption capacity and bioaccumulation, even in conditions where bioavailability is lower due to unfavorable pH (Flemming and Wingender 2010; Rodney 2002; Huerta, et al. 2016). Even so, pharmaceutical bioaccumulation in periphytic biofilms is highly site specific and affected by many factors (Aubertheau, et al. 2017). Additionally, biotransformation mechanisms in periphytic biofilms are not well understood and are dependent on community structure (Huerta, et al. 2016), which are commonly composed of filamentous algae, diatoms, bacteria, and fungi (Rier and Stevenson 2002).

Uptake and accumulation pathways of pharmaceuticals in aquatic invertebrates are also poorly understood (Miller, et al. 2017) and can be affected by multiple factors including respiration, locomotion, and utilization of the water column (Meredith-Williams, et al. 2012). The primary pathway of pharmaceutical uptake in truly aquatic invertebrate species appears to result from inhalation by the gills (Meredith-Williams, et al. 2012).

Pharmaceuticals are not expected to bioconcentrate to high levels in gill breathing invertebrates (Miller, et al. 2017) and internal concentrations are rapidly respondent to changes in stream concentration (Lagesson, et al. 2016). However, due to pharmaceutical sorptioning to particulate matter (Al-Khazrajy and Boxall 2016) and because higher concentrations are achieved in periphytic biofilms, as demonstrated in this study and others (Bostrom, et al. 2017; Ding, et al. 2015b; Ding, et al. 2015a; Du, et al. 2014a; Lagesson, et al. 2016; Ruhi, et al. 2016), diet as an exposure pathway may be more important for some APIs than aqueous concentrations for species that filter feed or graze on algae and biofilms (Du, et al. 2015; Meredith-Williams, et al. 2012; Baker and Kasprzyk-Hordern 2011; Hazelton, et al. 2014; Franzellitti, et al. 2014). In the present study, we examined *Helicopsyche sp*., *Hydropsyche sp*., *Lymnaeidea*, *Physidae* and *Ephemerella sp.*, which are grazers that feed on periphyton and detritus (Merritt and Cummins 1996). Whereas dietary routes of exposure to ionizable base APIs do not appear as important as inhalation for fish (Armitage, et al. 2017), recent studies examining diet as an exposure pathway have observed trophic transfer to invertebrates (Heynen, et al. 2016; Du, et al. 2015) and assimilation from ingested particulate matter and sediments (Du, et al. 2015; Franzellitti, et al. 2014; Karlsson, et al. 2017; Hazelton, et al. 2014). Though the ability of *G. pulex* to eliminate pharmaceuticals has been demonstrated, limited laboratory or field studies have examined differential biotransformation mechanisms and clearance of pharmaceuticals within and among invertebrates (Miller, et al. 2017; Lagesson, et al. 2016; Karlsson, et al. 2017). Clearly, this area warrants additional study when relatively higher levels of select APIs are observed in invertebrates.

Conclusions

We selected a unique study system, with instream flows influenced by municipal effluent discharge and snowmelt runoff, to examine spatiotemporal trophic transfer of ionizable APIs. Trophic dilution was observed at all sites across all seasons, regardless of different flow, temperature, or aqueous exposure concentrations. These observations suggest that ionizable weak base pharmaceuticals are not biomagnified, and that waterborne exposure of fish to APIs is more predictive of bioaccumulation than diet. Additional research is necessary to understand comparative uptake and elimination mechanisms in aquatic organisms. We further examined potential relationships between pharmaceutical bioaccumulation and fractions of neutral lipids, polar lipids, and proteins. Our results demonstrate that normalization of multiple ionizable pharmaceuticals to neutral lipid fractions is inappropriate, and normalization of pharmaceutical tissue residues to polar lipid or protein fractions did not appear particularly useful. Future studies examining influences of internal partitioning (e.g., plasma protein binding) on bioaccumulation of pharmaceuticals and other ionizable environmental contaminants are needed.

Acknowledgement

Support for this study was provided by the Snyderville Basin Water Reclamation District. We thank staff from the Snyderville Basin Water Reclamation District and the Utah Department of Natural Resources for assisting with field sampling. We also thank Dr. Bowen Du, Dr. Eric LeBrun, Leah Botkin, Kailey Reimen, Craig Calvert, and Nick Adams for additional support. A special thanks to Dr. Jeffery Back for assistance with invertebrate identification.

CHAPTER FOUR

Spatio-temporal Occurrence and Observed Fish Plasma Levels of Human Pharmaceuticals in a Semi-arid Stream Influenced by Snowmelt.

Abstract

An advanced, non-traditional approach incorporating the internal dose of pharmaceuticals in plasma and target tissues of aquatic organisms (e.g., fish) is required to address the unique potency of this class of contaminants. The therapeutic hazard value (THV) represents a diagnostic approach for translating waterborne instream concentrations to potential therapeutic hazards in fish. Thus, we selected East Canyon Creek in Park City, Utah, USA to develop a baseline understanding of the spatial and temporal occurrence of pharmaceuticals and to evaluate potential risks to fish at incremental distances (0.15, 1.4, 13 miles) downstream from a municipal effluent discharge during spring (May), Summer (August and September), and fall (October) seasons. 17 of 19 target analytes were detected in water from multiple sampling sites located upstream and incrementally downstream of the effluent discharge. Amitriptyline, diphenhydramine, fluoxetine, norfluoxetine, and sertraline exceeded the predicted THV (with 1000 fold safety factor) 100% of the time at all sites during all sampling events. Conversely, caffeine did not exceed the predicted THV (with 1000 fold safety factor) at any site during any sampling. Additionally, the measured concentrations of amitriptyline, diphenhydramine, fluoxetine, norfluoxetine, and sertraline in *Salmo trutta* plasma all exceeded the C_{min} value with the previously proposed 1000-fold safety factor, while CAF did not exceed the C_{min} with safety factor. In the present study,

amitriptyline, diphenhydramine, fluoxetine, norfluoxetine, and sertraline were all predicted to exceed the C_{min} with 1000-fold safety factor by the THV and the observed plasma concentrations did in fact correspond to the previous prediction. Further caffeine was not predicted to exceed the C_{min} with 1000-fold safety factor and the corresponding plasma levels also did not exceed the C_{min} value. Thus, the current study demonstrates the utility of the THV as a spatiotemporal diagnostic tool to translate water concentrations into potential aquatic hazards. However, future uptake and toxicological studies are necessary to decrease uncertainty associated with default 1000 fold safety factor use for the THV and to define rates of uptake and elimination in aquatic systems in responses to spatiotemporal changes in inhalational exposure.

Introduction

Due to rapid population growth and urbanization, modern day water plans have become more complex in response to increased demand for diminishing aquatic resources, the urbanizing water cycle, and multiplying anthropogenic stressors (Brooks 2018; Rice and Westerhoff 2017). Increased discharge of reclaimed water or untreated sewage to urban waterways has resulted in a unique exposure of contaminants of emerging concern (CECs), such as active pharmaceutical ingredients (APIs), to aquatic organisms in urban ecosystems (Brooks 2018). The occurrence of human pharmaceuticals in the aquatic environment is of concern due to the ~3000 APIs currently administered in Europe, the United States, and Asia that pose potential ecotoxicological risk to aquatic organisms (Rice and Westerhoff 2017; Xie, et al. 2015). Further, during dry months, the base flows of many semi-arid river systems are increasingly effluent dependent or dominated resulting in longer, pseudo-persistent, exposure durations to aquatic organisms (B. W. Brooks, et al. 2012; Brooks,

Riley, and Taylor 2006). A condition exacerbated by increased global temperatures and climate change causing decreased snowpack, relied upon by over 2 billion people annually for high quality surface water inflows and water resources (Mankin, et al. 2015). Such considerations are increasingly important for semi-arid southwestern river systems in the United States, which may represent worst case scenarios for potential exposure and effects from APIs in aquatic systems (Brooks, Riley, and Taylor 2006; Du, et al. 2014a; Du, et al. 2012). Thus, identifying conditions and scenarios where APIs pose higher risks to aquatic and terrestrial wildlife is important to reduce potential ecological perturbation, and was recently identified as a major research need (Boxall, et al. 2012a; Brooks 2014).

However, traditional assessment approaches and endpoints to predict the exposure and effects of other environmental organic contaminant classes are often inappropriate for APIs, which may over or under estimate risk (Kwon, et al. 2009; Daughton and Brooks 2011b; Brooks 2014). Unlike neutral organic contaminants, uptake and elimination of APIs in aquatic organisms is modified by physiological and surface water pH conditions (Nichols, et al. 2015; Armitage, et al. 2017), because approximately 80% of APIs are ionizable (Manallack 2007). Additionally, the partitioning dynamics of pharmaceuticals are not solely due to hydrophobic interactions, but can be influenced by active transport, ion exchange, ion bridging, hydrogen bonding, complexation, and sorption (Armitage, et al. 2017; Brooks, Huggett, and Boxall 2009). Further, pharmaceuticals and their metabolites were designed to be biologically active molecules, where specific internal concentrations can be linked to therapeutic activity (Gunnarsson, et al. 2008; Brodin, et al. 2014; Brooks 2014; Ebele, Abou-Elwafa Abdallah, and Harrad 2017). Thus, an advanced, non-traditional, approach incorporating the internal dose of APIs in plasma and target

tissues of aquatic organisms (e.g., fish) is required to address the unique potency of this class of contaminants (Tanoue, et al. 2014; Tanoue, et al. 2015; Brooks 2018).

Fortunately, lessons learned from the study of compounds active at the hypothalamic–pituitary–gonadal axis (endocrine disruptors/modulators) may reduce uncertainties associated with aquatic assessment and management of APIs (Ankley, et al. 2007). Because pharmacological targets are evolutionarily conserved in many aquatic organisms (Gunnarsson, et al. 2008), mammalian pharmacology and toxicology data may be leveraged to study and even predict adverse effects to aquatic life, because adverse effects are often linked to therapeutic activity (Ankley, et al. 2007; Berninger and Brooks 2010; Berninger, et al. 2015). Further, extensive mammalian pharmacology and toxicology data exists in the case of APIs, which is not the case for the majority of industrial chemicals (Brooks 2018). Recently, the therapeutic hazard value (THV) concept, which identifies water concentrations of a drug predicted to result in an internal dose in fish plasma equal to a mammalian therapeutic dose, was developed to translate water exposure concentrations of APIs to thresholds related to water quality hazards (Brooks 2014). The THV approach incorporates physiological-based pharmacokinetic (PBPK) inspired modeling based on evolutionary conservation of many pharmacological targets occurs in fish (Gunnarsson, et al. 2008; Fitzsimmons 2001; Huggett, et al. 2003). Fish plasma modeling appears to have much utility for prioritizing pharmaceuticals for advanced research, monitoring, and assessment (Caldwell, et al. 2014), independently demonstrated during recent fish toxicology studies (Valenti, et al. 2012; Margiotta-Casaluci, et al. 2014; Brooks 2018; Scott, et al. 2016; Tanoue, et al. 2017). Thus, the THV approach directly supports translation of surface water quality monitoring data to predict water quality

hazards, which can then support environmental assessment interpretation and management decisions (Kristofco and Brooks 2017; Saari, Scott, and Brooks 2017; Scott, et al. 2016).

However, additional studies to examine the robustness of the THV when applied to multiple classes of APIs are required (Saari, Scott, and Brooks 2017). Further, a recent review of pharmaceuticals and aquatic organisms, identified that spatio-temporal factors influencing bioaccumulation and potential risks of pharmaceuticals and other CECs to aquatic life is decidedly lacking (Daughton and Brooks 2011b). Herein, the current study seeks to develop a baseline understanding of the spatial and temporal occurrence of APIs from a semi-arid river, East Canyon Creek, Utah, USA, including an estimation of potential risks to aquatic life. In this dynamic system, instream flow fluctuates due to seasonal snow melt and continuous effluent discharge. Target pharmaceuticals were quantified in water and fish plasma samples from East Canyon Creek collected during spring, summer, and fall sampling events at an upstream reference site and incremental distances downstream from an effluent discharge. Spatial and temporal occurrence and attenuation patterns were examined by comparing the ratio concentrations of target pharmaceuticals and sucralose at each sampling site to effluent concentrations. The potential risks of API exposure to brown trout was evaluated spatially and temporally in East Canyon Creek using the fish plasma modeling approach and THV.

Materials and Methods

Study Site

The East Canyon Creek watershed is situated east of Salt Lake City, Utah. The water shed is spread over the western stretch of Summit and Morgan county. Within the water shed is the Snyderville Basin Water Reclamation District (SBWRD) which collects

wastewater from ~11,000 homes and businesses from around the basin. The SBWRD encompasses ~102 square miles, maintains two reclamation facilities, and 12 pumping stations. The current study will focus on the East Canyon Water Reclamation Facility (ECWRF) that discharge into East Canyon Creek near Park City, Utah. ECWRF has a design capacity of 4.0 million gallons/day (MGD) with a mean daily load of ~3 MGD. East Canyon Creek is located in the semiarid mountainous region of Utah and receives ~60% of annual precipitation during the winter. As a result, stream discharges in East Canyon Creek are elevated during the spring and summer snowmelt (Figure 4.1). The final destination for waters from the ECWRF discharge and East Canyon Creek is the East Canyon Reservoir.

Field Sampling

Samples from East Canyon Creek were collected during high flow conditions from snow melt, in the spring (4-7 May), and semi-arid conditions during summer (17-21 August & 15-19 September) and fall (27-31 October) of 2014 (Figure 4.1). Collection occurred at an upstream site and incremental distances downstream (0.15, 1.4, 13 miles) from the ECWRF discharge. A unique geological barrier exists between the upstream site and the ECWRF discharge that allows organisms to move downstream but not back upstream ensuring that organisms sampled from the upstream site had not been influenced by the ECWRF discharge. Duplicate water samples for targeted CECs were collected from each site using acetone cleaned 4 L amber glass bottles. Utah Department of Natural Resources (UDNR) protocols were followed for backpack electroshock collection of brown trout (Salmo trutta). Fish length and weight were measured on site immediately after anesthetization using MS-222. S. trutta blood was collected immediately after

anesthetization from the caudal artery with heparinized microhaematocrit capillary tubes. Blood was centrifuged at 13000g for 10 min, after which blood plasma was collected and immediately frozen on dry ice. All samples were transported to a field station on ice, then shipped to Baylor University for processing and extraction.

Chemicals and Analytical Standards

All chemicals and their corresponding isotopically-labeled analogs were obtained with various vendors. Acetaminophen (ACE), acetaminophen-d4, amitriptyline (AMI), amitriptyline-d3, aripiprazole (ARI), aripiprazole-d8, benzoylecgonine (BEN), benzoylecgonine -d3, buprenorphine (BUP), buprenorphine-d4, caffeine (CAF), carbamazepine (CAR), carbamazepine-d10, diclofenac (DIC), diltiazem (DIL), diphenhydramine (DIP), diphenhydramine-d3, duloxetine (DUL), duloxetine-d3, fluoxetine (FLU), fluoxetine-d6, methylphenidate (MPH), methylphenidate-d9, norfluoxetine (NOR), norfluoxetine-d6, , promethazine (PROM), promethazine-d3, and sertraline (SER) were purchased as certified analytical standards from Cerilliant (Round Rock, TX, USA). Amlodipine (AML), amlodipine-d4, caffeine-d9, desmethylsertraline (DES), desmethylsertraline-d4, diclofenac-d4, diltiazem-d3, and sertraline-d3 were purchased from Toronto Research Chemicals (Toronto, Ontario, Canada). Sucralose (SUC) was purchased from Sigma-Aldrich (St. Louis, MO, USA) and sucralose-d6 was purchased from Santa Cruz Biotechnology (Santa Cruz, CA, USA). All chemicals were reagent grade and used as received. HPLC grade methanol (MeOH), methyl tert-butyl ether (MTBE), and chloroform were obtained from Fisher Scientific (Fair Lawn, NJ, USA), formic acid was purchased from VWR Scientific (Radnor, PA, USA), and a Thermo Barnstead™

Nanopure™ (Dubuque, IA, USA) Diamond UV water purification system was used throughout sample analysis to provide 18 MΩ water.

Sample Preparation

Water samples were filtered and concentrated to solid phase extraction (SPE) cartridges following previously reported methods (Du, et al. 2014b; Lajeunesse, Gagnon, and Sauve 2008; Vanderford and Snyder 2006) with some modifications. Described briefly samples were filtered through three different sized filters to remove particulate: a glass fiber prefilter (1.0-μm pore size, 47 mm, Pall Corporation, Port Washington, NY, USA), a nitrocellulose filter (0.45-μm pore size, 47 mm, GE Healthcare, Little Chalfont, BUX, UK), and a Nylaflo™ filter (0.2-μm pore size, 47 mm, Pall Corporation, Port Washington, NY, USA). 2 L were separated into 2 – 1 L volumetric flasks for extraction with an Oasis HLB (6 cc, 200 mg, Waters Corporation, Milford, MA, USA) cartridge and a Strata SCX (6 cc, 500 mg, Phenomenex, Torrance, CA, USA) cartridge. 50 μL of prepared 2000 (ng mL^{-1}) internal standard was spiked into each sample. Strata SCX samples were then spiked with an additional 100 μL of 85 % phosphoric acid and 5 mL of MeOH. Oasis HLB cartridges were pretreated with 5 mL MTBE, 5 mL MeOH, and 5 mL nanopure water respectively. Strata SCX cartridges were pretreated with 5 mL MEOH and 5 mL nanopure water respectively. Samples were extracted via a 24 port Visiprep™ vacuum manifold (Supelco Inc., Bellefonte, PA, USA) with a flow rate of approximately 10 ml/min. Oasis HLB cartridges were eluted with 5 mL MeOH and 5 mL 10:90 (v v^{-1}) MeOH:MTBE. Strata SCX cartridges were first washed with 5 mL of aqueous 0.1% HCl solution, then eluted with 5 mL MeOH and 6 mL 5:95 (v v^{-1}) NH_4OH:MeOH. Eluates were blown to dryness

under a gentle stream of nitrogen in a Turbovap (Zynmark, Hopkinton, MA, USA) set to 45°C, then reconstituted to 1 mL with 5:95 (v v^{-1}) MeOH:aqueous 0.1% formic acid.

S. trutta blood plasma collected in the field was preserved at -80°C prior to analysis at Baylor University generally following previously reported methods (Du, et al. 2014a). Samples were thawed and a 500 µL aliquot was placed in a clean test tube. 50 µL of 2000 ppb ISS was spiked in each sample. 5 mL of aqueous 0.1% formic acid was then added to each test tube. HLB cartridges were used to concentrate and extract analytes from plasma. Cartridges were preconditioned with 5 mL of MeOH and 5 mL H_2O. Samples were then allowed to gravity drip through the cartridge. Cartridges were blown dry under nitrogen and eluted with 5mL MeOH. Eluates were blown to dryness under a gentle stream of nitrogen in a turbovap set to 45°C, and then reconstituted to 1 mL with 5:95 (v v^{-1}) MeOH:aqueous 0.1% formic acid.

All reconstituted samples were syringe filtered using a BD 1 mL TB syringe (BD, Franklin Lakes, NJ, USA) and Acrodisc® hydrophobic Teflon Supor membrane syringe filters (13-mm diameter; 0.2-µm pore size, Pall Corporation, Port Washington, NY, USA) and placed in 2 mL analytical vials (Agilent Technologies, Santa Clara, CA, USA) for analysis.

Instrumental Analysis

Samples were analyzed using isotope-dilution liquid chromatography-tandem mass spectrometry (LC-MS/MS) with an Agilent Infinity 1260 autosampler/quaternary pumping system, Agilent jet stream thermal gradient electrospray ionization source (ESI), and model 6420 triple quadrupole mass analyzer (Agilent Technologies, Santa Clara, CA, USA). A binary gradient method consisting of aqueous 0.1 % formic acid as solvent

A, and MeOH as solvent B, was used. Separation was performed using a 10 cm × 2.1 mm Poroshell 120 SB-AQ column (120Å, 2.7-μm, Agilent Technologies, Santa Clara, CA, USA) preceded by a 5 × 2.1 mm^2 Poroshell 120 SB-C18 attachable guard column (120Å, 2.7-μm, Agilent Technologies, Santa Clara, CA, USA). The flow rate was held constant at 0.5 mL/min with a column temperature maintained at 60°C and an injection volume of 10 μL. Multiple reaction monitoring (MRM) transitions, detection limits, and associated instrument parameters for target analytes can be found elsewhere (Bean, et al. 2018).

Quantitation was performed using an isotope dilution calibration method. Calibration standards, containing mixture of internal standards and variable concentrations of target compounds, were prepared in 95:5 0.1% (v v^{-1}) aqueous formic acid–methanol. The linear range for each analyte (0.1 – 500 ng mL^{-1}) was confirmed from plots of sensitivity (i.e., response factor; RF) versus analyte concentration. Our criterion for linearity required that the relative standard deviation of RFs for standards spanning the noted range was ≤ 15%. Internal standard calibration curves were constructed for each analyte using eight standards that were within the corresponding linear range. Calibration data were fit to a linear regression, and correlation coefficients (r^2) for all analytes were ≥ 0.995. Quality assurance and quality control measures included running a continued calibration verification (CCV) sample every five samples to check calibration validity during the run. A criterion of ± 20% of CCV concentration was held to be acceptable for all analytes. One blank (i.e., reference water with internal standards only), one field blank, and duplicate matrix spikes were included in each analytical sample batch. Method detection limits (MDLs) represented the lowest concentration of an analyte reported with 99% confidence that the concentration is different from zero in a given matrix. The EPA

guideline (40 CFR Part 136, Appendix B) for generating method detection limits was followed to generate MDLs in water and fish plasma. In the present study <MDL is defined as analytes that were detected in the matrices, but below corresponding MDLs.

Fish Plasma Modeling

Pharmaceutical uptake modeling was performed using a previously reported model to predict fish plasma concentrations of pharmaceuticals from water exposure (Scott, et al. 2016; Berninger, et al. 2011; Saari, Scott, and Brooks 2017).

$$FPC = [Aq] \cdot P_{BW}$$

where FPC is the fish plasma concentration, [Aq] is the aqueous concentration of analyte, and P_{BW} is the partitioning coefficient of analyte from water to blood across the gill membrane.

$$P_{BW} = (10^{(0.73 \cdot \text{Log Dmw})} \times 0.16) + 0.84$$

Estimated values of the acid dissociation constant (pK_a) and the octanol-water partitioning coefficient (K_{ow}) were obtained from SCIfinder. Log D_{mw} was determined following the method (Droge, et al. 2017):

$$\text{Log } D_{mw} = \text{Log}(f_{\text{nuetral}} \cdot K_{mw(\text{neutral})} + f_{\text{ion}} \cdot K_{mw(\text{ion})})$$

$$\text{Log } K_{mw(\text{neutral})} = 1.01 \cdot \text{Log } K_{ow} + 0.12 \text{ (Endo, Escher, and Goss 2011)}$$

$$\text{Log } K_{mw(\text{ion})} = \text{Log } K_{mw(\text{neutral})} - \Delta_{mw}$$

$$f_{\text{nuetral}} = 1/1+10^{(\text{pKa-pH})}$$

$$f_{\text{ion}} = 1- f_{\text{nuetral}}$$

where Δ_{mw} = -1.4 for 1˚ polar amines, -0.57 for 2˚ polar amines, and 0.35 for 3˚ polar amines, f_{ion} and f_{nuetral} are the fractions of ionized form and neutral form of the chemical

respectively as predicted by the Henderson-Hasselbalch equation based on measured pH at each site during each season.

Probabilistic Environmental Hazard Assessment

Probabilistic distributions of THVs modified by spatiotemporal gradients of surface water pH were created to identify whether pharmaceuticals measured in water potentially posed adverse effects to fish at each site following previously report methods (Scott, et al. 2016). Briefly, the THV represents an aqueous concentration of a pharmaceutical that, if approached, is expected to result in receptor-mediated therapeutic responses in fish (Brooks 2014). THVs were calculated following a previously published approach (Saari, Scott, and Brooks 2017):

$$THV = C_{min} / P_{BW}$$

where C_{min} values were from Schulz et al. (2012). THV distributions were generated for each chemical at 15-min intervals over a 24-h sampling period for each study site, during each sampling event. As noted by pharmaceutical industry scientists (Huggett, et al. 2003), therapeutic effects and associated adverse outcomes may be expected at plasma concentrations in fish that are below human therapeutic doses (C_{min}). Thus, Huggett, et al. (2003) recommended that a safety factor of 1000 (10-fold for extrapolation of humans to animals, 10-fold for sensitivity differences, 10-fold for extrapolation from mammalian to non-mammalian species) be employed to account for uncertainty when using human C_{min} values to estimate fish responses, which was incorporated into each distribution. The measured water concentrations of each contaminant were used to estimate the probability of exceeding a THV over a 24h period at each site during each sampling. THVs were ranked using the Weibull equation (Solomon and Takacs 2002):

$$j = (i \cdot 100) / (n + 1)$$

where i is the rank number of the data point, n is the total number of data points in the set, and j is the percent rank. This method assumes that this distribution is 1 value away from the true environmental distribution; therefore, a 1 is added to n (Posthuma, Suter II, and Traas 2001). THVs (ng/L) were plotted along the x axis against the percent rank along the y axis. The measured concentration of target analytes in water were then substituted for x in the linear regression equation to estimate the probability that the measured aqueous concentration would exceed a THV over the 24 hour period at each site during each sampling.

Statistical Analysis

SigmaPlot by Systat Software (San Jose, CA, USA) was used for statistical analysis. An alpha of 0.05 was assigned for all tests. Linear regressions were performed for water sample data relative to distance from the effluent discharge to East Canyon Creek. For plasma samples, a parametric one-way analysis of variance or an analysis of variance on ranks were performed with a Tukey's or Dunn's post-hoc multiple comparison test, respectively, to compare analyte concentrations across sites. When an analyte was not detected at more than two sites, a t-test was performed. For analytes that were not detected, or observed below a corresponding MDL, values were set at half the MDL for statistical analyses (Antweiler and Taylor 2008).

Results and Discussion

Stream Characterization

During 2014, Park City, UT received 32% less rainfall and 74% less snowfall than the annual mean, resulting in lower-than-average instream flows in East Canyon Creek. Discharge measurements were available from the U.S. Geological Survey for two gaging stations located in East Canyon Creek. Stations #10133800 and #10133980 are located approximately 0.15 and 13 miles downstream from the ECWRF discharge. Consistent with my hypothesis, the mean discharge immediately downstream from the effluent discharge was at least three-fold greater during the spring (May) sampling event than during the summer (August, September) or fall (October) sampling events (Figure 4.1). Stream discharge increased 14 ft^3/s during May, 4 ft^3/s during August, 6 ft^3/s during September, and 4 ft^3/s during October between the 0.15- and 13-mile sites. The effluent discharge was relatively consistent ranging from 0.73 to 6.97 ft^3/s over 2014 with an average of 4.29 ± 0.81 ft^3/s, similar to measurements made in a follow up study, with a similar design, in 2016 (Buswell 2017). Due to this consistency in effluent discharge, the percentage of effluent downstream of the discharge was seasonally dependent on the upstream base flow (Buswell 2017). In this study, the highest instream effluent percentage was observed in August (33.3%), followed by September (30.1), October (21.9%), and May (7.4%).

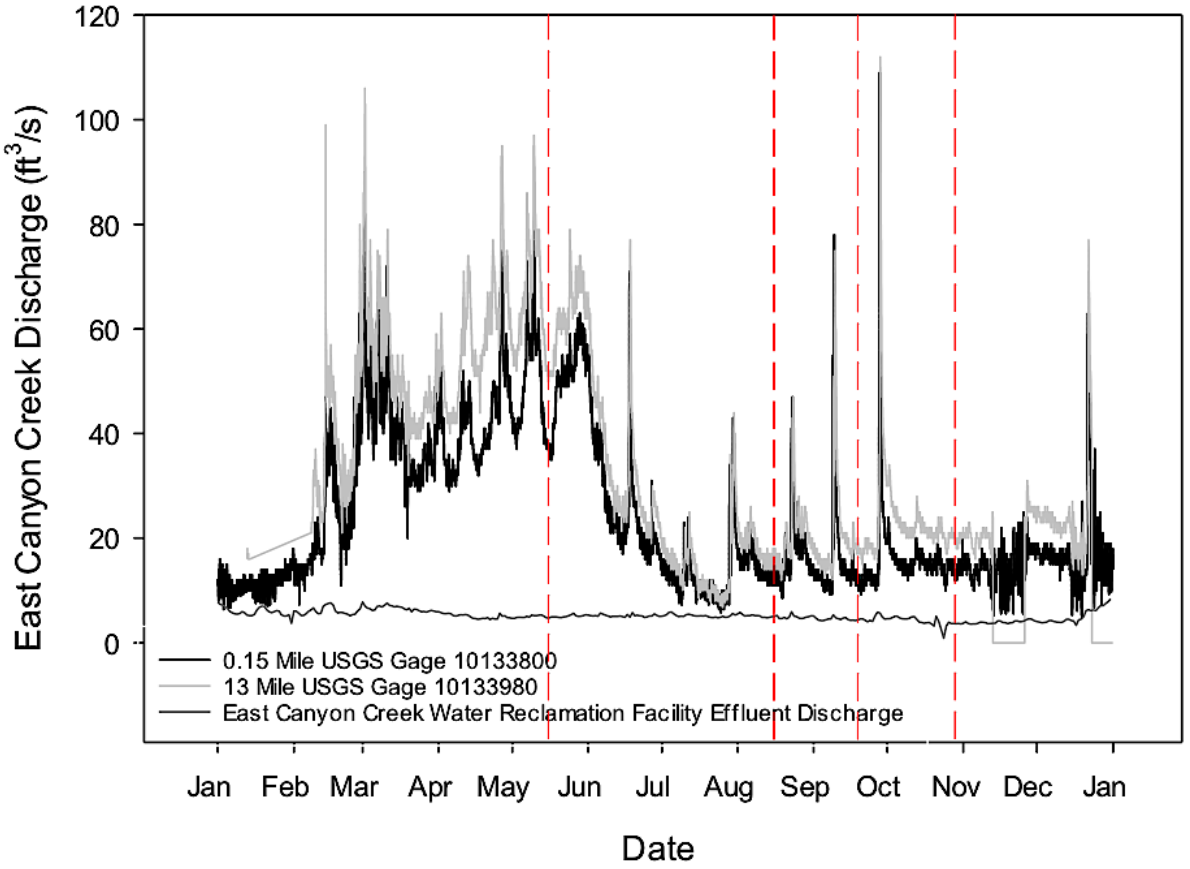

Figure 4.1. Flow (ft3/s) of East Canyon Creek, Utah, USA, from effluent and USGS gages during 2014. USGS gages are located at the 0.15 mile sampling site near Jeremy Ranch (10133800), which is directly downstream of an effluent discharge, and at the 13 mile sampling site near Morgan (10133980). Dashed vertical reference lines represent sampling events during the year.

Pharmaceuticals in Water

17 of 19 target analytes were detected in water from the ECWRF effluent and from sampling sites located upstream and incrementally downstream of the ECWRF discharge. Detection and frequency of detection for all target analytes in water is reported in Table 4.1. Of 19 target analytes, none were detected in field blanks and BEN, CAF, DIP, and SUC were detected the most frequently at all sites during all sampling events. Not surprisingly, target analytes were consistently higher in effluent samples. The highest effluent detections of target analytes were AMI, BEN, DIL, DIP, and MPH during May; CAR, DES, FLU, SER, and SUC during August; AML and BUP during September; and CAF, DIC, and NOR during October. Spatially, regression analysis resulted in observations of decreases of target analytes with distance downstream of the ECWRF discharge except for CAF (Figure 4.2.1). While temporally, consistent with our hypothesis and corresponding to differential stream discharge observations among sampling events (Figure 4.1), the lowest instream concentrations of target analytes were observed during the May sampling event (Table 4.1).

Table 4.1. Human pharmaceuticals in mean (N = 2) water samples collected from East Canyon Water Reclamation Facility (ECWRF) effluent and in East Canyon Creek, UT, USA, upstream and downstream (0.15 miles, 1.44 miles, 13 miles) from the ECWRF effluent discharge during four sampling events in 2014. ACE, acetaminophen; AMI, amitriptyline; AML, amlodipine; BEN, benzoylecgonine; BUP, buprenorphine; CAF, caffeine; CAR, carbamazepine; DES, desmethylsertraline; DIC, diclofenac; DIL, diltiazem; DIP, diphenhydramine; DUL, duloxetine; FLU, fluoxetine; MPH, methylphenidate; NOR, norfluoxetine; SER, sertraline; SUC, sucralose; ND, No Detect; <MDL, below method detection limit; MDL, method detection limit; SPE, solid phase extraction cartridge.

Sampling Period	Site	ACE (ng/L)	AMI (ng/L)	AML (ng/L)	BEN (ng/L)	BUP (ng/L)	CAF (ng/L)	CAR (ng/L)	DES (ng/L)	DIC (ng/L)	DIL (ng/L)	DIP (ng/L)	DUL (ng/L)	FLU (ng/L)	MPH (ng/L)	NOR (ng/L)	SER (ng/L)	SUC (ng/L)
May	Upstream	ND	ND	ND	2.3	ND	7.3	0.5	ND	ND	<MDL	0.11	ND	3.4	ND	ND	ND	3.6
	Effluent	<MDL	170	<MDL	77	<MDL	17	50	ND	94	87	320	<MDL	46	9.0	5.4	2.0	1600
	0.1 Mile	<MDL	ND	ND	5.2	ND	7.1	3.8	ND	ND	1.5	11	ND	ND	0.58	ND	ND	200
	1 Mile	<MDL	ND	ND	4.8	ND	6.7	3.5	ND	ND	6.3	6.7	ND	ND	0.41	ND	ND	170
	10 Mile	<MDL	ND	ND	3.1	ND	5.0	3.5	ND	ND	2.7	2.8	ND	ND	0.19	ND	ND	140
August	Upstream	ND	ND	ND	1.5	ND	22	<MDL	6.6	ND	<MDL	0.49	ND	ND	ND	ND	ND	8.5
	Effluent	15	140	<MDL	26	<MDL	21	110	55	69	32	82	<MDL	58	6.8	ND	37	1900
	0.1 Mile	7.6	29	ND	7.2	<MDL	30	34	ND	23	9.4	26	ND	15	2.0	ND	ND	750
	1 Mile	17	24	ND	11	<MDL	33	34	ND	14	9.0	20	ND	ND	1.4	ND	ND	770
	10 Mile	3.1	ND	ND	9.0	ND	20	26	ND	ND	1.5	1.6	ND	ND	<MDL	ND	ND	560
September	Upstream	ND	ND	ND	2.2	ND	10	0.14	ND	ND	0.7	0.17	ND	ND	ND	ND	ND	5.8
	Effluent	7.8	120	6.0	20	2.7	23	83	33	74	28.0	72	ND	26	8.0	ND	26	1300
	0.1 Mile	1.8	28	ND	6.9	3.2	14	27	ND	17	7.2	18	ND	ND	2.2	ND	ND	630
	1 Mile	1.8	21	ND	11	3.2	13	28	ND	19	7.4	14	ND	ND	1.8	ND	ND	700
	10 Mile	1.8	ND	ND	4.4	ND	16	14	ND	ND	1.0	1.5	ND	ND	0.17	ND	ND	470
October	Upstream	<MDL	ND	ND	0.36	ND	120	ND	<MDL	ND	ND	<MDL	ND	39	ND	ND	ND	7.1
	Effluent	23	150	ND	61	<MDL	105	100	36	160	38	140	<MDL	33	6.8	9.0	28	1700
	0.1 Mile	8.8	28	ND	16.5	<MDL	45	31	18	22	9.3	33	<MDL	38	1.6	28	15	820
	1 Mile	6.3	5.8	ND	8.6	<MDL	44	17	18	5.5	2.8	12	<MDL	39	0.58	47	11	545
	10 Mile	4.0	8.6	ND	6.8	<MDL	150	11	ND	ND	0.51	0.86	<MDL	22	<MDL	ND	7.5	435
MDL		3.47	5.30	12.03	0.05	6.35	4.43	0.27	7.16	4.74	0.31	0.11	6.79	2.39	0.14	1.77	1.52	2.62
SPE		HLB	SCX	SCX	SCX	SCX	HLB	HLB	SCX	HLB	HLB	SCX	SCX	SCX	SCX	SCX	SCX	HLB

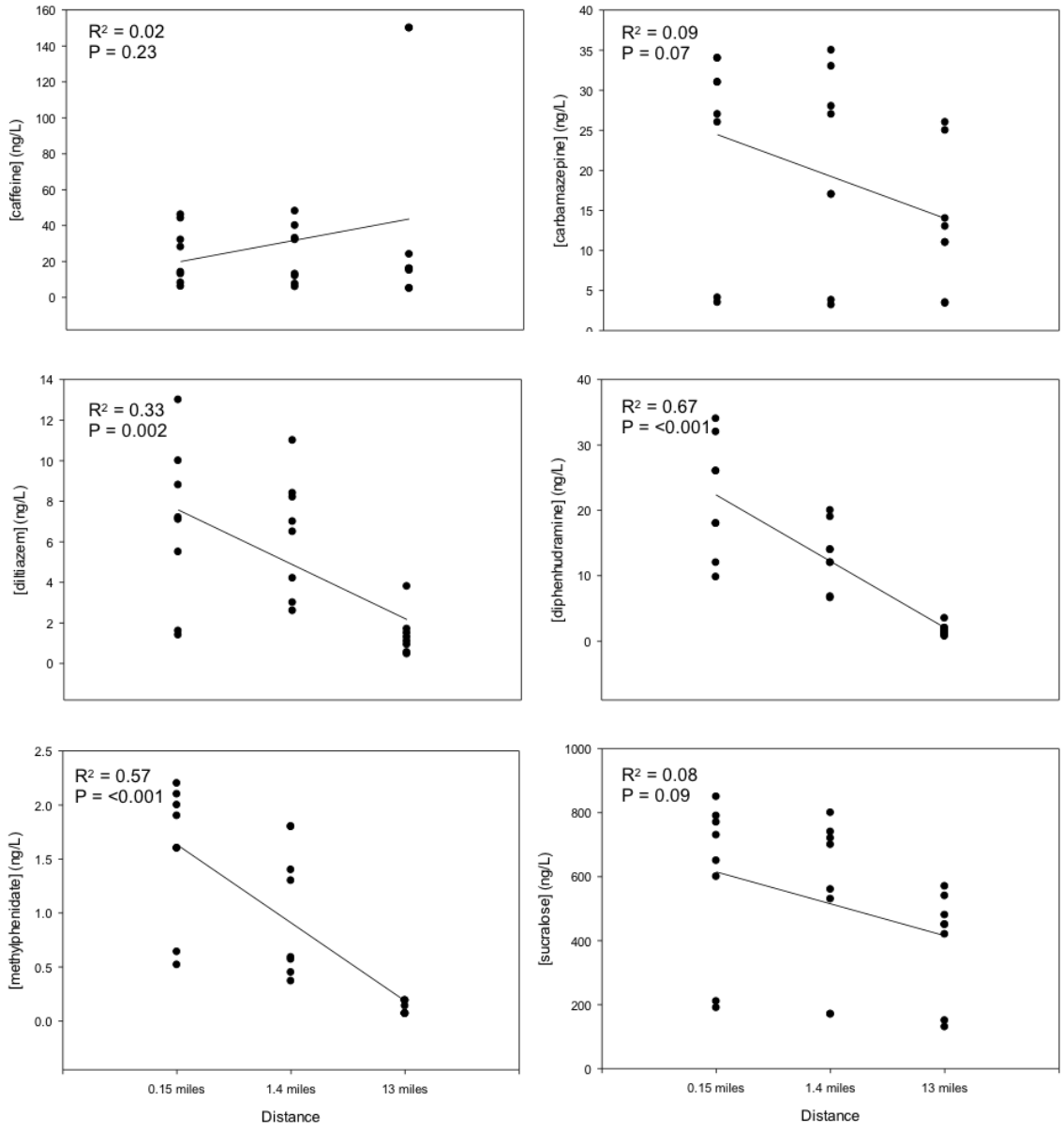

Figure 4.2. Water concentrations (ng/L) of caffeine, carbamazepine, diltiazem, diphenhydramine, methylphenidate, and sucralose over all seasons at each sampling site.

Decreasing pharmaceutical concentrations in water are likely due to attenuation and dilution from smaller tributaries along East Canyon Creek (Buswell 2017). Pharmaceutical concentrations often decrease due to instream dilution downstream of effluent discharges (Barber, et al. 2013). In addition to dilution, decreasing pharmaceutical concentrations

could be caused by sorptioning, biodegradation, photodegradation and hydrolysis, which are all mechanisms of instream attenuation (Brown, et al. 2015). However, the extent of pharmaceutical attenuation or transformation along the stream length will be reliant on compound specific physio-chemical properties and seasonal conditions (Acuna, et al. 2015). Differences in observed seasonal effluent concentrations may be explained by seasonal anthropogenic use patterns of pharmaceuticals in Park City, UT, which is a resort town with a changing population of visitors throughout the year. The resident population of Park City is 8, 128 (US Census Bureau 2015). However, the estimated visiting population of Park City during sampling was 24,207 during May, 60,740 during August, 53,739 during September, and 27,871 during October (Park City Chamber of Commerce and Visitors Bureau 2015). Thus, the observed visiting population in Park City was always greater than the resident population. The demographics of that visiting population would also be different during each season due to activities that are popular in Park City at different times of the year. Thus, a greater understanding of population demographics and pharmaceutical use among those populations would expand upon pharmaceutical occurrences in effluent during different seasons. Additional investigation into seasonal factors affecting pharmaceutical occurrences in effluent merits study to inform on spatial temporal conditions affecting exposure to aquatic species.

To further investigate spatial and temporal observations, the ratio of each target analyte was examined relative to the ratio of SUC along the stream distance (Figure 4.2). SUC, an artificial sweetener, does not undergo appreciable photodegradation, transformation at environmentally relevant pHs and temperatures, partition to other environmental compartments, or bioaccumulate. Thus, SUC is suitable as an

environmental tracer of effluent discharge due to low removal efficiency in WWTPs and high recalcitrance in surface waters (Du, et al. 2014b; Lim, Ong, and Hu 2017; Soh, et al. 2011). Because SUC is considered to be conserved as it moves downstream the ratio at each sampling site takes into account instream dilution. Therefore, all analytes with ratios below SUC are considered to be attenuating in some capacity. However, CAF was found at the upstream site at the same order of magnitude or higher than effluent, and levels remained consistent or increased downstream (Table 4.1). Caffeine is more readily degraded than SUC during the waste water treatment process and in the environment under environmentally relevant conditions (Soh, et al. 2011; Du, et al. 2014b). The present study identified that there was CAF at every sampling site and at ratios higher than SUC (Figure 4.2).

SUC appears to be a superior and more reliable indication of effluent discharge and flow than other tracers (Du, et al. 2016; Soh, et al. 2011). The current study provides a more complete picture of the behavior of SUC in an effluent dependent or dominated system than previous studies where a snap shot single site was sampled (Du, et al. 2016; Du, et al. 2014a). SUC also appears to be a more predictable indicator of waste water discharge when compared to CAF.

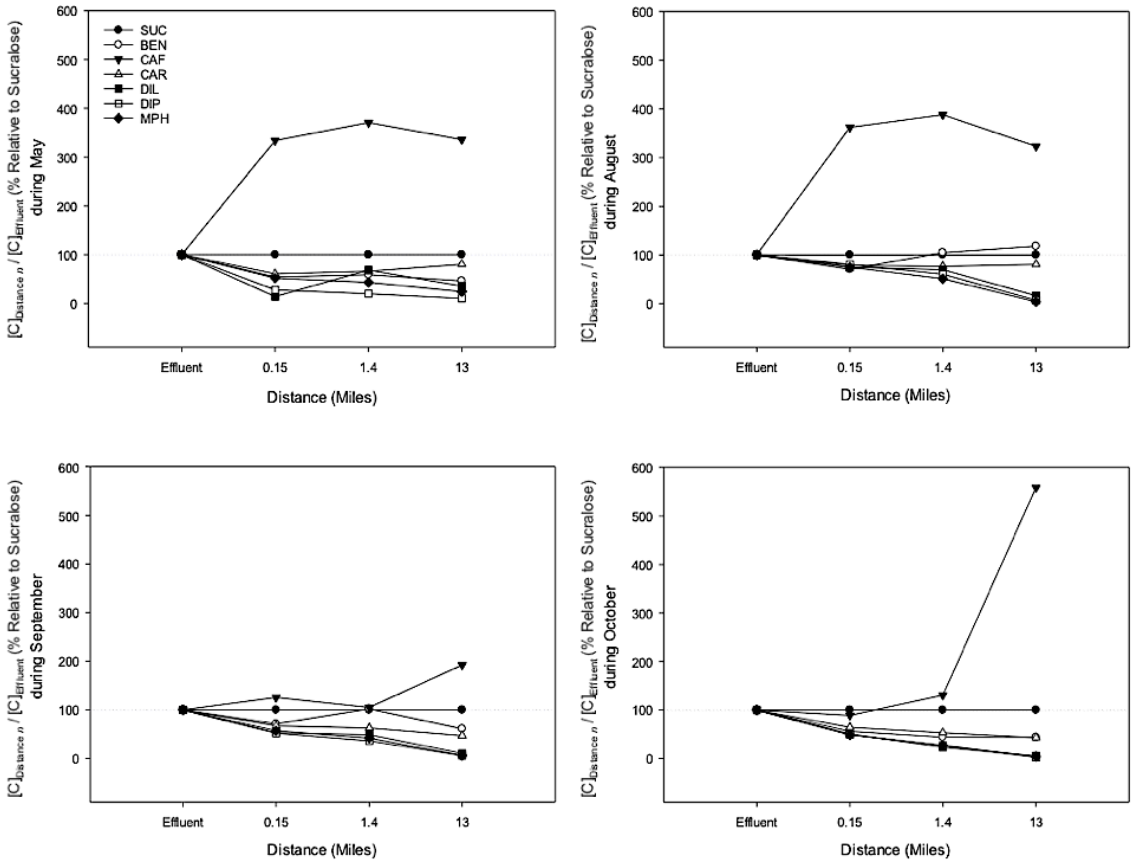

Figure 4.3. The ratio ([C]Distance / [C]Effluent) of target analytes relative to sucralose at three distances downstream (0.13, 1.44, 13 miles) during May, August, September, and October of 2014. BEN=benzoylecgonine, CAF=caffeine CAR=carbamazepine, DIL=diltiazem, DIP=diphenhydramine, MPH=methylphenidate, and SUC=sucralosee

The observation of target analytes in water at the upstream site (Table 4.1) and higher ratios of CAF can be attributed to non-point source contribution of treated waste water from onsite systems located near the reference site and along smaller tributaries flowing into East Canyon Creek. While CAF is removed efficiently during the WWTP process, onsite waste water system have much lower removal capacity (Du, et al. 2014b). Thus, it would appear that caffeine is a better indicator of non-point source inputs of CECs into streams. Further, increased dilution occurs progressively at each site downstream from the discharge, and instream discharge increases along the stream length (Figure 4.1),

suggesting addition sources of surface or groundwater to the system. Potential contributions of CECs from on-site (e.g., septic) or other sources (e.g., compromised infrastructure) may require additional sewage epidemiological study of sources, including targeted drugs of abuse and substances varying temporally for consumer use in response to cold and flu season, allergy season, or transient population shifts.

Therapeutic Hazard Assessment of Pharmaceuticals in Fish Plasma

Despite extensive surface water and effluent monitoring of pharmaceuticals and other CECs (Kolpin, et al. 2002; Ebele, Abou-Elwafa Abdallah, and Harrad 2017), translating measured environmental data to support robust water quality assessment and management for ecological uses have been inherently limited by data availability (Brooks, Huggett, and Boxall 2009; Berninger, et al. 2016; Brooks 2018). For example, potential ecological risks of most pharmaceuticals following introduction to surface water bodies is also not well understood (Brooks, Huggett, and Boxall 2009; Ankley, et al. 2007; Boxall, et al. 2012b). Fortunately, extensive mammalian pharmacology and toxicology data exists in the case of pharmaceuticals, which is not the case for the majority of industrial chemicals; this information is quite valuable for prioritizing substances of relatively higher environmental quality concern (Ankley, et al. 2007; Brooks 2014; Fick, et al. 2010b; Gunnarsson, et al. 2008; Huggett, et al. 2003; Brooks 2018; Berninger, et al. 2016). However, identifying ways to leverage such available chemical safety data for pharmaceuticals represents a major research need (Boxall, et al. 2012b; Rudd, et al. 2014; Berninger, et al. 2016).

As mentioned above, the THV represents a direct method for translating waterborne instream concentrations to potential therapeutic hazards in non-target species. Such a

comparison is achieved by relating the instream concentration to the C_{min} (Brooks 2018). In the present study, THVs over a 24 hour period were calculated for six compounds detected in *S. trutta* plasma (Table 4.3) at each site during each sampling event and compared to the observed water concentration (Figures 4.3-4.8). AMI, FLU, NOR, and SER exceeded the predicted THV (with 1000 fold safety factor) 100% of the time at all sites during all sampling events. Conversely, CAF did not exceed the predicted THV (with 1000 fold safety factor) at any site during any sampling. DIP exceeded the predicted THV (with 1000 fold safety factor) 100% of the time at the 0.15 and 1.4 mile sites during all sampling events and at the 13 mile site during the May sampling event. During the August and September sampling events DIP exceeded the predicted THV (with 1000 fold safety factor) 38.5% and 17.7% of the time, respectively, at the 13 mile site, while no exceedance was observed during October. At no time during the present study did any water concentration exceed a THV without the 1000 fold safety factor.

Alongside the THV, which is used to predict potential therapeutic hazards (Brooks 2018), we tested the previously proposed fish plasma modeling approach (Fitzsimmons 2001; Huggett, et al. 2003) to understand potential risks of CEC exposure to *S. trutta*, and how these risks may vary spatially and temporally in East Canyon Creek. A comparison of predicted and measured *S. trutta* plasma levels and the relationships among these observations to human therapeutic levels (C_{min}) are reported in Figures 4.9-4.14. The tricyclic antidepressant AMI, the selective serotonin reuptake inhibitor FLU and its primary active metabolite NOR were generally predicted from water concentrations within an order of magnitude of the observed internal dose levels in *S. trutta*.

Table 4.2. Human pharmaceuticals in fish plasma collected from Salmo trutta in East Canyon Creek at an upstream site and three downstream sites (0.15 miles, 1.44 miles, 13 miles) during 2014. AMI, amitriptyline; CAF, caffeine; DIP, diphenhydramine; FLU, fluoxetine; NOR, norfluoxetine; SER, sertraline; ND, No Detect; <MDL, below method detection limit; MDL, method detection limit.

		Analyte											
		AMI (ng/mL)		CAF (ng/mL)		DIP (ng/mL)		FLU (ng/mL)		NOR (ng/mL)		SER (ng/mL)	
Sampling Period	Site	Mean ± SD	Freq.	Mean ± SD	Freq.	Mean ± SD	Freq.	Mean ± SD	Freq.	Mean ± SD	Freq.	Mean ± SD	Freq.
May	Upstream	ND	0/10	<MDL	10/10	0.04	1/10	ND	10/10	ND	10/10	ND	0/10
	0.1 Mile	2.1 ± 1.1	5/10	<MDL	8/10	0.14 ± 0.05	10/10	<MDL	10/10	<MDL	9/10	<MDL	10/10
	1 Mile	ND	0/10	<MDL	3/10	0.15 ± 0.04	10/10	<MDL	10/10	<MDL	8/10	<MDL	8/10
	10 Mile	5.1 ± 2.0	6/10	<MDL	3/10	0.06 ± 0.03	10/10	<MDL	9/10	<MDL	7/10	<MDL	1/10
August	Upstream	ND	0/10	<MDL	10/10	ND	0/10	ND	0/10	ND	0/10	0.66	2/10
	0.1 Mile	1.6 ± 0.88	8/10	<MDL	10/10	0.41 ± 0.18	10/10	2.3 ± 1.3	10/10	1.4 ± 1.1	10/10	1.6 ± 0.81	10/10
	1 Mile	ND	0/10	<MDL	10/10	0.20 ± 0.07	10/10	0.77 ± 0.29	10/10	0.62 ± 0.30	9/10	0.47 ± 0.19	10/10
	10 Mile	ND	0/10	0.90 ± 0.56	10/10	0.07 ± 0.01	4/10	<MDL	1/10	ND	0/10	<MDL	1/10
September	Upstream	ND	0/5	<MDL	5/5	ND	0/5	ND	0/5	ND	0/5	2.4	1/5
	0.1 Mile	ND	0/5	<MDL	3/5	0.10 ± 0.02	5/5	<MDL	5/5	0.74 ± 0.37	5/5	<MDL	5/5
	1 Mile	ND	0/5	<MDL	5/5	0.06 ± 0.03	5/5	<MDL	3/5	<MDL	4/5	<MDL	3/5
	10 Mile	ND	0/5	<MDL	5/5	0.13 ± 0.04	5/5	<MDL	5/5	<MDL	5/5	<MDL	5/5
October	Upstream	ND	0/10	<MDL	8/10	0.05	2/10	<MDL	1/10	ND	0/10	<MDL	9/10
	0.1 Mile	4.8 ± 3.1	5/10	<MDL	10/10	0.19 ± 0.04	10/10	<MDL	10/10	<MDL	10/10	0.48 ± 0.27	10/10
	1 Mile	7.2 ± 7.7	9/10	<MDL	10/10	0.12 ± 0.06	10/10	<MDL	9/10	<MDL	9/10	<MDL	10/10
	10 Mile	7.0 ± 6.2	4/10	<MDL	10/10	0.06 ± 0.02	10/10	<MDL	2/10	<MDL	3/10	ND	0/10
MDL		1.99		1.44		0.03		1.37		0.94		0.7	

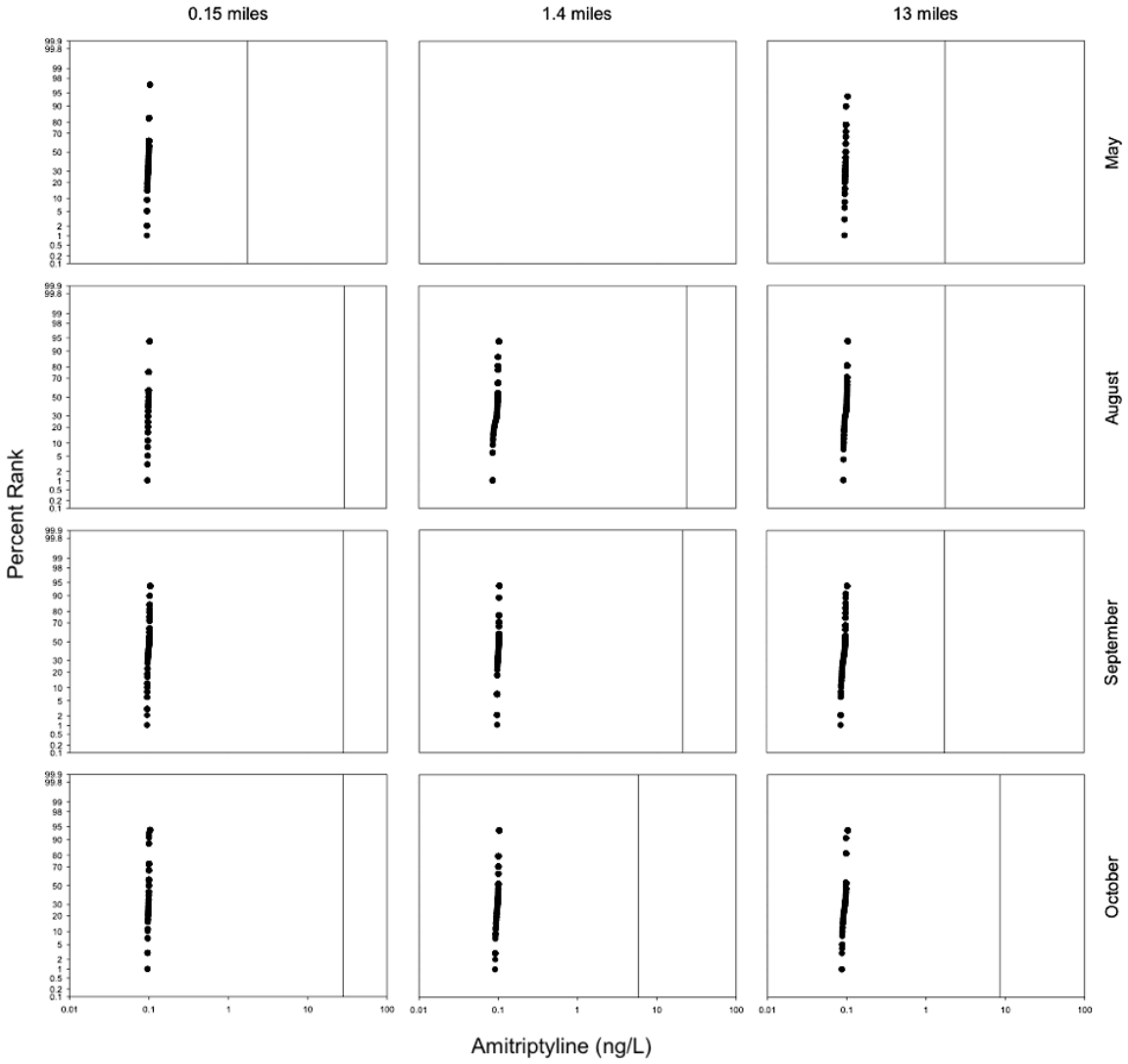

Figure 4.4. Probability distribution of therapeutic hazard values for amitriptyline, including a 1000-fold safety factor based on pH at 15-minute intervals over a 24-hour period in East Canyon Creek at the three sites downstream of the discharge (0.15, 1.44, 13 miles) during May, August, September, and October of 2014. The horizontal reference line represents the measured water concentration at that site during the sampling.

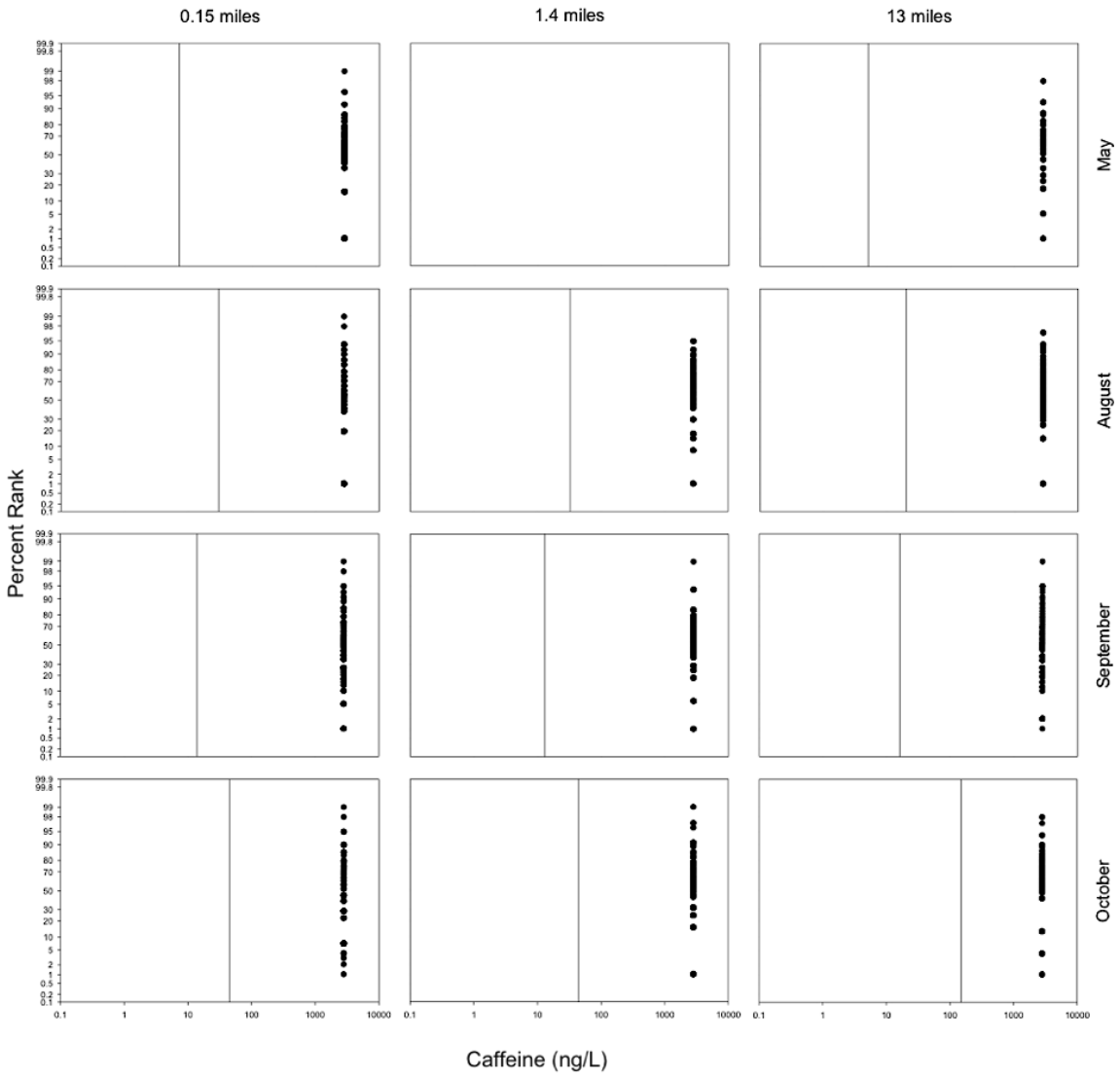

Figure 4.5. Probability distribution of therapeutic hazard values for caffeine, including a 1000-fold safety factor based on pH at 15-minute intervals over a 24-hour period in East Canyon Creek at the three sites downstream of the discharge (0.15, 1.44, 13 miles) during May, August, September, and October of 2014. The horizontal reference line represents the measured water concentration at that site during the sampling.

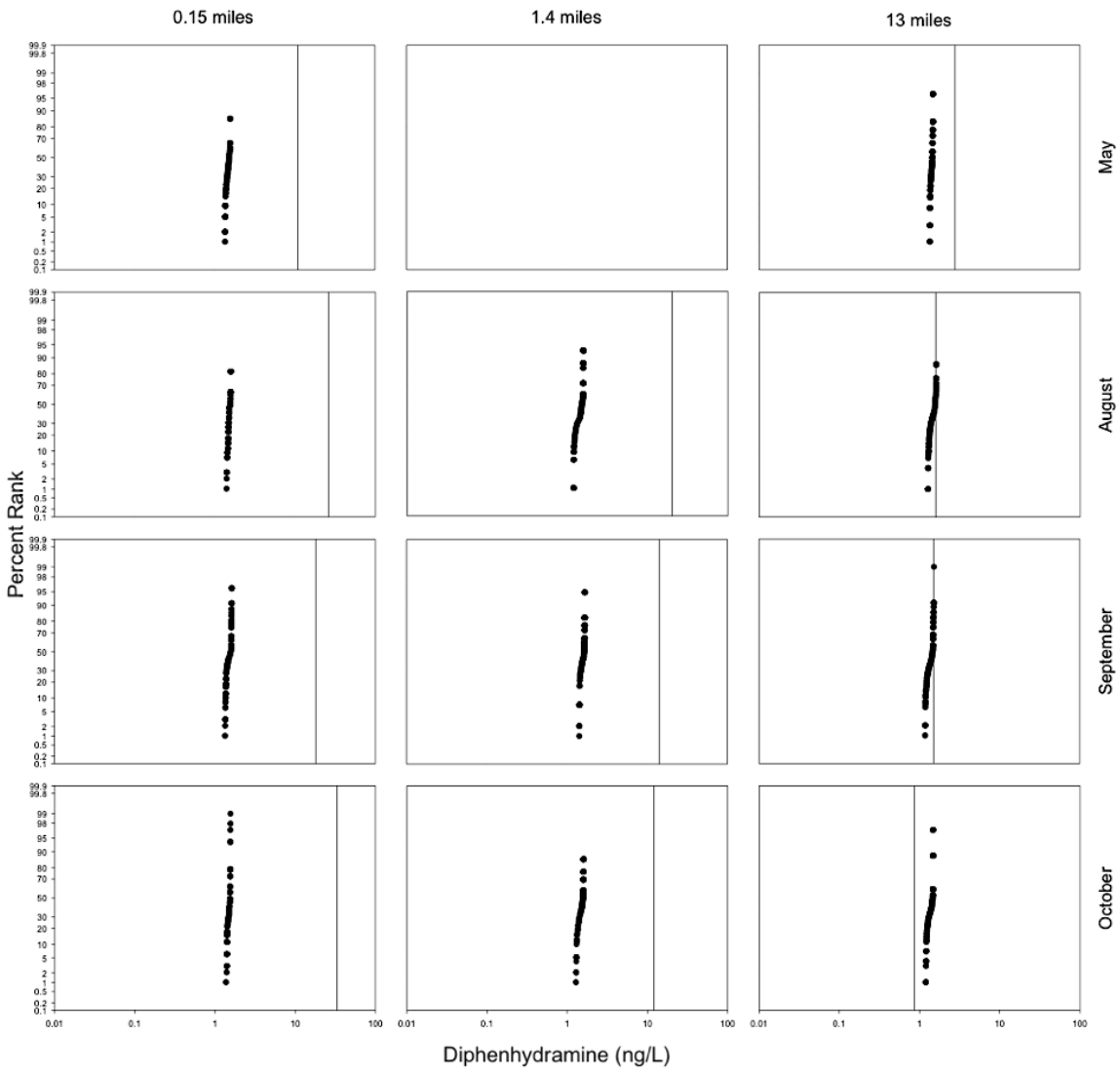

Figure 4.6. Probability distribution of therapeutic hazard values for diphenhydramine, including a 1000-fold safety factor based on pH at 15-minute intervals over a 24-hour period in East Canyon Creek at the three sites downstream of the discharge (0.15, 1.44, 13 miles) during May, August, September, and October of 2014. The horizontal reference line represents the measured water concentration at that site during the sampling.

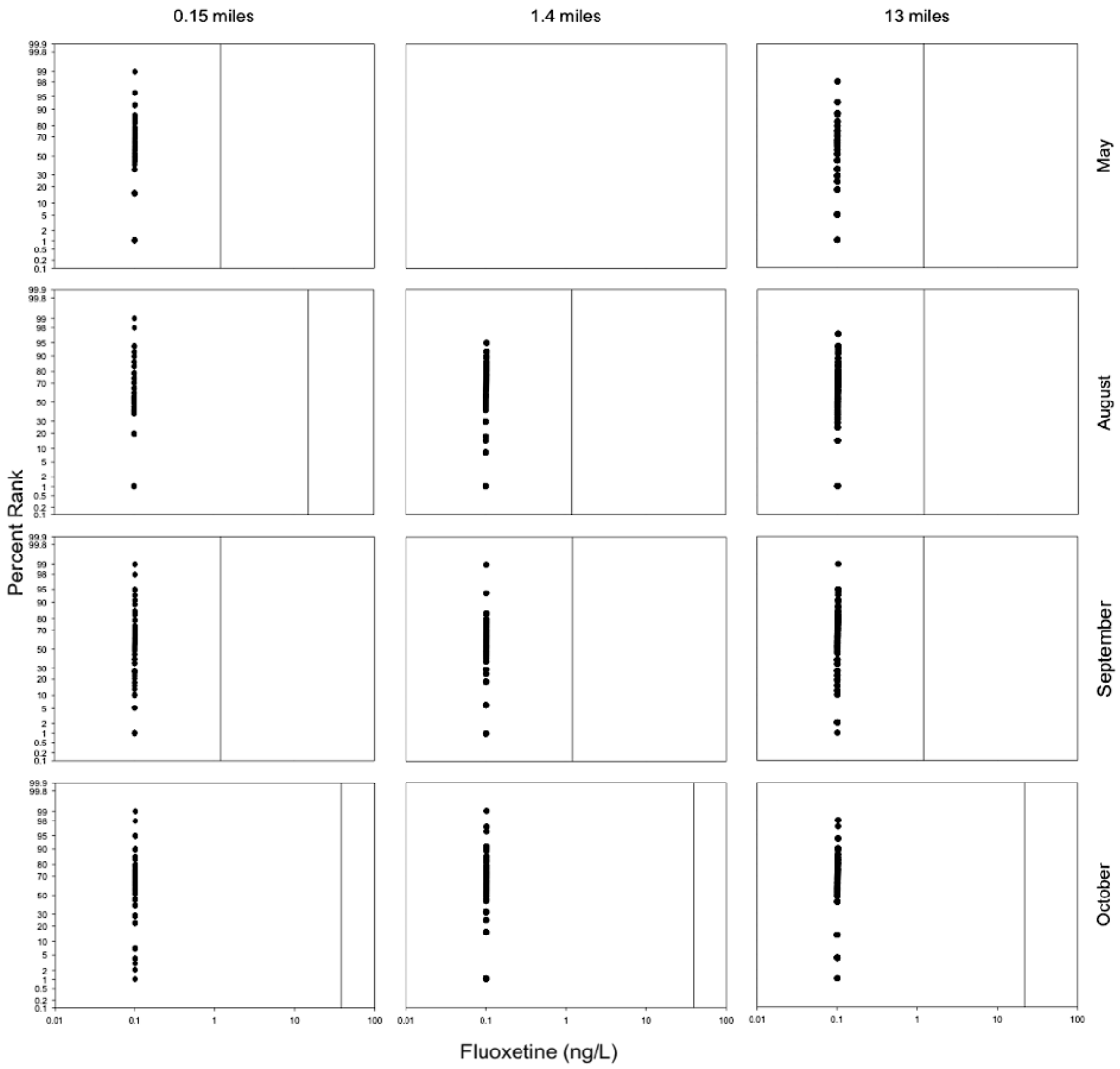

Figure 4.7. Probability distribution of therapeutic hazard values for fluoxetine, including a 1000-fold safety factor based on pH at 15-minute intervals over a 24-hour period in East Canyon Creek at the three sites downstream of the discharge (0.15, 1.44, 13 miles) during May, August, September, and October of 2014. The horizontal reference line represents the measured water concentration at that site during the sampling.

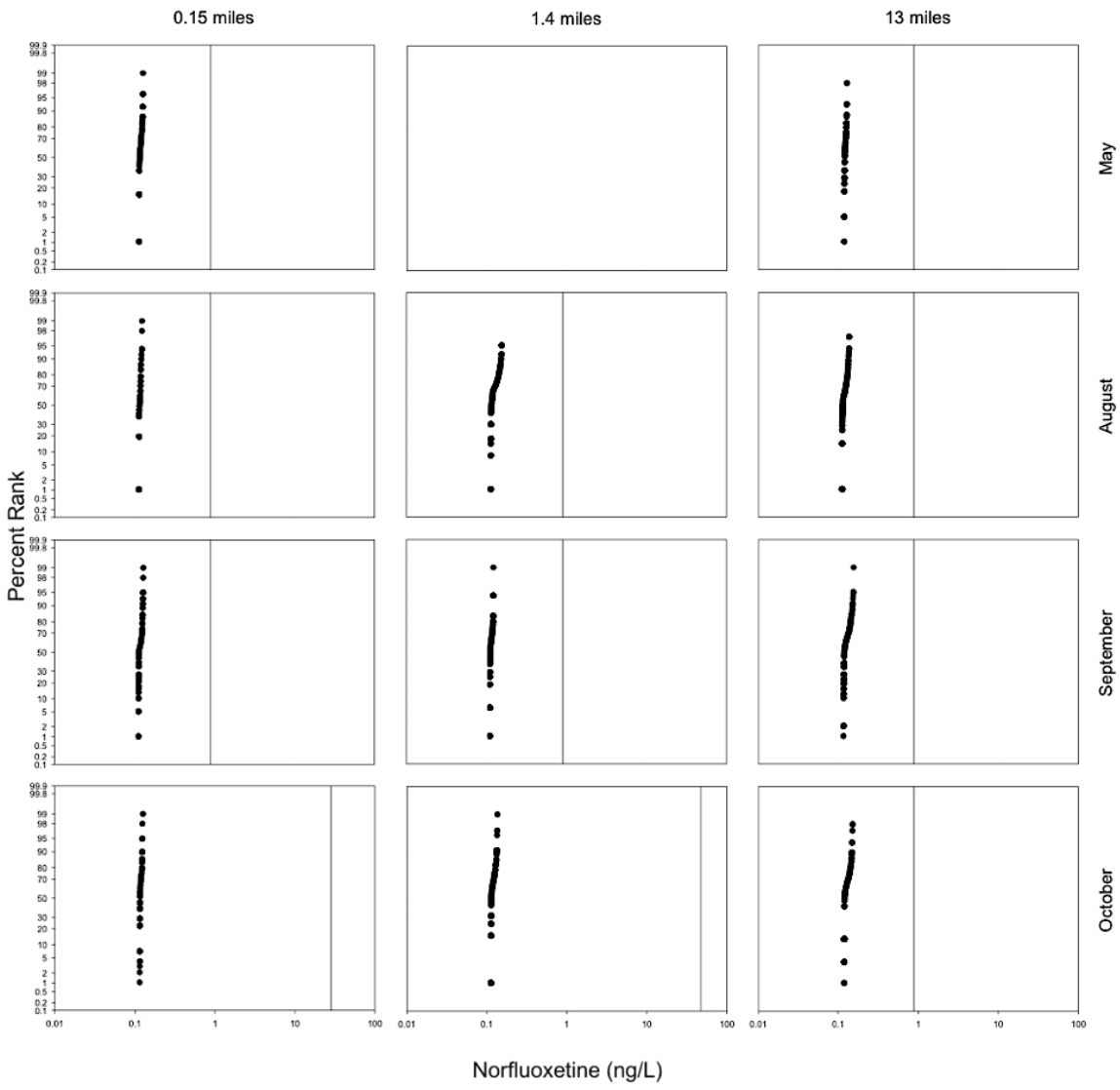

Figure 4.8. Probability distribution of therapeutic hazard values for norfluoxetine, including a 1000-fold safety factor based on pH at 15-minute intervals over a 24-hour period in East Canyon Creek at the three sites downstream of the discharge (0.15, 1.44, 13 miles) during May, August, September, and October of 2014. The horizontal reference line represents the measured water concentration at that site during the sampling.

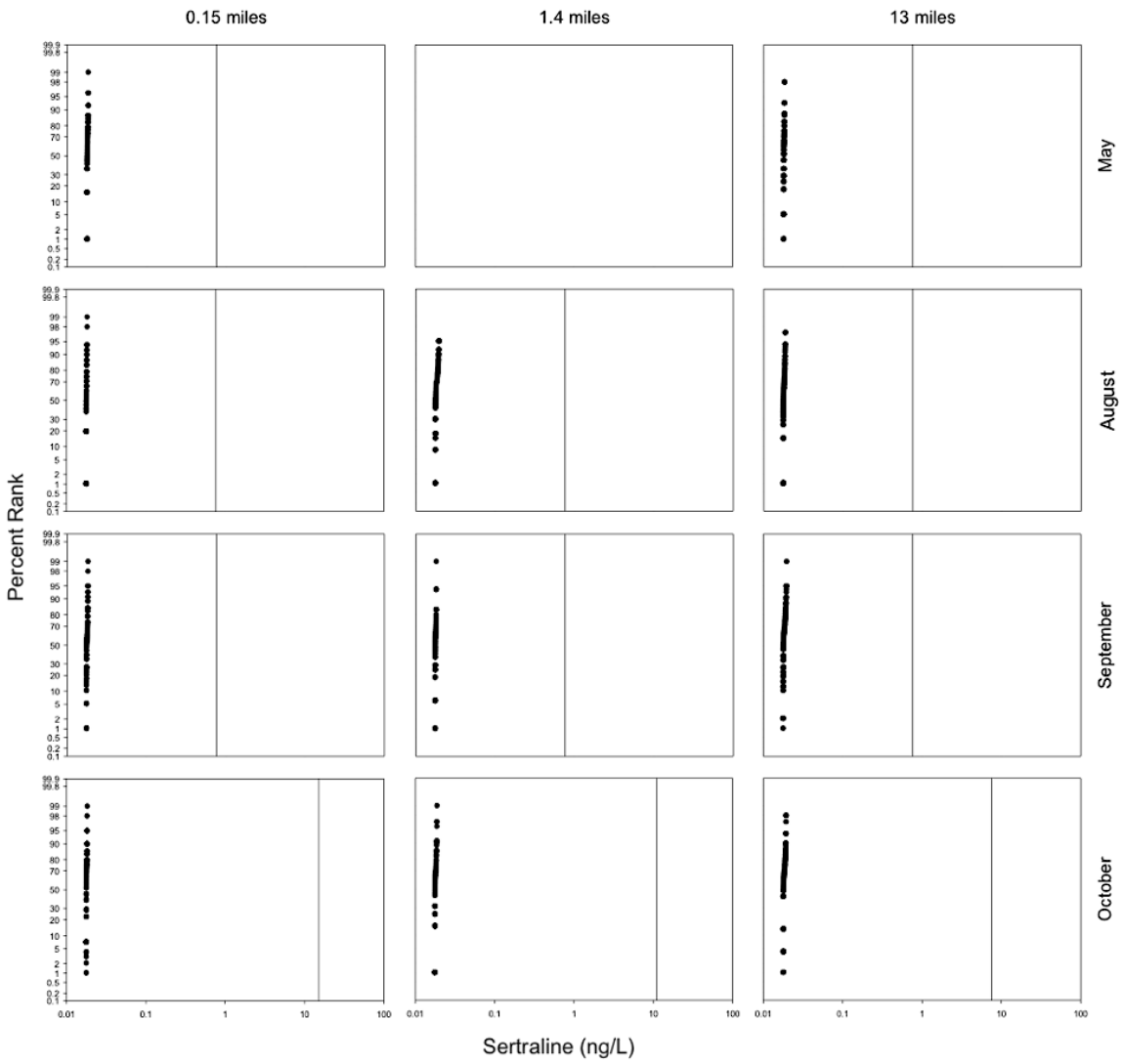

Figure 4.9. Probability distribution of therapeutic hazard values for sertraline, including a 1000-fold safety factor based on pH at 15-minute intervals over a 24-hour period in East Canyon Creek at the three sites downstream of the discharge (0.15, 1.44, 13 miles) during May, August, September, and October of 2014. The horizontal reference line represents the measured water concentration at that site during the sampling.

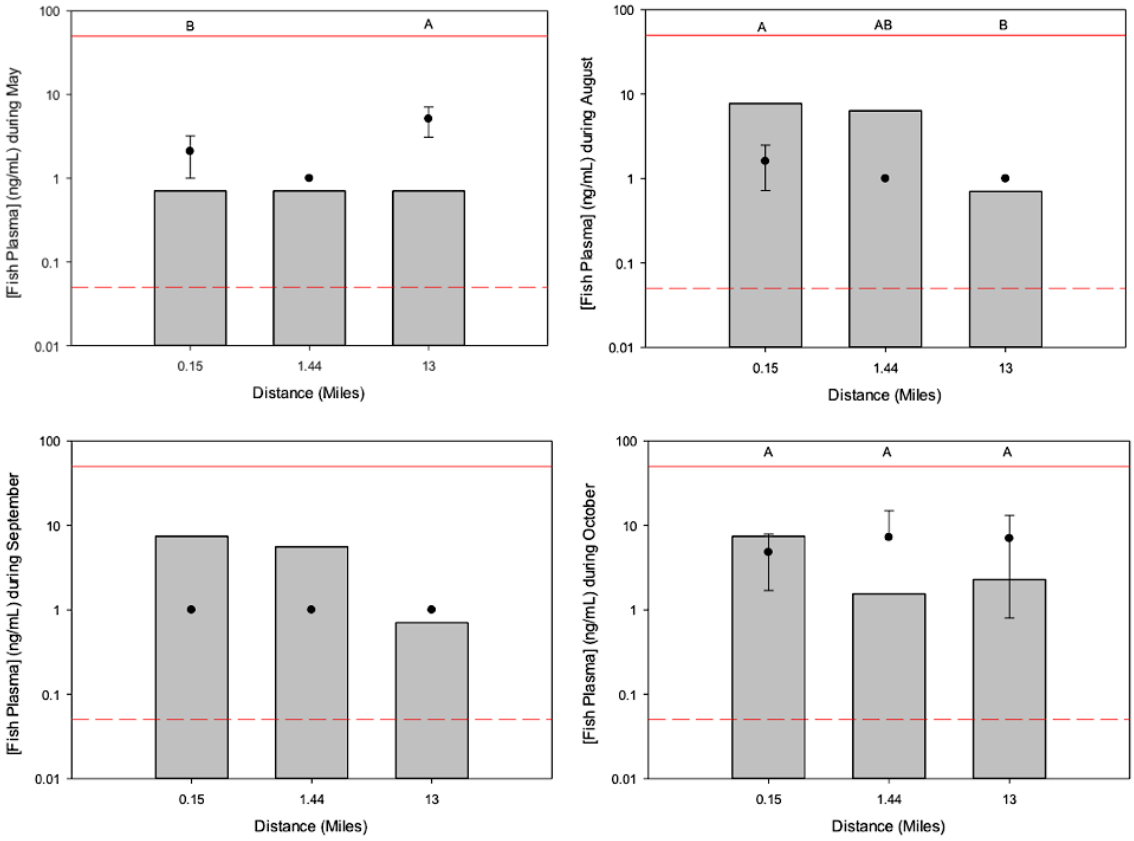

Figure 4.10. The predicted fish plasma concentration of amitriptyline (gray bars) compared to the mean (±SD) measured concentration of amitriptyline (dots) in Salmo trutta plasma at the three sites downstream of the discharge (0.15, 1.44, 13 miles) during May, August, September, and October of 2014. Letters represent accumulation in fish plasma at that site that is significantly different ($p<0.05$) from plasma accumulation at other sites along the sampling distance. The horizontal reference line represents the human Cmin. The dashed horizontal reference line represents the human Cmin with a 3-fold safety factor.

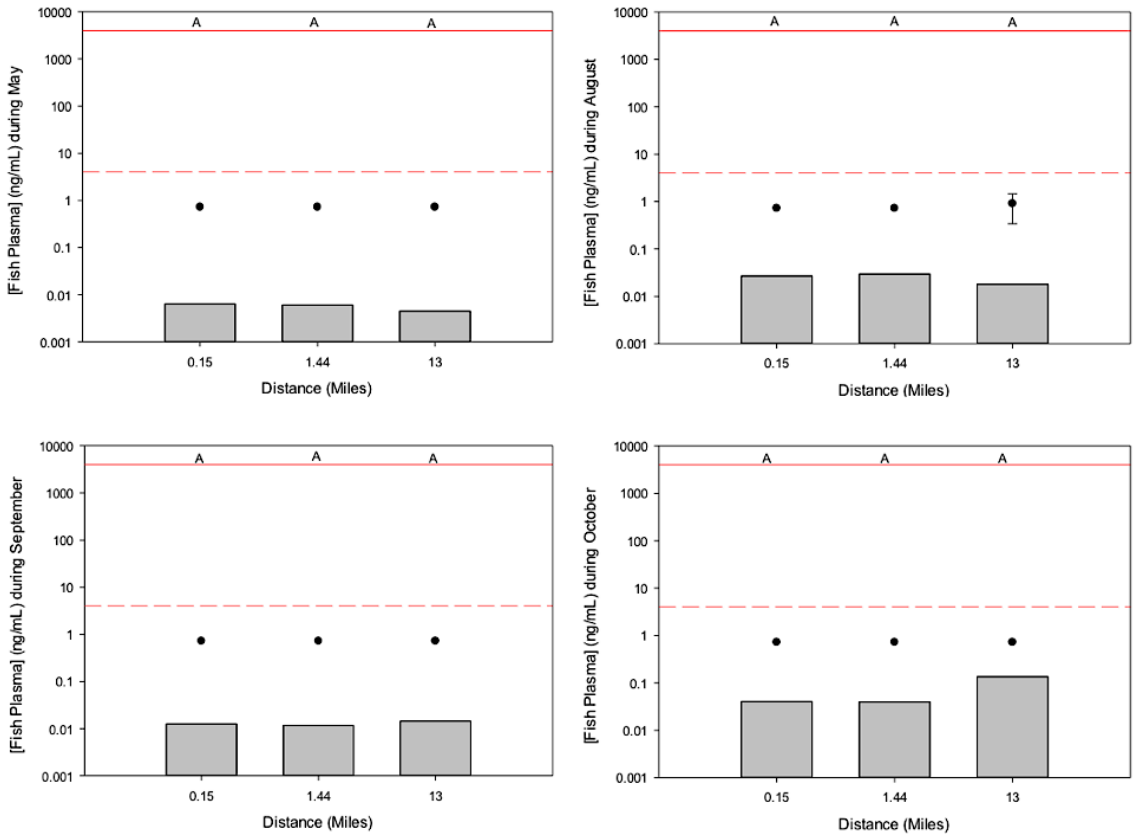

Figure 4.11. The predicted fish plasma concentration of caffeine (gray bars) compared to the mean (±SD) measured concentration of caffeine (dots) in Salmo trutta plasma at the three sites downstream of the discharge (0.15, 1.44, 13 miles) during May, August, September, and October of 2014. Letters represent accumulation in fish plasma at that site that is significantly different ($p<0.05$) from plasma accumulation at other sites along the sampling distance. The horizontal reference line represents the human Cmin. The dashed horizontal reference line represents the human Cmin with a 3-fold safety factor.

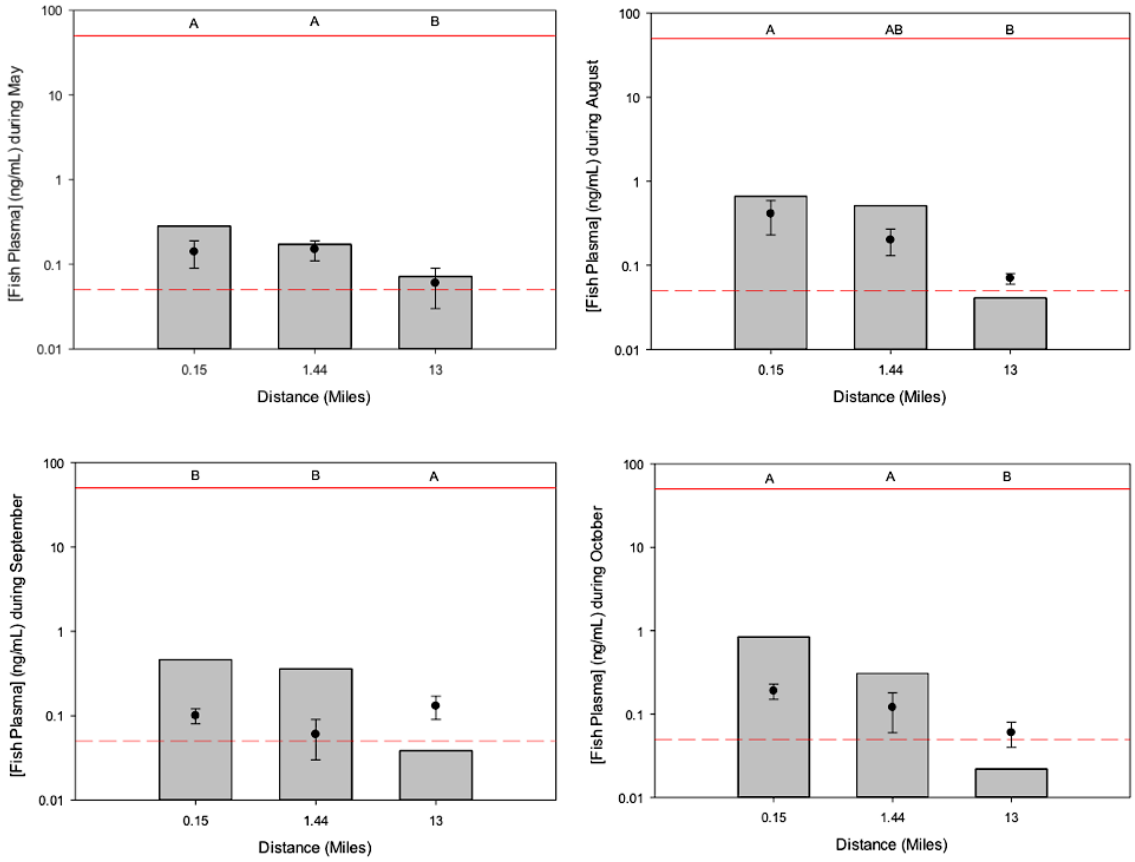

Figure 4.12. The predicted fish plasma concentration of diphenhydramine (gray bars) compared to the mean (±SD) measured concentration of diphenhydramine (dots) in Salmo trutta plasma at the three sites downstream of the discharge (0.15, 1.44, 13 miles) during May, August, September, and October of 2014. Letters represent accumulation in fish plasma at that site that is significantly different ($p<0.05$) from plasma accumulation at other sites along the sampling distance. The horizontal reference line represents the human Cmin. The dashed horizontal reference line represents the human Cmin with a 3-fold safety factor.

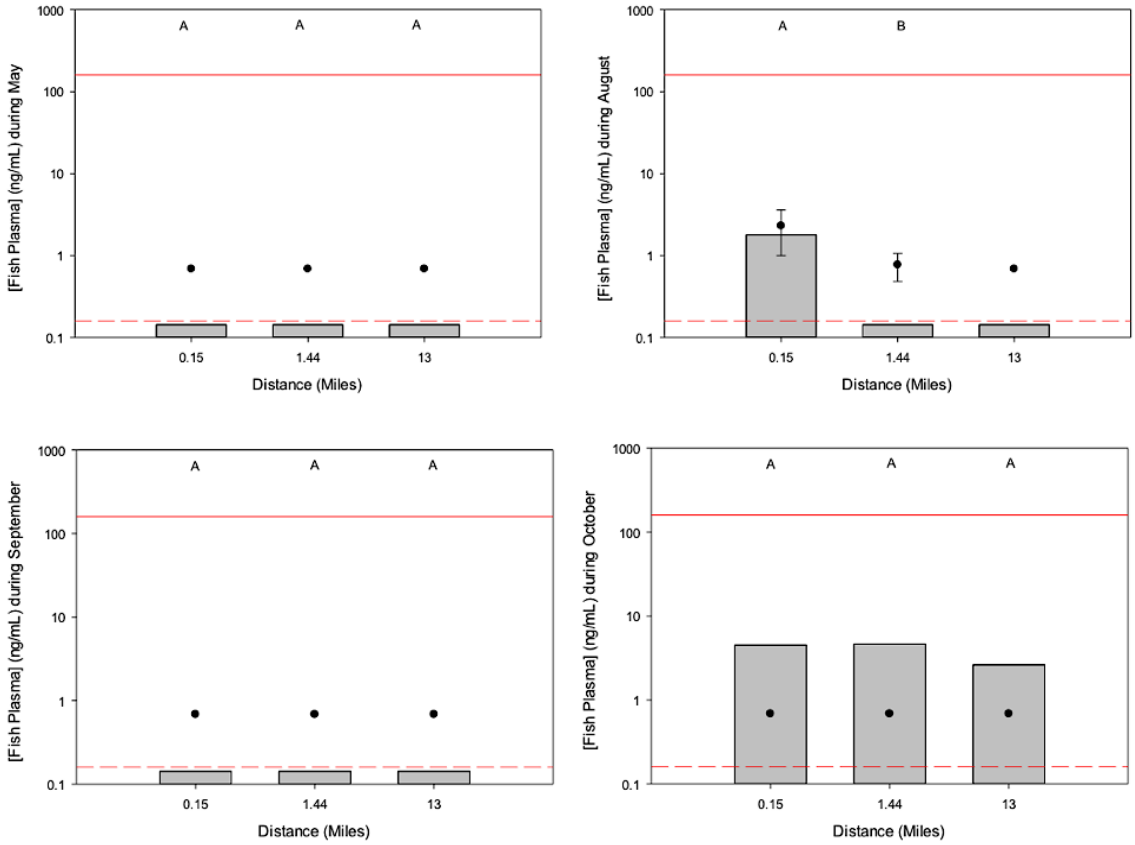

Figure 4.13. The predicted fish plasma concentration of fluoxetine (gray bars) compared to the mean (±SD) measured concentration of fluoxetine (dots) in Salmo trutta plasma at the three sites downstream of the discharge (0.15, 1.44, 13 miles) during May, August, September, and October of 2014. Letters represent accumulation in fish plasma at that site that is significantly different ($p<0.05$) from plasma accumulation at other sites along the sampling distance. The horizontal reference line represents the human Cmin. The dashed horizontal reference line represents the human Cmin with a 3-fold safety factor.

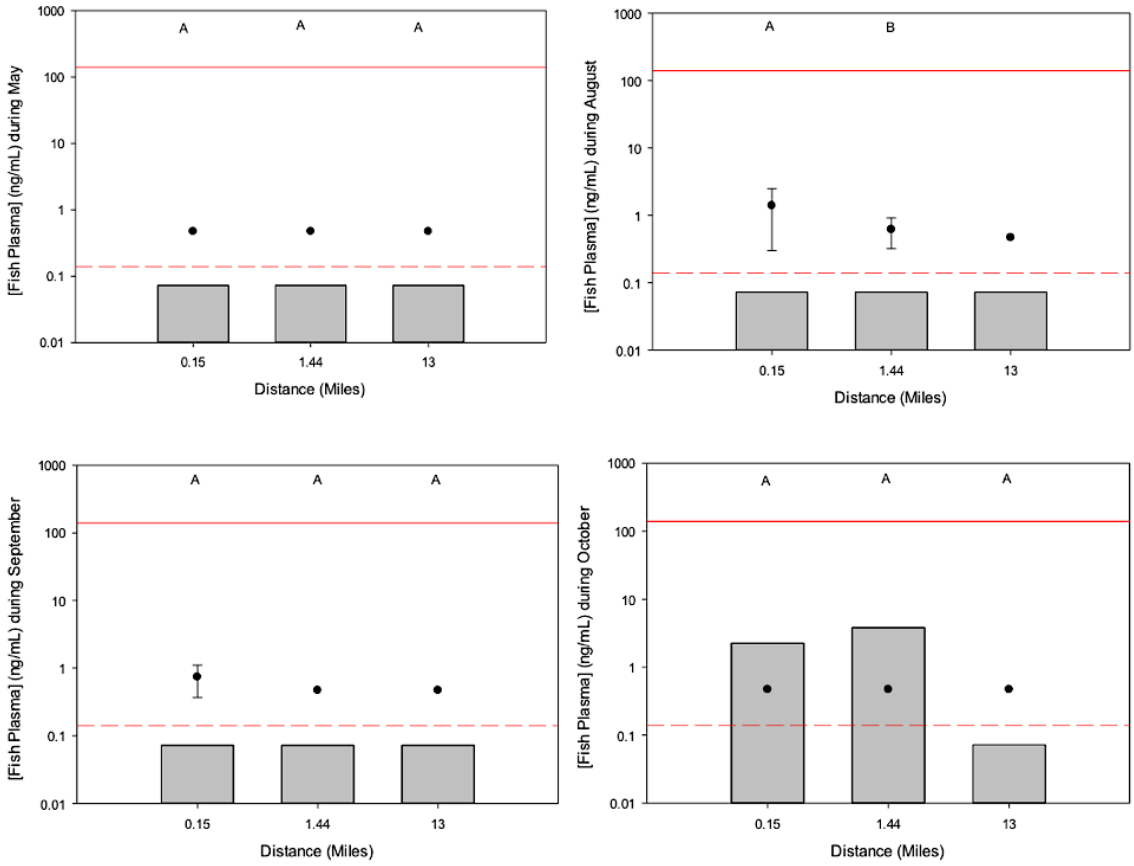

Figure 4.14. The predicted fish plasma concentration of norfluoxetine (gray bars) compared to the mean (±SD) measured concentration of norfluoxetine (dots) in Salmo trutta plasma at the three sites downstream of the discharge (0.15, 1.44, 13 miles) during May, August, September, and October of 2014. Letters represent accumulation in fish plasma at that site that is significantly different ($p<0.05$) from plasma accumulation at other sites along the sampling distance. The horizontal reference line represents the human Cmin. The dashed horizontal reference line represents the human Cmin with a 3-fold safety factor.

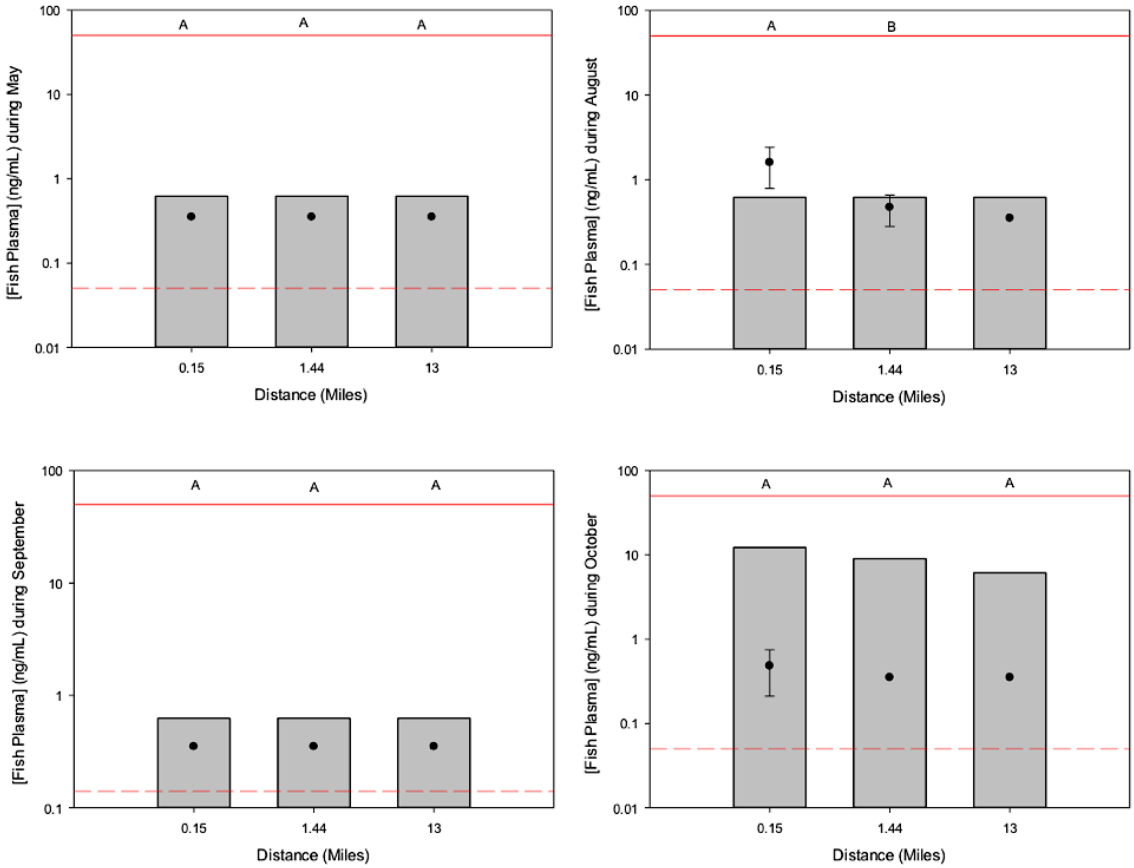

Figure 4.15. The predicted fish plasma concentration of sertraline (gray bars) compared to the mean (±SD) measured concentration of sertraline (dots) in Salmo trutta plasma at the three sites downstream of the discharge (0.15, 1.44, 13 miles) during May, August, September, and October of 2014. Letters represent accumulation in fish plasma at that site that is significantly different ($p<0.05$) from plasma accumulation at other sites along the sampling distance. The horizontal reference line represents the human Cmin. The dashed horizontal reference line represents the human Cmin with a 3-fold safety factor.

CAF was not predicted to accumulate in *S. trutta* plasma due to its relative hydrophobicity, but it was detected in fish plasma at all study sites during every sampling event. During the May sampling effort, DIP and SER were over-predicted because measured levels in *S. trutta* plasma were between 50 and 86% of predicted values at downstream sites. During the August, September, and October sampling events, DIP was over-predicted at the 0.15 and 1.44 mile sites, but under-predicted at the 13 mile site. The measured concentrations of AMI, DIP, FLU, NOR, and SER in *S. trutta* plasma all exceeded the C_{min} value with the

previously proposed 1000-fold safety factor (Huggett, et al. 2003), while CAF did not exceed the C_{min} with safety factor.

The THV concept has been previously evaluated and shown utility for advanced water quality assessments of pharmaceuticals (Kristofco and Brooks 2017; Saari, Scott, and Brooks 2017; Scott, et al. 2016; Valenti, et al. 2012); however, a need to evaluate the THV spatially and temporally within varying pH profiles was recently identified (Scott, et al. 2016; Saari, Scott, and Brooks 2017). Because the THV compares the water concentration to the C_{min} value with 1000-fold safety factor, the observed plasma concentrations in *S. trutta* can also be compared to the C_{min} with 1000-fold safety factor as a tool to identify whether the THV is accurately predicating compounds of concern during screening. In the present study, AMI, DIP, FLU, NOR, and SER were all predicted to exceed the C_{min} with 1000-fold safety factor by the THV and the observed plasma concentrations did in fact correspond to the previous prediction. Further CAF was not predicted to exceed the C_{min} with 1000-fold safety factor and the corresponding plasma levels also did not exceed the C_{min} value. Thus, the current study demonstrates the utility of the THV as a screening tool to translate water concentrations into potential aquatic hazards. In the current study several antidepressants were observed to accumulate in plasma of *S. trutta* within this safety factor of 1000 compared to human therapeutic doses (C_{min}). These antidepressants are considered endocrine disrupting compounds given the critical role of serotonin in neuroendocrine function (Foran, et al. 2004). Further, it is particularly important to note that levels of the tricyclic antidepressant AMI were observed within just one order of magnitude of its corresponding human C_{min} level during the October sampling event. Unfortunately, the bioaccumulation dynamics (e.g., uptake,

depuration) or toxicological implications of such observations are not understood but warrant additional study, particularly during low flow periods in East Canyon Creek. Further, though this water quality assessment approach is quite promising, additional studies are necessary to test the utility of and then extend such modeling efforts to fish species across environmental relevant surface water pH gradients for other ionizable contaminants.

Acknowledgments

Support for this study was provided by the Snyderville Basin Water Reclamation District. We thank staff from the Snyderville Basin Special Reclamation District and the Utah Department of Natural Resources for assisting with field sampling. We also thank Dr. Bowen Du, Leah Botkin, Kailey Reimen, Craig Calvert, and Nick Adams for additional support.

CHAPTER FIVE

Determination of Microcystins, Nodularin, Anatoxin-a, Cylindrospermopsin, and Saxitoxin in Water and Fish Tissue using Isotope Dilution Liquid Chromatography Tandem Mass Spectrometry

Abstract

Cyanobacteria can form dense blooms, under specific environmental conditions, and some species produce harmful secondary metabolites known as cyanotoxins, which present significant risks to public health and the environment. Identifying toxins produced by cyanobacteria present in surface water and fish is critical to ensuring high quality food and water for consumption, and recreation. Current analytical screening methods typically focus on one class of cyanotoxins in a single matrix and rarely include saxitoxin, a select agent. Thus, a cross-class screening method for microcystins, nodularin, anatoxin-a, cylindrospermopsin, and saxitoxin was developed to examine target analytes in environmental water and fish tissue. This was done, due to the broad range of cyanotoxin physicochemical properties, by pairing two extraction and separation techniques were paired to improve isolation and detection. For the first time a zwitterionic hydrophilic interaction liquid chromatography column was evaluated to separate anatoxin-a, cylindrospermopsin, and saxitoxin, demonstrating greater sensitivity for all three compounds over previous techniques. Further, the method for microcystins and nodularin was validated using isotopically labeled internal standards, again for the first time, resulting in improved compensation for recovery bias and matrix suppression. Optimized extractions for water and fish tissue can be extended to other congeners in the future. These improved

separation and isotope dilution techniques are a launching point for more complex, non-targeted analyses, with preliminary targeted screening.

Introduction

Cyanobacteria are prokaryotic microorganisms found globally in both inland waters and coastal and marine systems (Merel, et al. 2013; Buratti, et al. 2017). Across varying environmental conditions, cyanobacteria can produce harmful secondary metabolites called cyanotoxins, which possess various physiochemical properties, structures, and toxicological mechanisms of action (Pearson, et al. 2016; Buratti, et al. 2017). Microcystins (MCs) and nodularin (NOD) are hepatotoxic cyclic peptides (Buratti, et al. 2017; Merel, et al. 2013). Cylindrospermopsin (CLD) is a cytotoxic, dermotoxic, and hepatotoxic cyclic guanidinic alkaloid (de la Cruz, et al. 2013). Anatoxin-a (ANA) is a neurotoxic bicyclic secondary amine (Buratti, et al. 2017; Merel, et al. 2013). Saxitoxin (SAX) is a neurotoxic guanadinium derivative with two amine functional groups (Buratti, et al. 2017; Merel, et al. 2013). Occurrence of these cyanotoxins in the environment, resulting from cyanobacterial Harmful Algal Blooms (HABs), have been reported globally in surface waters (Buratti, et al. 2017).

Cyanobacterial HABs result in various water quality problems and severe economic damage by impairing water supplies, recreational activities and fisheries (Brooks, et al. 2016; Merel, et al. 2013). Further, exposures to cyanotoxins through food and water can be fatal to both humans and wildlife (Merel, et al. 2013; Buratti, et al. 2017; Pearson, et al. 2016). Despite the complexity of environmental exposures and economic losses caused by these compounds, few water quality criteria and regulations for exposure to cyanotoxins exist, especially in the developing world (Merel, et al. 2013; Brooks, et al. 2017). Many

countries have regulatory values for exposure to microcystin-LR that are in agreement with the recommended exposure level (1.0 µg L^{-1}) provided by the World Health Organization (Merel, et al. 2013; WHO 2011). In the United States, the Environmental Protection Agency (EPA) has revised the Unregulated Contaminant Monitoring Rule (UCMR 4) for Public Water Systems to add 10 cyanotoxins (U.S.EPA 2015b), has added several toxins to the Contaminant Candidate List 3 and 4 (CCL3&4) (U.S.EPA 2016a), and has proposed the Draft Human Health Recreational Ambient Water Quality Criteria or Swimming Advisories for MCs (4 µg L^{-1}) and CLD (8 µg L^{-1}) (U.S.EPA 2016b). However, a lesser studied pathway to exposure in humans is through the consumption of contaminated food, such as dietary supplements, invertebrates, and fish (Buratti, et al. 2017). Thus, a multi-toxin screening method for cyanotoxins in water and fish tissue is necessary to support environmental evaluations of cyanotoxins in surface waters and aquatic organisms that are consumed by human populations.

Recent developments in reverse phase chromatography (RPLC) stationary phases have resulted in separation methods that allow for the simultaneous detection of ANA, CLD, MCs, and NOD in water and fish tissue (Oehrle, Southwell, and Westrick 2010; Chrıstophorıdıs, et al. 2017; Greer, et al. 2017; Greer, et al. 2016; Zervou, et al. 2017). However, resolving all toxin classes on a single RPLC column is challenging due to the diverse range of physiochemical properties, charge states, and structures exhibited by cyanotoxins (Dell'Aversano, Eaglesham, and Quilliam 2004). For example, coelution of ANA and d-phenylalanine (DPA), which are isobaric and produce similar fragment ions (Dimitrakopoulos, et al. 2010; Furey, et al. 2005), can lead to misidentification of ANA (Greer, et al. 2017) on RPLC columns. Additionally, the high water solubility of some

cyanotoxins requires use of ion-pairing agents to achieve sufficient retention on an RPLC column, which increases background noise, decreases ionization efficiency, and results in higher detection limits (Dell'Aversano, Eaglesham, and Quilliam 2004). Alternatively, other multi-toxin screening methods obtain successful retention and separation of the polar cyanotoxins, ANA, CLD, and SAX using hydrophilic interaction liquid chromatography (HILIC) (Lajeunesse, et al. 2012; Dell'Aversano, Eaglesham, and Quilliam 2004; Ballot, Fastner, and Wiedner 2010; Hollingdale, et al. 2015; Heussner, et al. 2012). The advantage of HILIC includes functionality similar to traditional normal phase chromatography with the compatibility of solvents suitable for RPLC, allowing the same mobile phases to be used for both separation techniques (Salas, et al. 2017). Thus, use of HILIC separation in addition to RPLC separation would allow for the regular incorporation of SAX in analytical screening methods.

Another challenge for the development of cyanotoxin analytical methods is finding reliable strategies that account and correct for the influence of matrix effect on ionization efficiency, a frequent problem when using electrospray ionization (ESI), and during extraction recovery. Robust methods to correct for matrix effect and recovery involve use of a surrogate/internal standards that shares physiochemical and structural properties with that of the target compound, resulting in similar column retention, ionization efficiency, and extraction recovery (Kruve, et al. 2015a; Kruve, et al. 2015b). To date, several compounds have been used as internal standards for cyanotoxin method development (Dimitrakopoulos, et al. 2010; Lajeunesse, et al. 2012; Oehrle, Southwell, and Westrick 2010; Yen, Lin, and Liao 2011; Zervou, et al. 2017). Unfortunately, no compounds have been generally accepted as suitable internal standards because robust evaluation in terms

of observed variation in relative response and recoveries compared to the target compounds has not been performed (Zervou, et al. 2017). Ideally, an isotopically labeled version of all target analytes could be used in an isotope dilution method to correct for recovery bias and matrix effects because variations in retention, ionization efficiency, and recovery would be rendered negligible (Kruve, et al. 2015a; Kruve, et al. 2015b). However, commercially available isotopically labeled internal standards for cyanotoxins were not available until recently.

Herein, we report the first multi-toxin screening method to incorporate the use of commercially available isotopically labeled internal standards for microcystin-LA, LR, RR, and YR to correct for matrix effect and extraction bias of MCs. This protocol further evaluates use of a zwitterionic HILIC analytical column to separate ANA, CLD, and SAX simultaneously, for the first time. Use of optimized HILIC and RPLC separation methods allows for rapid detection of ANA, CLD, SAX, MCs, and NOD in water and fish tissue. Method development of solid phase extraction (SPE) for water and liquid-liquid extraction (LLE) for fish tissue involved the optimization of extraction techniques where highly polar cyanotoxins (ANA, CLD, and SAX) were isolated separately from moderately polar cyanotoxins (MCs and NOD). SPE extraction built from previously existing methods to incorporate SAX. Multiple solvent systems were evaluated for optimized extraction from fish tissue, followed by cleanup of extracted tissue samples using the SPE methods developed for water. This method was subsequently used to screen target analytes in water and fish from a caged fish study staged in a hypereutrophic impoundment located in Waco, TX, USA.

Experimental Section

Chemicals and Reagents

All chemicals were reagent grade or better, obtained from various commercial venders, and used as received. The cyanotoxin standards microcystin-LA (M-LA), microcystin-LR (M-LR), microcystin-LY (M-LY), microcystin-RR (M-RR), microcystin-YR (M-YR), nodularin, anatoxin-a, cylindrospermopsin, and saxitoxin were purchased from Abraxis (Warminster, PA, USA). Isotopically labeled ^{15}N internal standards (IS) microcystin-LA-$^{15}N_7$ (M-LA-^{15}N), microcystin-LR-$^{15}N_{10}$ (M-LR-^{15}N), microcystin-RR-$^{15}N_{13}$ (M-RR-15N), microcystin-YR-$^{15}N_{10}$ (M-YR-^{15}N), and D-phenylalanine-d_5 (DPA-d_5) were obtained from Cambridge Isotope Laboratory (Tewksbury, MA, USA). Methanol (MeOH), acetonitrile (MeCN), and dichloromethane (DCM) were obtained from Fisher Scientific (Fair Lawn, NJ, USA). Formic acid (FA) was purchased from VWR Scientific (Radnor, PA, USA). Ammonium formate was purchased from Sigma-Aldrich (St. Louis, MO, USA). A Thermo Barnstead™ Nanopure™ (Dubuque, IA, USA) Diamond UV water purification system was used throughout sample analysis to provide 18 MΩ nanopure (NP) water.

Liquid Chromatography – Tandem Mass Spectrometry

Chromatographic separation was carried out using an Agilent HPLC system consisting of an Agilent 1260 Quaternary Pump (G1311B), Agilent 1260 Infinity Standard Autosampler, and Agilent 1260 Infinity Thermostatted Column Compartment (G1316A). The HPLC system was interfaced with an Agilent G6420 Triple Quadrupole Mass Spectrometer. The goal of the current method was to incorporate SAX in the screening methodology; thus, we decided to employ complimentary RPLC and HILIC separation.

ANA, CLD, and SAX were separated using a Poroshell HILIC-Z column (2.1 x 150 mm, 2.7 µm, 120Å), produced by Agilent Technologies (Santa Clara, CA, USA), with a binary gradient consisting of water as solvent B, and 5:95 water:MeCN (v v^{-1}) as solvent A, both buffered with 5mM NH_4OOCH_3 and 3.6 mM HCOOH (pH 3.7). Flow rate was held constant at 0.5 mL min^{-1} with column temperature maintained at 30 °C. MCs and NOD were separated using a Poroshell SB-C18 RPLC column (2.1 × 100 mm, 2.7 µm, 120Å), produced by Agilent Technologies (Santa Clara, CA, USA), with a binary gradient method consisting of water as solvent A, and 5:95 water:MeCN (v v^{-1}) as solvent B, both buffered with 5mM NH_4OOCH_3 and 3.6 mM HCOOH (pH 3.7). Flow rate was held constant at 0.5 mL min^{-1} with column temperature maintained at 60 °C. Both methods used an injection volume of 50 µL and monitored for target analytes ionized in positive mode via ESI. Cycle time was adjusted to 200 ms for the dynamic MRM acquisition mode.

Nontarget Mass Spectrometry

Nontarget analysis was carried out using the above chromatographic separations ported to a Dionex Ultimate 3000 RS HPLC system (Thermo Scientific, Waltham, Massachusetts, USA) coupled with a Thermo Scientific Q Exactive™ Focus Hybrid Quadrupole-Orbitrap™ Mass Spectrometer. An injection volume of 20 µL and a flow rate of 0.5 mL min^{-1} was used in both separation methods. The first minute of each separation was diverted to waste to keep the detector free of salts. All samples were run in triplicate. Eluting analytes were ionized using heated electrospray ionization (HESI) with a spay voltage of 4000 V and a capillary temperature of 350 °C. The spectrometer was operated in positive full-scan mode with spectra ranging from 200 to 1200 *m/z* and 150 to 1000 *m/z* for RPLC and HILIC separations, respectively. The full width at half maximum resolution

was set to 70,000 with the automatic gain control (AGC) at 1×10^6. After nontarget analysis, samples were rerun on the Q Exactive™ with an inclusion list using confirmation mode (dd-MS^2). MS^2 spectra were collected with a resolution of 17,500 *m/z* with a 1.0 m/z isolation window. A stepped normalized collision energy (NCE) of 30, 60, and 90 was used with the AGC set to 2×10^4. To minimize data size, all spectra were collected in centroid mode.

Nontarget data was analyzed using the open-source software MZmine 2 version 2.32 (Pluskal, et al. 2010; Myers, et al. 2017). The general MZmine 2 nontarget workflow consists of five steps: mass detection, chromatogram builder, chromatogram deconvolution, retention time normalization, peak list alignment. The complete MZmine 2 nontarget workflow used in the analysis of environmental water samples is shown in Table S2. A comprehensive custom database containing exact masses and common salt adducts (adapted from Bogialli et al. 2017 (Bogialli, et al. 2017)) was used to screen samples. MS^2 data and the custom database were used to acquire nontarget data; however, settings were optimized for peak lists before further analysis was done. The open source software MZmine 2 provides superior control over peak list settings, and future nontarget analyses should modify the settings (Table 5.1) to fit the chromatographic data. The minimum peak height and minimum time span in the chromatogram builder setting control the number of features present in a peak list. This is important for minimizing false positives, and even after background correction peak lists contained approximately 20,000 different features. Peak lists were filtered using the following criteria: 1) features for a specific sample must be present in the triplicate LC-MS runs and 2) features must contain at least 2 *m/z* peaks in the isotope pattern. After filtering and database screening,

Table 5.1. MZmine 2 workflow parameters.

Workflow	Parameters	Values
Mass Detection	MS level	1
	Mass detector	centroid
	noise level	1.0×10^3
Chromatogram Builder	Retention Time (min)	1.00 to 10.00
	Min time span (min)	0.03
	Min height	1.0×10^3
	m/z tolerance	10.0 ppm
Smoothing	Filter Width	7
Chromatogram Deconvolution	Algorithm	Wavelets (ADAP)
	S/N threshold	20
	S/N estimator	Intensity Window SN
	min feature height	1000
	coefficient/area threshold	250
	peak duration range	0.03 to 0.30
	RT wavelet Range	0.03 to 0.40
Isotopic peak grouper	m/z tolerance	10 ppm
	RT Tolerance	2%
	Monotonic Shape	✓
	maximum charge	1
	Representative iosotope	Most Intense
Duplicate Peak Filter	m/z tolerance	10 ppm
	RT Tolerance	2%
RT Normalizer	m/z tolerance	10 ppm
	RT Tolerance	2%
	Minimum Standard Inensity	1.0×10^3
Join Aligner	m/z tolerance	10 ppm
	Weight for m/z	20
	RT Tolerance	2%
	Weight for RT	10
	Require same charge state	✓
	Compare isotope pattern	Ü
	m/z tolerance	10 ppm
	Min absolute intensity	1.0×10^3
	Min score	65.00%
Peak list rows filter	min peaks in a row	3
	min peaks in an isotope patter	2
	Renumber	✓

approximately 50 to 100 features were left depending on the given sample. The remaining features were manually inspected and added to the inclusion list for further confirmation

measurements using the Q Exactive™ if the isotope patterns were within 10 ppm of the theoretical patterns.

Solid Phase Extraction (SPE)

Due to the variety of physiochemical properties that cyanotoxins possess, isolation of target analytes from water was split into two SPE extractions methods, corresponding to the HILIC or RPLC separation methods. SPE extraction methodology and optimization were developed from a previously reported study (Zervou, et al. 2017), with modifications for individual SPE extraction and the incorporation of SAX. Water samples were filtered through two filters: a glass fiber prefilter (1.0-μm pore size, 47 mm, Pall Corporation, Port Washington, NY, USA) and a nitrocellulose filter (0.45-μm pore size, 47 mm, GE Healthcare, Little Chalfont, BUX, UK). 2 Ls were separated into 2 – 1 L volumetric flasks for extraction. ANA, CLD, and SAX were extracted on a Supelclean ENVI-carb (6cc, 500mg, Supelco Inc., Bellefonte, PA, USA). MCs and NOD were extracted using an Oasis HLB (6 cc, 200 mg, Waters Corporation, Milford, MA, USA). Prior to extraction all samples were spiked with 100 μg L^{-1} of corresponding ISs. HLB cartridges were pretreated with 6 mL of MeOH and 6 mL of nanopure water. ENVI-carb cartridges were pretreated with 6 mL of DCM, 6 mL of MeOH, and 6 mL of nanopure H_2O (Barnstead™ Nanopure™). 1 L of sample was loaded on each cartridge separately at ~10 mL/min (visible dripping) via a 24 port Visiprep™ vacuum manifold (Supelco Inc., Bellefonte, PA, USA). Cartridges were then blown dry under nitrogen. HLB cartridges were eluted with 10 mL of MeOH (0.5% formic acid) into 20 mL test tubes. ENVI-carb cartridges were eluted with 10 mL 60:40 (v v^{-1}) MeOH:DCM (0.5% formic acid) into 20 mL test tubes. Eluates were blown to dryness under a gentle stream of nitrogen in a Turbovap (Zynmark,

Hopkinton, MA, USA) set to 55°C. HLB samples were reconstituted with 1 mL 90:10 (v v^{-1}) H_2O:MeCN buffered with 5mM NH_4OOCH_3 and 3.6 mM HCOOH (pH 3.7). ENVI-carb samples were reconstituted with 1 mL 10:90 (v v^{-1}) H_2O:MeCN buffered with 5mM NH_4OOCH_3 and 3.6 mM HCOOH (pH 3.7). All reconstituted samples were syringe filtered using a BD 1 mL TB syringe (BD, Franklin Lakes, NJ, USA) and Acrodisc® hydrophobic Teflon Supor membrane syringe filters (13-mm diameter; 0.2-μm pore size, Pall Corporation, Port Washington, NY, USA) and placed in 2 mL analytical vials (Agilent Technologies, Santa Clara, CA, USA) for analysis.

Fish Tissue Extraction

Similar to water extractions, isolation of target analytes from fish tissue was split into two extractions methods, corresponding to the HILIC or RPLC separation methods. Fish whole body homogenates were prepared for extraction by grinding frozen samples to a paste. Two - 1g w/w aliquots were placed in separate preweighed 20 mL borosilicate glass vial (Wheaton; VWR Scientific, Rockwood, TN, USA). Samples were lyophilized for 72 hours using a VirTis BenchTop Pro freeze dryer (SP Scientific, Garnider, NY, USA) and the dry weight of each sample was determined. Samples were then spiked with 100 μg kg^{-1} of corresponding ISs. ANA, CLD, and SAX were extracted with 10 mL of 25:75 (v v^{-1}) MeCN:NP water added to each vial. MCs and NOD were extracted using 10 mL of 75:25 (v v^{-1}) MeCN:aqueous 0.1% formic acid added to each vial. Vials were inverted by hand for 30 seconds to mix the contents prior to sonicating for 30 minutes on a CPHX ultrasonicator (Fisher Scientific, Fair Lawn, NJ, USA). Samples were then placed on a rotating table at 40 rpm for 30 minutes. After rotation, samples were centrifuged at 25,000 rpm for 20 minutes using an Avanti JXN-26 centrifuge (Beckman Coulter, Brea,

CA, USA). Following centrifugation, supernatant was collected, and syringe filtered using a Kendall monoject 6 mL luer lock syringe (Tyco, Milwaukee, WI, USA) and Whatman puradisc 25 polypropylene filter (0.45-μm pore size, 47 mm, GE Healthcare, Little Chalfont, BUX, UK). Supernatants were blown down under a gentle stream of nitrogen in a Turbovap (Zynmark, Hopkinton, MA, USA) set to 55°C for 1 hour to remove the organic solvent (MeCN). Samples were then diluted to 20 mL with nanopure water and loaded to SPE cartridges following the same protocols described above for water extractions.

Extraction Recovery

To calculate absolute extraction recoveries two groups of samples were prepared for each matrix. Group 1 samples were spiked with corresponding IS and each target analyte for the given extraction method, while Group 2 samples were not spiked. Both groups were carried through complete and identical extraction procedures. Following reconstitution, group 2 samples were spiked with each target analyte and IS at the same concentration previously used in group 1 samples. Samples were analyzed, and absolute recoveries were calculated using the following equation:

$$Absolute\ extraction\ recovery\ (\%) = \frac{A_{X_1}/A_{IS_1}}{A_{X_2}/A_{IS_2}} \times 100$$

where A_{X1}, A_{IS1}, A_{X2}, and A_{IS2} are the peak areas of the analyte (X) and internal standard (IS) for groups 1 and 2, respectively.

Analysis of Environmental Samples

The developed method was applied to water and fish samples collected during two seven-day caged fish studies executed in Lake Waco, Waco, Texas, USA during September (19^{th}-26^{th}) 2017 and January (7^{th}-14^{th}) 2018. Naïve channel catfish (*Ictalurus punctatus*)

housed at Baylor University were caged in a sheltered cove (31°35'40.48"N, 97°13'54.41"W). Caged fish were sampled every 24 hours (n=3) by anesthetization using MS-222, bagged onsite, then frozen at Baylor University until analysis. Duplicate water samples for targeted cyanotoxins analysis were collected using acetone cleaned 4 L amber glass bottles. Water samples were split into two 1 L subsamples where one sample (filtered) was filtered immediately, representing freely available dissolved toxins, and the second sample (seston) was frozen and thawed three times to lyse algal cells present in the sample, representing intracellular toxins.

Results and Discussion

LC-MS/MS Methodology

Compound specific mass spectrometry parameters were automatically determined using MassHunter Optimizer (Agilent Technologies, Santa Clara, CA, USA) by flow injection analysis. Optimized MS/MS transitions and instrument parameters are provided in Table 5.2. Typically, MCs containing a single arginine residue will form $[M+H]^+$ precursor ions at the arginine moiety (Kaloudis, et al. 2013). Similarly, M-RR will form $[M+2H]^{2+}$ precursor ions due to the presence of two arginine residues (Yuan, et al. 1999). In contrast, MCs without an arginine residue typically form $[M+H]^+$ precursors ions where protonation occurs on the methoxy group present within the ADDA side chain (Hiller, et al. 2007; Yuan, et al. 1999). However, in the current study, the doubly protonated precursor ions $[M+2H]^{2+}$ for M-LR, M-LY, M-RR, M-YR, M-LR-^{15}N, M-RR-^{15}N, and M-YR-^{15}N were found to be the most abundant, while the single protonated $[M+H]^+$ precursor was most abundant for M-LA and M-LA-^{15}N, and NOD. The observed precursor ions used in this work are in agreement with those observed in previous studies (Hiller, et al. 2007; Li,

Chu, and Hsientang Hsieh 2006; Draper, et al. 2013; Yuan, et al. 1999; Maizels and Budde 2004). For all MCs and NOD the most abundant fragment ion, used as the quantitation ion, was *m/z* 135, except for M-LA where *m/z* 776 was the most abundant fragment. The qualification ion employed for all MCs and NOD was *m/z* 103, except for M-LA where *m/z* 135 was used. Observed formation of $[M+2H]^{2+}$ precursor ions for M-LR and M-YR is not surprising due to the ubiquitous use of ammonium formate, added to the mobile phases, which actively minimized sodium replacement ions causing an increased abundance of the doubly protonated species (Draper, et al. 2013; Yuan, et al. 1999; Draper, Xu, and Perera 2009). M-LR and M-YR form $[M+2H]^{2+}$ precursor ion when protonation occurs on both the arginine residue and methoxy residue of the ADDA side chain (Yuan, et al. 1999). Further, previous studies have demonstrated the utility of selecting the unconventional $[M+2H]^{2+}$ precursor for M-LR, M-RR, and M-YR noting that a higher abundance of *m/z* 135 fragments are produced, resulting in lower overall detection limits (Li, Chu, and Hsientang Hsieh 2006; Yuan, et al. 1999). Formation of the $[M+2H]^{2+}$ precursor ion for M-LY is surprising and suggests a second protonation site other than the methoxy residue of the ADDA side chain (Hiller, et al. 2007). ANA formed a $[M+H]^{+}$ precursor ion of *m/z* 166 with major fragment ions of *m/z* 131, used as the quantitation ion, and *m/z* 91, employed as the qualification ion. The $[M+H]^{+}$ precursor ion of *m/z* 416 formed for CLD and produced fragment ions of *m/z* 194, used as the quantitation ion, and *m/z* 176, for the qualification ion. The $[M+H]^{+}$ precursor ion of *m/z* 300 was observed for SAX and major fragment ions of *m/z* 204, employed as the quantitation ion, and *m/z* 138, used as the qualification ion, were produced.

Table 5.2. Target analyte mass spectrometry parameters

Method	Analyte	Formula	Precurser ion (m/z)		Product ions (m/z)	Fragmentor (V)	Collision Energy (V)	t_R (mins)
HILIC	ANA	$C_{10}H_{15}NO$	166.1	$[M+H]^+$	91.1, 131	103	29, 17	1.5
	CLD	$C_{15}H_{21}N_5O_7S$	416.1	$[M+H]^+$	194.1, 176	152	37, 41	4.0
	SAX	$C_{10}H_{17}N_7O_4$	300.1	$[M+H]^+$	204.1, 138	152	25, 33	5.2
	DPA-*d5* (IS)	$C_9D_5H_6NO_2$	171.1	$[M+H]^+$	125	103	17	2.0
RPLC	M-LA	$C_{46}H_{67}N_7O_{12}$	910.5	$[M+H]^+$	776.4, 135	200	21, 69	5.3
	M-LA-15N (IS)	$C_{46}H_{67}{}^{15}N_7O_{12}$	917.2		783.4, 135			
	M-LR	$C_{49}H_{74}N_{10}O_{12}$	498.2	$[M+2H]^{2+}$	135.1, 103	103	9, 69	3.7
	M-LR-15N (IS)	$C_{49}H_{74}{}^{15}N_{10}O_{12}$	502.5					
	M-LY	$C_{52}H_{71}N_7O_{13}$	501.7	$[M+2H]^{2+}$	135.1, 103	103	13, 69	5.7
	M-RR	$C_{49}H_{75}N_{13}O_{12}$	519.7	$[M+2H]^{2+}$	135.1, 103	152	33, 69	2.5
	M-RR-15N (IS)	$C_{49}H_{75}{}^{15}N_{13}O_{12}$	525.7					
	M-YR	$C_{52}H_{72}N_{10}O_{13}$	523.2	$[M+2H]^{2+}$	135.1, 103	103	13, 69	3.4
	M-YR-15N (IS)	$C_{52}H_{72}{}^{15}N_{10}O_{13}$	527.5					
	NOD	$C_{41}H_{60}N_8O_{10}$	825.4	$[M+H]^+$	135.1, 103	201	69, 137	2.4
	CLA-*d3* (IS)	$C_{38}H_{66}D_3NO_{13}$	751.5	$[M+H]^+$	161.1	152	33	5.7

Excellent separation of MCs and NOD was achieved using RPLC (Figure 5.1A), with retention order similar to previous reports (Draper, et al. 2013; Greer, et al. 2016; Kaloudis, et al. 2013; Lajeunesse, et al. 2012; Oehrle, Southwell, and Westrick 2010; Yen, Lin, and Liao 2011; Zervou, et al. 2017). Further, observation of overlapping retention times for MC ^{15}N ISs with unlabeled counterparts demonstrates minimalized isotope effect (Figure 5.2), consistent with previous studies reporting reduced isotope effect from ^{15}N labeled IS (Szarka, Prokai-Tatrai, and Prokai 2014). Initial development of a HILIC separation method was performed on a TSKgel amide-80 due to previous reports and used for ANA, CLD, and SAX (Dell'Aversano, Eaglesham, and Quilliam 2004; Dell'Aversano, Hess, and Quilliam 2005; Lajeunesse, et al. 2012; Hollingdale, et al. 2015; Kikuchi, Kubo, and Kaya 2007; Ballot, Fastner, and Wiedner 2010; Salas, et al. 2017; Heussner, et al. 2012). Complete separation of ANA, DPA-*d5*, CLD, and SAX was achieved using HILIC (Figure 5.3), solving the issue of ANA and DPA coelution (Furey, et al. 2005; Greer, et al.

2017), and providing excellent retention of the polar cyanotoxins, similar to previous results (Lajeunesse, et al. 2012; Dell'Aversano, Eaglesham, and Quilliam 2004; Ballot, Fastner, and Wiedner 2010; Hollingdale, et al. 2015; Heussner, et al. 2012). Further, in agreement with previous work, the current study found that target analyte peak shape and retention when using HILIC were greatly affected by mobile phase buffer conditions (Dell'Aversano, Eaglesham, and Quilliam 2004); thus, a previously reported optimized buffer with 5mM NH_4OOCH_3 and 3.6 mM HCOOH (pH 3.7) was utilized.(Lajeunesse, et al. 2012)

Whereas excellent separation was observed on the TSKgel amide-80, amide HILIC columns are designed to target polar compounds with hydroxyl groups (weak acids). However, ANA and SAX have ionizable amine groups (Dimitrakopoulos, et al. 2010; Dell'Aversano, Hess, and Quilliam 2005), while CLD is zwitterionic at relevant pH (de la Cruz, et al. 2013).

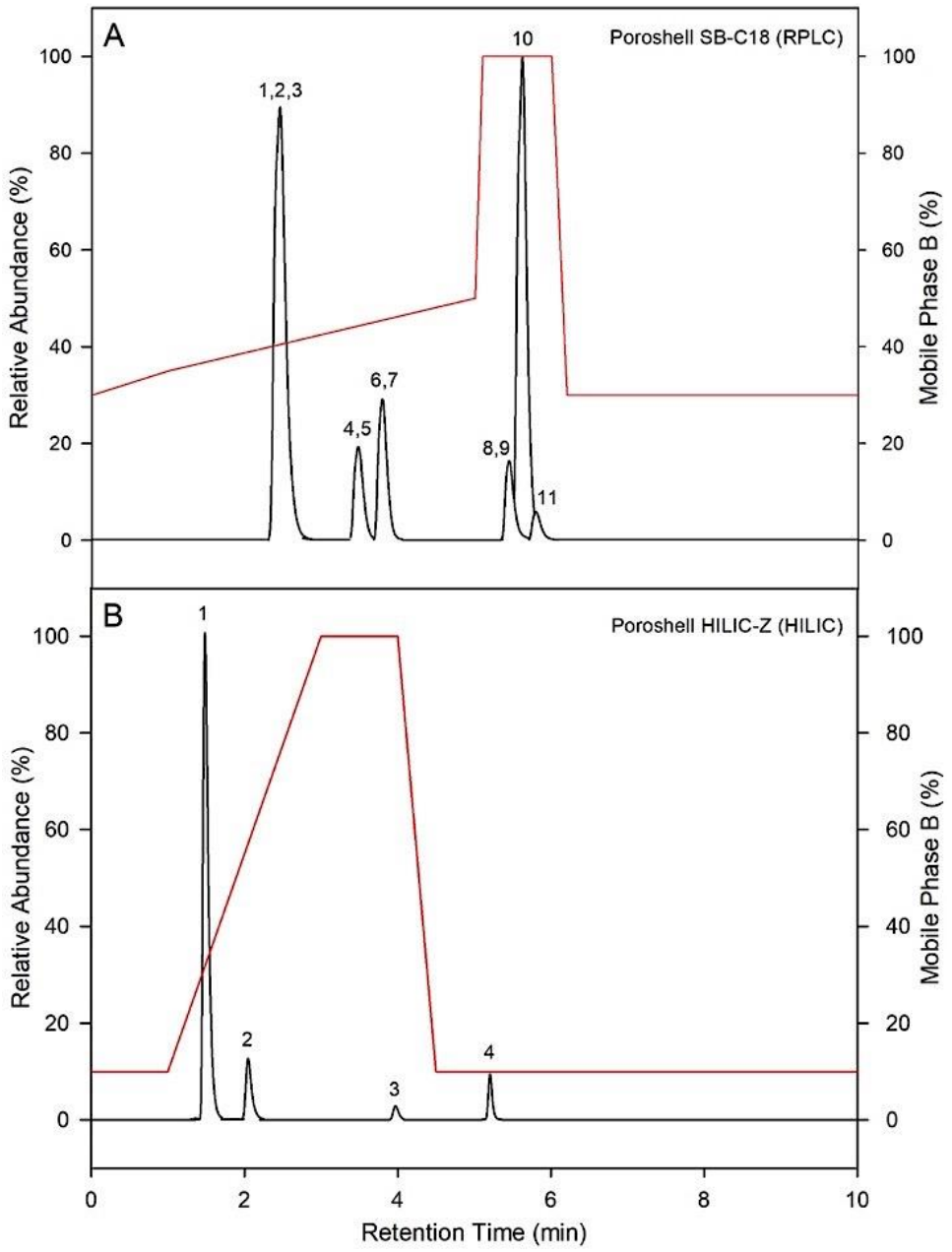

Figure 5.1. LC-MS/MS total ion chromatograms for compounds separated by the RPLC method on the Agilent Poroshell SB-C18 (A) and the HILIC method on the Agilent Poroshell HILIC-Z (B), monitored in a 10 ng mL^{-1} standard solution. Peak identifications for the RPLC method (A) are as follows: (1) microcystin-RR, (2) microcystin-RR-$^{15}N_{13}$, (3) nodularin, (4) microcystin-YR, (5) microcystin-YR-$^{15}N_{10}$, (6) microcystin-LR, (7) microcystin-LR-$^{15}N_{10}$, (8) microcystin-LA, (9) microcystin-LR-$^{15}N_{7}$, (10) clarithromycin-d_3, (11) microcystin-LY. Peak identifications for the HILIC method (B) are as follows: (1) anatoxin-a, (2) D-phenylalanine-d_5, (3) cylindrospermopsin, (4) saxitoxin. The red line represents the mobile phase gradient conditions in percentage of the strong solvent B for each separation respectively.

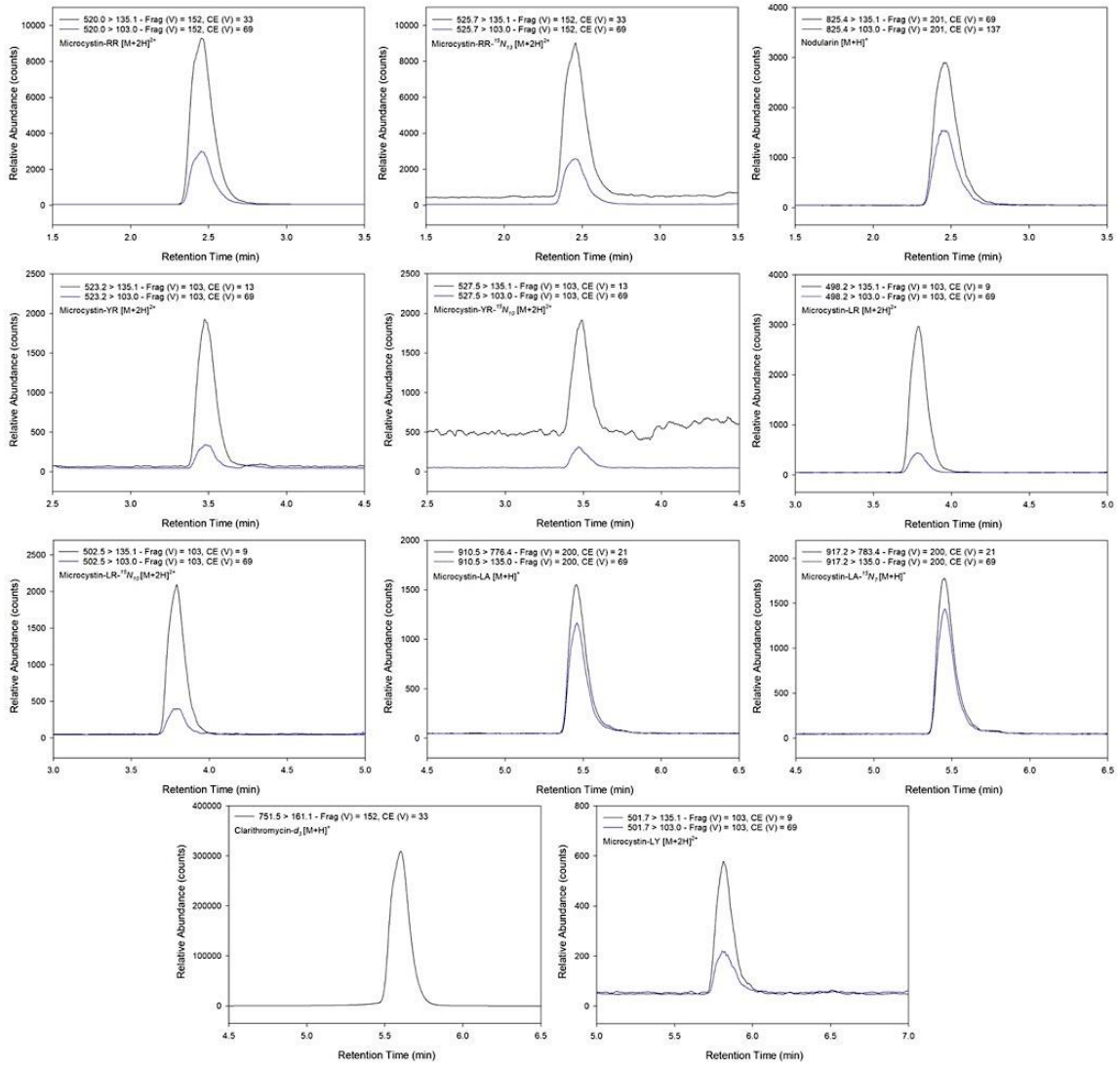

Figure 5.2. LC-MS/MS reconstituted ion chromatograms for compounds separated on the Agilent Poroshell SB-C18 (RPLC) column displaying analyte-specific quantitation (black) and qualifier (blue) ions monitored in a 10 ng mL^{-1} standard solution with internal standard concentrations at 10 ng mL^{-1}. Compound name, MRM transitions for the quantitation and qualifier ion, Fragmentor voltage (Frag), and Collision Energy voltage (CE) are displayed in the upper left-hand corner of each chromatogram respectively.

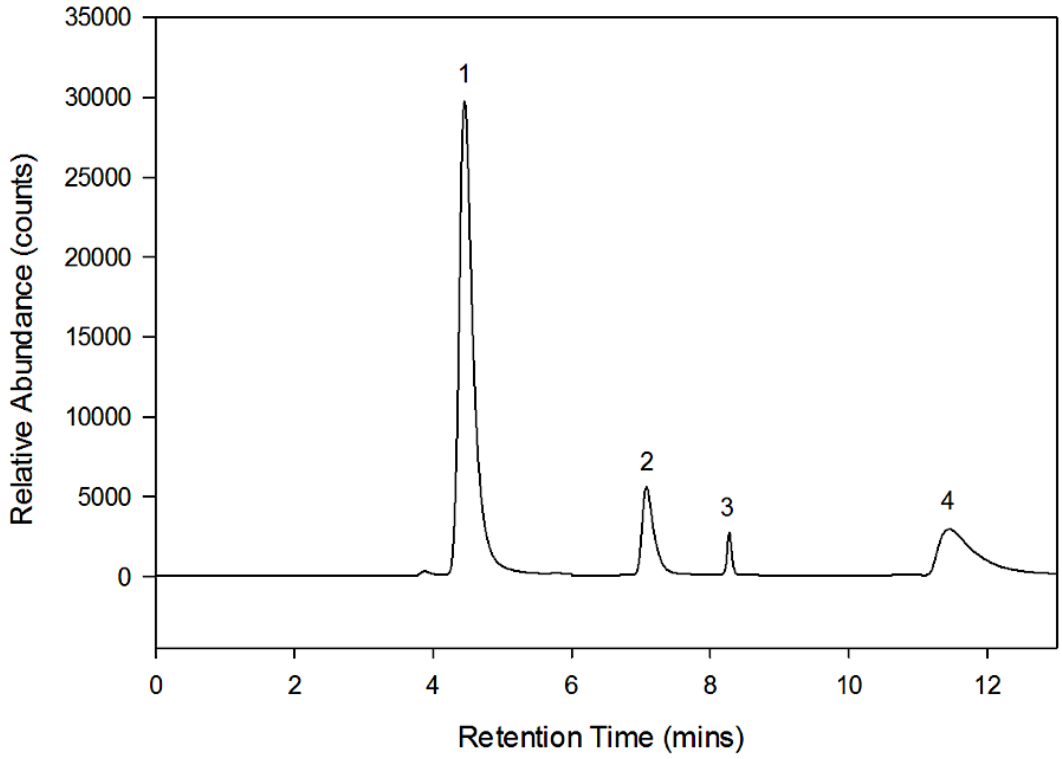

Figure 5.3. LC-MS/MS total ion chromatograms for compounds separated by the HILIC method on the TOSOH TSKgel amide-80 monitored in a 10 ng mL^{-1} standard solution. Peak identifications are as follows: (1) anatoxin-a, (2) D-phenylalanine-d_5, (3) cylindrospermopsin, (4) saxitoxin.

Therefore, the use of a zwitterionic HILIC column may improve retention, method sensitivity, matrix interference, and separation of the polar cyanotoxins (Salas, et al. 2017). This has previously been demonstrated for SAX (Diener, et al. 2007), though no such studies have been performed for ANA or CLD to date (Salas, et al. 2017). Recently, a new zwitterionic HILIC column, the Agilent Poroshell HILIC-Z, which demonstrated excellent separation of small polar molecules (Huang, et al. 2018), became commercially available and was tested using the current method. Complete separation of all target analytes was observed on the HILIC-Z (Figure 5.1B & 5.4).

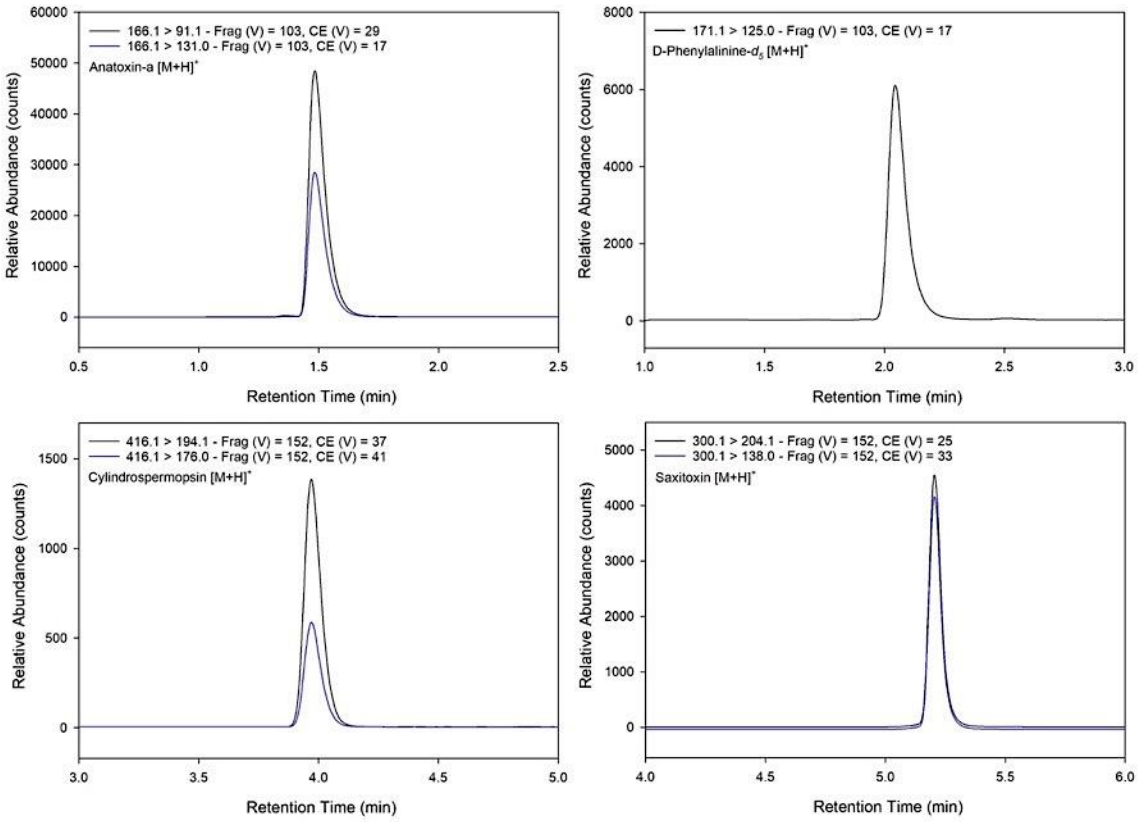

Figure 5.4. LC-MS/MS reconstituted ion chromatograms for compounds separated on the Agilent HILIC-Z (HILIC) column displaying analyte-specific quantitation (black) and qualifier (blue) ions monitored in a 10 ng mL^{-1} standard solution with internal standard concentration at 10 ng mL^{-1}. Compound name, MRM transitions for the quantitation and qualifier ion, Fragmentor voltage (Frag), and Collision Energy voltage (CE) are displayed in the upper left-hand corner of each chromatogram respectively.

To evaluate analytical differences between each column calibration curves for the TSKgel amide-80 and HILIC-Z are plotted side by side using target analyte peak areas and response factors (RF). Differences in the slope are statistically evaluated as a measure of sensitivity (Figure 5.5) (Kruve, et al. 2015a; Kruve, et al. 2015b). The HILIC-Z produced greater peak areas for all target analytes along the range of the calibration curve and calibration slopes were significantly ($p<0.05$) greater on the HILIC-Z, resulting in greater method sensitivity. Interestingly, slope of the RF calibration curves is significantly

($p<0.05$) greater for ANA and CLD, but significantly ($p<0.05$) lower for SAX. The observed decrease in slope for the SAX RF calibration curve is due to a 6-fold increase in the abundance of DPA-*d5* on the HILIC-Z column, while SAX abundance only increased 2.5-fold. Likewise, abundance of ANA increased 6-fold and CLD increased 11-fold, resulting in the observed differences in RF calibration slope. DPA-*d5* is the most similar to ANA and has previously been recommended as an IS for ANA and CLD (Dimitrakopoulos, et al. 2010; Meriluoto, Spoof, and Codd 2017).

Solid Phase Extraction

The current study provides the first report of matched IS corrected mean recoveries for MCs and NOD on the Oasis HLB ranging from 73-98% (Table 5.3). Recoveries of MCs and NOD in the current study were in agreement with previous reports (Zervou, et al. 2017; Kaloudis, et al. 2013; Greer, et al. 2016) demonstrating high recoveries when using the Oasis HLB. Mean recoveries on the ENVI-carb were 53% for SAX, 90% for CLD, 97% for ANA (Table 5.3) and 80% (± 4.4) for DPA-*d5* (IS). Recoveries of CLD in the current study are similar to previous reports that used graphitic carbon SPE (Greer, et al. 2016; Yen, Lin, and Liao 2011; Zervou, et al. 2017). Higher recoveries of ANA and some MCs from water samples which have been modified to pH 10.5 have been previously reported with no IS correction (Zervou, et al. 2017). In the current study, filtered surface water samples from local Texas streams and lakes were pH modified and a soapy residue formed in the sample due to the high organic content. This material clogged SPE cartridges and produced unacceptable recoveries. Use of IS correction for recovery bias was tested by comparing water samples modified to pH 10.5 without IS correction and unmodified water samples with IS correction in laboratory water. Similar results were obtained.

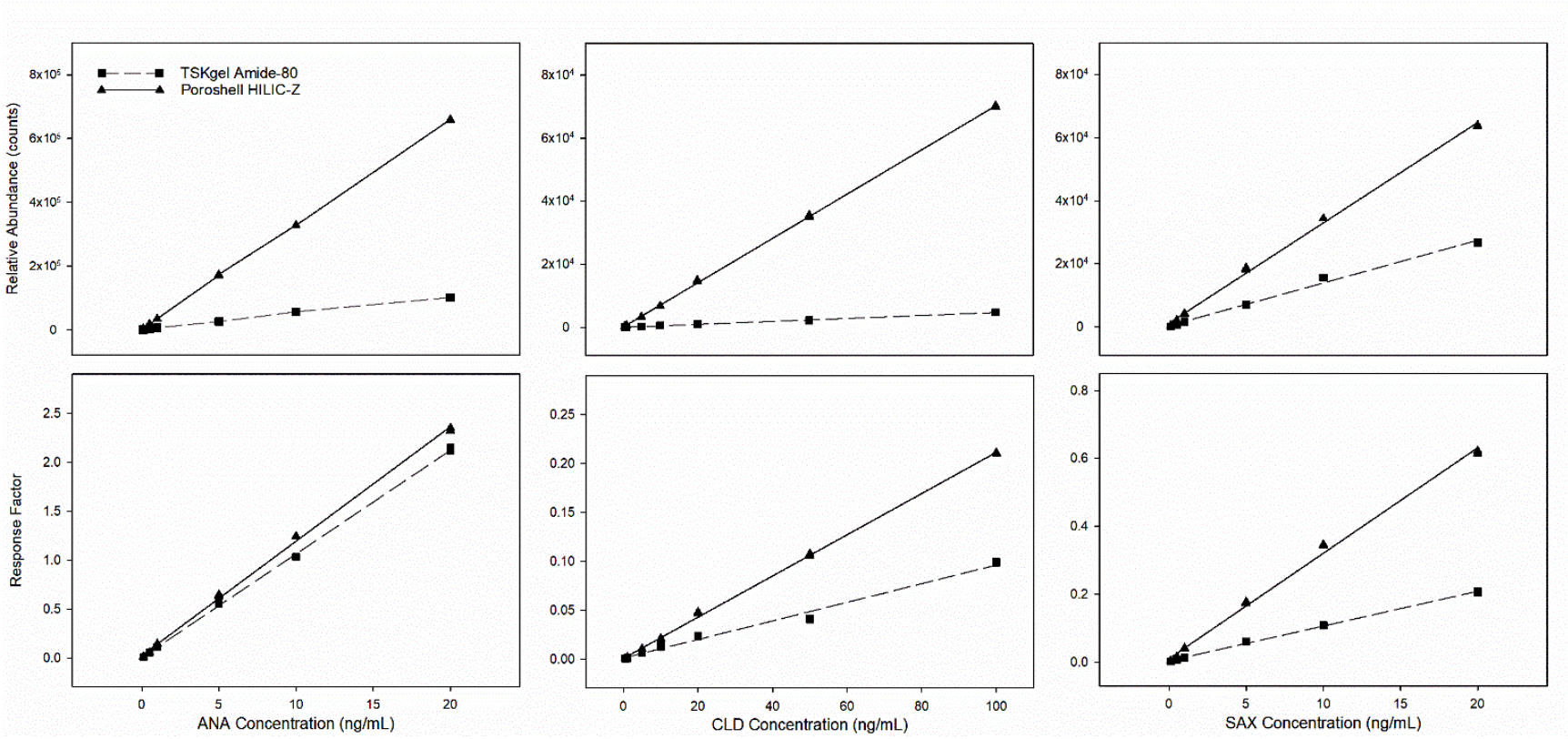

Figure 5.5. Comparison of calibration curves across the linear range for anatoxin-a, cylindrospermopsin, and saxitoxin on the TSKgel Amide-80 and Poroshell HILIC-Z.

Table 5.3. Validation data for target analytes in water and fish tissue.

Analyte	Linear Range (ng mL^{-1})	Correlation Coefficient (r^2)	Recovery (%, CV) Water	Recovery (%, CV) Fish	Precision (%, CV) Water	Precision (%, CV) Fish	Detection Limits (pg) LOD	Detection Limits (pg) LOQ	MDL Water (ng L^{-1})	MDL Fish (μg kg^{-1})
ANA	0.1-20	0.999	97 (1.2)	103 (1.3)	1.9	3.4	4.0	10	0.08	0.14
CLD	0.5-100	0.998	90 (2.6)	90 (1.8)	5.0	8.2	70	230	0.43	0.12
SAX	0.1-20	0.995	53 (2.7)	45 (4.4)	1.6	5.6	10	40	0.22	0.04
M-LA	0.5-100	0.998	97 (1.8)	96 (5.7)	0.8	5.7	20	70	0.60	0.61
M-LR	0.1-100	0.998	94 (2.4)	97 (5.1)	0.6	5.1	40	130	0.38	0.31
M-LY	0.5-100	0.998	73 (7.3)	75 (7.1)	7.2	4.7	40	140	0.83	0.35
M-RR	0.1-100	0.999	97 (3.0)	90 (5.9)	2.4	6.3	60	220	0.91	0.28
M-YR	0.5-100	0.999	93 (4.6)	77 (4.7)	3.9	1.2	80	280	0.80	0.70
NOD	0.5-100	0.996	98 (3.1)	90 (7.9)	2.9	4.7	50	180	0.96	0.57

Limit of detection (LOD) was defined as LOD = (3σ/b) where σ is the standard deviation of the quantified value from replicate blank samples (n=8), and b is the slope of the calibration for the target analyte. Limit of quantification (LOQ) was defined as LOQ = (10σ/b). Method detection limits (MDL) were defined as MDL = $t_{(n-1,0.99)}$ x SD, where $t_{(n-1,0.99)}$ is the one-sided Student's t-statistic at the 99% confidence limit for n-1 degrees of freedom, (2.998 for n = 8), and SD is the standard deviation of replicate spiked matrix sample (spiking level $\leq$ 10 x MDL).

Thus, extraction of water was carried out under neutral conditions with IS correction. Higher ANA recoveries in the current method extracted at neutral conditions are attributed to IS correction using DPA-*d5*, previously reported to have similar extraction recoveries to ANA (Dimitrakopoulos, et al. 2010). Recoveries of SAX utilizing current methods represent a useful first step toward development of greater all-in-one extraction protocols.

Fish Tissue Extraction

The large variation in pK_a and lipophilicity of cyanotoxins led to a systematic study of extraction behaviors using different solvent systems to optimize extraction from fish tissue. Varying ratios of MeCN, nanopure water, and aqueous 0.1% formic acid were tested side by side. Mean recoveries (n = 3) for each solvent system are given in Table 5.4. Individual target analyte recoveries were averaged for each method and plotted for comparison (Figure 5.6). Data in each graph have not been statistically examined but

provide a convenient visual metric for comparing overall solvent performance, where the most effective solvents are those displaying a maximum recovery and minimum error. Error bars represent the standard deviation from the mean of recoveries and provide an assessment of variability among mean recoveries for individual analytes. Recoveries for MCs and NOD were highest in solvent systems that utilized a mixture of MeCN and aqueous 0.1% formic acid, with the overall highest recoveries observed for 75:25 MeCN:aqueous 0.1% formic acid ranging from 75% to 97%, in agreement with previous reports utilizing the same or similar solvent systems (Geis-Asteggiante, et al. 2011; Chrıstophorıdıs, et al. 2017; Greer, et al. 2017). Recoveries for ANA, CLD, and SAX were highest using 75:25 nanopure:MeCN ranging from 45% to 103%, with recovery of DPA-*d5* measured at 92 ± 2.3%. Whereas a higher recovery for SAX (99%) was observed using 50:50 nanopure:MeCN (Table 5.4), 75:25 nanopure:MeCN was used because of higher overall recoveries for ANA and CLD.

Table 5.4. Absolute recovery (%, CV) of target analytes from clean whole-body homogenates of fish tissue for each tested extraction solvent mixtures.

Extraction Solvent	ANA	CLD	SAX	M-LA	M-LR	M-LY	M-RR	M-YR	NOD
75:25 MeCN:0.1% FA	27 (23)	81 (30)	26 (15)	96 (5.7)	97 (5.1)	75 (7.1)	90 (5.9)	77 (4.7)	90 (7.9)
50:50 MeCN:0.1% FA	23 (9.4)	93 (12)	9.4 (16)	100 (22)	52 (20)	57 (24)	23 (23)	47 (19)	93 (22)
25:75 MeCN:0.1% FA	43 (12)	73 (32)	23 (82)	55 (27)	37 (21)	24 (18)	36 (41)	32 (19)	72 (22)
75:25 NP:MeCN	103 (1.3)	90 (1.8)	45 (4.4)	4.4 (52)	17 (5.7)	1.1 (78)	48 (10)	14 (6.1)	49 (11)
50:50 NP:MeCN	79 (15)	46 (19)	99 (16)	20 (8.9)	37 (7.8)	1.9 (97)	46 (54)	29 (8.3)	88 (7.4)
25:75 NP:MeCN	86 (24)	43 (21)	32 (63)	16 (81)	23 (82)	5.7 (65)	39 (61)	19 (81)	38 (85)
0.1% FA	80 (12)	50 (15)	12 (25)	18 (98)	11 (64)	1.7 (150)	17 (63)	14 (72)	60 (71)
MeCN	77 (6.1)	12 (6.1)	2.9 (83)	39 (63)	6.1 (71)	22 (32)	0.01 (110)	1.3 (94)	0.1 (78)
NP	57 (10)	57 (8)	74 (12)	42 (6.1)	14 (4.8)	15 (31)	30 (4.3)	10 (5.7)	58 (5.8)

All solvent systems were prepared by mixing the noted ratio of solvents in a binary mixture. Solvents without a ratio can be assumed to be pure solvent. Solvent system notations are as follows: MeCN, acetonitrile; 0.1% FA, 0.1% aqueous formic acid (v v^{-1}); NP, nanopure water. Target analyte notation are as follows: ANA, anatoxin-a; CLD, cylindrospermopsin; SAX, saxitoxin; M-LA, microcystin-LA; M-LR, microcystin-LR; M-LY, microcystin-LY; M-RR, microcystin-RR; M-YR, microcystin-YR; NOD, nodularin.

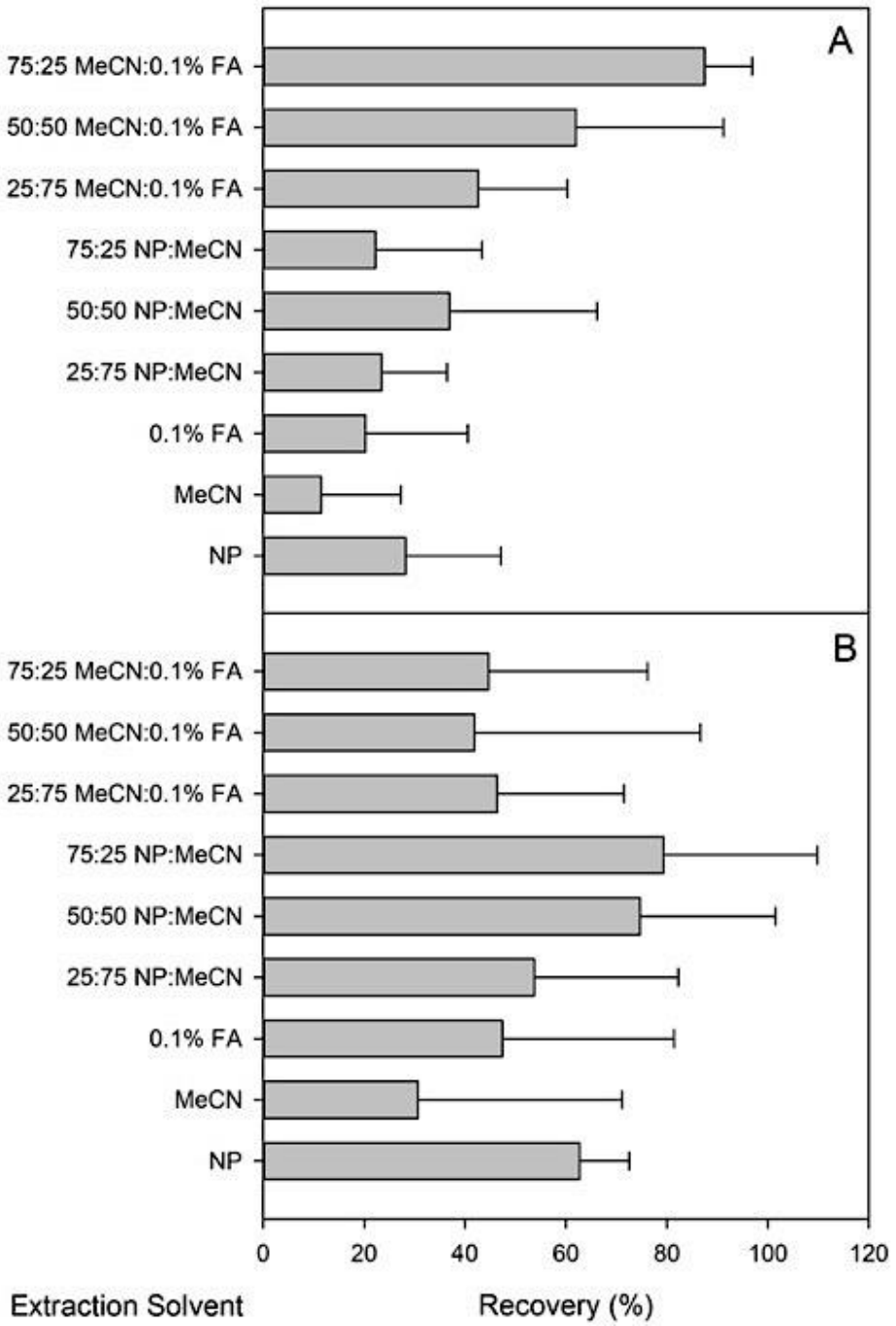

Figure 5.6. Average recoveries for extraction of anatoxin-a, cylindrospermopsin, and saxitoxin (A) and microcystin-LA, microcystin-LR, microcystin-LY microcystin-RR, microcystin-YR, and noduklarin (B) from clean whole-body homogenates of fish tissue. Extraction solvents were prepared by combining the noted ratios of solvents in a binary mixture equal to 10 mL.

Matrix Effect

Absolute matrix effect was quantified by the addition of standards to post-extraction samples. Water and fish tissue were carried through the extraction procedures detailed above then spiked with both internal standard and target analytes immediately prior to analysis. Peak areas of target analytes from post-extraction samples and standard solution were compared to calculate absolute matrix effect. To examine IS compensation for matrix effect, matched ^{15}N labeled M-LA, M-LR, M-RR, and M-YR were used for MCs and NOD, while DPA-*d5*, previously suggested as a suitable IS for ANA (Dimitrakopoulos, et al. 2010), was used for ANA, CLD, and SAX. Relative matrix effect (IS corrected) was calculated from an internal standard calibration curve. Absolute matrix effect and relative matrix effect for water and fish tissue (n = 3) are presented in Table 5.5, where positive values indicate ion enhancement while negative values indicate ion suppression. No pair matched ^{15}N standards were available for M-LY or NOD, however M-LA-15N was used for M-LY and M-RR-15N was used for NOD with acceptable results. An ion suppression ranging from -22% to -77% was observed for MCs and NOD in water, with IS corrections showing improvement where ion suppression and enhancement range from -4.2% to +5.4%. Similar to water, ion suppression for fish tissue ranged from -26% to -58%, which was improved with IS correction, where relative values ranged from -17% to +17%. Percent CV of relative matrix values for water and fish tissue are all <15% demonstrating acceptable reproducibility. ANA, CLD, and SAX showed ion suppression in water ranging from -44% to -50%. Ion suppression was still observed when the IS DPA-*d5* was used with relative values ranging from -16% to -26%, where percent CV was <15% for ANA and SAX, but not for CLD. The greatest ion suppression was observed for ANA,

CLD, and SAX in fish tissue ranging from -60% to -81%. Surprisingly, ion suppression was corrected to -42% for ANA with a CV of 23%. Ion enhancement was observed for CLD (+13%) and SAX (+26%) when DPA-*d5* was used to correct for matrix effect, with percent CV of 15% for CLD and 46% for SAX. While DPA-*d5* is structurally similar to ANA (Dimitrakopoulos, et al. 2010), use as an IS to correct for matrix effect in ANA, CLD, and SAX may be limited, but at present represents an acceptable option until commercially available isotopically labeled standards are available.

Table 5.5. Absolute and relative (IS corrected) matrix effect for target analytes in water and fish tissue.

	Absolute matrix effect (%, CV)		Relative matrix effect (%, CV)	
Analyte	Water	Fish	Water	Fish
ANA	-50 (12)	-81 (15)	-26 (5.0)	-42 (23)
CLD	-45 (23)	-61 (27)	-17 (27)	+13 (15)
SAX	-44 (14)	-60 (7.0)	-16 (14)	+26 (46)
M-LA	-55 (18)	-53 (41)	+2.9 (12)	+2.5 (5.1)
M-LR	-45 (11)	-49 (36)	+5.4 (12)	-1.3 (4.4)
M-LY	-77 (28)	-50 (45)	-4.2 (10)	-17 (7.8)
M-RR	-35 (6.0)	-26 (33)	+0.5 (11)	-2.5 (2.3)
M-YR	-48 (12)	-58 (36)	+5.3 (13)	+17 (7.2)
NOD	-22 (7.0)	-49 (24)	+3.6 (10)	+16 (2.7)

Method Validation

Method validation results are presented in Table 5.3. Method linearity and range of measurement for each target analyte was examined with an eight-point internal standard calibration curves ranging from 0.1-100 ng mL^{-1}, run in triplicate. Linear range was confirmed with plots of sensitivity (i.e., relative response factor; RRF) versus analyte concentration. Our criterion for linearity required that the percent CV of RRFs spanning the calibration range was ≤ 15%. Linear range calibration data were fit to a linear regression

with a minimum of six points to determine correlation coefficients (r^2), which were greater than ≥0.995 for all target analytes. Method precision was evaluated in terms of repeatability calculated as the percent CV of the quantified values in spiked water (10 ng L^{-1}) and fish tissue (10 µg kg^{-1}) replicates (n=3), and were <9.0% for all target analytes indicating excellent reproducibility in water and fish tissue. Method trueness was measured as the IS corrected absolute recovery (% ± CV) in spiked water (10 ng L^{-1}) and fish tissue (10 µg kg^{-1}) replicates (n=3), with the results discussed previously. Method LODs ranged from 4.0 to 80 pg (0.004-0.08 ng mL^{-1}), LOQs ranged from 10 to 280 pg (0.01-0.28 ng mL^{-1}), and MDLs ranged from 80 to 960 pg (0.08-0.96 ng L^{-1}) in water and 120 to 700 pg (0.12-0.70 µg kg^{-1}) in fish tissue. While LOD and LOQ are recognized performance metrics, MDL is more appropriate as a threshold in environmental analyses (Ramirez, et al. 2007). LOD and LOQ are calculated from laboratory blank samples, while MDL is derived from replicate matrix spikes following an accepted US EPA regulatory protocol (40 CFR Part 136, Appendix B). In most cases, matrix specific MDLs for all target analytes were an order of magnitude higher than reported LODs or LOQs demonstrating the effect sample matrix and the extraction process has on detection of target analytes. Using LOD or LOQ values developed in laboratory blanks as a reporting threshold could lead to the reporting of questionable environmental detections. Thus, MDLs were used in the current study as the detection and quantitation threshold for reporting cyanotoxin concentrations in water and fish tissue.

Analysis of Environmental Samples

Only M-LA and M-LR were detected in all water samples from both sampling periods (Table 5.6); however, no cyanotoxins were observed in fish tissue. As expected,

concentrations of M-LA and M-LR were higher in water samples subjected to freezing and thawing to release bound intercellular components. M-LA levels were higher in September than in January, when conditions for cyanobacterial growth were predicted to be optimal. Surprisingly, M-LR concentrations did not differ to a high degree from September to January in either filtered or seston water samples. Two MCs not present in the targeted analysis were identified in the September seston samples (Table 5.7). The *m/z* 103 and 135 peaks in MS^2 spectra were used for confirmation of MCs. Further, the nontarget method identified MC-LR in September and January samples as expected from the results from the targeted method. However, due to low instrument sensitivity, MC-LA was identified by the nontarget method when the minimum peak height setting was adjusted to a lower value. However, this produced more features in the peak lists which lead to more false positives. To avoid this the minimum peak height was set to 1000, which did not allow for a positive identification of MC-LA given the parameters specified in Table 5.1. There were no observed features in the nontarget method using the HILIC separation.

In the current study uncontaminated fish from laboratory cultures were caged in Lake Waco and subsampled daily to examine potential uptake of cyanotoxins detected in the filtered and seston water samples. It is not surprising that cyanotoxins were not detected in the fish samples because the major route of exposure for aquatic organisms to MCs is via diet (Ferrao-Filho Ada and Kozlowsky-Suzuki 2011), with very little inhalational accumulation expected from freely dissolved MCs (de Maagd, et al. 1999). Fish were caged in wire mesh cages, partially exposed to the sediment, to allow for the free movement of water and potential feeding of fish on native organisms. However, the current study was

conducted for 7 days, while previous caged fish studies in natural environments were conducted for 60 days and even then bioconcentration factors of MCs in fish ranged from 0.6 to 13.3 (Adamovský, et al. 2007) with elimination half-life calculated to be 0.7 to 8.4 $days^{-1}$. The findings of the current study appear to reinforce previous observations of diet as the major route of exposure for MCs to fish (Ferrao-Filho Ada and Kozlowsky-Suzuki 2011) because no uptake of M-LA or M-LR was measured in fish. However, water concentrations were similar to a recent study conducted in aquaculture ponds from Southeast Asia, where accumulation of MCs in fish was observed (Greer, et al. 2017). It is also important to note that these improved separation and isotope dilution techniques can be extended to other congeners in the future and further represent a launching point for more complex, non-targeted analyses, with preliminary targeted screening in fish tissue.

Table 5.6. Concentrations of target analytes detected in water samples collected during September and January from Lake Waco, Waco, TX, USA.

	M-LA ($ng\ L^{-1}$)		M-LR ($ng\ L^{-1}$)	
Sample Type	range	mean	range	mean
September filtered	7.0-26	13	11-38	23
September seston	43-81	59	43-120	86
January filtered	0.5-6.3	3.5	4.0-27	13
January seston	2.3-28	17	10-160	92

Table 5.7. List of nontarget compounds found in environmental water samples.

Compound	Adduct	m/z	RT (min)	Sample Type
MC-LR	$[M+H]^+$	995.5553	3.56	SF, SS, JS
MC-LM	$[M+H]^+$	970.4951	5.84	SS
MC-LL	$[M+H]^+$	952.5385	6.78	SS

SS – September seston; SF – September filtered; JS – January seston

Acknowledgment

Funding for this work was provided by the United States Department of Agriculture (USDA), National Institute of Food and Agriculture (NIFA). Samuel Haddad would like to thank Bjorn Ogren, John Palmer, Travis Thompson, Lisa Perkins, and Dr. Carol Haney Ball of Agilent Technologies for technical training, mentorship, and the Poroshell HILIC-Z column used in the current study. A special thanks to Dr. Gavin Saari for aid and education on maintaining channel catfish cultures. Additional thanks to Dr. Alejandro Ramirez and the Baylor University Mass Spectrometry Core Facility for technical support, training, and aid with instrument maintenance.

REFERENCES

Abraham, M. H., and W. E. Acree, Jr. 2010. "Equations for the Transfer of Neutral Molecules and Ionic Species from Water to Organic Phases." *J Org Chem* 75, no. 4 (Feb 19): 1006-15. http://dx.doi.org/10.1021/jo902388n.

Acuna, V., et al. 2015. "Occurrence and in-Stream Attenuation of Wastewater-Derived Pharmaceuticals in Iberian Rivers." *Sci Total Environ* 503-504 (Jan 15): 133-41. http://dx.doi.org/10.1016/j.scitotenv.2014.05.067.

Adamovský, Ondřej, et al. 2007. "Microcystin Kinetics (Bioaccumulation and Elimination) and Biochemical Responses in Common Carp (Cyprinus Carpio) and Silver Carp (Hypophthalmichthys Molitrix) Exposed to Toxic Cyanobacterial Blooms." *Environmental Toxicology and Chemistry* 26, no. 12: 2687-2693. http://dx.doi.org/doi:10.1897/07-213.1.

Akin, S., and K. O. Winemiller. 2006. "Seasonal Variation in Food Web Composition and Structure in a Temperate Tidal Estuary." *Estuaries and Coasts* 29, no. 4 (Aug): 552-567. <Go to ISI>://WOS:000240601900002.

Al-Khazrajy, O. S., and A. B. Boxall. 2016. "Impacts of Compound Properties and Sediment Characteristics on the Sorption Behaviour of Pharmaceuticals in Aquatic Systems." *J Hazard Mater* 317 (May 21): 198-209. http://dx.doi.org/10.1016/j.jhazmat.2016.05.065.

Allinger, L. E., and E. D. Reavie. 2013. "The Ecological History of Lake Erie as Recorded by the Phytoplankton Community." *Journal of Great Lakes Research* 39, no. 3 (Sep): 365-382. http://dx.doi.org/10.1016/j.jglr.2013.06.014.

Alvarez, David A., et al. 2014. "Occurrence of Contaminants of Emerging Concern Along the California Coast (2009–10) Using Passive Sampling Devices." *Marine Pollution Bulletin* 81, no. 2: 347-354. http://dx.doi.org/http://dx.doi.org/10.1016/j.marpolbul.2013.04.022.

Amuer, Btissam, Abdellatif Bayed, and Touria Benazzou. 2003. "Rôle De La Communication De La Lagune De Merja Zerga (Gharb, Maroc) Avec L'océan Atlantique Dans La Reproduction D'une Population De Mugil Cephalus L. (Poisson Mugilidae)." *Bulletin de l'Institut Scientifique, Rabat, section Sciences de la Vie*, 25: 77-82.

Anderson, Caroline, and Gilbert Cabana. 2005. "Δ15n in Riverine Food Webs: Effects of N Inputs from Agricultural Watersheds." *Canadian Journal of Fisheries and Aquatic Sciences* 62, no. 2: 333-340. http://dx.doi.org/10.1139/f04-191.

Anderson, Marti J. 2001. "A New Method for Non-Parametric Multivariate Analysis of Variance." *Austral Ecology* 26, no. 1: 32-46. http://dx.doi.org/10.1111/j.1442-9993.2001.01070.pp.x.

Ankley, G. T., et al. 2009. "White Paper: Aquatic Life Criteria for Contaminants of Emerging Concern, Part 1 General Challenges and Recommendations>." *U.S. Environmental Protection Agency, Washington, DC*: 86.

Ankley, G. T., et al. 2007. "Repeating History: Pharmaceuticals in the Environment." *Environmental Science & Technology* 41, no. 24 (Dec): 8211-8217. http://dx.doi.org/10.1021/es072658j.

Antweiler, R. C., and H. E. Taylor. 2008. "Evaluation of Statistical Treatments of Left-Censored Environmental Data Using Coincident Uncensored Data Sets: I. Summary Statistics." *Environmental Science & Technology* 42, no. 10 (May): 3732-3738. http://dx.doi.org/10.1021/es071301c.

Arheimer, Berit, et al. 2005. "Climate Change Impact on Water Quality: Model Results from Southern Sweden." *AMBIO: A Journal of the Human Environment* 34, no. 7: 559-566. http://dx.doi.org/10.1579/0044-7447-34.7.559.

Armitage, J. M., et al. 2017. "Assessing the Bioaccumulation Potential of Ionizable Organic Compounds: Current Knowledge and Research Priorities." *Environmental Toxicology and Chemistry* 36, no. 4 (Apr): 882-897. http://dx.doi.org/10.1002/etc.3680.

Armitage, James M., et al. 2013. "Development and Evaluation of a Mechanistic Bioconcentration Model for Ionogenic Organic Chemicals in Fish." *Environmental Toxicology and Chemistry* 32, no. 1 (Jan): 115-128. http://dx.doi.org/10.1002/etc.2020.

Arnold, Kathryn E., et al. 2014. "Medicating the Environment: Assessing Risks of Pharmaceuticals to Wildlife and Ecosystems." *Philosophical Transactions of the Royal Society B-Biological Sciences* 369, no. 1656 (Nov 19). http://dx.doi.org/10.1098/rstb.2013.0569.

Arnot, Jon A., and Frank A. P. C. Gobas. 2006. "A Review of Bioconcentration Factor (Bcf) and Bioaccumulation Factor (Baf) Assessments for Organic Chemicals in Aquatic Organisms." *Environmental Reviews* 14, no. 4: 257-297. http://dx.doi.org/10.1139/a06-005.

Aubertheau, E., et al. 2017. "Impact of Wastewater Treatment Plant Discharge on the Contamination of River Biofilms by Pharmaceuticals and Antibiotic Resistance." *Sci Total Environ* 579 (Feb 01): 1387-1398. http://dx.doi.org/10.1016/j.scitotenv.2016.11.136.

Baker, David R., and Barbara Kasprzyk-Hordern. 2011. "Multi-Residue Determination of the Sorption of Illicit Drugs and Pharmaceuticals to Wastewater Suspended Particulate Matter Using Pressurised Liquid Extraction, Solid Phase Extraction and Liquid Chromatography Coupled with Tandem Mass Spectrometry." *Journal of Chromatography A* 1218, no. 44 (Nov 4): 7901-7913. http://dx.doi.org/10.1016/j.chroma.2011.08.092.

Ballot, A., J. Fastner, and C. Wiedner. 2010. "Paralytic Shellfish Poisoning Toxin-Producing Cyanobacterium Aphanizomenon Gracile in Northeast Germany." *Appl Environ Microbiol* 76, no. 4 (Feb): 1173-80. http://dx.doi.org/10.1128/AEM.02285-09.

Barber, Larry B., et al. 2013. "Persistence and Potential Effects of Complex Organic Contaminant Mixtures in Wastewater-Impacted Streams." *Environmental Science & Technology* 47, no. 5 (2013/03/05): 2177-2188. http://dx.doi.org/10.1021/es303720g.

Bean, T. G., et al. 2018. "Pharmaceuticals in Water, Fish and Osprey Nestlings in Delaware River and Bay." *Environ Pollut* 232 (Jan): 533-545. http://dx.doi.org/10.1016/j.envpol.2017.09.083.

Berninger, J. P., and B. W. Brooks. 2010. "Leveraging Mammalian Pharmaceutical Toxicology and Pharmacology Data to Predict Chronic Fish Responses to Pharmaceuticals." *Toxicology Letters* 193, no. 1 (Mar): 69-78. http://ac.els-cdn.com/S0378427409015434/1-s2.0-S0378427409015434-main.pdf?_tid=e53d5d3e-7346-11e5-9295-00000aacb360&acdnat=1444918583_fbd16b8be2232563ebda3dba2e9ee4e5.

Berninger, J. P., et al. 2011. "Effects of the Antihistamine Diphenhydramine on Selected Aquatic Organisms." *Environmental Toxicology and Chemistry* 30, no. 9 (Sep): 2065-2072. http://dx.doi.org/10.1002/etc.590.

Berninger, J. P., et al. 2015. "Prioritization of Pharmaceuticals for Potential Environmental Hazard through Leveraging a Large Scale Mammalian Pharmacological Dataset." *Environ Toxicol Chem* (Mar 13). http://dx.doi.org/10.1002/etc.2965.

Berninger, Jason P., et al. 2016. "Prioritization of Pharmaceuticals for Potential Environmental Hazard through Leveraging a Large-Scale Mammalian Pharmacological Dataset." *Environmental Toxicology and Chemistry* 35, no. 4 (Apr): 1007-1020. http://dx.doi.org/10.1002/etc.2965.

Blaber, S. J. M., and A. K. Whitfield. 1977. "Feeding Ecology of Juvenile Mullet (Mugilidae) in Southeast African Estuaries " *Biological Journal of the Linnean Society* 9, no. 3 (1977): 277-284. http://dx.doi.org/10.1111/j.1095-8312.1977.tb00270.x.

Bligh, E. G., and W. J. Dyer. 1959. "A Rapid Method of Total Lipid Extraction and Purification." *Canadian Journal of Biochemistry and Physiology* 37, no. 8: 911-917. <Go to ISI>://WOS:A1959WM52500001.

Bogialli, S., et al. 2017. "Liquid Chromatography-High Resolution Mass Spectrometric Methods for the Surveillance Monitoring of Cyanotoxins in Freshwaters." *Talanta* 170 (Aug 01): 322-330. http://dx.doi.org/10.1016/j.talanta.2017.04.033.

Borga, K., et al. 2012. "Trophic Magnification Factors: Considerations of Ecology, Ecosystems, and Study Design." *Integrated Environmental Assessment and Management* 8, no. 1 (Jan): 64-84. http://dx.doi.org/10.1002/ieam.244.

Bostrom, M. L., et al. 2017. "Bioaccumulation and Trophodynamics of the Antidepressants Sertraline and Fluoxetine in Laboratory-Constructed, 3-Level Aquatic Food Chains." *Environmental Toxicology and Chemistry* 36, no. 4 (Apr): 1029-1037. http://dx.doi.org/10.1002/etc.3637.

Boxall, Alistair, et al. 2012a. "Pharmaceuticals and Personal Care Products in the Environment: What Are the Big Questions?" *Environ Health Perspect* 120, no. 9 (Sep): 1221-9. http://dx.doi.org/10.1289/ehp.1104477.

Boxall, Alistair, et al. 2012b. "Pharmaceuticals and Personal Care Products in the Environment: What Are the Big Questions?" *Environmental Health Perspectives* 120, no. 9 (Sep): 1221-1229. http://dx.doi.org/10.1289/ehp.1104477.

Bradford, Marion M. 1976. "A Rapid and Sensitive Method for the Quantitation of Microgram Quantities of Protein Utilizing the Principle of Protein-Dye Binding." *Analytical Biochemistry* 72, no. 1 (1976/05/07/): 248-254. http://dx.doi.org/http://dx.doi.org/10.1016/0003-2697(76)90527-3.

Brinkmann, Lars, Joseph B Rasmussen, and Karen Kidd. 2012. "Elevated Mercury Levels in Biota Along an Agricultural Land Use Gradient in the Oldman River Basin, Alberta." *Canadian Journal of Fisheries and Aquatic Sciences* 69, no. 7: 1202-1213. http://dx.doi.org/10.1139/f2012-056.

Brodin, Tomas, et al. 2014. "Ecological Effects of Pharmaceuticals in Aquatic Systems-Impacts through Behavioural Alterations." *Royal Society Philosophical Transactions Biological Sciences* 369, no. 1656 (Nov 19): 20130580-20130580. <Go to ISI>://ZOOREC:ZOOR15101004770 http://www.ncbi.nlm.nih.gov/pmc/articles/PMC4213591/pdf/rstb20130580.pdf.

Brooks, B. W. 2014. "Fish on Prozac (and Zoloft): Ten Years Later." *Aquatic Toxicology* 151 (Jan 19): 61-67. http://dx.doi.org/10.1016/j.aquatox.2014.01.007.

Brooks, B. W., et al. 2012. "Pharmaceuticals in the Environment: Lessons Learned for Reducing Uncertainties in Environmental Risk Assessment." *Prog Mol Biol Transl Sci* 112: 231-58. http://dx.doi.org/10.1016/B978-0-12-415813-9.00008-8.

Brooks, B. W., et al. 2005. "Determination of Select Antidepressants in Fish from an Effluent-Dominated Stream." *Environmental Toxicology and Chemistry* 24, no. 2 (Feb): 464-469. http://dx.doi.org/10.1897/04-081r.1.

Brooks, B. W., et al. 2003. "Aquatic Ecotoxicology of Fluoxetine." *Toxicology Letters* 142, no. 3 (May): 169-183. http://dx.doi.org/10.1016/s0378-4274(03)00066-3.

Brooks, B. W., D. B. Huggett, and A. B. A. Boxall. 2009. "Pharmaceuticals and Personal Care Products: Research Needs for the Next Decade." *Environmental Toxicology and Chemistry* 28, no. 12 (Dec): 2469-2472. <Go to ISI>://WOS:000271694000001.

Brooks, B. W., et al. 2017. " In Some Places, in Some Cases, and at Some Times, Harmful Algal Blooms Are the Greatest Threat to Inland Water Quality." *Environmental Toxicology and Chemistry* 36, no. 5 (May): 1125-1127. http://dx.doi.org/10.1002/etc.3801.

Brooks, B. W., et al. 2016. "Are Harmful Algal Blooms Becoming the Greatest Inland Water Quality Threat to Public Health and Aquatic Ecosystems?" *Environ Toxicol Chem* 35, no. 1 (Jan): 6-13. http://dx.doi.org/10.1002/etc.3220.

Brooks, B. W., T. M. Riley, and R. D. Taylor. 2006. "Water Quality of Effluent-Dominated Ecosystems: Ecotoxicological, Hydrological, and Management Considerations." *Hydrobiologia* 556 (Feb): 365-379. http://dx.doi.org/10.1007/s10750-004-0189-7.

Brooks, Bryan W. 2018. "Urbanization, Environment and Pharmaceuticals: Advancing Comparative Physiology, Pharmacology and Toxicology." *Conservation Physiology* 6, no. 1. http://dx.doi.org/10.1093/conphys/cox079.

Brooks, Bryan W., et al. 2012. "Perspectives on Human Pharmaceuticals in the Environment." In *Human Pharmaceuticals in the Environment: Current and Future Perspectives*, edited by Bryan W. Brooks and Duane B. Huggett, 1-16. New York, NY: Springer New York.

Brown, A. R., et al. 2014. "Assessing Variation in the Potential Susceptibility of Fish to Pharmaceuticals, Considering Evolutionary Differences in Their Physiology and Ecology." *Philos Trans R Soc Lond B Biol Sci* 369, no. 1656 (Nov 19). http://dx.doi.org/10.1098/rstb.2013.0576.

Brown, D., et al. 2015. "Persistence of Pharmaceuticals in Effluent-Dominated Surface Waters." *J Environ Qual* 44, no. 1 (Jan): 299-304. http://dx.doi.org/10.2134/jeq2014.08.0334.

Buratti, F. M., et al. 2017. "Cyanotoxins: Producing Organisms, Occurrence, Toxicity, Mechanism of Action and Human Health Toxicological Risk Evaluation." *Arch Toxicol* 91, no. 3 (Mar): 1049-1130. http://dx.doi.org/10.1007/s00204-016-1913-6.

Burkhard, L. P., et al. 2013. "Improving the Quality and Scientific Understanding of Trophic Magnification Factors (Tmfs)." *Environ Sci Technol* 47, no. 3 (Feb 5): 1186-7. http://dx.doi.org/10.1021/es305253r.

Buswell, Bradley R. 2017. "Pharmaceuticals and Personal Care Products in an Effluent-Dominated Stream: Seasonal Variability and Downstream Fate." *All Graduate Theses and Dissertations* 5812. https://digitalcommons.usu.edu/etd/5812.

Byth, S. 1980. "Palm Island Mystery Disease." *Medical Journal of Australia* 2, no. 1: 40-42. https://www.scopus.com/inward/record.uri?eid=2-s2.0-0019191617&partnerID=40&md5=9c76cc76d5a66c9cd38e31c1a21a7dd1.

Caldwell, D. J., et al. 2014. "An Integrated Approach for Prioritizing Pharmaceuticals Found in the Environment for Risk Assessmerit, Monitoring and Advanced Research." *Chemosphere* 115 (Nov): 4-12. http://dx.doi.org/10.1016/j.chemosphere.2014.01.021.

Cardona, Luis. 2006. "Habitat Selection by Grey Mullets (Osteichthyes : Mugilidae) in Mediterranean Estuaries: The Role of Salinity." *Scientia Marina* 70, no. 3 (Sep): 443-455. <Go to ISI>://WOS:000240879800011.

Carey, R. O., and K. W. Migliaccio. 2009. "Contribution of Wastewater Treatment Plant Effluents to Nutrient Dynamics in Aquatic Systems: A Review." *Environ Manage* 44, no. 2 (Aug): 205-17. http://dx.doi.org/10.1007/s00267-009-9309-5.

Chapman, P. M. 2015. "Harmful Algal Blooms Should Be Treated as Contaminants." *Integrated Environmental Assessment and Management* 11, no. 4 (Oct): 523-524. http://dx.doi.org/10.1002/ieam.1698.

Chen, F., Z. Gong, and B. C. Kelly. 2017. "Bioaccumulation Behavior of Pharmaceuticals and Personal Care Products in Adult Zebrafish (Danio Rerio): Influence of Physical-Chemical Properties and Biotransformation." *Environ Sci Technol* 51, no. 19 (Oct 3): 11085-11095. http://dx.doi.org/10.1021/acs.est.7b02918.

Chrıstophorıdıs, C., et al. 2017. "Analysis of Multi-Class Cyanotoxins in Fish Tissue. Application to Fish from Greek Lakes." Paper presented at the 15th International Conference on Environmental Science and Technology, Rhodes, Greece, 31 August to 2 September 2017.

Codd, Geoffrey A., et al. 2005. "Harmful Cyanobacteria." In *Harmful Cyanobacteria*, edited by Jef Huisman, Hans C. P. Matthijs, and Petra M. Visser, 1-23. Dordrecht: Springer Netherlands.

Conder, J. M., et al. 2012. "Use of Trophic Magnification Factors and Related Measures to Characterize Bioaccumulation Potential of Chemicals." *Integr Environ Assess Manag* 8, no. 1 (Jan): 85-97. http://dx.doi.org/10.1002/ieam.216.

Connors, K. A., et al. 2013. "Comparative Pharmaceutical Metabolism by Rainbow Trout (Oncorhynchus Mykiss) Liver S9 Fractions." *Environmental Toxicology and Chemistry* 32, no. 8 (Aug): 1810-1818. http://dx.doi.org/10.1002/etc.2240.

Costanzo, S. D., et al. 2005. "Using Nitrogen Stable Isotope Ratios (Delta N-15) of Macroalgae to Determine the Effectiveness of Sewage Upgrades: Changes in the Extent of Sewage Plumes over Four Years in Moreton Bay, Australia." *Marine Pollution Bulletin* 51, no. 1-4 (2005): 212-217. http://dx.doi.org/10.1016/j.marpolbul.2004.10.018.

Dale, B., M. Edwards, and P. C. Reid. 2006. "Climate Change and Harmful Algal Blooms." In *Ecology of Harmful Algae*, edited by Edna Granéli and Jefferson T. Turner, 367-378. Berlin, Heidelberg: Springer Berlin Heidelberg.

Daughton, C. G., and T. A. Ternes. 1999. "Pharmaceuticals and Personal Care Products in the Environment: Agents of Subtle Change?" *Environmental Health Perspectives* 107 (Dec): 907-938. http://dx.doi.org/10.2307/3434573.

Daughton, CG, and BW Brooks. 2011a. "Active Pharmaceutical Ingredients and Aquatic Organisms." In *Environmental Contaminants in Biota*, edited by WN Beyer and JP Meador, 286-347. Boca Raton: CRC Press, Taylor and Francis.

---. 2011b. "Active Pharmaceuticals Ingredients and Aquatic Organisms. In: Environmental Contaminants in Wildlife: Interpreting Tissue Concentrations, 2nd Ed. Meador J, Beyer N (Eds). Taylor and Francis." 281-341.

de la Cruz, Armah A., et al. 2013. "A Review on Cylindrospermopsin: The Global Occurrence, Detection, Toxicity and Degradation of a Potent Cyanotoxin." *Environmental Science: Processes & Impacts* 15, no. 11: 1979-2003. http://dx.doi.org/10.1039/C3EM00353A.

de Maagd, P. Gert-Jan, et al. 1999. "Ph-Dependent Hydrophobicity of the Cyanobacteria Toxin Microcystin-Lr." *Water Research* 33, no. 3 (1999/02/01/): 677-680. http://dx.doi.org/https://doi.org/10.1016/S0043-1354(98)00258-9.

Dell'Aversano, Carmela, Geoffrey K. Eaglesham, and Michael A. Quilliam. 2004. "Analysis of Cyanobacterial Toxins by Hydrophilic Interaction Liquid Chromatography–Mass Spectrometry." *Journal of Chromatography A* 1028, no. 1: 155-164. http://dx.doi.org/10.1016/j.chroma.2003.11.083.

Dell'Aversano, Carmela, Philipp Hess, and Michael A. Quilliam. 2005. "Hydrophilic Interaction Liquid Chromatography–Mass Spectrometry for the Analysis of Paralytic Shellfish Poisoning (Psp) Toxins." *Journal of Chromatography A* 1081, no. 2: 190-201. http://dx.doi.org/10.1016/j.chroma.2005.05.056.

Desilva, S. S., and M. J. S. Wijeyaratne. 1977. "Studies on Biology of Young Grey Mullet, Mugil-Cephalus L .2. Food and Feeding." *Aquaculture* 12, no. 2 (1977): 157-167. http://dx.doi.org/10.1016/0044-8486(77)90183-1.

Diener, M., et al. 2007. "Application of a New Zwitterionic Hydrophilic Interaction Chromatography Column for Determination of Paralytic Shellfish Poisoning Toxins." *J Sep Sci* 30, no. 12 (Aug): 1821-6. http://dx.doi.org/10.1002/jssc.200700025.

Dimitrakopoulos, I. K., et al. 2010. "Development of a Fast and Selective Method for the Sensitive Determination of Anatoxin-a in Lake Waters Using Liquid Chromatography-Tandem Mass Spectrometry and Phenylalanine-D5 as Internal Standard." *Anal Bioanal Chem* 397, no. 6 (Jul): 2245-52. http://dx.doi.org/10.1007/s00216-010-3727-3.

Ding, J., et al. 2015a. "Evaluation of the Potential for Trophic Transfer of Roxithromycin Along an Experimental Food Chain." *Environmental Science and Pollution Research* 22, no. 14 (Jul): 10592-10600. http://dx.doi.org/10.1007/s11356-015-4265-5.

Ding, J., et al. 2015b. "Biological Fate and Effects of Propranolol in an Experimental Aquatic Food Chain." *Sci Total Environ* 532 (Nov 01): 31-9. http://dx.doi.org/10.1016/j.scitotenv.2015.06.002.

Downing, John A., Susan B. Watson, and Edward McCauley. 2001. "Predicting Cyanobacteria Dominance in Lakes." *Canadian Journal of Fisheries and Aquatic Sciences* 58, no. 10: 1905-1908. http://dx.doi.org/10.1139/f01-143.

Draper, William M., et al. 2013. "Optimizing Lc-Ms-Ms Determination of Microcystin Toxins in Natural Water and Drinking Water Supplies." *Analytical Methods* 5, no. 23: 6796. http://dx.doi.org/10.1039/c3ay41328d.

Draper, William M., Dadong Xu, and S. Kusum Perera. 2009. "Electrolyte-Induced Ionization Suppression and Microcystin Toxins: Ammonium Formate Suppresses Sodium Replacement Ions and Enhances Protiated and Ammoniated Ions for Improved Specificity in Quantitative Lc-Ms-Ms." *Anal Chem* 81, no. 10 (2009/05/15): 4153-4160. http://dx.doi.org/10.1021/ac802735t.

Droge, S. T., et al. 2017. "Predicting the Phospholipophilicity of Monoprotic Positively Charged Amines." *Environ Sci Process Impacts* (Feb 20). http://dx.doi.org/10.1039/c6em00615a.

Drouillard, K. G., H. Hagen, and G. D. Haffner. 2004. "Evaluation of Chloroform/Methanol and Dichloromethane/Hexane Extractable Lipids as Surrogate Measures of Sample Partition Capacity for Organochlorines in Fish Tissues." *Chemosphere* 55, no. 3 (Apr): 395-400. http://dx.doi.org/10.1016/j.chemosphere.2003.11.010.

Du, B., et al. 2015. "Pharmaceutical Bioaccumulation by Periphyton and Snails in an Effluent-Dependent Stream During an Extreme Drought." *Chemosphere* 119 (Jan): 927-34. http://dx.doi.org/10.1016/j.chemosphere.2014.08.044.

Du, B., et al. 2012. "Evaluation of an Isotope Dilution Liquid Chromatography Tandem Mass Spectrometry Method for Pharmaceuticals in Fish." *Journal of Chromatography A* 1253, no. 0: 177-183. http://dx.doi.org/http://dx.doi.org/10.1016/j.chroma.2012.07.026.

Du, Bowen, et al. 2016. "Bioaccumulation of Human Pharmaceuticals in Fish across Habitats of a Tidally Influenced Urban Bayou." *Environmental Toxicology and Chemistry* 35, no. 4: 966-974. http://dx.doi.org/10.1002/etc.3221.

Du, Bowen, et al. 2014a. "Bioaccumulation and Trophic Dilution of Human Pharmaceuticals across Trophic Positions of an Effluent-Dependent Wadeable Stream." *Philosophical transactions of the Royal Society of London Series B, Biological Science* 369: 20140058.

Du, Bowen, et al. 2014b. "Comparison of Contaminants of Emerging Concern Removal, Discharge, and Water Quality Hazards among Centralized and on-Site Wastewater Treatment System Effluents Receiving Common Wastewater Influent." *Sci Total Environ* 466-467C (Aug 26): 976-984. http://dx.doi.org/10.1016/j.scitotenv.2013.07.126.

Ebele, Anekwe Jennifer, Mohamed Abou-Elwafa Abdallah, and Stuart Harrad. 2017. "Pharmaceuticals and Personal Care Products (Ppcps) in the Freshwater Aquatic Environment." *Emerging Contaminants* 3, no. 1: 1-16. http://dx.doi.org/10.1016/j.emcon.2016.12.004.

Eggold, B. T., and P. J. Motta. 1992. "Ontogenic Dietary Shifts and Morphological Correlates in Stripped Mullet, Mugil-Cephalus." *Environmental Biology of Fishes* 34, no. 2 (Jun): 139-158. http://dx.doi.org/10.1007/bf00002390.

El-Shehawy, R., et al. 2012. "Global Warming and Hepatotoxin Production by Cyanobacteria: What Can We Learn from Experiments?" *Water Res* 46, no. 5 (Apr 01): 1420-9. http://dx.doi.org/10.1016/j.watres.2011.11.021.

Endo, S., B. I. Escher, and K. U. Goss. 2011. "Capacities of Membrane Lipids to Accumulate Neutral Organic Chemicals." *Environ Sci Technol* 45, no. 14 (Jul 15): 5912-21. http://dx.doi.org/10.1021/es200855w.

Ferrao-Filho Ada, S., and B. Kozlowsky-Suzuki. 2011. "Cyanotoxins: Bioaccumulation and Effects on Aquatic Animals." *Mar Drugs* 9, no. 12 (Dec): 2729-72. http://dx.doi.org/10.3390/md9122729.

Ferreira, M., P. Moradas-Ferreira, and M. A. Reis-Henriques. 2005. "Oxidative Stress Biomarkers in Two Resident Species, Mullet (Mugil Cephalus) and Flounder (Platichtkys Flesus), from a Polluted Site in River Douro Estuary, Portugal." *Aquatic Toxicology* 71, no. 1 (Jan 18): 39-48. http://dx.doi.org/10.1016/j.aquatox.2004.10.009.

Fick, J., et al. 2010a. "Therapeutic Levels of Levonorgestrel Detected in Blood Plasma of Fish: Results from Screening Rainbow Trout Exposed to Treated Sewage Effluents." *Environmental Science & Technology* 44, no. 7 (Apr): 2661-2666. http://dx.doi.org/10.1021/es903440m.

Fick, J., et al. 2010b. "Predicted Critical Environmental Concentrations for 500 Pharmaceuticals." *Regul Toxicol Pharmacol* 58, no. 3 (Dec): 516-23. http://dx.doi.org/10.1016/j.yrtph.2010.08.025.

Fitzsimmons, P.N., Fernandez, J.D., Hoffman, A.D., Butterworth, B.C., Nichols, J.W. 2001. "Branchial Elimination of Superhydrophobic Organic Compounds by Rainbow Trout (Oncorhynchus Mykiss)." *Aquatic Toxicology* 55: 23-34. http://ac.els-cdn.com/S0166445X01001746/1-s2.0-S0166445X01001746-main.pdf?_tid=466cf826-7347-11e5-a1ef-00000aab0f26&acdnat=1444918746_2b0095be6fa8fc91856ab15110af88ea.

Flemming, Hans-Curt, and Jost Wingender. 2010. "The Biofilm Matrix." *Nat Rev Micro* 8, no. 9 (09//print): 623-633. http://dx.doi.org/10.1038/nrmicro2415.

Foran, Christy M., et al. 2004. "Reproductive Assessment of Japanese Medaka (Oryzias Latipes) Following a Four-Week Fluoxetine (Ssri) Exposure." *Archives of Environmental Contamination and Toxicology* 46, no. 4. http://dx.doi.org/10.1007/s00244-003-3042-5.

Francis, G. 1878. "Poisonous Australian Lake." *Nature* 18: 11-12.

Franzellitti, Silvia, et al. 2014. "An Exploratory Investigation of Various Modes of Action and Potential Adverse Outcomes of Fluoxetine in Marine Mussels." *Aquatic Toxicology* 151, no. 0 (6//): 14-26. http://dx.doi.org/http://dx.doi.org/10.1016/j.aquatox.2013.11.016.

Furey, Ambrose, et al. 2005. "Strategies to Avoid the Mis-Identification of Anatoxin-a Using Mass Spectrometry in the Forensic Investigation of Acute Neurotoxic Poisoning." *Journal of Chromatography A* 1082, no. 1: 91-97. http://dx.doi.org/10.1016/j.chroma.2005.05.040.

Gaw, S., K. V. Thomas, and T. H. Hutchinson. 2014. "Sources, Impacts and Trends of Pharmaceuticals in the Marine and Coastal Environment." *Philosophical transactions of the Royal Society of London Series B, Biological Science* 369, no. 1656 (Nov 19). http://dx.doi.org/10.1098/rstb.2013.0572.

Geis-Asteggiante, L., et al. 2011. "Development and Validation of a Rapid Method for Microcystins in Fish and Comparing Lc-Ms/Ms Results with Elisa." *Anal Bioanal Chem* 401, no. 8 (Nov): 2617-30. http://dx.doi.org/10.1007/s00216-011-5345-0.

Gisbert, E., L. Cardona, and F. Castello. 1996. "Resource Partitioning among Planktivorous Fish Larvae and Fry in a Mediterranean Coastal Lagoon." *Estuarine Coastal and Shelf Science* 43, no. 6 (Dec): 723-735. http://dx.doi.org/10.1006/ecss.1996.0099.

Greer, B., et al. 2017. "Detection of Freshwater Cyanotoxins and Measurement of Masked Microcystins in Tilapia from Southeast Asian Aquaculture Farms." *Anal Bioanal Chem* 409, no. 16 (Jun): 4057-4069. http://dx.doi.org/10.1007/s00216-017-0352-4.

Greer, Brett, et al. 2016. "A Validated Uplc–Ms/Ms Method for the Surveillance of Ten Aquatic Biotoxins in European Brackish and Freshwater Systems." *Harmful Algae* 55: 31-40. http://dx.doi.org/10.1016/j.hal.2016.01.006.

Gunnarsson, L., et al. 2008. "Evolutionary Conservation of Human Drug Targets in Organisms Used for Environmental Risk Assessments." *Environmental Science & Technology* 42, no. 15 (Aug): 5807-5813. http://dx.doi.org/10.1021/es8005173.

Hammer, Ø, D.A.T Harper, and P.D. Ryan. 2001. "Past: Paleontological Statistics Software Package for Education and Data Analysis." *Palaeontologia Electronica* 4, no. 1: 9.

Hazelton, Peter D., et al. 2014. "Chronic Fluoxetine Exposure Alters Movement and Burrowing in Adult Freshwater Mussels." *Aquatic Toxicology* 151 (Jun): 27-35. http://dx.doi.org/10.1016/j.aquatox.2013.12.019.

Heisler, J., et al. 2008. "Eutrophication and Harmful Algal Blooms: A Scientific Consensus." *Harmful Algae* 8, no. 1: 3-13. http://dx.doi.org/10.1016/j.hal.2008.08.006.

Henneberger, L., K. U. Goss, and S. Endo. 2016a. "Equilibrium Sorption of Structurally Diverse Organic Ions to Bovine Serum Albumin." *Environ Sci Technol* 50, no. 10 (May 17): 5119-26. http://dx.doi.org/10.1021/acs.est.5b06176.

---. 2016b. "Partitioning of Organic Ions to Muscle Protein: Experimental Data, Modeling, and Implications for in Vivo Distribution of Organic Ions." *Environ Sci Technol* 50, no. 13 (Jul 05): 7029-36. http://dx.doi.org/10.1021/acs.est.6b01417.

Heussner, A. H., et al. 2012. "Toxin Content and Cytotoxicity of Algal Dietary Supplements." *Toxicol Appl Pharmacol* 265, no. 2 (Dec 1): 263-71. http://dx.doi.org/10.1016/j.taap.2012.10.005.

Heynen, Martina, et al. 2016. "Effect of Bioconcentration and Trophic Transfer on Realized Exposure to Oxazepam in 2 Predators, the Dragonfly Larvae (Aeshna Grandis) and the Eurasian Perch (Perca Fluviatilis)." *Environmental Toxicology and Chemistry* 35, no. 4: 930-937. http://dx.doi.org/10.1002/etc.3368.

Hiller, S., et al. 2007. "Rapid Detection of Cyanobacterial Toxins in Precursor Ion Mode by Liquid Chromatography Tandem Mass Spectrometry." *J Mass Spectrom* 42, no. 9 (Sep): 1238-50. http://dx.doi.org/10.1002/jms.1257.

Hollingdale, C., et al. 2015. "Feasibility Study on Production of a Matrix Reference Material for Cyanobacterial Toxins." *Analytical and Bioanalytical Chemistry* 407, no. 18 (Jul): 5353-5363. http://dx.doi.org/10.1007/s00216-015-8695-1.

Hsu, Chih-Chieh, et al. 2009. "A Growth Check Deposited at Estuarine Arrival in Otoliths of Juvenile Flathead Mullet (Mugil Cephalus L.)." *Zoological Studies* 48, no. 3 (May): 315-324. <Go to ISI>://WOS:000266522900003.

Huang, Yuxiong, et al. 2018. "Quantitative Analysis of Underivatized Amino Acids in Plant Matrix by Hydrophilic Interaction Chromatography (Hilic) with Lc/Ms Detection." *Application Note*.

Huerta, B., et al. 2016. "Determination of a Broad Spectrum of Pharmaceuticals and Endocrine Disruptors in Biofilm from a Waste Water Treatment Plant-Impacted River." *Sci Total Environ* 540 (Jan 01): 241-9. http://dx.doi.org/10.1016/j.scitotenv.2015.05.049.

Huggett, D. B., et al. 2003. "A Theoretical Model for Utilizing Mammalian Pharmacology and Safety Data to Prioritize Potential Impacts of Human Pharmaceuticals to Fish." *Human and Ecological Risk Assessment* 9, no. 7 (Dec): 1789-1799. http://dx.doi.org/10.1080/10807030390260498.

Ibanez, A. L., and O. G. Benitez. 2004. "Climate Variables and Spawning Migrations of the Striped Mullet and White Mullet in the North-Western Area of the Gulf of Mexico." *Journal of Fish Biology* 65, no. 3 (Sep): 822-831. http://dx.doi.org/10.1111/j.1095-8649.2004.00488.x.

Jardine, T. D., K. A. Kidd, and A. T. Fisk. 2006. "Applications, Considerations, and Sources of Uncertainty When Using Stable Isotope Analysis in Ecotoxicology." *Environmental Science & Technology* 40, no. 24 (Dec): 7501-7511. http://dx.doi.org/10.1021/es061263h.

Jiang, Jheng-Jie, Chon-Lin Lee, and Meng-Der Fang. 2014. "Emerging Organic Contaminants in Coastal Waters: Anthropogenic Impact, Environmental Release and Ecological Risk." *Marine Pollution Bulletin* 85, no. 2: 391-399. http://dx.doi.org/http://dx.doi.org/10.1016/j.marpolbul.2013.12.045.

Johnk, Klaus D., et al. 2008. "Summer Heatwaves Promote Blooms of Harmful Cyanobacteria." *Global Change Biology* 14, no. 3: 495-512. http://dx.doi.org/10.1111/j.1365-2486.2007.01510.x.

Juaneda, P., and G. Rocquelin. 1985. "Rapid and Convenient Separation of Phospholipids and Non Phosphorus Lipids from Rat-Heart Using Silica Cartridges." *Lipids* 20, no. 1: 40-41. http://dx.doi.org/10.1007/bf02534360.

Kaloudis, T., et al. 2013. "Determination of Microcystins and Nodularin (Cyanobacterial Toxins) in Water by Lc-Ms/Ms. Monitoring of Lake Marathonas, a Water Reservoir of Athens, Greece." *J Hazard Mater* 263 Pt 1 (Dec 15): 105-15. http://dx.doi.org/10.1016/j.jhazmat.2013.07.036.

Karlsson, M. V., et al. 2017. "Novel Approach for Characterizing Ph-Dependent Uptake of Ionizable Chemicals in Aquatic Organisms." *Environ Sci Technol* 51, no. 12 (Jun 20): 6965-6971. http://dx.doi.org/10.1021/acs.est.7b01265.

Kikuchi, S., T. Kubo, and K. Kaya. 2007. "Cylindrospermopsin Determination Using 2-[4-(2-Hydroxyethyl)-1-Piperazinyl]Ethanesulfonic Acid (Hepes) as the Internal Standard." *Anal Chim Acta* 583, no. 1 (Jan 30): 124-7. http://dx.doi.org/10.1016/j.aca.2006.10.007.

Kim, J., et al. 2016. "Evaluating the Roles of Biotransformation, Spatial Concentration Differences, Organism Home Range, and Field Sampling Design on Trophic Magnification Factors." *Sci Total Environ* 551-552 (May 1): 438-51. http://dx.doi.org/10.1016/j.scitotenv.2016.02.013.

Klosterhaus, S. L., et al. 2013. "Method Validation and Reconnaissance of Pharmaceuticals, Personal Care Products, and Alkylphenols in Surface Waters, Sediments, and Mussels in an Urban Estuary." *Environ Int* 54 (Apr): 92-9. http://dx.doi.org/10.1016/j.envint.2013.01.009.

Kolpin, D. W., et al. 2002. "Pharmaceuticals, Hormones, and Other Organic Wastewater Contaminants in Us Streams, 1999-2000: A National Reconnaissance." *Environmental Science & Technology* 36, no. 6 (Mar): 1202-1211. http://dx.doi.org/10.1021/es011055j.

Kraemer, L. D., D. Evans, and P. J. Dillon. 2012. "The Impacts of Ontogenetic Dietary Shifts in Yellow Perch (Perca Flavescens) on Zn and Hg Accumulation." *Ecotoxicology and Environmental Safety* 78 (Apr): 246-252. http://dx.doi.org/10.1016/j.ecoenv.2011.11.033.

Kristofco, L. A., and B. W. Brooks. 2017. "Global Scanning of Antihistamines in the Environment: Analysis of Occurrence and Hazards in Aquatic Systems." *Sci Total Environ* 592 (Aug 15): 477-487. http://dx.doi.org/10.1016/j.scitotenv.2017.03.120.

Kruve, A., et al. 2015a. "Tutorial Review on Validation of Liquid Chromatography-Mass Spectrometry Methods: Part I." *Anal Chim Acta* 870 (Apr 22): 29-44. http://dx.doi.org/10.1016/j.aca.2015.02.017.

---. 2015b. "Tutorial Review on Validation of Liquid Chromatography-Mass Spectrometry Methods: Part Ii." *Anal Chim Acta* 870 (Apr 22): 8-28. http://dx.doi.org/10.1016/j.aca.2015.02.016.

Kurmayer, Rainer, and Guntram Christiansen. 2009. "The Genetic Basis of Toxin Production in Cyanobacteria." *Freshwater Reviews* 2, no. 1 (2009/06/01): 31-50. Accessed 2017/01/18. http://dx.doi.org/10.1608/FRJ-2.1.2.

Kwon, J. W., et al. 2009. "Determination of 17alpha-Ethynylestradiol, Carbamazepine, Diazepam, Simvastatin, and Oxybenzone in Fish Livers." *J AOAC Int* 92, no. 1 (Jan-Feb): 359-69.

Lagesson, A., et al. 2016. "Bioaccumulation of Five Pharmaceuticals at Multiple Trophic Levels in an Aquatic Food Web - Insights from a Field Experiment." *Sci Total Environ* 568 (Jun 10): 208-215. http://dx.doi.org/10.1016/j.scitotenv.2016.05.206.

Lajeunesse, A., C. Gagnon, and S. Sauve. 2008. "Determination of Basic Antidepressants and Their N-Desmethyl Metabolites in Raw Sewage and Wastewater Using Solid-Phase Extraction and Liquid Chromatography - Tandem Mass Spectrometry." *Analytical Chemistry* 80, no. 14 (Jul): 5325-5333. http://dx.doi.org/10.1021/ac800162q.

Lajeunesse, A., C. Gagnon, and S. Sauvé. 2008. "Determination of Basic Antidepressants and Their N-Desmethyl Metabolites in Raw Sewage and Wastewater Using Solid-Phase Extraction and Liquid Chromatography−Tandem Mass Spectrometry." *Analytical Chemistry* 80, no. 14: 5325-5333. http://dx.doi.org/10.1021/ac800162q.

Lajeunesse, A., et al. 2012. "Detection and Confirmation of Saxitoxin Analogues in Freshwater Benthic Lyngbya Wollei Algae Collected in the St. Lawrence River (Canada) by Liquid Chromatography-Tandem Mass Spectrometry." *Journal of Chromatography A* 1219 (Jan): 93-103. http://dx.doi.org/10.1016/j.chroma.2011.10.092.

Lawson, Emmanuel O.; Jimoh, Abayomi A.-A. 2010. "Aspects of the Biology of Grey Mullet, Mugil Cephalus, in Lagos Lagoon, Nigeria." *AACL Bioflux* 3, no. 3: 181-194.

Lazarus, R. S., et al. 2015. "Exposure and Food Web Transfer of Pharmaceuticals in Ospreys (Pandion Haliaetus): Predictive Model and Empirical Data." *Integrated Environmental Assessment and Management* 11, no. 1 (Jan): 118-29. http://dx.doi.org/10.1002/ieam.1570.

Li, C. M., R. Y. Chu, and D. P. Hsientang Hsieh. 2006. "An Enhanced Lc-Ms/Ms Method for Microcystin-Lr in Lake Water." *J Mass Spectrom* 41, no. 2 (Feb): 169-74. http://dx.doi.org/10.1002/jms.972.

Li, Jun, et al. 2015. "Mercury Bioaccumulation in the Food Web of Three Gorges Reservoir (China): Tempo-Spatial Patterns and Effect of Reservoir Management." *Science of the Total Environment* 527 (Sep 15): 203-210. http://dx.doi.org/10.1016/j.scitotenv.2015.04.115.

Lim, Fang, Say Ong, and Jiangyong Hu. 2017. "Recent advances in the use of chemical markers for Tracing wastewater contami nation in aquatic Environment: a review." *Water* 9, no. 2: 143. http://dx.doi.org/10.3390/w9020143.

Loomer, H. A., et al. 2015. "Use of Stable Isotopes to Trace Municipal Wastewater Effluents into Food Webs within a Highly Developed River System." *River Research and Applications* 31, no. 9 (Nov): 1093-1100. http://dx.doi.org/10.1002/rra.2826.

Mackay, Donald, et al. 2016. "Processes Influencing Chemical Biomagnification and Trophic Magnification Factors in Aquatic Ecosystems: Implications for Chemical Hazard and Risk Assessment." *Chemosphere* 154 (Jul): 99-108. http://dx.doi.org/10.1016/j.chemosphere.2016.03.048.

Maizels, M., and W. L. Budde. 2004. "A Lc/Ms Method for the Determination of Cyanobacteria Toxins in Water." *Analytical Chemistry* 76, no. 5 (Mar): 1342-1351. http://dx.doi.org/10.1021/ac035118n.

Manallack, David T. 2007. "The Pk(a) Distribution of Drugs: Application to Drug Discovery." *Perspectives in Medicinal Chemistry* 1 (09/17): 25-38. http://www.ncbi.nlm.nih.gov/pmc/articles/PMC2754920/.

Mankin, Justin S., et al. 2015. "The Potential for Snow to Supply Human Water Demand in the Present and Future." *Environmental Research Letters* 10, no. 11: 114016. http://dx.doi.org/10.1088/1748-9326/10/11/114016.

Marais, J. F. K. 1978. "Routine Oxygen Consumption of Mugil Cephalus, Liza Dumerili and L. Richardsoni at Different Temperatures and Salinities." *Marine Biology* 50, no. 1 (1978/03/01): 9-16. http://dx.doi.org/10.1007/BF00390537.

Margiotta-Casaluci, L., et al. 2014. "Quantitative Cross-Species Extrapolation between Humans and Fish: The Case of the Anti-Depressant Fluoxetine." *PLoS One* 9, no. 10: e110467. http://dx.doi.org/10.1371/journal.pone.0110467.

Maruya, K. A., L. Francendese, and R. O. Manning. 2005. "Residues of Toxaphene Decrease in Estuarine Fish after Removal of Contaminated Sediments." *Estuaries* 28, no. 5 (Oct): 786-793. http://dx.doi.org/10.1007/bf02732916.

Maruya, Keith A., et al. 2014. "The Mussel Watch California Pilot Study on Contaminants of Emerging Concern (Cecs): Synthesis and Next Steps." *Marine Pollution Bulletin* 81, no. 2: 355-363. http://dx.doi.org/http://dx.doi.org/10.1016/j.marpolbul.2013.04.023.

McDonough, C. J., and C. A. Wenner. 2003. "Growth, Recruitment, and Abundance of Juvenile Striped Mullet (Mugil Cephalus) in South Carolina Estuaries." *Fishery Bulletin* 101, no. 2 (Apr): 343-357. <Go to ISI>://WOS:000182389600012.

McLeod, Anne M., et al. 2015. "Quantifying Uncertainty in the Trophic Magnification Factor Related to Spatial Movements of Organisms in a Food Web." *Integrated Environmental Assessment and Management* 11, no. 2 (Apr): 306-318. http://dx.doi.org/10.1002/ieam.1599.

Meador, J. P., et al. 2016. "Contaminants of Emerging Concern in a Large Temperate Estuary." *Environ Pollut* 213 (Feb 20): 254-267. http://dx.doi.org/10.1016/j.envpol.2016.01.088.

Meredith-Williams, Melanie, et al. 2012. "Uptake and Depuration of Pharmaceuticals in Aquatic Invertebrates." *Environmental Pollution* 165 (Jun): 250-258. http://dx.doi.org/10.1016/j.envpol.2011.11.029.

Merel, S., et al. 2013. "State of Knowledge and Concerns on Cyanobacterial Blooms and Cyanotoxins." *Environment International* 59 (Sep): 303-327. http://dx.doi.org/10.1016/j.envint.2013.06.013.

Meriluoto, J., L. Spoof, and G.A. Codd. 2017. *Handbook of Cyanobacterial Monitoring and Cyanotoxin Analysis*: Wiley.

Merritt, R.W., and K.W. Cummins. 1996. *An Introduction to the Aquatic Insects of North America*: Kendall/Hunt Publishing Company.

Metcalfe, Chris D., et al. 2010. "Antidepressants and Their Metabolites in Municipal Wastewater, and Downstream Exposure in an Urban Watershed." *Environmental Toxicology and Chemistry* 29, no. 1 (Jan): 79-89. http://dx.doi.org/10.1002/etc.27.

Meynecke, Jan-Olaf, and Shing Yip Lee. 2011. "Climate-Coastal Fisheries Relationships and Their Spatial Variation in Queensland, Australia." *Fisheries Research* 110, no. 2 (Jul): 365-376. http://dx.doi.org/10.1016/j.fishres.2011.05.004.

Meynecke, Jan-Olaf, et al. 2006. "Effect of Rainfall as a Component of Climate Change on Estuarine Fish Production in Queensland, Australia." *Estuarine Coastal and Shelf Science* 69, no. 3-4 (Sep): 491-504. http://dx.doi.org/10.1016/j.ecss.2006.05.011.

Michalak, A. M., et al. 2013. "Record-Setting Algal Bloom in Lake Erie Caused by Agricultural and Meteorological Trends Consistent with Expected Future Conditions." *Proceedings of the National Academy of Sciences of the United States of America* 110, no. 16 (Apr): 6448-6452. http://dx.doi.org/10.1073/pnas.1216006110.

Miller, T. H., et al. 2017. "Uptake, Biotransformation and Elimination of Selected Pharmaceuticals in a Freshwater Invertebrate Measured Using Liquid Chromatography Tandem Mass Spectrometry." *Chemosphere* 183 (Sep): 389-400. http://dx.doi.org/10.1016/j.chemosphere.2017.05.083.

Moreno, Clara E., et al. 2015. "Seasonal Variation of Mercury and Delta N-15 in Fish from Lake Heddalsvatn, Southern Norway." *Journal of Limnology* 74, no. 1 (2015): 21-30. http://dx.doi.org/10.4081/jlimnol.2014.918.

Myers, O. D., et al. 2017. "One Step Forward for Reducing False Positive and False Negative Compound Identifications from Mass Spectrometry Metabolomics Data: New Algorithms for Constructing Extracted Ion Chromatograms and Detecting Chromatographic Peaks." *Analytical Chemistry* 89, no. 17 (Sep): 8696-8703. http://dx.doi.org/10.1021/acs.analchem.7b00947.

Nash, C. E., C. M. Kuo, and S. C. McConnel. 1974. "Operational Procedures for Rearing Larvae of Grey Mullet (Mugil-Cephalus L)." *Aquaculture* 3, no. 1 (1974): 15-24. http://dx.doi.org/10.1016/0044-8486(74)90095-7.

Nichols, J. W., et al. 2015. "Observed and Modeled Effects of Ph on Bioconcentration of Diphenhydramine, a Weakly Basic Pharmaceutical, in Fathead Minnows." *Environ Toxicol Chem* 34, no. 6 (Jun): 1425-35. http://dx.doi.org/10.1002/etc.2948.

O'Reilly, C. M., et al. 2002. "Interpreting Stable Isotopes in Food Webs: Recognizing the Role of Time Averaging at Different Trophic Levels." *Limnology and Oceanography* 47, no. 1: 306-309. http://dx.doi.org/10.4319/lo.2002.47.1.0306.

O'Neil, J. M., et al. 2012. "The Rise of Harmful Cyanobacteria Blooms: The Potential Roles of Eutrophication and Climate Change." *Harmful Algae* 14: 313-334. http://dx.doi.org/10.1016/j.hal.2011.10.027.

Oehrle, S. A., B. Southwell, and J. Westrick. 2010. "Detection of Various Freshwater Cyanobacterial Toxins Using Ultra-Performance Liquid Chromatography Tandem Mass Spectrometry." *Toxicon* 55, no. 5 (May): 965-72. http://dx.doi.org/10.1016/j.toxicon.2009.10.001.

Oksanen, Jari, et al. 2017. "Vegan: Community Ecology Package." https://CRAN.R-project.org/package=vegan.

Oksyuzyan, E. B., and A. S. Sokolovsky. 2003. "The Marine Component of Ichthyofauna in the Mouth Area and Lower Course of the Tumen River." *Russian Journal of Marine Biology* 29, no. 1 (2003/01/01): 18-22. http://dx.doi.org/10.1023/A:1022819718963.

Orias, Frederic, Laurent Simon, and Yves Perrodin. 2015. "Respective Contributions of Diet and Medium to the Bioaccumulation of Pharmaceutical Compounds in the First Levels of an Aquatic Trophic Web." *Environmental Science and Pollution Research* 22, no. 24 (Dec): 20207-20214. http://dx.doi.org/10.1007/s11356-015-5243-7.

Pearson, L. A., et al. 2016. "The Genetics, Biosynthesis and Regulation of Toxic Specialized Metabolites of Cyanobacteria." *Harmful Algae* 54 (Apr): 98-111. http://dx.doi.org/10.1016/j.hal.2015.11.002.

Pluskal, T., et al. 2010. "Mzmine 2: Modular Framework for Processing, Visualizing, and Analyzing Mass Spectrometry-Based Molecular Profile Data." *Bmc Bioinformatics* 11 (Jul): 11. http://dx.doi.org/10.1186/1471-2105-11-395.

Post, D. M. 2002. "Using Stable Isotopes to Estimate Trophic Position: Models, Methods, and Assumptions." *Ecology* 83, no. 3 (Mar): 703-718. http://dx.doi.org/10.2307/3071875.

Postel, S. 2010. "Water: Adapting to a New Normal." In *The Post Carbon Reader: Managing the 21st Century's Sustainability Crises*, edited by R Heinberg and D Lerch. California: Watershed Media/University of California Press.

Posthuma, Leo, Glenn W Suter II, and Theo P Traas. 2001. *Species Sensitivity Distributions in Ecotoxicology*: CRC press.

Pouria, Shideh, et al. 1998. "Fatal Microcystin Intoxication in Haemodialysis Unit in Caruaru, Brazil." *The Lancet* 352, no. 9121 (7/4/): 21-26. http://dx.doi.org/http://dx.doi.org/10.1016/S0140-6736(97)12285-1.

Ramirez, A. J., et al. 2009. "Occurrence of Pharmaceuticals and Personal Care Products in Fish: Results of a National Pilot Study in the United States." *Environmental Toxicology and Chemistry* 28, no. 12 (Dec): 2587-2597. <Go to ISI>://WOS:000271694000014.

Ramirez, A. J., et al. 2007. "Analysis of Pharmaceuticals in Fish Using Liquid Chromatography-Tandem Mass Spectrometry." *Analytical Chemistry* 79, no. 8 (Apr): 3155-3163. http://dx.doi.org/10.1021/ac062215i.

Rhind, S. M. 2009. "Anthropogenic Pollutants: A Threat to Ecosystem Sustainability?" *Philosophical Transactions of the Royal Society B: Biological Sciences* 364, no. 1534: 3391-3401. http://dx.doi.org/10.1098/rstb.2009.0122.

Rice, Jacelyn, and Paul Westerhoff. 2017. "High Levels of Endocrine Pollutants in Us Streams During Low Flow Due to Insufficient Wastewater dilution." *Nature Geoscience* 10, no. 8: 587-591. http://dx.doi.org/10.1038/ngeo2984.

Rier, S. T., and R. J. Stevenson. 2002. "Effects of Light, Dissolved Organic Carbon, and Inorganic Nutrients on the Relationship between Algae and Heterotrophic Bacteria in Stream Periphyton." *Hydrobiologia* 489, no. 1-3 (Dec): 179-184. http://dx.doi.org/10.1023/a:1023284821485.

Rodney, M. Donlan. 2002. "Biofilms: Microbial Life on Surfaces." *Emerging Infectious Disease journal* 8, no. 9: 881. http://dx.doi.org/10.3201/eid0809.020063.

Roegner, A. F., et al. 2014. "Microcystins in Potable Surface Waters: Toxic Effects and Removal Strategies." *J Appl Toxicol* 34, no. 5 (May): 441-57. http://dx.doi.org/10.1002/jat.2920.

Rudd, M. A., et al. 2014. "International Scientists' Priorities for Research on Pharmaceutical and Personal Care Products in the Environment." *Integrated environmental assessment and management* 10, no. 4 (Oct): 576-87. http://dx.doi.org/10.1002/ieam.1551.

Rudd, Murray A. 2014. "Scientists' Perspectives on Global Ocean Research Priorities." *Frontiers in Marine Science* 1. http://dx.doi.org/10.3389/fmars.2014.00036.

Ruhi, Albert, et al. 2016. "Bioaccumulation and Trophic Magnification of Pharmaceuticals and Endocrine Disruptors in a Mediterranean River Food Web." *Science of the Total Environment* 540 (Jan 1): 250-259. http://dx.doi.org/10.1016/j.scitotenv.2015.06.009.

Saari, G. N., W. C. Scott, and B. W. Brooks. 2017. "Global Scanning Assessment of Calcium Channel Blockers in the Environment: Review and Analysis of Occurrence, Ecotoxicology and Hazards in Aquatic Systems." *Chemosphere* 189 (Dec): 466-478. http://dx.doi.org/10.1016/j.chemosphere.2017.09.058.

Salas, Daniela, et al. 2017. "Hydrophilic Interaction Liquid Chromatography Coupled to Mass Spectrometry-Based Detection to Determine Emerging Organic Contaminants in Environmental Samples." *TrAC Trends in Analytical Chemistry* 94: 141-149. http://dx.doi.org/10.1016/j.trac.2017.07.017.

Sarazin, G., et al. 2002. "Première Évaluation Du Risque Toxique Lié Aux Cyanobactéries D'eau Douce En France : Le Programme " Efflocya "." *Revue des sciences de l'eau* 15, no. 1: 315. http://dx.doi.org/10.7202/705455ar.

Schulz, M., et al. 2012. "Therapeutic and Toxic Blood Concentrations of Nearly 1,000 Drugs and Other Xenobiotics." *Critical Care* 16, no. 4: 4. http://dx.doi.org/10.1186/cc11441.

Scott, J. Thad, et al. 2009. "Nitrogen Fixation and Phosphatase Activity in Periphyton Growing on Nutrient Diffusing Substrata: Evidence for Differential Nutrient Limitation in Stream Periphyton." *Journal of the North American Benthological Society* 28, no. 1 (Mar): 57-68. http://dx.doi.org/10.1899/07-107.1.

Scott, William C. Casan, et al. 2016. "Predicted and Observed Therapeutic Dose Exceedences of Ionizable Pharmaceuticals in Fish Plasma from Urban Coastal Systems." *Environmental Toxicology and Chemistry* 35, no. 4: 983-995. http://dx.doi.org/10.1002/etc.3236.

Soh, L., et al. 2011. "Fate of Sucralose through Environmental and Water Treatment Processes and Impact on Plant Indicator Species." *Environ Sci Technol* 45, no. 4 (Feb 15): 1363-9. http://dx.doi.org/10.1021/es102719d.

Solomon, Keith, and P. Takacs. 2002. *Probabilistic Risk Assessment Using Species Sensitivity Distributions*.

Sotton, B., et al. 2015. "Nodularin and Cylindrospermopsin: A Review of Their Effects on Fish." *Reviews in Fish Biology and Fisheries* 25, no. 1 (Mar): 1-19. http://dx.doi.org/10.1007/s11160-014-9366-6.

Sowby, Robert. 2014. "The Urban Water Cycle: Sustaining Our Modern Cities." *Water Currents*.

Starrfelt, Jostein, et al. 2013. "Estimating Trophic Levels and Trophic Magnification Factors Using Bayesian Inference." *Environmental Science & Technology* 47, no. 20 (Oct 15): 11599-11606. http://dx.doi.org/10.1021/es401231e.

Strydom, N. A., and B. D. d'Hotman. 2005. "Estuary-Dependence of Larval Fishes in a Non-Estuary Associated South African Surf Zone: Evidence for Continuity of Surf Assemblages." *Estuarine Coastal and Shelf Science* 63, no. 1-2 (Apr): 101-108. http://dx.doi.org/10.1016/j.ecss.2004.10.013.

Subedi, B., et al. 2012. "Occurrence of Pharmaceuticals and Personal Care Products in German Fish Tissue: A National Study." *Environmental Science & Technology* 46, no. 16 (Aug): 9047-9054. http://dx.doi.org/10.1021/es301359t.

Szarka, S., K. Prokai-Tatrai, and L. Prokai. 2014. "Application of Screening Experimental Designs to Assess Chromatographic Isotope Effect Upon Isotope-Coded Derivatization for Quantitative Liquid Chromatography-Mass Spectrometry." *Anal Chem* 86, no. 14 (Jul 15): 7033-40. http://dx.doi.org/10.1021/ac501309s.

Szczebak, J. T., and D. L. Taylor. 2011. "Ontogenetic Patterns in Bluefish (Pomatomus Saltatrix) Feeding Ecology and the Effect on Mercury Biomagnification." *Environ Toxicol Chem* 30, no. 6 (Jun): 1447-58. http://dx.doi.org/10.1002/etc.516.

Tanoue, R., et al. 2017. "Uptake and Metabolism of Human Pharmaceuticals by Fish: A Case Study with the Opioid Analgesic Tramadol." *Environ Sci Technol* 51, no. 21 (Nov 7): 12825-12835. http://dx.doi.org/10.1021/acs.est.7b03441.

Tanoue, Rumi, et al. 2014. "Simultaneous Determination of Polar Pharmaceuticals and Personal Care Products in Biological Organs and Tissues." *Journal of Chromatography A* 1355, no. 0: 193-205. http://dx.doi.org/http://dx.doi.org/10.1016/j.chroma.2014.06.016.

Tanoue, Rumi, et al. 2015. "Uptake and Tissue Distribution of Pharmaceuticals and Personal Care Products in Wild Fish from Treated-Wastewater-Impacted Streams." *Environmental Science & Technology* 49, no. 19 (Oct 6): 11649-11658. http://dx.doi.org/10.1021/acs.est.5b02478.

TCEQ. 2007. "Surface Water Quality Management Procedures, Volume 2: Methods for Collecting and Analyzing Biological Assemblage and Habitat Data. Rg-416. Texas Commission on Environmental Quality, Austin Tx.".

---. 2008. " Surface Water Quality Management Procedures, Volume 1: Physical and Chemical Monitoring Methods for Water, Sediment, and Tissue. Rg-415. Texas Commission on Environmental Quality, Austin Tx.".

Thompson, J. 1966. "The Grey Mullets." *Oceanography and Marine Biology Annual Review* 4: 301-305.

Trapp, Stefan, and Richard W. Horobin. 2005. "A Predictive Model for the Selective Accumulation of Chemicals in Tumor Cells." *European Biophysics Journal* 34, no. 7 (October 01): 959-966. http://dx.doi.org/10.1007/s00249-005-0472-1.

U.S.EPA. 2015a. "2015 Drinking Water Health Advisories for Two Cyanobacterial Toxins." *https://www.epa.gov/sites/production/files/2015-06/documents/cyanotoxins-fact_sheet-2015.pdf*.

---. 2015b. "Revisions to the Unregulated Contaminant Monitoring Rule (Ucmr 4) for Public Water Systems and Announcement of a Public Meeting. 40 Cfr Part 121. Fed Reg 80:76897–76923. [Cited 2018 April 7]." *https://federalregister.gov/a/2015-30824*.

---. 2016a. "Drinking Water Contaminant Candidate List (Ccl) and Regulatory Determination." *https://www.epa.gov/ccl*.

---. 2016b. "Human Health Recreational Ambient Water Quality Criteria or Swimming Advisories for Microcystins and Cylindrospermopsin. Epa 822-P-16-002. [Cited 2018 April 7]." *https://www.epa.gov/sites/production/files/2016-12/documents/draft-hh-rec-ambient-water-swimming-document.pdf*.

Ulrich, N., et al. 2017. "Ufz-Lser Database V 3.2 [Internet]." http://www.ufz.de/lserd.

"United Nations, World Urbanization Prospects: The 2017 Revision, United Nations Population Division." 2017.

USEPA. 1989. "Risk Assessment Guidance for Superfund, Volume I: Human Health Evaluation Manual. (Part a), Interim Final." *EPA 540/1-89/002*. Office of Emergency and Remedial Response, Washington, DC.

Valenti, T. W., et al. 2012. "Human Therapeutic Plasma Levels of the Selective Serotonin Reuptake Inhibitor (Ssri) Sertraline Decrease Serotonin Reuptake Transporter Binding and Shelter-Seeking Behavior in Adult Male Fathead Minnows." *Environmental Science & Technology* 46, no. 4 (Feb): 2427-2435. http://dx.doi.org/10.1021/es204164b.

Valenti, T. W., et al. 2011. "Influence of Drought and Total Phosphorus on Diel Ph in Wadeable Streams: Implications for Ecological Risk Assessment of Ionizable Contaminants." *Integrated environmental assessment and management* 7, no. 4 (Oct): 636-47. http://dx.doi.org/10.1002/ieam.202.

Valenti, Theodore W., Jr., et al. 2009. "Aquatic Toxicity of Sertraline to Pimephales Promelas at Environmentally Relevant Surface Water Ph." *Environmental Toxicology and Chemistry* 28, no. 12 (Dec): 2685-2694. <Go to ISI>://WOS:000271694000025.

van Apeldoorn, M. E., et al. 2007. "Toxins of Cyanobacteria." *Mol Nutr Food Res* 51, no. 1 (Jan): 7-60. http://dx.doi.org/10.1002/mnfr.200600185.

Vander Zanden, M. J., and J. B. Rasmussen. 1999. "Primary Consumer Delta C-13 and Delta N-15 and the Trophic Position of Aquatic Consumers." *Ecology* 80, no. 4 (Jun): 1395-1404. <Go to ISI>://WOS:000081368500027.

Vanderford, B. J., and S. A. Snyder. 2006. "Analysis of Pharmaceuticals in Water by Isotope Dilution Liquid Chromatography/Tandem Mass Spectrometry." *Environmental Science & Technology* 40, no. 23 (Dec): 7312-7320. http://dx.doi.org/10.1021/es0613198.

Walters, D. M., et al. 2016. "Trophic Magnification of Organic Chemicals: A Global Synthesis." *Environ Sci Technol* 50, no. 9 (May 3): 4650-8. http://dx.doi.org/10.1021/acs.est.6b00201.

Waltham, N. J., P. R. Teasdale, and R. M. Connolly. 2013. "Use of Flathead Mullet (Mugil Cephalus) in Coastal Biomonitor Studies: Review and Recommendations for Future Studies." *Marine Pollution Bulletin* 69, no. 1-2 (Apr): 195-205. http://dx.doi.org/10.1016/j.marpolbul.2013.01.012.

Watkins, C. D., et al. 2014. "Assessment of Mosquitofish (Gambusia Affinis) Health Indicators in Relation to Domestic Wastewater Discharges in Suburbs of Houston, USA." *Bulletin of environmental contamination and toxicology* 93, no. 1 (Jul): 13-8. http://dx.doi.org/10.1007/s00128-014-1248-z.

Whitfield, A. K., J. Panfili, and J. D. Durand. 2012. "A Global Review of the Cosmopolitan Flathead Mullet Mugil Cephalus Linnaeus 1758 (Teleostei: Mugilidae), with Emphasis on the Biology, Genetics, Ecology and Fisheries Aspects of This Apparent Species Complex." *Reviews in Fish Biology and Fisheries* 22, no. 3 (Sep): 641-681. http://dx.doi.org/10.1007/s11160-012-9263-9.

WHO. 2011. *Guidelines for Drinking-Water Quality*, edited by 4th. Geneva, Switzerland: World Health Organization.

Wickham, Hadley. 2016. *Ggplot2: Elegant Graphics for Data Analysis*. 2nd ed., Use R! New York: Springer

Wiegand, C., and S. Pflugmacher. 2005. "Ecotoxicological Effects of Selected Cyanobacterial Secondary Metabolites: A Short Review." *Toxicol Appl Pharmacol* 203, no. 3 (Mar 15): 201-18. http://dx.doi.org/10.1016/j.taap.2004.11.002.

Xie, Z. X., et al. 2017. "Bioaccumulation and Trophic Transfer of Pharmaceuticals in Food Webs from a Large Freshwater Lake." *Environmental Pollution* 222 (Mar): 356-366. http://dx.doi.org/10.1016/j.envpol.2016.12.026.

Xie, Zhengxin, et al. 2015. "Occurrence, Bioaccumulation, and Trophic Magnification of Pharmaceutically Active Compounds in Taihu Lake, China." *Chemosphere* 138 (Nov): 140-147. http://dx.doi.org/10.1016/j.chemosphere.2015.05.086.

Yen, H. K., T. F. Lin, and P. C. Liao. 2011. "Simultaneous Detection of Nine Cyanotoxins in Drinking Water Using Dual Solid-Phase Extraction and Liquid Chromatography-Mass Spectrometry." *Toxicon* 58, no. 2 (Aug): 209-218. http://dx.doi.org/10.1016/j.toxicon.2011.06.003.

Yuan, M., et al. 1999. "Low-Energy Collisionally Activated Decomposition and Structural Characterization of Cyclic Heptapeptide Microcystins by Electrospray Ionization Mass Spectrometry." *Journal of Mass Spectrometry* 34, no. 1 (Jan): 33-43. http://dx.doi.org/10.1002/(sici)1096-9888(199901)34:1<33::aid-jms754>3.0.co;2-l.

Zervou, S. K., et al. 2017. "New Spe-Lc-Ms/Ms Method for Simultaneous Determination of Multi-Class Cyanobacterial and Algal Toxins." *J Hazard Mater* 323, no. Pt A (Feb 05): 56-66. http://dx.doi.org/10.1016/j.jhazmat.2016.07.020.

Zismann, L., V. Berdugo, and B. Kimor. 1975. "Food and Feeding Habits of Early Stages of Grey Mullets in Haifa Bay Region." *Aquaculture* 6, no. 1 (1975): 59-75. http://dx.doi.org/10.1016/0044-8486(75)90089-7.